UNIVERSITA' DEGLI STUDI DI BARI ALDO MORO

Dipartimento di Scienze del Suolo, della Pianta e degli Alimenti

DOTTORATO DI RICERCA IN "BIODIVERSITÀ, AGRICOLTURA E AMBIENTE"
Curriculum: Genetica e biotecnologie vegetali

CICLO XXXVII

Settore Scientifico Disciplinare AGRI-06/A (AGR/07)

TITOLO DELLA TESI:

"CHARACTERIZATION OF GRAIN LEGUME BIODIVERSITY FOR STRESS ADAPTATION AND INNOVATIVE INDUSTRIAL USES WITH LOW ENVIRONMENTAL INPUTS"

Dottorando: Dott. Francesco Arcieri

Coordinatori: Ch.mo Prof. Enrico de Lillo e Ch.ma Prof.ssa Cinzia Montemurro

Supervisore (Tutor): Ch.mo Prof. Stefano Pavan

ESAME FINALE 2025

Borsa di Dottorato finanziata nell'ambito del Programma Operativo Nazionale Ricerca e Innovazione 2014-2020 (CCI 2014IT16M2OP005), risorse FSE REACT-EU, Azione IV.4 "Dottorati e contratti di ricerca su tematiche dell'innovazione" e Azione IV.5 "Dottorati su tematiche Green"

Summary

This thesis focuses on the characterization of the biodiversity of grain legumes, pea (*Pisum sativum* L.) and lentil (*Lens culinaris* Medik.), with the aim of improving stress adaptation and promoting innovative industrial uses with low environmental inputs. Research activities were carried out at the Department of Soil, Plant and Food Sciences of the University of Bari "Aldo Moro". A part of the work was conducted in collaboration with the industrial partner Innovaprot S.r.l. and the valuable support of Dr. Luigi Manfredi.

After a general introduction (Chapter 1), Chapters 2 and 3 focus on the interaction between pea and the holoparasitic root plant *Orobanche crenata* (*Oc*), today representing one of the major biotic stresses affecting grain legumes cultivation in the Mediterranean area. Specifically, Chapter 2 reports experimental activities aimed at investigating the genetic basis of *Oc* resistance displayed by the pea breeding line ROR12. Quantitative trait loci (QTLs) associated with this trait were identified, and marker assays were developed to assist selection in breeding programs. Chapter 3 reports another experimental study aimed at investigating the relation between strigolactone (SL) exudation and field response to *Oc* in pea, using a global pea germplasm collection, SL biosynthetic mutants and a set of segregating RILs originating from ROR12 as resistant parent. Phenotypic screening, SLs quantification, and RNA-seq were used in this case as investigation methods.

Chapter 4 reports a study, based on transcriptomics and hormonal quantification, carried out to investigate the physiological roles of SLs and the SL-biosynthetic enzymes Carotenoid Cleavage Dioxygenase (CCD)7 and 8. This led, among other, to the definition of association between SLs and response to multiple abiotic stresses (hydrogen peroxide and salt, oxidative and heat). In addition, hormonal cross-talks were identified between SLs and the stress-related hormones jasmonic acid and abscissic acid.

Chapter 5 reports the characterization of a lentil germplasm collection for seed color, phenolic profile and antioxidant activity. Superior lines were identified, and association among traits were defined.

Finally, Chapter 6 discusses the results of the thesis as a whole and provides a conclusion with future perspectives.

TABLE OF CONTENTS

Chapter 1
Introduction

1. Agrobiodiversity: definition, genetic erosion and conservation

Biodiversity is defined as the diversity of life on earth across all levels, from genes to ecosystems (The Convention on Biological Diversity, 2006; Andres et al., 2023; Hailu, 2025). Agrobiodiversity, on the other hand, encompasses the diversity of all domesticated crops and livestock, their wild relatives, and associated interacting species, including pollinators, symbionts, pests, parasites, predators, and competitors (Qualset et al., 1995; Hammer et al., 2003).

Agrobiodiversity provides essential resources for breeding programs aimed at developing higher-yielding crops, with enhanced resistance to biological and environmental stresses, and enhanced qualitative features (Rao, 2004; Cruz-Cruz et al., 2013, Zegeye, 2017).

Despite its critical importance, agrobiodiversity is gradually threatened by a combination of anthropogenic and environmental factors, resulting in a phenomenon known as genetic erosion (Khoury et al., 2022). Agricultural intensification, characterized by adoption of monocultures and the dominance of a limited number of high-yielding varieties, is recognized as the primary driver of genetic erosion (Kehoe et al., 2017; Zabel et al., 2019; Khatri et al., 2024).

Considering the current high rate of genetic erosion, the conservation of agrobiodiversity is essential for ensuring agricultural productivity, and preserving ecosystem services, species, and genetic diversity for future generations (Schwartz et al., 2017; Borrell et al., 2020; Hailu, 2025). This can be carried out through two mutually reinforcing and complementary approaches: *in-situ* conservation and *ex-situ* conservation (Zegeye, 2017).

In-situ (on-site) conservation refers to the preservation of genetic resources within their original ecosystems. *In-situ* conservation is a dynamic process, as the evolution of species continues in the same environment where plants grow, involving gene pools and the process of co-evolution (Maxted et al., 1997; Heywood, 2014). For cultivated species, *in situ* conservation takes place in farmers' fields, especially in the centers of biodiversity where crops were originally domesticated (Harlan, 1971; Gepts, 2006; Zegeye, 2017). As for wild species, *in situ* conservation mainly occurs in natural areas (with limited or no human activities) and national parks (carefully regulated human activities) (Gepts, 2006).

Ex-situ (off-site) conservation consists in maintaining genetic resources outside of their original (agro)-ecosystem, and mainly occurs in genebanks (Zegeye, 2017; Engels et al., 2021). These are repositories that store plant genetic resources, typically in the form of seeds, but also as seedlings, vegetative organs and tissues, and whole plant (Smale et al., 2020; Aribi, 2024). There are approximately 1,800 genebanks worldwide, conserving around 7.4 million germplasm accessions (i.e. populations collected in a given place at a specific time) from over 16,500 plant species relevant

to agriculture (Engels, 2004; FAO, 2010; Paton et al., 2020). Approximately two million of these accessions are considered unique, and one-third is conserved in Europe (Eangels, 2004; FAO, 2010; Kell et al., 2012).

In order to fully utilize the agrobiodiversity within genebanks, crop breeders and researchers require detailed information on passport, morpho-agronomic and genetic traits. Unfortunately, this information is not always available, thus representing a bottleneck that should be addressed by research efforts (Mascher et al., 2019; Volk et al., 2021; Aubry, 2023).

2. Identification of marker-trait associations by QTL Mapping

Genetic and phenotypic data on segregant populations can be integrated to map genomic regions associated with quantitative phenotypic traits, a process also referred to as QTL mapping. QTL mapping provides a basis for the identification of genes underlying quantitative traits by means of positional cloning; in addition, it might be exploited for the development of molecular markers assisting selection in breeding programs (Pavan et al., 2019).

QTL mapping requires, at its basis, the availability of a linkage map, displaying the position and relative genetic distances between markers along linkage groups. The three main steps necessary for the construction of linkage map are the following:

(1) production of a mapping segregant population, such as an F_2 population or a recombinant inbred lines (RIL) population, obtained by repeated selfing of individual F_2 plants (Collard et al., 2005; Alqudah et al., 2020);
(2) identification of molecular markers segregating within the population;
(3) linkage analysis, in which linkage between markers is assessed and genetic distances are estimated using a mapping function (such as the Haldane or Kosambi's functions). The logarithm of the odd (LOD) ratio (i.e. the ratio of the probability of linkage versus no linkage) is typically used to assess linkage. LOD values of ≥ 3 are typically used to declare linkage between markers and construct linkage map (Collard et al., 2005; Sing et al., 2015).

The QTL mapping procedure searches for statistical associations between trait and genetic marker variation. Indeed, if a marker is closely linked to a QTL, genotypic groups for that marker exhibit significant phenotypic differences (Zeng, 2001; Collard et al., 2005). Thus, to perform QTL mapping, linkage maps and phenotypic data collecting on mapping population are necessary. Three widely used methods for QTL detection are single-marker analysis, simple interval mapping, and composite interval mapping (Tanksley, 1993; Liu, 1998).

Interval mapping methods generate a profile of potential QTL locations between adjacent linked markers. The results of are typically presented as LOD score profiles along the linkage map. In order to declare a significant QTL, the LOD score must exceed a specified significance threshold. This is typically determined using permutation tests, which shuffle phenotypic values while keeping genotypes fixed, therefore simulating the null hypothesis of no true association. Repeated iterations (e.g. 500–1000) generate an empirical distribution of the LOD score. Finally, a reliable threshold was established based on false positive rates (Churchill et al., 1994; Zeng 2001; Collard et al., 2005; Manichaikul et al., 2007; Zou et al., 2008; Xu et al., 2017).

Although the most probable position of a QTL corresponds to the LOD score peak, QTL confidence intervals are typically estimated by QTL mapping algorithms, based on LOD score drop-off or bootstrap (Collard et al., 2005; Sing et al., 2015). This interval provides indication on genomic regions in which genes underlying quantitative traits are likely to be located.

3. Grain Legumes: Botanical features, context and economic importance

The Fabaceae (Leguminosae) family, comprising approximately 800 genera and 20,000 species, is the third largest family of flowering plants. It represents an exceptionally diverse and globally distributed plant family, encompassing a wide variety of life forms across different ecosystems (Lewis et al., 2005; Smýkal et al., 2014; Stagnari et al., 2017). Members of the Fabaceae family are characterized by butterfly-like (papilionoid) flower and distinct fruit, termed a legume, which gives the family its original name (Smýkal et al., 2014).

Grain legumes (also known as pulses) are members (species) of the Fabaceae family whose seeds are harvested dry (other legumes are those used as vegetables, forage and other uses). Based on the growth seasons, grain legumes are also classified in cool-season legumes, such as pea (*Pisum sativum*), lentil (*Lens culinaris*) and faba bean (*Vicia faba*), and warm-season legumes, such as soybean (*Glycine max*), common bean (*Phaseolus vulgaris*), peanut (*Arachis hypogaea*) and *Vigna* spp. (Smýkal et al., 2014; Zhang et al., 2022).

Grain legume domestication occurred independently in several distinct geographical regions, such as South America, Southwest Asia, and Europe. Then, their cultivation dispersed through human migration or trade. Key traits of domestication include pod shattering/dehiscence, seed dormancy (especially in cool-season legumes), and seed size. Additionally, other traits, such as phenology, grain shape, nutritional quality and taste, were enhanced over time (Abbo et al., 2014; Vaz Patto et al., 2015; Zhang et al., 2022).

Grain legumes play a crucial role in providing essential ecosystem services and supporting sustainable farming systems. They can fix atmospheric nitrogen by establishing a root-nodule symbiosis with

nitrogen-fixing soil bacteria called rhizobia, thereby reducing the need for synthetic nitrogen fertilization and lowering greenhouse gases (GHG) emissions (Sultani et al., 2007; Stagnari et al., 2017; Ferreira et al., 2021; Zhang et al., 2022). In addition, grain legume cultivation improves several aspects of soil fertility, such as humus content, and the availability of nitrogen and phosphorus. Thus, introducing grain legume in crop rotations or intercropping system can significantly improve the yield and quality of subsequent crops or intercropped plants (Kirkegaard et al., 2008; Preissel et al., 2015; St. Luce et al., 2015; Stagnari et al., 2017). Finally, the inclusion of legumes in intensive cropping and cereal-based farming systems helps to conserve habitat diversity and protect agrobiodiversity, supporting the survival of key species for nature conservation, such as insects (including pollinators), birds, and small mammals (Peoples et al., 2019; Ferreira et al., 2021).

Regarding nutritional properties, grain legumes are an affordable and important source of dietary proteins, therefore playing a crucial role in global food security. They offer a fairly balanced amino acid profile, making them an excellent protein source. However, low amounts of some essential sulfur-containing amino acids (cystine and methionine) are present, which are instead present in cereals. In addition to protein, grain legumes provide essential nutrients such as fatty acids, fibers, carbohydrates, phytochemicals, minerals and bioactive compounds while maintaining a low glycemic index (Campos-Vega et al., 2010; Smýkal et al., 2014; Ferreira et al., 2021; Affrifah et al., 2023; Zhang et al., 2024).

Grain legumes (excluding soybean) are cultivated on approximately 97 million ha globally, with total production exceeding 94 Mt (FAOSTAT, 2023). Asia leads both in production and cultivated area, followed by Africa and the Americas (FAOSTAT, 2023). Among grain legumes, bean represents the most widely cultivated crop, with 38 million ha dedicated to its production, followed by dry cowpea and dry chickpea (FAOSTAT, 2023). In terms of production, dry beans also dominate, with a total of 28 million tonnes harvested, followed by dry chickpeas and dry peas (FAOSTAT, 2023). India is the top producer of grain legumes, contributing approximately 25.7 million tonnes, and leads in both cultivated area and overall production, followed by Australia, China, and Canada (FAOSTAT, 2023).

Despite the significant ecosystem services and agricultural sustainability benefits provided by grain legume cultivation, European Union has undergone a notable decline in the area dedicated to these crops. From 1961 to the present, this decreased from 5.7 million hectares to 2.4 million hectares, representing a 50% reduction (FAOSTAT, 2023). Such a trend contrasts the developing grain legume sectors in other regions such as Australia and Canada (Preissel et al., 2015). In the same period the legume cultivated area expanded from 53,000 to 2.9 million ha in Canada, and from 26,000 to 2.5 million ha in Australia (FAOSTAT, 2023). These changes represent impressive increases of

approximately 5,000% and 9,000%, respectively. Nowadays, Canada is the second-largest producer of dry peas and lentils in the world, while Australia is the leading producer of lentils and the second-largest producer of dry chickpeas (FAOSTAT, 2023).

The decline in legume cultivation in Europe is linked to broader changes in farming systems, with a shift towards more specialized and intensive agriculture based on cereals and oil crops. This trend has made grain legumes less economically attractive compared to crops like cereals, which benefit from high production intensity and significantly higher yields. In addition, low and unpredictable policy support, along with the low and unstable yields of grain legumes, are other important factors contributing to the decline of grain legume cultivation in Europe (Preissel et al., 2015; Reckling et al., 2016). Finally, the low profitability of legumes, especially in Mediterranean countries, has led to minimal breeding activities and inadequate exposure of farmers to new cultivars (Rubiales et al., 2021).

The global population is expected to reach 9.6 billion by 2050, bringing major challenges such as ensuring food security and mitigating climate change. In this context, grain legumes emerge as a strategic resource due to their ability to adapt to critical environmental conditions and contribute to the sustainability of agricultural systems (United Nations 2012; Stagnari et al., 2017; de Jager et al., 2019). Increasing the production of grain legumes is therefore essential to safeguard food and nutritional security while preserving agrobiodiversity (Zhang et al., 2022). At the same time, animal-based diets are increasingly considered as unsustainable, inefficient, environmentally unfriendly and unhealthy. Consequently, the limited sustainability of meat has driven a transition from animal-based to plant-based foods (Zhang et al., 2024). Globally, this dietary transition is recognized as a key strategy to address both malnutrition and the environmental impact of food systems (Ferreira et al., 2021).

The protein transition, together with sustainable crop farming, constitutes a core element of the Farm to Fork strategy within the European Green Deal, which aims to make food systems fair, healthy, and environmentally friendly (Omar et al., 2024). Within this framework, grain legumes are considered one of the most promising alternatives to meat products, playing a pivotal role in sustainable crop farming (Stagnari et al., 2017; Ferreira et al., 2021). In fact, the United Nations recognized the importance of pulses by declaring 2016 the International Year of Pulses under the theme "Nutritious Seeds for a Sustainable Future" (United Nations, 2013). Therefore, increasing grain legume production in the European Union, either by expanding cultivation areas or intensifying crop production, is a crucial step in meeting the protein needs of the European population, within the

broader context of the transition from animal-based to plant-based protein sources (Van Loon et al., 2023).

4. Grain Legume breeding

Modern plant breeding is an applied and multidisciplinary science that utilizes genetic principles and practices to develop cultivars better suited to human needs (Ceccarelli et al., 2010). Plant breeding can take great advantage from pre-breeding activities, such as phenotypic and genetic evaluation of germplasm collections, that can provide, for example, key information to select parental lines for hybridization and inheritance patterns of economically important traits. The characterization of global germplasm banks in grain legume crops is therefore of main importance to the implementation of breeding activities on these crops (Smýkal et al., 2014; Jacob et al., 2016).

Key breeding targets for grain legumes include yield, nutritional quality, and resistance to biotic and abiotic stresses (Tayeh at al., 2015; Jacob et al., 2016; Dixit et al., 2022; Dikshit et al., 2022), which are discussed below. Details will be given on the genetic improvement of legumes for resistance to Crenate broomrape (*Orobanche crenata* Forsk.), which represents one of the most serious constraints to grain legume cultivation in Mediterranean environments (Pavan et al., 2016; Negewo et al., 2022).

4.1 Yield

High inter-annual yield variability is one of the main factors contributing to the decline in grain legume cultivation in Europe, where farmers tend to prefer crops such as cereals, oilseeds, and tubers (Cernay et al., 2015). High and stable yields are complex traits, influenced by various traits, such as plant architecture, leaf development, pod and seed traits, stresses resistance, nodulation, and responses to fertilization and irrigation (Klein et al., 2020; Dixit et al., 2022; Dikshit et al., 2022; Xia et al., 2023). Thus, breeding for these traits is essential for yield improvement.

In pea, major yield increases have been achieved by the introduction of semi-leafless cultivars, carrying the *afila* (*af*) recessive mutation. This modifies plant architecture and leaf development by causing the replacement of leaflets with a branched mass of tendrils, leading to higher yield while facilitating mechanical harvesting (Tayeh et al., 2024).

Several QTL mapping studied have allowed the detection of QTLs associated with yield in grain legumes, such as chickpea (Jingade et al., 2019; Barmukh et al., 2021), faba bean (Cruz-Izquierdo et al., 2012; Ávila et al., 2017; Zhao et al., 2023; Aguilar-Benitez et al., 2025), lentil (Fratini et al., 2007; Verma et al., 2015; Kumar et al., 2018; Shing et al., 2019) and pea (Tar'an et al., 2004; Krajewski et al., 2011; Gali et al., 2018; Guindon et al., 2019; Klein et al., 2020). Genome-wide association studies (GWAS) identified additional QTLs in yield-related QTLs in chickpea (Sari et al., 2024), faba bean

(Gutierrez et al., 2024), lentil (Lorenzetti et al., 2024) and pea (Gali et al., 2019). All this information can be efficiently used to enhance productivity in improved varieties by marker assisted selection (MAS), while providing a basis for the characterization of genes functionally related to yield.

4.2 Nutritional Traits

The improvement of legume quality is a long-standing objective for plant breeding, with ongoing efforts focusing on enhancing nutritional content, organoleptic properties and other key quality attributes (Limenie, 2024).

Nowadays, in line with the increasing global demand for plant proteins, the food industry is incorporating legumes and legume-based ingredients in food products (e.g. meat analogs, extruded products, fermented foods and nutritionally balanced protein snacks) (Ferreira et al., 2021; Goldstein et al., 2022). Therefore, breeding for enhanced protein content is of main importance (Gaur et al., 2016; Dikshit et al., 2022; Parihar et al., 2022). Several genotypes with high seed protein were identified in chickpea (Serrano et al., 2017), lentil wild relatives (Kumar et al., 2016) and pea (Gabriel et al., 2008; Mohammed et al., 2018), making these materials of main interest for breeding purposes. In addition, several QTLs associated with protein content in chickpea (Wang et al., 2019) and pea (Gali et al., 2018), were detected starting from biparental populations. However, biparental QTL mapping is limited by the low genetic diversity explored. Importantly, advances in next-generation sequencing and high-throughput phenotyping have enabled GWAS in grain legumes, also leading to the identification of multiple genomic regions associated with protein content (Jha et al., 2022), as in the case of chickpea (Upadhyaya et al., 2016; Samineni et al., 2022), lentil (Johnson et al., 2023) and pea (Gali et al., 2019; Uhdre et al., 2024).

The genetic biofortification of these crops offers a cost-effective, practical, and sustainable approach to enhancing the bioavailability of micronutrients, thereby helping to alleviate malnutrition and reduce hidden hunger (Rehman et al., 2018; Kumar et al., 2020; Joshi-Saha et al., 2022). Several studies were conducted to enhance micronutrients contents in grain legume seeds. As example, in chickpea, lentil and pea, genomic regions associated with mineral concentration, especially Fe and Zn were identified (Diapari et al., 2014; Upadhyaya et al., 2016; Khazaei et al., 2017; Dissanayaka et al., 2020; Sab et al., 2020; Power et al., 2021).

Another crucial point of improvement of grain legumes concerns certain secondary metabolites, which can reduce the bioavailability of nutrients. These, collectively termed anti-nutritional factors, include tannins, lectins, phytates, vicine, and convicine (Björnsdotter et al., 2021; Kumar et al., 2022). In addition, vicine and convicine cause a hemolytic anemia known as favism. Legume breeding successfully developed improved varieties with reduced levels of anti-nutritional factors (Zhang et

al., 2022). For example, in faba bean, a key regulatory gene involved in the biosynthesis of vicine and convicine was identified (Björnsdotter et al., 2021). In addition, another example is the development of lentil "zero-tannin" varieties like CDC Gold, released in Canada, and Shasta and Cedar, released in USA (Muehlbauer et al., 2011; Mirali et al., 2016). In pea, low-lectin varieties have been developed, which are less likely to cause digestive issues and enhance the absorption of nutrients like iron (Warkentin et al., 2012; Liu et al., 2015).

Legumes are a rich source of bioactive molecules, such as polyphenolic compounds (e.g., phenolic acids and flavonoids), which not only contribute to their organoleptic properties but also offer various health benefits. The presence of these phenolic compounds in legume seeds, along with their antioxidant activity, makes legumes valuable candidates for the development of functional foods that can be incorporated into the daily diet. Therefore, enhancing these nutritional features is essential to support food security (Singh et al., 2017a). Despite their importance, the genetic basis of these traits have been poorly investigated. In faba bean, GWAS led to the identification of a candidate gene associated with phenolic content (Lippolis et al. 2025). Similarly, in pigeon pea, molecular markers linked to phenolic compounds were identified through GWAS (Ujinwal et al., 2025). Additional research on other legume species is required to highlighted genetic determinants of this trait.

4.3 Resistance to abiotic and biotic stresses

Climate change is expected to exacerbate both individual and combined abiotic stresses (i.e. drought, cold, salinity and heat). This escalating severity underscores the urgent need for crop varieties that are resilient to these conditions (Pandey et al., 2017; Ali et al., 2022).

Drought stress is a major constraint to grain legume production, particularly in arid and semi-arid regions. Its impact is most severe during the reproductive and grain-filling stages (terminal drought), often resulting in substantial yield losses. However, the extent of these losses depends on both stress duration and intensity (Farooq et al., 2016; Ullah et al., 2021). Drought escape (DE) is a primary adaptation mechanism which involves rapid plant growth and development to facilitate the completion of the life span prior to the onset of drought events (Nadeem et al., 2019).

Several mapping studies were conducted to identify QTLs related to drought stress. In chickpea, Rehman et al. (2011) identified QTLs associated with early flowering and early maturity that can be used to improve elite cultivars. In lentil, eighteen QTLs related to root and shoot traits contributing to drought tolerance, such as dry root biomass, root-shoot ratio, and specific root length, were identified (Idrissi et al., 2016). Finally, in pea, ten QTLs related to response to drought stress were identified (Iglesias-García et al., 2015). In addition, GWASs performed on chickpea, lentil and pea

were successfully carried out to identify QTLs associated with drought tolerance (Li et al., 2018; Johnson et al., 2021; Tafesse et al., 2021).

Salt stress significantly reduces agricultural productivity by severely affecting plant growth. Salinity-affected soils are common in arable and irrigated lands of arid and semi-arid regions. Key factors contributing to soil salinity include low precipitation, high surface evaporation, groundwater depletion, and inappropriate agricultural practices, such as poor drainage in irrigated areas. To sustain crop yield under saline conditions, the development of improved cultivars with enhanced salt tolerance is essential (Jha et al., 2019).

QTL mapping studies indicated tolerance to salinity as a complex trait governed by several genes (Jha et al., 2019). Nonetheless, several QTLs with a major effect on the phenotype were identified. For example, in chickpea, Vadez et al. (2012) identified a major QTL associated with high seed yield under saline conditions. In addition, Pushpavalli et al. (2015) identified two major QTLs controlling salinity tolerance. In lentil and pea, QTLs related to salinity stress tolerance were also identified (Leonforte et al., 2013; Singh et al., 2020). Moreover, GWAS studies to identify genomic regions associated to salt tolerance were conducted in chickpea, cowpea and lentil (Ahmed et al., 2021; Dissanayake et al., 2021; Ravelombola et al., 2021).

Extreme temperature (either cold or heat) is one of the most important factors affecting overall developmental stages of plant and crop phenology that leads to loss in productivity and yield (Bhat et al., 2022). During the life cycle of grain legumes, heat stress is particularly critical in the reproductive stage, as it compromises seed setting and/or subsequent seed filling (Liu et al., 2019). Heat stress tolerance is a complex trait controlled by multiple genes. Mapping studies carried out in chickpea allowed identifying major QTLs for yield components (number of filled pods per plot, total number of seeds per plot, grain yield per plot and percentage of pod setting) under heat stress (Paul et al., 2018). Mapping studies were also carried out in lentil, leading to the identification of major QTLs associated with seedling survival and pod set under heat stress (Singh et al., 2017b). GWAS conducted in pea, conducted using 135 accessions of peas in five environments, identified thirty-two markers and forty-eight candidates for ten heat stress responsive traits (Tafesse et al., 2020).

Cold stress is one of the major abiotic factors affecting global crop production, leading to plant necrosis, chlorosis, and growth delay that determine loss in productivity and yield (Bhat et al., 2022). In chickpea, lentil, pea, mapping studies led to the identification of QTLs for cold tolerance (Kahraman et al., 2004; Klein et al., 2014; Mugabe et al., 2019). In addition, GWAS on cold tolerance was conducted in pea, allowing the identification of candidate genes that could be used in winter pea breeding programs (Beji et al., 2020).

Although legumes are essential to global food security, their productivity is often limited by a wide range of biotic agents, including nematodes, viruses, fungi, bacteria, insects and parasitic plants. Therefore, the development of new varieties with enhanced adaptability and resistance to these biotic challenges represents a key priority in grain legume breeding programs (Makhumbila et al., 2022).

Fusarium oxysporum is a soil-borne pathogen responsible for fusarium wilt (FW) and is considered one of the most destructive fungal agents affecting grain legumes. It causes severe yield losses in several species, including chickpea, faba bean, lentil, and pea. Moreover, it has the ability to develop distinct *formae speciales* and races based on host specificity (Jha et al., 2020). The development of host plant resistance represents the most durable, cost-effective, and environmentally sustainable strategy to mitigate FW losses in grain legumes (Jain et al., 2015; Jha et al., 2020). In chickpea, lentil and pea, several genotypes displaying resistance to FW were identified (McPhee et al., 1999; Neumann et al., 2003; Bani et al., 2012; Mohammadi et al., 2012; Pouralibaba et al., 2015; Schuba et al., 2016; Sharma et al., 2019). In addition, QTLs and genes associated with FW resistance have been successfully identified in several legume species (Hamwieh et al., 2005; McPhee et al., 2012; Jain et al., 2015; Jendoubi et al., 2016; Mannur et al., 2019).

Anthracnose, caused by the hemibiotrophic *Colletotrichum* spp., is another destructive disease affecting grain legumes. It impacts food and forage legumes during all growth stages, leading to significant yield losses (Pandey et al., 2023). Several genotypes with resistance to anthracnose were identified in different legume species, including common bean, cowpea and lentil (Méndez-Vigo et al., 2005; Pradhan et al., 2018; Banoo et al., 2020; Barilli et al., 2020; Gela et al., 2021; Bawa et al., 2022). In addition, QTLs and genes related to anthracnose resistance were found in grain legume species (Trabanco et al., 2015; Zuiderveen et al., 2016; Bhadauria et al., 2017; Gilio et al., 2020).

Another significant disease of legumes is powdery mildew, caused by parasitic fungi from the order of *Erysiphales*, which can lead to yield losses of up to 50%. The most effective strategy to control this disease is through genetic approaches (Sulima et al., 2022). In pea, loss of function mutations of the gene *PsMLO1* gene (also known as *Er1*) was previously associated with powdery mildew resistance (Humphry et al., 2001; Pavan et al., 2011). The search for *mlo*-based immunity in other legumes, based on the introduction of loss-of-function mutations of *MLO* homologs, is in progress (Rispail et al., 2016; Polanco et al., 2018; Binagwa et al., 2021).

Aphids are recognized as key pests of grain legume crops worldwide, as they can cause yield losses of up to 30% and act as vectors for numerous plant viruses. Insect-resistant cultivars offer a cost-effective, eco-friendly, and sustainable alternative to insecticides, playing a central role in integrated pest management (Sandhi et al., 2020). In lentil and pea, several genotypes displaying different levels

of resistance against aphids were characterized (Andarge et al., 2004; Ali et al., 2005; Aznar-Fernández et al., 2018a; Mitku et al., 2019). In addition, genomic regions associate to resistance to aphids were found in cowpea, lentil and pea (Qin et al., 2017; Das et al., 2022; Ollivier et al., 2022; Rahman et al., 2023).

Finally, bruchids (also known as seed weevils) are the most damaging storage pests of grain legumes. Developing resistant cultivars represents the most effective and sustainable strategy to mitigate these losses, ensuring durable protection and supporting sustainable agriculture (Mishra et al., 2017; Carrillo-Perdomo et al., 2019). Studies were conducted to identify genotypes displaying enhanced resistance to bruchids in chickpea, faba bean, lentil and pea (Clement et al., 2002; Shaheen et al., 2006; Laserna-Ruiz et al., 2012; Mishra et al., 2017; Aznar-Fernández et al., 2018b, Eker et al., 2018). Furthermore, recent studies have led to the identification of genomic regions associated with bruchid resistance in grain legume species, such as common bean and pea (Li et al., 2022; Yan et al., 2023; Osuna-Caballero et al., 2024).

4.4 Resistance to crenate broomrape

Crenate broomrape (*Orobanche crenata* Forsk.) is a root holoparasitic plant belonging to the family Orobanchaceae, which primarily infects cool-season legumes (e.g. faba bean, lentil and pea) cultivated in the Mediterranean region and Middle Eastern countries, with potential to cause up to 100% yield loss (Pavan et al., 2016; Negewo et al., 2022).

Crenate broomrape, like other species in the Orobanchaceae family, has a life cycle comprising two distinct phases: an underground phase and an aboveground phase. During the first phase, following a period of conditioning, seeds located near host roots germinate in response to specific signalling molecules released by the host plant into the rhizosphere. Upon germination, the seedling attaches to the host root and penetrates the host tissues, forming a specialized absorption structure known as a haustorium. This structure facilitates stable attachment to host and enables the transfer of water and nutrients from the host to the parasite. The underground phase concludes with the formation of small tubercles that act as storage organs for the acquired resources. The aerial phase begins with the emergence of a branched floral stem bearing blue to violet flowers. These flowers can produce up to 250,000 seeds, significantly increasing the seed bank in the soil (Pérez-de-Luque et al., 2007; Cartry et al., 2021; Wohor et al., 2022).

Strigolactones (SLs) are carotenoid-derived compounds secreted by host roots that act as germination stimulants for root-parasitic plants, including crenate broomrape (Bouwmeester et al., 2021). Seeds of these obligate parasites germinate upon perceiving SLs released into the rhizosphere, which signal the proximity of a suitable host essential for their survival. Beyond their role in parasitic seed

germination, SLs function as plant hormones involved in regulating various aspects of plant development, such as inhibiting shoot branching, shaping root architecture, promoting leaf senescence, and controlling secondary growth (Wang et al., 2024). Additionally, SLs are exuded into the soil to attract arbuscular mycorrhizal fungi (AMF), facilitating a symbiotic association in which the plant receives water and mineral nutrients, while supplying carbohydrates to the fungal partner (Pavan et al., 2016; Flematti et al., 2016; Jia et al., 2017; Mashiguchi et al., 2021).

Nowadays, three strigolactones have been identified in pea root exudates, i.e., orobanchol, orobanchyl acetate, and fabacyl acetate, with the latter having the highest biological activity toward the pea parasitic plant species (Xie et al., 2009; Pavan et al., 2016).

Among the available control strategies for broomrape management, breeding for resistance is considered as the most economically feasible and environment friendly control method for broomrape management (Amri et al., 2019). However, breeding for resistance to rhizosphere diseases (e.g. crenate broomrape) is complex, as the quantitative nature of resistance that to involve a complex inheritance governed by minor genes with small effects. In addition, resistance to broomrape is highly influenced by the environment, complicating the selection of the most resistant genotypes (Rubiales et al., 2020; Wohor et al., 2022).

In general, resistance mechanisms to Orobanchaceae can operate at the pre-attachment, pre-haustorial, or post-haustorial stages of Orobanche–host plant interactions (Pérez-de-Luque et al., 2009). At the pre-attachment stage, resistance may be related to the reduced production or altered composition of germination stimulants, such as SLs (Dor et al., 2011; Pavan et al., 2016; Mallu et al., 2021; Li et al., 2023). In addition, the resistance mechanisms may involve the formation of physical barriers or the local accumulation of toxic compounds (Pérez-de-Luque et al., 2005; Letousey et al., 2007; Sisou et al., 2021). Finally, at the post-haustorial stage, resistance may result from the necrosis and death of broomrape nodules or the sealing of host vascular tissues (Martín-Sanz et al., 2019).

Due to their pivotal role in mediating interactions between parasitic plants and their hosts, SLs have emerged as a key target in breeding strategies aimed at enhancing host resistance. Selecting crop genotypes that exude reduced levels of these compounds into the rhizosphere represents a promising approach for conferring resistance to parasitic weeds (Cardoso et al., 2011; Jamil et al., 2011). The pea mutants *rms5* and *rms1* were generated by mutations in the *RMS5* and *RMS1* genes encoding enzymes carotenoid cleavage dioxygenase (CCD)7 and CCD8, respectively. These enzymes are critical for the production of SLs (Gomez-Roldan et al., 2008; Al-Babili et al., 2015; Mashiguchi et al., 2021). CCD7 is responsible for cleaving 9-*cis*-β-carotene (C40), resulting in the production of β-ionone and 9-*cis*-β-apo-10'-carotenal (C27) (Al-Babili et al., 2015; Jia et al., 2018). Next, CCD8

cleaves 9-*cis*-apo-10'-carotenal (C27) to form carlactone (C19), a percursor of SL (Alder et al., 2012; Bouwmeester et al., 2021). CCD7 exhibits a wide range of substrate specificity, whereas CCD8 appears to be more specialized for the synthesis of SLs (Bruno et al., 2014; Hou et al., 2016).

Although such mutants were shown to induce significantly lower germination of crenate broomrape seeds, they exhibit severe pleiotropic effects, including dwarfism and excessive shoot branching, which limit their applicability in breeding programs (Rameau et al., 1997; Gomez-Roldan et al., 2008; Pavan et al., 2016).

For faba bean, several cultivars (mostly derived from the Egyptian donor line Giza402) have shown different levels of resistance to crenate broomrape. This resistance is associated with a reduced penetration of the parasite into the host vascular system (Cuccurullo et al., 2022). In addition, two breeding lines, Quijote and Navio, showing a lower induction of crenata broomrape seed germination, due to reduced release of germination stimulants in the root exudate, were identified (Fernández-Aparicio et al., 2012). Also in lentil, genotypes showing different levels of resistance against crenate broomrape were identified (Fernández-Aparicio et al., 2008; Mbasani-Mansi et al., 2019; En-nahli et al., 2021). For pea, no cultivar with resistance to crenate broomrape is currently available on the market (Wohor et al., 2022). However, some resistant lines with different level of resistance have been characterized, each exhibiting different resistance mechanisms: one acting at the pre-attachment stage and another at the post-haustorial stage (Pavan et al., 2016; Rubiales et al., 2020). Finally, several QTL related to crenate broomrape resistance were identified in faba bean and pea (Romàn et al., 2002; Valderamma et al., 2004; Fondevilla et al., 2010; Gutiérrez et al., 2013; Bardaro et al., 2016; Abd El-Fatah et al., 2020). However, many of them explain only a small proportion of phenotypic variation and are therefore not yet suitable for MAS.

In conclusion, durable resistance can be achieved by pyramiding genes with different mechanisms of action, creating multiple barriers that are not easily overcome by the parasite. For instance, combining low germination induction with other resistance mechanisms acting at different stages represents a valuable strategy (Rubiales et al., 2020).

5. Aims of the thesis

The general aim of this PhD thesis, reflected in its title, is to characterize legume biodiversity for stress adaptation and innovative industrial uses. Considering the major impact of the parasitic species *Oc* in Mediterranean agro-ecosystems, focus was given to the study of genetic mechanisms of resistance to this parasite (Chapters 2 and 3). Chapter 4 aims to elucidate multifunctional physiological roles of SLs, including adaptation to several environmental stresses. In addition, it addresses the characterization of SL-independent physiological roles of the SL biosynthetic genes

rms1 and *rms5*. Chapter 5 offers data on the characterization of a lentil germplasm collection for its phenolic profile and antioxidant activity. Altogether, these insights can support the legume value chain in challenging environments, including Mediterranean area.

REFERENCES

Abbo, S., van-Oss, R. P., Gopher, A., Saranga, Y., Ofner, I., & Peleg, Z. (2014). Plant domestication versus crop evolution: a conceptual framework for cereals and grain legumes. *Trends in Plant Science*, *19*(6), 351-360.

Abd El-Fatah, B. E., & Nassef, D. M. (2020). Inheritance of faba bean resistance to Broomrape, genetic diversity and QTL mapping analysis. *Molecular Biology Reports*, *47*(1), 11-32.

Affrifah, N. S., Uebersax, M. A., & Amin, S. (2023). Nutritional significance, value-added applications, and consumer perceptions of food legumes: A review. *Legume Science*, *5*(4), e192.

Aguilar-Benitez, D., Gutierrez, N., Casimiro-Soriguer, I., & Torres, A. M. (2025). A high-density linkage map and fine QTL mapping of architecture, phenology, and yield-related traits in faba bean (*Vicia faba* L.). *Frontiers in Plant Science*, *16*, 1457812.

Ahmed, S. M., Alsamman, A. M., Jighly, A., Mubarak, M. H., Al-Shamaa, K., Istanbuli, T., ... & Hamwieh, A. (2021). Genome-wide association analysis of chickpea germplasms differing for salinity tolerance based on DArTseq markers. *Plos One*, *16*(12), e0260709.

Al-Babili, S., & Bouwmeester, H. J. (2015). Strigolactones, a novel carotenoid-derived plant hormone. *Annual Review of Plant Biology*, *66*(1), 161-186.

Alder, A., Jamil, M., Marzorati, M., Bruno, M., Vermathen, M., Bigler, P., ... & Al-Babili, S. (2012). The path from β-carotene to carlactone, a strigolactone-like plant hormone. *Science*, *335*(6074), 1348-1351.

Ali, K., Louw, S. V. D. M., & Swart, W. J. (2005). Components and mechanisms of resistance in selected field pea *Pisum sativum* lines to the pea aphid *Acyrthosiphon pisum* (Homoptera: Aphididae). *International Journal of Tropical Insect Science*, *25*(2), 114-121.

Ali, A., Altaf, M. T., Nadeem, M. A., Karaköy, T., Shah, A. N., Azeem, H., ... & Chung, Y. S. (2022). Recent advancement in OMICS approaches to enhance abiotic stress tolerance in legumes. *Frontiers in Plant Science*, *13*, 952759.

Alqudah, A. M., Sallam, A., Baenziger, P. S., & Börner, A. (2020). GWAS: fast-forwarding gene identification and characterization in temperate cereals: lessons from barley–a review. *Journal of Advanced Research*, *22*, 119-135.

Amri, M., Trabelsi, I., Abbes, Z., & Kharrat, M. (2019). Release of a new faba bean variety" chourouk" resistant to the parasitic plants *Orobanche foetida* and *O. crenata* in Tunisia. *International Journal of Agriculture and Biology*, *23*, 499-505.

Andarge, A., & Van Der Westhuizen, M. C. (2004). Mechanisms of resistance of lentil *Lens culinaris* Medikus, genotypes to the pea aphid *Acyrthosiphon pisum* Harris (Hemiptera: Aphididae). *International Journal of Tropical Insect Science*, *24*(3), 249-254.

Andres, S. E., Standish, R. J., Lieurance, P. E., Mills, C. H., Harper, R. J., Butler, D. W., ... & Gallagher, R. V. (2023). Defining biodiverse reforestation: Why it matters for climate change mitigation and biodiversity. *Plants, People, Planet*, *5*(1), 27-38.

Aribi, M. M. (2024). Plant gene banks: conservation of genetic resources. In *Sustainable Utilization and Conservation of Plant Genetic Diversity* (pp. 753-775). Singapore: Springer Nature Singapore.

Aubry, S. (2023). Genebanking plant genetic resources in the postgenomic era. *Agriculture and Human Values*, *40*(3), 961-971.

Ávila, C. M., Ruiz-Rodríguez, M. D., Cruz-Izquierdo, S., Atienza, S. G., Cubero, J. I., & Torres, A. M. (2017). Identification of plant architecture and yield-related QTL in *Vicia faba* L. *Molecular Breeding*, *37*, 1-13.

Aznar-Fernández, T., & Rubiales, D. (2018a). Identification and characterisation of antixenosis and antibiosis to pea aphid (*Acyrthosiphon pisum*) in Pisum spp. germplasm. *Annals of Applied Biology*, *172*(3), 268-281.

Aznar-Fernández, T., Carrillo-Perdomo, E., Flores, F., & Rubiales, D. (2018b). Identification and multi-environment validation of resistance to pea weevil (*Bruchus pisorum*) in *Pisum* germplasm. *Journal of Pest Science*, *91*, 505-514.

Bani, M., Rubiales, D., & Rispail, N. (2012). A detailed evaluation method to identify sources of quantitative resistance to *Fusarium oxysporum* f. sp. *pisi* race 2 within a *Pisum* spp. germplasm collection. *Plant Pathology*, *61*(3), 532-542.

Banoo, A., Nabi, A., Rasool, R. S., Shah, M. D., Ahmad, M., Sofi, P. A., ... & Padder, B. A. (2020). North-western Himalayan common beans: population structure and mapping of quantitative anthracnose resistance through genome wide association study. *Frontiers in Plant Science*, *11*, 571618.

Bardaro, N., Marcotrigiano, A. R., Bracuto, V., Mazzeo, R., Ricciardi, F., Lotti, C., ... & Ricciardi, L. (2016). Genetic analysis of resistance to *Orobanche crenata* (Forsk.) in a pea (*Pisum sativum* L.) low-strigolactone line. *Journal of Plant Pathology*, 671-675.

Barilli, E., Moral, J., Aznar-Fernández, T., & Rubiales, D. (2020). Resistance to anthracnose (*Colletotrichum lentis*, race 0) in *Lens* spp. germplasm. *Agronomy*, *10*(11), 1799.

Barmukh, R., Soren, K. R., Madugula, P., Gangwar, P., Shanmugavadivel, P. S., Bharadwaj, C., ... & Varshney, R. K. (2021). Construction of a high-density genetic map and QTL analysis for yield, yield components and agronomic traits in chickpea (*Cicer arietinum* L.). *Plos One*, *16*(5), e0251669.

Bawa, P. K., Halliday, J., Kapoor, K., & Banniza, S. (2022). Identification of candidate genes associated with resistance against race 0 of *Colletotrichum lentis* in *Lens ervoides*. *Scientific Reports*, *12*(1), 18447.

Beji, S., Fontaine, V., Devaux, R., Thomas, M., Negro, S. S., Bahrman, N., ... & Lejeune-Hénaut, I. (2020). Genome-wide association study identifies favorable SNP alleles and candidate genes for frost tolerance in pea. *BMC Genomics*, *21*, 1-21.

Bhadauria, V., Vijayan, P., Wei, Y., & Banniza, S. (2017). Transcriptome analysis reveals a complex interplay between resistance and effector genes during the compatible lentil-*Colletotrichum lentis* interaction. *Scientific Reports*, *7*(1), 42338.

Bhat, K. A., Mahajan, R., Pakhtoon, M. M., Urwat, U., Bashir, Z., Shah, A. A., ... & Zargar, S. M. (2022). Low temperature stress tolerance: An insight into the omics approaches for legume crops. *Frontiers in Plant Science*, *13*, 888710.

Binagwa, P. H., Traore, S. M., Egnin, M., Bernard, G. C., Ritte, I., Mortley, D., ... & Bonsi, C. (2021). Genome-wide identification of powdery mildew resistance in common bean (*Phaseolus vulgaris* L.). *Frontiers in Genetics*, *12*, 673069.

Björnsdotter, E., Nadzieja, M., Chang, W., Escobar-Herrera, L., Mancinotti, D., Angra, D., ... & Geu-Flores, F. (2021). *VC1* catalyses a key step in the biosynthesis of vicine in faba bean. *Nature Plants*, *7*(7), 923-931.

Borrell, J. S., Dodsworth, S., Forest, F., Pérez-Escobar, O. A., Lee, M. A., Mattana, E., ... & Pironon, S. (2020). The climatic challenge: Which plants will people use in the next century?. *Environmental and Experimental Botany*, *170*, 103872.

Bouwmeester, H., Li, C., Thiombiano, B., Rahimi, M., & Dong, L. (2021). Adaptation of the parasitic plant lifecycle: germination is controlled by essential host signaling molecules. *Plant Physiology*, *185*(4), 1292-1308.

Bruno, M., Hofmann, M., Vermathen, M., Alder, A., Beyer, P., & Al-Babili, S. (2014). On the substrate-and stereospecificity of the plant carotenoid cleavage dioxygenase 7. *FEBS letters*, *588*(9), 1802-1807.

Campos-Vega, R., Loarca-Piña, G., & Oomah, B. D. (2010). Minor components of pulses and their potential impact on human health. *Food Research International*, *43*(2), 461-482.

Cardoso, C., Ruyter-Spira, C., & Bouwmeester, H. J. (2011). Strigolactones and root infestation by plant-parasitic *Striga*, *Orobanche* and *Phelipanche* spp. *Plant Science*, *180*(3), 414-420.

Carrillo-Perdomo, E., Raffiot, B., Ollivier, D., Deulvot, C., Magnin-Robert, J. B., Tayeh, N., & Marget, P. (2019). Identification of novel sources of resistance to seed weevils (*Bruchus* spp.) in a faba bean germplasm collection. *Frontiers in Plant Science*, *9*, 1914.

Cartry, D., Steinberg, C., & Gibot-Leclerc, S. (2021). Main drivers of broomrape regulation. A review. *Agronomy for Sustainable Development*, *41*(2), 17.

Ceccarelli, S., Galie, A., & Grando, S. (2013). Participatory breeding for climate change-related traits. In *Genomics and Breeding for Climate-Resilient Crops: Vol. 1 Concepts and Strategies* (pp. 331-376). Berlin, Heidelberg: Springer Berlin Heidelberg.

Cernay, C., Ben-Ari, T., Pelzer, E., Meynard, J. M., & Makowski, D. (2015). Estimating variability in grain legume yields across Europe and the Americas. *Scientific Reports*, *5*(1), 11171.

Churchill, G. A., & Doerge, R. (1994). Empirical threshold values for quantitative trait mapping. *Genetics*, *138*(3), 963-971.

Clemen`t, S. L., Hardie, D. C., & Elberson, L. R. (2002). Variation among accessions of *Pisum fulvum* for resistance to pea weevil. *Crop Science*, *42*(6), 2167-2173.

Collard, B. C., Jahufer, M. Z. Z., Brouwer, J. B., & Pang, E. C. K. (2005). An introduction to markers, quantitative trait loci (QTL) mapping and marker-assisted selection for crop improvement: the basic concepts. *Euphytica*, *142*, 169-196.

Convention on Biological Diversity. (2006). Article 2. Use of Terms. https://www.cbd.int/convention/articles/?a=cbd-02

Cruz-Cruz, C. A., González-Arnao, M. T., & Engelmann, F. (2013). Biotechnology and conservation of plant biodiversity. *Resources*, *2*(2), 73-95.

Cruz-Izquierdo, S., Avila, C. M., Satovic, Z., Palomino, C., Gutiérrez, N., Ellwood, S. R., ... & Torres, A. M. (2012). Comparative genomics to bridge *Vicia faba* with model and closely-related legume species: stability of QTLs for flowering and yield-related traits. *Theoretical and Applied Genetics*, *125*, 1767-1782.

Cuccurullo, A., Nicolia, A., Vurro, M., & Cardi, T. (2022). Genetic and agronomic approaches to control *Orobanche* and *Phelipanche* spp. parasitic weeds in vegetables and legumes. *Romanian Journal of Horticulture*, *3*(3), 63-82.

Das, S., Porter, L. D., Ma, Y., Coyne, C. J., Chaves-Cordoba, B., & Naidu, R. A. (2022). Resistance in lentil (*Lens culinaris*) genetic resources to the pea aphid (*Acyrthosiphon pisum*). *Entomologia Experimentalis et Applicata*, *170*(8), 755-769.

de Jager, I., Borgonjen-van den Berg, K. J., Giller, K. E., & Brouwer, I. D. (2019). Current and potential role of grain legumes on protein and micronutrient adequacy of the diet of rural Ghanaian infants and young children: using linear programming. *Nutrition Journal*, *18*, 1-16.

Diapari, M., Sindhu, A., Bett, K., Deokar, A., Warkentin, T. D., & Tar'an, B. (2014). Genetic diversity and association mapping of iron and zinc concentrations in chickpea (*Cicer arietinum* L.). *Genome*, *57*(8), 459-468.

Dikshit, H. K., Mishra, G. P., Aski, M. S., Singh, A., Tripathi, K., Bansal, R., ... & Kumar, S. (2022). Lentil breeding. In *Fundamentals of field crop breeding* (pp. 1181-1236). Singapore: Springer Nature Singapore.

Dissanayaka, D. N., Gali, K. K., Jha, A. B., Lachagari, V. R., & Warkentin, T. D. (2020). Genome-wide association study to identify single nucleotide polymorphisms associated with Fe, Zn, and Se concentration in field pea. *Crop Science*, *60*(4), 2070-2084.

Dissanayake, R., Cogan, N. O., Smith, K. F., & Kaur, S. (2021). Application of genomics to understand salt tolerance in lentil. *Genes*, *12*(3), 332.

Dixit, G. P., Srivastava, A. K., Jayalakshmi, V., Bindra, S., & Singh, S. (2022). Chickpea Breeding. In *Fundamentals of Field Crop Breeding* (pp. 1009-1062). Singapore: Springer Nature Singapore.

Dor, E., Yoneyama, K., Wininger, S., Kapulnik, Y., Yoneyama, K., Koltai, H., ... & Hershenhorn, J. (2011). Strigolactone deficiency confers resistance in tomato line *SL-ORT1* to the parasitic weeds *Phelipanche* and *Orobanche* spp. *Phytopathology*, *101*(2), 213-222.

Eker, T., Erler, F., Adak, A., Imrek, B., Guven, H., Tosun, H. S., ... & Ikten, C. (2018). Screening of chickpea accessions for resistance against the pulse beetle, *Callosobruchus chinensis* L. (Coleoptera: Bruchidae). *Journal of Stored Products Research*, *76*, 51-57.

Engels, J. M. M. (2002, August). Plant genetic resources management and conservation strategies: problems and progress. In *XXVI International Horticultural Congress: Plant Genetic Resources, The Fabric of Horticultures Future 623* (pp. 179-192).

Engels, J. M., & Ebert, A. W. (2021). A critical review of the current global *ex situ* conservation system for plant agrobiodiversity. I. History of the development of the global system in the context of the political/legal framework and its major conservation components. *Plants*, *10*(8), 1557.

En-Nahli, Y., El Arroussi, H., Kumar, S., Bouhlal, O., Mentag, R., Hejjaoui, K., ... & Amri, M. (2021). Resistance to *Orobanche crenata* Forsk. in lentil (*Lens culinaris* Medik.): exploring some potential altered physiological and biochemical defense mechanisms. *Journal of Plant Interactions*, *16*(1), 321-331.

FAO. 2010. *The second report on the state of the world's plant genetic resources for food and agriculture*. Rome. https://www.fao.org/agriculture/crops/thematic-sitemap/theme/seeds-pgr/sow/sow2/en/.

FAOSTAT, (2025) https://www.fao.org/faostat/en/#data/QCL (last updated 30/05/2025)

Farooq, M., Gogoi, N., Barthakur, S., Baroowa, B., Bharadwaj, N., Alghamdi, S. S., & Siddique, K. H. (2017). Drought stress in grain legumes during reproduction and grain filling. *Journal of Agronomy and Crop Science*, *203*(2), 81-102.

Fernández-Aparicio, M., Sillero, J. C., Pérez-de-Luque, A., & Rubiales, D. (2008). Identification of sources of resistance to crenate broomrape (*Orobanche crenata*) in Spanish lentil (*Lens culinaris*) germplasm. *Weed Research*, *48*(1), 85-94.

Fernández-Aparicio, M., Moral, A., Kharrat, M., & Rubiales, D. (2012). Resistance against broomrapes (*Orobanche* and *Phelipanche* spp.) in faba bean (*Vicia faba*) based in low induction of broomrape seed germination. *Euphytica*, *186*, 897-905.

Ferreira, H., Pinto, E., & Vasconcelos, M. W. (2021). Legumes as a cornerstone of the transition toward more sustainable agri-food systems and diets in Europe. *Frontiers in Sustainable Food Systems, 5,* 694121.

Flematti, G. R., Scaffidi, A., Waters, M. T., & Smith, S. M. (2016). Stereospecificity in strigolactone biosynthesis and perception. *Planta*, *243*, 1361-1373.

Fondevilla, S., Fernández-Aparicio, M., Satovic, Z., Emeran, A. A., Torres, A. M., Moreno, M. T., & Rubiales, D. (2010). Identification of quantitative trait loci for specific mechanisms of resistance to *Orobanche crenata* Forsk. in pea (*Pisum sativum* L.). *Molecular Breeding*, *25*, 259-272.

Fratini, R., Durán, Y., García, P., & De La Vega, M. P. (2007). Identification of quantitative trait loci (QTL) for plant structure, growth habit and yield in lentil. *Spanish Journal of Agricultural Research*, *5*(3), 348-356.

Gabriel, I., Quillien, L., Cassecuelle, F., Marget, P., Juin, H., Lessire, M., ... & Burstin, J. (2008). Variation in seed protein digestion of different pea (*Pisum sativum* L.) genotypes by cecectomized broiler chickens: 2. Relation between in vivo protein digestibility and pea seed characteristics, and identification of resistant pea polypeptides. *Livestock Science*, *113*(2-3), 262-273.

Gali, K. K., Liu, Y., Sindhu, A., Diapari, M., Shunmugam, A. S., Arganosa, G., ... & Warkentin, T. D. (2018). Construction of high-density linkage maps for mapping quantitative trait loci for multiple traits in field pea (*Pisum sativum* L.). *BMC Plant Biology*, *18*, 1-25.

Gali, K. K., Sackville, A., Tafesse, E. G., Lachagari, V. R., McPhee, K., Hybl, M., ... & Warkentin, T. D. (2019). Genome-wide association mapping for agronomic and seed quality traits of field pea (*Pisum sativum* L.). *Frontiers in Plant Science*, *10*, 1538.

Gaur, P. M., Singh, M. K., Samineni, S., Sajja, S. B., Jukanti, A. K., Kamatam, S., & Varshney, R. K. (2016). Inheritance of protein content and its relationships with seed size, grain yield and other traits in chickpea. *Euphytica*, *209*, 253-260.

Gela, T., Ramsay, L., Haile, T. A., Vandenberg, A., & Bett, K. (2021). Identification of anthracnose race 1 resistance loci in lentil by integrating linkage mapping and genome-wide association study. *The Plant Genome*, *14*(3), e20131.

Gepts, P. (2006). Plant genetic resources conservation and utilization: the accomplishments and future of a societal insurance policy. *Crop Science*, *46*(5), 2278-2292.

Gilio, T. A. S., Hurtado-Gonzales, O. P., Gonçalves-Vidigal, M. C., Valentini, G., Ferreira Elias, J. C., Song, Q., & Pastor-Corrales, M. A. (2020). Fine mapping of an anthracnose-resistance locus in Andean common bean cultivar Amendoim Cavalo. *Plos One*, *15*(10), e0239763.

Goldstein, N., & Reifen, R. (2022). The potential of legume-derived proteins in the food industry. *Grain & Oil Science and Technology*, *5*(4), 167-178.

Gomez-Roldan, V., Fermas, S., Brewer, P. B., Puech-Pagès, V., Dun, E. A., Pillot, J. P., ... & Rochange, S. F. (2008). Strigolactone inhibition of shoot branching. *Nature*, *455*(7210), 189-194.

Guindon, M. F., Martin, E., Cravero, V., Gali, K. K., Warkentin, T. D., & Cointry, E. (2019). Linkage map development by GBS, SSR, and SRAP techniques and yield-related QTLs in pea. *Molecular Breeding*, *39*, 1-16.

Gutiérrez, N., Palomino, C., Satovic, Z., Ruiz-Rodríguez, M. D., Vitale, S., Gutiérrez, M. V., ... & Ávila, C. M. (2013). QTLs for *Orobanche* spp. resistance in faba bean: identification and validation across different environments. *Molecular Breeding*, *32*, 909-922.

Gutiérrez, N., Pégard, M., Solis, I., Sokolovic, D., Lloyd, D., Howarth, C., & Torres, A. M. (2024). Genome-wide association study for yield-related traits in faba bean (*Vicia faba* L.). *Frontiers in Plant Science*, *15*, 1328690.

Hailu, F. (2025). The role of agrobiodiversity and diverse causes of its losses and methods of conservation: A review. *Food and Humanity*, 100500.

Hammer, K., Arrowsmith, N., & Gladis, T. (2003). Agrobiodiversity with emphasis on plant genetic resources. *Naturwissenschaften*, *90*, 241-250.

Hamwieh, A., Udupa, S. M., Choumane, W., Sarker, A., Dreyer, F., Jung, C., & Baum, M. (2005). A genetic linkage map of *Lens* sp. based on microsatellite and AFLP markers and the localization of fusarium vascular wilt resistance. *Theoretical and Applied Genetics*, *110*, 669-677.

Harlan, J. R. (1971). Agricultural Origins: Centers and Noncenters: Agriculture may originate in discrete centers or evolve over vast areas without definable centers. *Science*, *174*(4008), 468-474.

Heywood, V. H. (2014). An overview of in situ conservation of plant species in the Mediterranean. *Flora Mediterranea*, *24*, 5-24.

Hou, X., Rivers, J., León, P., McQuinn, R. P., & Pogson, B. J. (2016). Synthesis and function of apocarotenoid signals in plants. *Trends in Plant Science*, *21*(9), 792-803.

Humphry, M., Reinstaedler, A., Ivanov, S., Bisseling, T. O. N., & Panstruga, R. (2011). Durable broad-spectrum powdery mildew resistance in pea *er1* plants is conferred by natural loss-of-function mutations in *PsMLO1*. *Molecular Plant Pathology*, *12*(9), 866-878.

Idrissi, O., Udupa, S. M., De Keyser, E., McGee, R. J., Coyne, C. J., Saha, G. C., ... & De Riek, J. (2016). Identification of quantitative trait loci controlling root and shoot traits associated with drought tolerance in a lentil (*Lens culinaris* Medik.) recombinant inbred line population. *Frontiers in Plant Science*, *7*, 1174.

Iglesias-García, R., Prats, E., Fondevilla, S., Satovic, Z., & Rubiales, D. (2015). Quantitative trait loci associated to drought adaptation in pea (*Pisum sativum* L.). *Plant Molecular Biology Reporter*, *33*, 1768-1778.

Jacob, C., Carrasco, B., & Schwember, A. R. (2016). Advances in breeding and biotechnology of legume crops. *Plant Cell, Tissue and Organ Culture (PCTOC)*, *127*, 561-584.

Jain, S., Weeden, N. F., Kumar, A., Chittem, K., & McPhee, K. (2015). Functional codominant marker for selecting the *Fw* gene conferring resistance to Fusarium wilt race 1 in pea. *Crop Science*, *55*(6), 2639-2646.

Jamil, M., Rodenburg, J., Charnikhova, T., & Bouwmeester, H. J. (2011). Pre-attachment *Striga hermonthica* resistance of New Rice for Africa (NERICA) cultivars based on low strigolactone production. *New Phytologist*, *192*(4), 964-975.

Jendoubi, W., Bouhadida, M., Millán, T., Kharrat, M., Gil, J., Rubio, J., & Madrid, E. (2016). Identification of the target region including the *Foc0 1*/*foc0 1* gene and development of near isogenic lines for resistance to Fusarium Wilt race 0 in chickpea. *Euphytica*, *210*, 119-133.

Jha, U. C., Bohra, A., Jha, R., & Parida, S. K. (2019). Salinity stress response and 'omics' approaches for improving salinity stress tolerance in major grain legumes. *Plant Cell Reports*, *38*, 255-277.

Jha, U. C., Bohra, A., Pandey, S., & Parida, S. K. (2020). Breeding, genetics, and genomics approaches for improving Fusarium wilt resistance in major grain legumes. *Frontiers in Genetics*, *11*, 1001.

Jha, U. C., Nayyar, H., Parida, S. K., Deshmukh, R., von Wettberg, E. J., & Siddique, K. H. (2022). Ensuring global food security by improving protein content in major grain legumes using breeding and 'Omics' tools. *International Journal of Molecular Sciences*, *23*(14), 7710.

Jia, K. P., Baz, L., & Al-Babili, S. (2018). From carotenoids to strigolactones. *Journal of Experimental Botany*, *69*(9), 2189-2204.

Jingade, P., & Ravikumar, R. L. (2019). QTL mapping and identification of QTLs linked to yield and yield attributing traits in chickpea. *Proceedings of the National Academy of Sciences, India Section B: Biological Sciences*, *89*(3), 815-821.

Johnson, N., Boatwright, J. L., Bridges, W., Thavarajah, P., Kumar, S., Shipe, E., & Thavarajah, D. (2021). Genome-wide association mapping of lentil (*Lens culinaris* Medikus) prebiotic carbohydrates toward improved human health and crop stress tolerance. *Scientific Reports*, *11*(1), 13926.

Johnson, N., Boatwright, J. L., Bridges, W., Thavarajah, P., Kumar, S., & Thavarajah, D. (2024). Targeted improvement of plant-based protein: Genome-wide association mapping of a lentil (*Lens culinaris* Medik.) diversity panel. *Plants, People, Planet*, *6*(3), 640-655.

Joshi-Saha, A., Sethy, S. K., Misra, G., Dixit, G. P., Srivastava, A. K., & Sarker, A. (2022). Biofortified legumes: Present scenario, possibilities and challenges. *Field Crops Research*, *279*, 108467.

Kahraman, A., Kusmenoglu, I., Aydin, N., Aydogan, A., Erskine, W., & Muehlbauer, F. J. (2004). QTL mapping of winter hardiness genes in lentil. *Crop Science*, *44*(1), 13-22.

Kehoe, L., Romero-Muñoz, A., Polaina, E., Estes, L., Kreft, H., & Kuemmerle, T. (2017). Biodiversity at risk under future cropland expansion and intensification. *Nature Ecology & Evolution*, *1*(8), 1129-1135.

Kell, S. P., Maxted, N., Frese, L., & Iriondo, J. M. (2012). *In situ* conservation of crop wild relatives: a strategy for identifying priority genetic reserve sites. In *Agrobiodiversity conservation: securing the diversity of crop wild relatives and landraces* (pp. 7-19). Wallingford UK: CABI.

Khatri, P., Kumar, P., Shakya, K. S., Kirlas, M. C., & Tiwari, K. K. (2024). Understanding the intertwined nature of rising multiple risks in modern agriculture and food system. *Environment, Development and Sustainability*, *26*(9), 24107-24150.

Khazaei, H., Podder, R., Caron, C. T., Kundu, S. S., Diapari, M., Vandenberg, A., & Bett, K. E. (2017). Marker–trait association analysis of iron and zinc concentration in lentil (*Lens culinaris* Medik.) seeds. *The Plant Genome*, *10*(2), plantgenome2017-02.

Khoury, C. K., Brush, S., Costich, D. E., Curry, H. A., De Haan, S., Engels, J. M., ... & Thormann, I. (2022). Crop genetic erosion: understanding and responding to loss of crop diversity. *New Phytologist*, *233*(1), 84-118.

Kirkegaard, J., Christen, O., Krupinsky, J., & Layzell, D. (2008). Break crop benefits in temperate wheat production. *Field Crops Research*, *107*(3), 185-195.

Klein, A., Houtin, H., Rond, C., Marget, P., Jacquin, F., Boucherot, K., ... & Burstin, J. (2014). QTL analysis of frost damage in pea suggests different mechanisms involved in frost tolerance. *Theoretical and Applied Genetics*, *127*, 1319-1330.

Klein, A., Houtin, H., Rond-Coissieux, C., Naudet-Huart, M., Touratier, M., Marget, P., & Burstin, J. (2020). Meta-analysis of QTL reveals the genetic control of yield-related traits and seed protein content in pea. *Scientific Reports*, *10*(1), 15925.

Krajewski, P., Bocianowski, J., Gawłowska, M., Kaczmarek, Z., Pniewski, T., Święcicki, W., & Wolko, B. (2012). QTL for yield components and protein content: a multienvironment study of two pea (*Pisum sativum* L.) populations. *Euphytica*, *183*, 323-336.

Kumar, J., Singh, J., Kanaujia, R., & Gupta, S. (2016). Protein content in wild and cultivated taxa of lentil (Lens culinaris ssp. culinaris Medikus). *Indian Journal of Genetics and Plant Breeding*, *76*(04), 631-634.

Kumar, J., Gupta, S., Gupta, D. S., & Singh, N. P. (2018). Identification of QTLs for agronomic traits using association mapping in lentil. *Euphytica*, *214*, 1-15.

Kumar, S., & Pandey, G. (2020). Biofortification of pulses and legumes to enhance nutrition. *Heliyon*, *6*(3).

Kumar, Y., Basu, S., Goswami, D., Devi, M., Shivhare, U. S., & Vishwakarma, R. K. (2022). Anti-nutritional compounds in pulses: Implications and alleviation methods. *Legume Science*, *4*(2), e111.

Laserna-Ruiz, I., De-Los-Mozos-Pascual, M., Santana-Méridas, O., Sánchez-Vioque, R., & Rodríguez-Conde, M. F. (2012). Screening and selection of lentil (*Lens Miller*) germplasm resistant to seed bruchids (*Bruchus* spp.). *Euphytica*, *188*(2), 153-162.

Leonforte, A., Sudheesh, S., Cogan, N. O., Salisbury, P. A., Nicolas, M. E., Materne, M., ... & Kaur, S. (2013). SNP marker discovery, linkage map construction and identification of QTLs for enhanced salinity tolerance in field pea (*Pisum sativum* L.). *BMC Plant Biology*, *13*, 1-14.

Letousey, P., De Zélicourt, A., Vieira Dos Santos, C., Thoiron, S., Monteau, F., Simier, P., ... & Delavault, P. (2007). Molecular analysis of resistance mechanisms to *Orobanche cumana* in sunflower. *Plant Pathology*, *56*(3), 536-546.

Li, C., Dong, L., Durairaj, J., Guan, J. C., Yoshimura, M., Quinodoz, P., ... & Bouwmeester, H. J. (2023). Maize resistance to witchweed through changes in strigolactone biosynthesis. *Science*, *379*(6627), 94-99.

Li, X., Tang, Y., Wang, L., Chang, Y., Wu, J., & Wang, S. (2022). QTL mapping and identification of genes associated with the resistance to *Acanthoscelides obtectus* in cultivated common bean using a high-density genetic linkage map. *BMC Plant Biology*, *22*(1), 260.

Li, Y., Ruperao, P., Batley, J., Edwards, D., Khan, T., Colmer, T. D., ... & Sutton, T. (2018). Investigating drought tolerance in chickpea using genome-wide association mapping and genomic selection based on whole-genome resequencing data. *Frontiers in Plant Science*, *9*, 190.

Limenie, A. D. (2025). Advancement of genetic engineering applications for enhancing legume crop improvement in agriculture. *Cogent Food & Agriculture*, *11*(1), 2446652.

Lippolis, A., Hollebrands, B., Acierno, V., de Jong, C., Pouvreau, L., Paulo, J., ... & Trindade, L. M. (2025). GWAS Identifies SNP Markers and Candidate Genes for Off-Flavours and Protein Content in Faba Bean (*Vicia faba* L.). *Plants*, *14*(2), 193.

Liu, B. H. (2017). *Statistical genomics: linkage, mapping, and QTL analysis*. CRC press.

Liu, X., Glahn, R. P., Arganosa, G. C., & Warkentin, T. D. (2015). Iron bioavailability in low phytate pea. *Crop Science*, *55*(1), 320-330.

Liu, Y., Li, J., Zhu, Y., Jones, A., Rose, R. J., & Song, Y. (2019). Heat stress in legume seed setting: effects, causes, and future prospects. *Frontiers in Plant Science*, *10*, 938.

Lock, M. (2005). *Legumes of the World* (Vol. 577). G. P. Lewis, B. Schrire, & B. Mackinder (Eds.). Kew: Royal Botanic Gardens.

Lorenzetti, E., Macharia, M. W., Mager, S., Dell'Acqua, M., Carlesi, S., & Bàrberi, P. (2024). Unlocking genetic diversity for low-input systems in a changing climate through participatory characterization and GWAS of lentil landraces. *Scientific Reports*, *14*(1), 31979.

Makhumbila, P., Rauwane, M., Muedi, H., & Figlan, S. (2022). Metabolome profiling: A breeding prediction tool for legume performance under biotic stress conditions. *Plants*, *11*(13), 1756.

Mallu, T. S., Mutinda, S., Githiri, S. M., Achieng Odeny, D., & Runo, S. (2021). New pre-attachment *Striga* resistant sorghum adapted to African agro-ecologies. *Pest Management Science*, *77*(6), 2894-2902.

Manichaikul, A., Palmer, A. A., Sen, S., & Broman, K. W. (2007). Significance thresholds for quantitative trait locus mapping under selective genotyping. *Genetics*, *177*(3), 1963-1966.

Mannur, D. M., Babbar, A., Thudi, M., Sabbavarapu, M. M., Roorkiwal, M., Yeri, S. B., ... & Varshney, R. K. (2019). Super Annigeri 1 and improved JG 74: two Fusarium wilt-resistant introgression lines developed using marker-assisted backcrossing approach in chickpea (*Cicer arietinum* L.). *Molecular Breeding*, *39*, 1-13.

Martín-Sanz, A., Pérez-Vich, B., Rueda, S., Fernández-Martínez, J. M., & Velasco, L. (2020). Characterization of post-haustorial resistance to sunflower broomrape. *Crop Science*, *60*(3), 1188-1198.

Mascher, M., Schreiber, M., Scholz, U., Graner, A., Reif, J. C., & Stein, N. (2019). Genebank genomics bridges the gap between the conservation of crop diversity and plant breeding. *Nature Genetics*, *51*(7), 1076-1081.

Mashiguchi, K., Seto, Y., & Yamaguchi, S. (2021). Strigolactone biosynthesis, transport and perception. *The Plant Journal*, *105*(2), 335-350.

Maxted, N., Ford-Lloyd, b., Hawkes, J. G.(1997). Plant Genetic Conservation: The *In situ* Approach. Eds Chapman & Hall. London

Mbasani-Mansi, J., Briache, F. Z., Ennami, M., Gaboun, F., Benbrahim, N., Triqui, Z. E. A., & Mentag, R. (2019). Resistance of Moroccan lentil genotypes to *Orobanche crenata* infestation. *Journal of Crop Improvement*, *33*(3), 306-326.

McPhee, K. E., Tullu, A., Kraft, J. M., & Muehlbauer, F. J. (1999). Resistance to Fusarium wilt race 2 in the *Pisum* core collection. *Journal of the American Society for Horticultural Science*, *124*(1), 28-31.

Mc Phee, K. E., Inglis, D. A., Gundersen, B., & Coyne, C. J. (2012). Mapping QTL for Fusarium wilt race 2 partial resistance in pea (*Pisum sativum*). *Plant Breeding*, *131*(2), 300-306.

Méndez-Vigo, B., Rodríguez-Suárez, C., Paneda, A., Ferreira, J. J., & Giraldez, R. (2005). Molecular markers and allelic relationships of anthracnose resistance gene cluster B4 in common bean. *Euphytica*, *141*, 237-245.

Mirali, M., Purves, R. W., Stonehouse, R., Song, R., Bett, K., & Vandenberg, A. (2016). Genetics and biochemistry of zero-tannin lentils. *Plos One*, *11*(10), e0164624.

Mishra, S. K., Macedo, M. L. R., Panda, S. K., & Panigrahi, J. (2018). Bruchid pest management in pulses: past practices, present status and use of modern breeding tools for development of resistant varieties. *Annals of Applied Biology*, *172*(1), 4-19.

Mitku, G., Damte, T., & Wakgari, M. (2019). Category of resistance, antixenosis, antibiosis, and tolerance to *Acyrthosiphon pisum* (H.) (Hemiptera: Aphididae) in selected lentil genotypes (*Lens culinaris* M.). *Journal of Plant Science*, *7*(1), 26-35.

Mohammadi, N., Puralibaba, H., Goltapeh, E. M., Ahari, A. B., & Sardrood, B. P. (2012). Advanced lentil lines screened for resistance to *Fusarium oxysporum* f. sp. *lentis* under greenhouse and field conditions. *Phytoparasitica*, *40*, 69-76.

Mohammed, Y. A., Chen, C., Walia, M. K., Torrion, J. A., McVay, K., Lamb, P., ... & Khan, Q. (2018). Dry pea (*Pisum sativum* L.) protein, starch, and ash concentrations as affected by cultivar and environment. *Canadian Journal of Plant Science*, *98*(5), 1188-1198.

Muehlbauer, F. J., & Sarker, A. (2011). Tannin free lentils: A promising development for specialty use and increased value. *Grain Legumes*, *57*, pp. 27-28.

Mugabe, D., Coyne, C. J., Piaskowski, J., Zheng, P., Ma, Y., Landry, E., ... & Abbo, S. (2019). Quantitative trait loci for cold tolerance in chickpea. *Crop Science*, *59*(2), 573-582.

Nadeem, M., Li, J., Yahya, M., Sher, A., Ma, C., Wang, X., & Qiu, L. (2019). Research progress and perspective on drought stress in legumes: A review. *International Journal of Molecular Sciences*, *20*(10), 2541.

Negewo, T., Ahmed, S., Tessema, T., & Tana, T. (2022). Biological characteristics, impacts, and management of crenate broomrape (*Orobanche crenata*) in faba bean (*Vicia faba*): a review. *Frontiers in Agronomy*, *4*, 708187.

Neumann and AG Xue, S. (2003). Reactions of field pea cultivars to four races of *Fusarium oxysporum* f. sp. *pisi*. *Canadian Journal of Plant Science*, *83*(2), 377-379.

Ollivier, R., Glory, I., Cloteau, R., Le Gallic, J. F., Denis, G., Morlière, S., ... & Sugio, A. (2022). A major-effect genetic locus, *ApRVII*, controlling resistance against both adapted and non-adapted aphid biotypes in pea. *Theoretical and Applied Genetics*, *135*(5), 1511-1528.

Omar, A., & Thorsøe, M. H. (2024). Rebalance power and strengthen farmers' position in the EU food system? A CDA of the Farm to Fork Strategy. *Agriculture and Human Values*, *41*(2), 631-646.

Osuna-Caballero, S., Cobos, M. J., Ruiz, C. M., Wohor, O. Z., Rispail, N., & Rubiales, D. (2024). Genome-wide association studies on resistance to pea weevil: identification of novel sources of resistance and associated markers. *International Journal of Molecular Sciences*, *25*(14), 7920.

Pandey, A. K., Kumar, A., Mbeyagala, E. K., Barbetti, M. J., Basandrai, A., Basandrai, D., ... & Lamichhane, J. R. (2023). Anthracnose resistance in legumes for cropping system diversification. *Critical Reviews in Plant Sciences*, *42*(4), 177-216.

Pandey, R., Aretano, R., Gupta, A. K., Meena, D., Kumar, B., & Alatalo, J. M. (2017). Agroecology as a climate change adaptation strategy for smallholders of Tehri-Garhwal in the Indian Himalayan region. *Small-scale Forestry*, *16*, 53-63.

Parihar, A. K., Yadav, R., Lamichaney, A., Mishra, R. K., Chandra, A., Gupta, D. S., ... & Dixit, G. P. (2022). Field pea breeding. In *Fundamentals of field crop breeding* (pp. 1237-1321). Singapore: Springer Nature Singapore.

Paton, A., Antonelli, A., Carine, M., Forzza, R. C., Davies, N., Demissew, S., ... & Dickie, J. (2020). Plant and fungal collections: Current status, future perspectives. *Plants, People, Planet*, *2*(5), 499-514.

Paul, P. J., Samineni, S., Thudi, M., Sajja, S. B., Rathore, A., Das, R. R., ... & Gaur, P. M. (2018). Molecular mapping of QTLs for heat tolerance in chickpea. *International Journal of Molecular Sciences*, *19*(8), 2166.

Pavan, S., Schiavulli, A., Appiano, M., Marcotrigiano, A. R., Cillo, F., Visser, R. G., ... & Ricciardi, L. (2011). Pea powdery mildew *er1* resistance is associated to loss-of-function mutations at a *MLO* homologous locus. *Theoretical and Applied Genetics*, *123*, 1425-1431.

Pavan, S., Schiavulli, A., Marcotrigiano, A. R., Bardaro, N., Bracuto, V., Ricciardi, F., ... & Ricciardi, L. (2016). Characterization of low-strigolactone germplasm in pea (*Pisum sativum* L.) resistant to crenate broomrape (*Orobanche crenata* Forsk.). *Molecular Plant-Microbe Interactions*, *29*(10), 743-749.

Pavan, S., Bardaro, N., Fanelli, V., Marcotrigiano, A. R., Mangini, G., Taranto, F., ... & Ricciardi, L. (2019). Genotyping by sequencing of cultivated lentil (*Lens culinaris* Medik.) highlights population structure in the Mediterranean gene pool associated with geographic patterns and phenotypic variables. *Frontiers in Genetics*, *10*, 872.

Peoples, M. B., Hauggaard-Nielsen, H., Huguenin-Elie, O., Jensen, E. S., Justes, E., & Williams, M. (2019). The contributions of legumes to reducing the environmental risk of agricultural production. In *Agroecosystem diversity* (pp. 123-143). Academic Press.

Pérez-de-Luque, A., Jorrín, J., Cubero, J. I., & Rubiales, D. (2005). *Orobanche crenata* resistance and avoidance in pea (*Pisum* spp.) operate at different developmental stages of the parasite. *Weed Research*, *45*(5), 379-387.

Pérez-de-Luque, A., Lozano, M. D., Maldonado, A. M., Jorrín, J. V., Dita, M. A., Die, J., ... & Rubiales, D. (2007). *Medicago truncatula* as a model for studying interactions between root parasitic plants and legumes. *The Medicago truncatula Handbook. The Samuel Roberts Noble Foundation, Ardmore, OK*, 1-31.

Pérez-de-Luque, A., Fondevilla, S., Pérez-Vich, B., Aly, R., Thoiron, S., Simier, P., ... & Delavault, P. (2009). Understanding *Orobanche* and *Phelipanche*–host plant interactions and developing resistance. *Weed Research*, *49*, 8-22.

Polanco, C., Saenz de Miera, L. E., Bett, K., & Perez de la Vega, M. (2018). A genome-wide identification and comparative analysis of the lentil *MLO* genes. *Plos One*, *13*(3), e0194945.

Pouralibaba, H. R., Rubiales, D., & Fondevilla, S. (2015). Identification of resistance to *Fusarium oxysporum* f. sp. *lentis* in Spanish lentil germplasm. *European Journal of Plant Pathology*, *143*, 399-405.

Powers, S., Boatwright, J. L., & Thavarajah, D. (2021). Genome-wide association studies of mineral and phytic acid concentrations in pea (*Pisum sativum* L.) to evaluate biofortification potential. *G3*, *11*(9), jkab227.

Pradhan, D., Mathew, D., Mathew, S. K., & Nazeem, P. A. (2018). Identifying the markers and tagging a leucine-rich repeat receptor-like kinase gene for resistance to anthracnose disease in vegetable cowpea [*Vigna unguiculata* (L.) Walp.]. *The Journal of Horticultural Science and Biotechnology*, *93*(3), 225-231.

Preissel, S., Reckling, M., Schläfke, N., & Zander, P. (2015). Magnitude and farm-economic value of grain legume pre-crop benefits in Europe: A review. *Field Crops Research*, *175*, 64-79.

Pushpavalli, R., Krishnamurthy, L., Thudi, M., Gaur, P. M., Rao, M. V., Siddique, K. H., ... & Vadez, V. (2015). Two key genomic regions harbour QTLs for salinity tolerance in ICCV 2× JG 11 derived chickpea (*Cicer arietinum* L.) recombinant inbred lines. *BMC Plant Biology*, *15*, 1-15.

Qin, J., Shi, A., Mou, B., Bhattarai, G., Yang, W., Weng, Y., & Motes, D. (2017). Association mapping of aphid resistance in USDA cowpea (*Vigna unguiculata* L. Walp.) core collection using SNPs. *Euphytica*, *213*, 1-10.

Qualset, C., McGuire, P., & Warburton, M. (1995). In California:'Agrobiodiversity'key to agricultural productivity. *California Agriculture*, *49*(6), 45-49.

Rahman, M. M., Porter, L. D., Ma, Y., Coyne, C. J., Zheng, P., Chaves-Cordoba, B., & Naidu, R. A. (2023). Resistance in pea (*Pisum sativum*) genetic resources to the pea aphid, *Acyrthosiphon pisum*. *Entomologia Experimentalis et Applicata*, *171*(6), 435-448.

Rameau, C., Bodelin, C., Cadier, D., Grandjean, O., Miard, F., & Murfet, I. C. (1997). New *ramosus* mutants at loci *Rms1*, *Rms3* and *Rms4* resulting from the mutation breeding program at Versailles. *Pisum Genetics, 29*, 7–12.

Rao, N. K. (2004). Plant genetic resources: Advancing conservation and use through biotechnology. *African Journal of Biotechnology*, *3*(2), 136-145.

Ravelombola, W., Shi, A., & Huynh, B. L. (2021). Loci discovery, network-guided approach, and genomic prediction for drought tolerance index in a multi-parent advanced generation intercross (MAGIC) cowpea population. *Horticulture Research*, *8*.

Reckling, M., Bergkvist, G., Watson, C. A., Stoddard, F. L., Zander, P. M., Walker, R. L., ... & Bachinger, J. (2016). Trade-offs between economic and environmental impacts of introducing legumes into cropping systems. *Frontiers in Plant Science*, *7*, 669.

Rehman, A. U., Malhotra, R. S., Bett, K., Tar'An, B., Bueckert, R., & Warkentin, T. D. (2011). Mapping QTL associated with traits affecting grain yield in chickpea (*Cicer arietinum* L.) under terminal drought stress. *Crop Science*, *51*(2), 450-463.

Rehman, H. M., Cooper, J. W., Lam, H. M., & Yang, S. H. (2019). Legume biofortification is an underexploited strategy for combatting hidden hunger. *Plant, Cell & Environment*, *42*(1), 52-70.

Rispail, N., & Rubiales, D. (2016). Genome-wide identification and comparison of legume *MLO* gene family. *Scientific reports*, *6*(1), 32673.

Román, B., Torres, A. M., Rubiales, D., Cubero, J. I., & Satovic, Z. (2002). Mapping of quantitative trait loci controlling broomrape (*Orobanche crenata* Forsk.) resistance in faba bean (*Vicia faba* L.). *Genome*, *45*(6), 1057-1063.

Rubiales, D., Fondevilla, S., & Fernández-Aparicio, M. (2020). Development of pea breeding lines with resistance to *Orobanche crenata* derived from pea landraces and wild *Pisum* spp. *Agronomy*, *11*(1), 36.

Rubiales, D., Annicchiarico, P., Vaz Patto, M. C., & Julier, B. (2021). Legume breeding for the agroecological transition of global agri-food systems: A European perspective. *Frontiers in Plant Science*, *12*, 782574.

Sab, S., Lokesha, R., Mannur, D. M., Somasekhar, Jadhav, K., Mallikarjuna, B. P., ... & Thudi, M. (2020). Genome-wide SNP discovery and mapping QTLs for seed iron and zinc concentrations in chickpea (*Cicer arietinum* L.). *Frontiers in Nutrition*, *7*, 559120.

Samineni, S., Mahendrakar, M. D., Hotti, A., Chand, U., Rathore, A., & Gaur, P. M. (2022). Impact of heat and drought stresses on grain nutrient content in chickpea: Genome-wide marker-trait associations for protein, Fe and Zn. *Environmental and Experimental Botany*, *194*, 104688.

Sandhi, R. K., & Reddy, G. V. (2020). Biology, ecology, and management strategies for pea aphid (Hemiptera: Aphididae) in pulse crops. *Journal of Integrated Pest Management*, *11*(1), 18.

Sari, H., Uhdre, R., Wallace, L., Coyne, C. J., Bourland, B., Zhang, Z., ... & Warburton, M. L. (2024). Genome-wide association study in Chickpea (*Cicer arietinum* L.) for yield and nutritional components. *Euphytica*, *220*(6), 84.

Schwartz, K. R., Parsons, E. C. M., Rockwood, L., & Wood, T. C. (2017). Integrating *in-situ* and *ex-situ* data management processes for biodiversity conservation. *Frontiers in Ecology and Evolution*, *5*, 120.

Serrano, C., Carbas, B., Castanho, A., Soares, A., Patto, M. C. V., & Brites, C. (2017). Characterisation of nutritional quality traits of a chickpea (*Cicer arietinum*) germplasm collection exploited in chickpea breeding in Europe. *Crop and Pasture Science*, *68*(11), 1031-1040.

Shaheen, F. A., Khaliq, A., & Aslam, M. (2006). Resistance of chickpea (*Cicer arietinum* L.) cultivars against pulse beetle. *Pakistan Journal of Botany*, *38*(4), 1237.

Sharma, M., Ghosh, R., Tarafdar, A., Rathore, A., Chobe, D. R., Kumar, A. V., ... & Harer, P. N. (2019). Exploring the genetic cipher of chickpea (*Cicer arietinum* L.) through identification and multi-environment validation of resistant sources against Fusarium wilt (*Fusarium oxysporum* f. sp. *ciceris*). *Frontiers in Sustainable Food Systems*, *3*, 78.

Shubha, K., Dhar, S., Choudhary, H., Dubey, S. C., & Sharma, R. K. (2016). Identification of resistant sources and inheritance of *Fusarium* wilt resistance in garden pea (*Pisum sativum* ssp. *hortense*). *Indian Journal of Horticulture*, *73*(3), 356-361.

Singh, A., Dikshit, H. K., Mishra, G. P., Aski, M., & Kumar, S. (2019). Association mapping for grain diameter and weight in lentil using SSR markers. *Plant Gene*, *20*, 100204.

Singh, B.D., Singh, A.K. (2015). Mapping of Quantitative Trait Loci. In: Marker-Assisted Plant Breeding: Principles and Practices. Springer, New Delhi

Singh, B., Singh, J. P., Kaur, A., & Singh, N. (2017a). Phenolic composition and antioxidant potential of grain legume seeds: A review. *Food Research International*, *101*, 1-16.

Singh, D., Singh, C. K., Singh Tomar, R. S., & Pal, M. (2017b). Genetics and molecular mapping of heat tolerance for seedling survival and pod set in lentil. *Crop Science*, *57*(6), 3059-3067.

Singh, D., Singh, C. K., Tomar, R. S. S., Sharma, S., Karwa, S., Pal, M., ... & Sharma, P. C. (2020). Genetics and molecular mapping for salinity stress tolerance at seedling stage in lentil (*Lens culinaris* Medik). *Crop Science*, *60*(3), 1254-1266.

Sisou, D., Tadmor, Y., Plakhine, D., Ziadna, H., Hübner, S., & Eizenberg, H. (2021). Biological and transcriptomic characterization of pre-haustorial resistance to sunflower broomrape (*Orobanche cumana* W.) in sunflowers (*Helianthus annuus*). *Plants*, *10*(9), 1810.

Smale, M., & Jamora, N. (2020). Valuing genebanks. *Food Security*, *12*(5), 905-918.

Smýkal, P., Coyne, C. J., Ambrose, M. J., Maxted, N., Schaefer, H., Blair, M. W., ... & Varshney, R. K. (2015). Legume crops phylogeny and genetic diversity for science and breeding. *Critical Reviews in Plant Sciences*, *34*(1-3), 43-104.

Stagnari, F., Maggio, A., Galieni, A., & Pisante, M. (2017). Multiple benefits of legumes for agriculture sustainability: an overview. *Chemical and Biological Technologies in Agriculture*, *4*, 1-13.

St Luce, M., Grant, C. A., Zebarth, B. J., Ziadi, N., O'Donovan, J. T., Blackshaw, R. E., ... & Smith, E. G. (2015). Legumes can reduce economic optimum nitrogen rates and increase yields in a wheat–canola cropping sequence in western Canada. *Field Crops Research*, *179*, 12-25.

Sulima, A. S., & Zhukov, V. A. (2022). War and Peas: Molecular bases of resistance to powdery mildew in pea (*Pisum sativum* L.) and other legumes. *Plants*, *11*(3), 339.

Sultani, M. I., Gill, M. A., Anwar, M. M., & Athar, M. (2007). Evaluation of soil physical properties as influenced by various green manuring legumes and phosphorus fertilization under rain fed conditions. *International Journal of environmental Science & Technology*, *4*, 109-118.

Tafesse, E. G., Gali, K. K., Lachagari, V. R., Bueckert, R., & Warkentin, T. D. (2020). Genome-wide association mapping for heat stress responsive traits in field pea. *International Journal of Molecular Sciences*, *21*(6), 2043.

Tafesse, E. G., Gali, K. K., Lachagari, V. R., Bueckert, R., & Warkentin, T. D. (2021). Genome-wide association mapping for heat and drought adaptive traits in pea. *Genes*, *12*(12), 1897.

Tanksley, S. D. (1993). Mapping polygenes. *Annual Review of Genetics*, *27*(1), 205-233.

Tar'an, B., Warkentin, T., Somers, D. J., Miranda, D., Vandenberg, A., Blade, S., & Bing, D. (2004). Identification of quantitative trait loci for grain yield, seed protein concentration and maturity in field pea (*Pisum sativum* L.). *Euphytica*, *136*, 297-306.

Tayeh, N., Aubert, G., Pilet-Nayel, M. L., Lejeune-Hénaut, I., Warkentin, T. D., & Burstin, J. (2015). Genomic tools in pea breeding programs: status and perspectives. *Frontiers in Plant Science*, *6*, 1037.

Tayeh, N., Hofer, J. M., Aubert, G., Jacquin, F., Turner, L., Kreplak, J., ... & Burstin, J. (2024). *afila*, the origin and nature of a major innovation in the history of pea breeding. *New Phytologist*, *243*(3), 1247-1261.

Trabanco, N., Campa, A., & Ferreira, J. J. (2015). Identification of a new chromosomal region involved in the genetic control of resistance to anthracnose in common bean. *The Plant Genome*, *8*(2), plantgenome2014-10.

Uhdre, R., Coyne, C. J., Bourland, B., Piaskowski, J., Zheng, P., Ganjyal, G. M., ... & Warburton, M. L. (2025). Association study of crude seed protein and fat concentration in a USDA pea diversity panel. *The Plant Genome*, *18*(1), e20485.

Ujinwal, M., Singh, N., Langyan, S., & Singh, N. K. (2025). Genetic dissection of total protein content, phenolic content and seed quality traits in pigeonpea (*Cajanus cajan*) using 62K pigeonpea genic SNP chip. *Molecular Genetics and Genomics*, *300*(1), 1-18.

Ullah, A., & Farooq, M. (2022). The challenge of drought stress for grain legumes and options for improvement. *Archives of Agronomy and Soil Science*, *68*(11), 1601-1618.

United Nations, Department of Economic and Social Affairs. (2013). World population prospects: the 2012 revision, key findings and advance tables. Working Paper No. ESA/P/WP.227. New York: United Nations.

Upadhyaya, H. D., Bajaj, D., Narnoliya, L., Das, S., Kumar, V., Gowda, C. L. L., ... & Parida, S. K. (2016). Genome-wide scans for delineation of candidate genes regulating seed-protein content in chickpea. *Frontiers in Plant Science*, *7*, 302.

Vadez, V., Krishnamurthy, L., Thudi, M., Anuradha, C., Colmer, T. D., Turner, N. C., ... & Varshney, R. K. (2012). Assessment of ICCV 2× JG 62 chickpea progenies shows sensitivity of reproduction to salt stress and reveals QTL for seed yield and yield components. *Molecular Breeding*, *30*, 9-21.

Valderrama, M. R., Román, B., Satovic, Z., Rubiales, D., Cubero, J. I., & Torres, A. M. (2004). Locating quantitative trait loci associated with *Orobanche crenata* resistance in pea. *Weed Research*, *44*(4), 323-328.

van Loon, M. P., Alimagham, S., Pronk, A., Fodor, N., Ion, V., Kryvoshein, O., ... & van Ittersum, M. K. (2023). Grain legume production in Europe for food, feed and meat-substitution. *Global Food Security*, *39*, 100723.

Vaz Patto, M. C., Amarowicz, R., Aryee, A. N., Boye, J. I., Chung, H. J., Martin-Cabrejas, M. A., & Domoney, C. (2015). Achievements and challenges in improving the nutritional quality of food legumes. *Critical Reviews in Plant Sciences*, *34*(1-3), 105-143.

Verma, P., Goyal, R., Chahota, R. K., Sharma, T. R., Abdin, M. Z., & Bhatia, S. (2015). Construction of a genetic linkage map and identification of QTLs for seed weight and seed size traits in lentil (*Lens culinaris* Medik.). *Plos One*, *10*(10), e0139666.

Volk, G. M., Byrne, P. F., Coyne, C. J., Flint-Garcia, S., Reeves, P. A., & Richards, C. (2021). Integrating genomic and phenomic approaches to support plant genetic resources conservation and use. *Plants*, *10*(11), 2260.

Wang, J. Y., Chen, G. T. E., Braguy, J., & Al-Babili, S. (2024). Distinguishing the functions of canonical strigolactones as rhizospheric signals. *Trends in Plant Science*, *29*(8), 925 – 936.

Wang, R., Gangola, M. P., Irvine, C., Gaur, P. M., Båga, M., & Chibbar, R. N. (2019). Co-localization of genomic regions associated with seed morphology and composition in a desi chickpea (*Cicer arietinum* L.) population varying in seed protein concentration. *Theoretical and Applied Genetics*, *132*, 1263-1281.

Warkentin, T. D., Delgerjav, O., Arganosa, G., Rehman, A. U., Bett, K. E., Anbessa, Y., ... & Raboy, V. (2012). Development and characterization of low-phytate pea. *Crop Science*, *52*(1), 74-78.

Wohor, O. Z., Rispail, N., Ojiewo, C. O., & Rubiales, D. (2022). Pea breeding for resistance to rhizospheric pathogens. *Plants*, *11*(19), 2664.

Xia, Z., Song, Q., Harada, K., Chen, J., & Zhou, C. (2023). Genetic characterization of yield-and quality-related traits in legumes. *Frontiers in Plant Science*, *14*, 1281138.

Xie, X., Yoneyama, K., Harada, Y., Fusegi, N., Yamada, Y., Ito, S., ... & Yoneyama, K. (2009). Fabacyl acetate, a germination stimulant for root parasitic plants from *Pisum sativum*. *Phytochemistry*, *70*(2), 211-215.

Xu, Y., Li, P., Yang, Z., & Xu, C. (2017). Genetic mapping of quantitative trait loci in crops. *The Crop Journal*, *5*(2), 175-184.

Yan, J., Chen, J., Lin, Y., Yuan, X., Somta, P., Zhang, Y., ... & Chen, X. (2023). Mapping of quantitative trait locus reveals *PsXI* gene encoding xylanase inhibitor as the candidate gene for bruchid (*Callosobruchus* spp.) resistance in pea (*Pisum sativum* L.). *Frontiers in Plant Science*, *14*, 1057577.

Zabel, F., Delzeit, R., Schneider, J. M., Seppelt, R., Mauser, W., & Václavík, T. (2019). Global impacts of future cropland expansion and intensification on agricultural markets and biodiversity. *Nature Communications*, *10*(1), 2844.

Zegeye, H. (2017). *In situ* and *ex situ* conservation: complementary approaches for maintaining biodiversity. *International Journal of Research in Environmental Studies*, *4*(1), 1-12.

Zeng, Z.B. (2001). QTL Mapping. In *Brenner's Encyclopedia of Genetics* (pp. 8–12), 2nd ed.; Maloy, S., Hughes, K., Eds.; Academic Press: San Diego, MA, USA.

Zhang, H., Mascher, M., Abbo, S., & Jayakodi, M. (2022). Advancing grain legumes domestication and evolution studies with genomics. *Plant and Cell Physiology*, *63*(11), 1540-1553.

Zhang, X., Zhang, Z., Shen, A., Zhang, T., Jiang, L., El-Seedi, H., ... & Sui, X. (2024). Legumes as an alternative protein source in plant-based foods: Applications, challenges, and strategies. *Current Research in Food Science*, 100876.

Zhao, N., Xue, D., Miao, Y., Wang, Y., Zhou, E., Zhou, Y., ... & Wang, X. (2023). Construction of a high-density genetic map for faba bean (*Vicia faba* L.) and quantitative trait loci mapping of seed-related traits. *Frontiers in Plant Science*, *14*, 1201103.

Zou, W., & Zeng, Z. B. (2008). Statistical methods for mapping multiple QTL. *International Journal of Plant Genomics*, *2008*(1), 286561.

Zuiderveen, G. H., Padder, B. A., Kamfwa, K., Song, Q., & Kelly, J. D. (2016). Genome-wide association study of anthracnose resistance in Andean beans (*Phaseolus vulgaris*). *Plos One*, *11*(6), e0156391.

Chapter 2

High-density linkage mapping and genetic dissection of resistance to broomrape (*Orobanche crenata* Forsk.) in pea (*Pisum sativum* L.)

High-density linkage mapping and genetic dissection of resistance to broomrape (*Orobanche crenata* Forsk.) in pea (*Pisum sativum* L.)

Chiara Delvento[1], **Francesco Arcieri[1]**, Angelo Raffaele Marcotrigiano[1], Marzia Guerriero[1], Valentina Fanelli[1], Maria Dellino[1], Pasquale Luca Curci[2], Harro Bouwmeester[3], Concetta Lotti[4], Luigi Ricciardi[1], Stefano Pavan[1*]

[1]Department of Soil, Plant and Food Sciences, Section of Plant Genetics and Breeding, University of Bari Aldo Moro, Bari, Italy.

[2]Institute of Biosciences and Bioresources, National Research Council (CNR), Bari, Italy.

[3]Plant Hormone Biology group, Swammerdam Institute for Life Sciences, University of Amsterdam, Amsterdam, The Netherlands.

[4]Department of Agricultural, Food and Environmental Sciences, University of Foggia, Foggia, Italy.

[*]Authors to whom correspondence should be addressed

Published in Frontiers in Plant Science 2023, 14:1216297. Doi: 10.3389/fpls.2023.1216297

ABSTRACT

Pea (*Pisum sativum* L.) is a widely cultivated legume of major importance for global food security and agricultural sustainability. Crenate broomrape (*Orobanche crenata* Forsk.) (*Oc*) is a parasitic weed severely affecting legumes, including pea, in the Mediterranean Basin and the Middle East. Previously, the identification of the pea line 'ROR12', displaying resistance to *Oc*, was reported. Two-year field trials on a segregant population of 148 F_7 recombinant inbred lines (RILs), originating from a cross between 'ROR12' and the susceptible cultivar 'Sprinter', revealed high heritability (0.84) of the 'ROR12' resistance source. Genotyping-by-sequencing (GBS) on the same RIL population allowed the construction of a high-density pea linkage map, which was compared with the pea reference genome and used for quantitative trait loci (QTL) mapping.

Three QTLs associated with the response to Oc infection, named *PsOcr-1*, *PsOcr-2* and *PsOcr-3,* were identified, with *PsOcr-1* explaining 69.3% of the genotypic variance. Evaluation of the effects of different genotypic combinations indicated additivity between *PsOcr-1* and *PsOcr-2*, and between *PsOcr-1* and *PsOcr-3,* and epistasis between *PsOcr-2* and *PsOcr-3*. Finally, three Kompetitive Allele Specific PCR (KASP) marker assays were designed on the single nucleotide polymorphisms (SNPs) associated with the QTL significance peaks.

Besides contributing to the development of pea genomic resources, this work lays the foundation for the obtainment of pea cultivars resistant to *Oc* and the identification of genes involved in resistance to parasitic Orobanchaceae.

Keywords: Pea, broomrape, resistance, mapping, breeding

INTRODUCTION

Pea (*Pisum sativum* L.) is the second most widely cultivated cool season legume in the world, yielding 12.4 Mt of dry seeds and 20.5 Mt of green productions in 2021 (FAOSTAT data, 2021). In Europe there is a positive trend towards the rise of pea cultivation, mostly related to the increased awareness of consumers on the beneficial effects of legumes on human health, the implementation of political incentives in favor of sustainable farming systems, and the growing demand for non-transgenic alternatives to soybean (Daryanto et al., 2015; Centrone et al., 2020; Costantini et al., 2021; Pavan et al., 2022).

Crenate broomrape (*Orobanche crenata* Forsk.) (*Oc*) is an obligate root parasite, which occurs widespread in the Mediterranean area and the Middle East and may cause up to complete yield loss on several cultivated legumes, including pea (Pavan et al., 2016; Negewo et al., 2022). The life cycle of *Oc* includes the stages of seed germination, attachment to the host roots, establishment of vascular connections, development of underground tubercles, emergence of floral shoots and dispersal of seeds, which may remain viable in the soil for several decades (Xie et al., 2010; Fernández-Aparicio et al., 2016b).

Breeding for resistance proved to be a valuable strategy to cope with *Oc* and other parasitic weeds belonging to the botanic family of Orobanchaceae (Jamil et al., 2011; Fernández-Aparicio et al., 2014; Jamil et al., 2021; Li et al., 2023a), whereas agronomic and chemical control methods displayed limited efficacy (Fernández-Aparicio et al., 2016a). However, no *Oc* resistant pea cultivar is commercially available (Rubiales 2014; Wohor et al., 2022), thus pea cultivation has been abandoned in several areas with a large *Oc* seed bank (Renna et al., 2015).

We previously reported the selection, from an Italian garden pea landrace, of the breeding line 'ROR12', displaying resistance to *Oc* (Pavan et al., 2016). Characterization of root extracts and exudates indicated that 'ROR12' resistance might be due, at least partially, to reduced biosynthesis of strigolactones, a class of carotenoid-derived compounds acting in the rhizosphere as germination stimulants for Orobanchaceae (Yoneyama et al., 2010; Pavan et al., 2016; Bouwmeester et al., 2021). The response to *Oc* infection, assessed as the number of parasitic shoots emerged aboveground at crop maturity, significantly deviated from normality in an F_2 population generated from a cross between 'ROR12' and the susceptible cultivar 'Sprinter', suggesting the occurrence of one or a few loci having a major effect on the phenotype (Bardaro et al., 2016). In addition, testing a few polymorphic marker loci on resistant and susceptible F_2 bulks revealed a significant association between response to *Oc* infection and a genomic region on the pea chromosome 5LG3 (Bardaro et al., 2016).

The wild pea accession ‘P665’ was previously reported as partially resistant to *Oc* (Fondevilla et al., 2010). QTL mapping based on a segregant recombinant inbred line (RIL) population originating from ‘P665’ and the susceptible cultivar ‘Messire’ identified four QTLs associated with the number of parasitic shoots emerged per host plant (n°br03_1, n°br03_2, n°br03_3 and n°br04), located on the pea chromosomes 2LG1, 5LG3, 3LG5 and 1LG6, respectively (Fondevilla et al., 2010).

Genotyping-by-sequencing (GBS) is a reduced representation library sequencing strategy allowing the cost-effective identification of thousands of single nucleotide polymorphisms (SNPs) (Elshire et al., 2011; Pavan et al., 2020). GBS was successfully used in pea to generate high-density linkage maps, in which loci associated with economically important traits were positioned (Ma et al., 2017a; Barilli et al., 2018; Guindon et al., 2019). In addition, dense linkage maps can be compared to reference genome assemblies to provide genomic context to unanchored contigs and scaffolds, resolving allelism and identifying mis-joins (Fierst, 2015; Walve et al., 2019). Currently, the genome assemblies of the cultivars ‘Cameor’ and ‘ZW6’ are available for the scientific community working on pea (Kreplak et al., 2019; Yang et al., 2022).

Here, we describe the use of GBS for the construction of a high-density linkage map in pea, which was compared with the pea reference genome. SNP data and two-year phenotypic observations collected on the ‘ROR12’ x ‘Sprinter’ RIL segregant population were used to identify and annotate genomic loci associated with *Oc* resistance. Finally, marker assays were designed and validated to assist selection in breeding programs.

MATERIALS AND METHODS

Plant material

The breeding line ‘ROR12’ and the cultivar ‘Sprinter’ were used in this study, together with a population of 148 F_7 RILs obtained from their F_2 progeny by single seed descent. ‘ROR12’ was obtained from a local garden pea landrace by pure line selection (Pavan et al., 2016). Low strigolactone levels occurring in ‘ROR12’ result in a slightly branched phenotype, which, however, does not cause a major penalty effect on the agronomic performance (Pavan et al., 2016). ‘Sprinter’ is an old garden pea commercial cultivar previously shown to be highly susceptible to *Oc* (Bardaro et al., 2016; Pavan et al., 2016).

Phenotyping

Two field trials (sowing dates October 3, 2020, and January 8, 2021) were carried out at the experimental farm ‘P. Martucci’ of the University of Bari (41°01′22.1″N 16°54′21.0″E) in a silty-clayey experimental field continuously cultivated with legumes, known to be highly infested by *Oc*. RILs were arranged according to a randomized block design with three blocks and one replication

per block, with each replicate consisting of ten plants distant 0.15 m in a single row. The blocks were placed orthogonally to a gradient of *Oc* infestation observed in the previous two years. To check for the homogeneity of the *Oc* seedbank distribution within blocks, five replicates of the parental cultivar 'Sprinter' were randomly allocated in each block as positive control. No fertilization and irrigation were applied during the growing season. Pest and pathogen management was performed using single applications of deltamethrin and difenoconazole, whereas weed control was performed with pendimethalin in pre-emergence and manual weeding in post-emergence. Genotypic response to *Oc* infection was evaluated at crop maturity on May 25, 2020, and May 31, 2021, as the average number of parasitic shoots emerged aboveground per plant.

DNA extraction, GBS assay and quality control

Leaf tissue samples were collected from three individuals of the parental lines and one individual of each RIL. DNA was isolated using the DNeasy Plant Mini Kit (Qiagen) according to the manufacturer's protocol and checked for quality and concentration using agarose gel (0.8%) electrophoresis and the Qubit 3.0 fluorometer (Life Technologies). A multiplexed *Ape*KI-GBS library was prepared as described by Elshire et al. (2011) and sequenced by a paired-end approach using the Illumina Novoseq 6000 sequencing system (Elshire Group Ltd.). After demultiplexing with the Axe algorithm (Murray et al., 2018), reads were trimmed for adapter and reverse-barcode sequences using the batch_trim.pl script from github (https://github.com/Lanilen/GBS-PreProcess). Alignment to the *Pisum sativum* v1.0 reference genome (Kreplak et al., 2019) was performed using bowtie2 (Langmead et al., 2012). After pooling together alignments of the biological replicates of the parental lines, the Stacks pipeline (Catchen et al., 2013) with the biparental filtering mode was used for SNP calling. Further filtering was performed in TASSEL 5.2.31 (Bradbury et al., 2007) by selecting SNP loci showing polymorphism between the parental lines and associated with call rate >90%, minor allele frequency (MAF) >0.25 and heterozygous calls <5%, and maintaining individuals displaying heterozygosity <10%.

Linkage map construction and evaluation

The *mstmap* function of the ASMap R package (Taylor et al., 2017), implementing the Minimum Spanning Tree algorithm described by Wu et al. (2008), was used for linkage map construction. Default arguments within the function were applied, except for choosing the p-value threshold of 10^{-11} for clustering marker loci in linkage groups. Marker loci associated with double cross-over events or displaying skewed segregation ($P<0.05$ after the Bonferroni correction) were removed from analysis using the *drop.markers* function of ASMap. The performance of the *mstmap* function was checked by plotting the heat map of pairwise recombination fractions (RFs) between markers and

their pairwise logarithm of odd (LOD) score of linkage. Graphical representation of the linkage map was obtained using the *iplotMap* function of the qtlcharts R package (Broman, 2015). The relation between the linkage map and the pea reference genome was investigated by plotting genetic vs. physical positions for each chromosome, using the ggplot2 R package (Wickham, 2016).

Estimation of heritability and QTL analysis

Broad sense heritability (H^2_B) was estimated according to Schmidt et al. (2019), using the formula:

$$H_B^2 = \frac{\sigma_G^2}{(\sigma_G^2 + \frac{\sigma_{GY}^2}{n_Y} + \frac{\sigma_\varepsilon^2}{n_Y \times n_r})}$$

in which σ^2_G is the genotypic variance, σ^2_{GY} is the genotype-by-year variance, σ^2_ε is the error variance, n_y is the number of years, and n_r is the number of replicates within each year. Restricted maximum likelihood (REML) estimates of variance components were obtained by fitting a random effect model with the *lmer* function of the lme4 R package (Bates et al., 2015), in which: genotype, genotype-by-year, year, and replicates within years were set as random effects; the square root of phenotypic data was set as the dependent variable, with this transformation being necessary to correct for the right-skewness of the distribution. The model assumption of normality was assessed using the *qqnorm* function of the Stats R package (R Core Team 2013). The *ranova* function of the lmerTest R package (Kutnesova et al., 2017) was used to test the significance of the random effect terms of the model.

Mapping of quantitative trait loci (QTLs) was performed using linkage map data and best linear unbiased predictors (BLUPs) of RIL genotypic effects, which are widely used as alternative to phenotypic means to estimate genotypic values in QTL mapping studies (Ben Sadok et al., 2013; Allard et al., 2016; Molenaar et al., 2018; Wang et al., 2023). BLUPs were extracted by applying the *ranef* function of lme4 to the random effect model above described for H^2_B estimation. The *cim* function of the Rqtl R package (Broman et al., 2003) was used to search for marker-trait associations by composite interval mapping (CIM). Arguments within the function were set to perform the Haley-Knott regression method and identify a LOD score QTL significance threshold based on a permutation test with 1,000 iterations. The *plot* function of the Stats R package (R Core Team 2013) was applied on the output of the *cim* function to obtain graphs for chromosomal LOD scores. The percentage of the variance of RIL genotypic effects on the phenotype (PGE) explained by markers at QTL peaks was calculated with the formula:

$$\mathrm{PGE} = 100 \times (1 - 10^{\left(-2 \times \frac{LOD}{n}\right)})$$

Confidence intervals were identified using the *lodint* function of Rqtl, based on two LOD score units drop from the QTL peak. Genes included in the QTL confidence intervals were extracted from the pea reference genome annotation general feature format (gff) file, which was downloaded from the Unité de Recherche Génomique Info (URGI) bioinformatics platform (https://urgi.versailles.inra.fr/). The BLAST tools implemented by the same platform were used: a) to search, in QTL confidence intervals, for homologs of the strigolactone biosynthetic genes reviewed by Mashiguchi et al. (2021); b) physical mapping of the simple sequence repeat (SSR) marker AD174 (Loridon et al., 2005), previously associated with 'ROR12' resistance (Bardaro et al., 2016); c) physical mapping of the carbonic anhydrase gene *Psat1g058960* that, according to the map of Carrillo et al. (2014), is closely linked to the RAPD marker OPAA19_702, in turn linked to the *Oc* resistance QTL N°br04 by Fondevilla et al. (2010). Search for defense response genes enrichment in QTL confidence intervals was performed by the gprofiler2 R package (Kolberg et al., 2020), using p=0.05 as significance threshold and the Benjamini-Hochberg false discovery rate correction for multiple tests.

The effect of the different QTL combinations on the phenotype was investigated using the *effectplot* function of the Rqtl R package, which returned BLUP means and standard errors relative to different genotypic combinations at QTL pairs. Data were used to produce a custom plot using the ggplot2 R package (Wickham, 2016).

KASP marker development

Kompetitive Allele Specific PCR (KASP) assays were performed using two allele-specific forward primers, marked with the FAM and HEX fluorescence dyes, and a common reverse primer (Table 1). PCR reactions were performed at LGC genomics (Shanghai, China) according to standard protocols. Output fluorescence data were used to produce scatter plots, using the ggplot2 R package (Wickham, 2016).

Table 1 Details of the KASP assays designed on the QTLs *PsOcr*-1, *PsOcr*-2 *and PsOcr*-3 identified in this study

QTL	Target SNP	Allele specific primer 1	Allele specific primer 2	Common primer
PsOcr-1	C/G	GCAGGTTTTCTA CTTCGATGACG	GCAGGTTTTCTAC TTCGATGACC	GTCAATCCTTTTTGACC CTTGGACTAATT
PsOcr-2	T/C	TCATCCAAGTGG CTCCCTTTCATT	CATCCAAGTGGCT CCCTTTCATC	TGAAAGTGAATAGTGC AGATCCTTTGAATT
PsOcr-3	G/T	TCTACGATCAAA TGCCGGATACC	GTTCTACGATCAA ATGCCGGATACA	ATGCTGCAGCTCCCAA ACTTCTCAT

RESULTS

Phenotypic variation and heritability of *Oc* resistance

Two-year trials were carried out in an experimental field known to be severely infested by *Oc*, aiming to evaluate the response of a segregant population of 148 F_7 RILs originating from a cross between 'ROR12' and 'Sprinter'. Scoring of the average number of parasitic shoots emerged aboveground per host plant indicated a fairly good uniformity of infestation within blocks, as relatively low dispersion around the mean was observed for five 'Sprinter' replicates randomly allocated in each block (mean±SD were 5.65±0.35, 2.9±0.14 and 2.95±0.21 for the three blocks arranged in 2020, and 1.53±0.12, 2.7±0.46 and 3.4±0.46 for the three blocks arranged in 2021).

The average number of parasitic shoots emerged aboveground per host plant ranged, for RILs, from 0 to 6.03 in 2020, and from 0 to 3.07 in 2021. In addition, in both years this variable exhibited a distribution clearly deviating from normality, indicating the occurrence of one or a few major loci involved in resistance (Figure 1). 'ROR12' displayed very high resistance levels, with an average number of *Oc* shoots emerged per host plant of 0.13 and 0.06 in 2020 and 2021, respectively, suggesting the absence of transgressive segregation (Figure 1). The estimated broad sense heritability (H^2_B) was 0.84, indicating a minor effect of environmental factors on phenotypic variation.

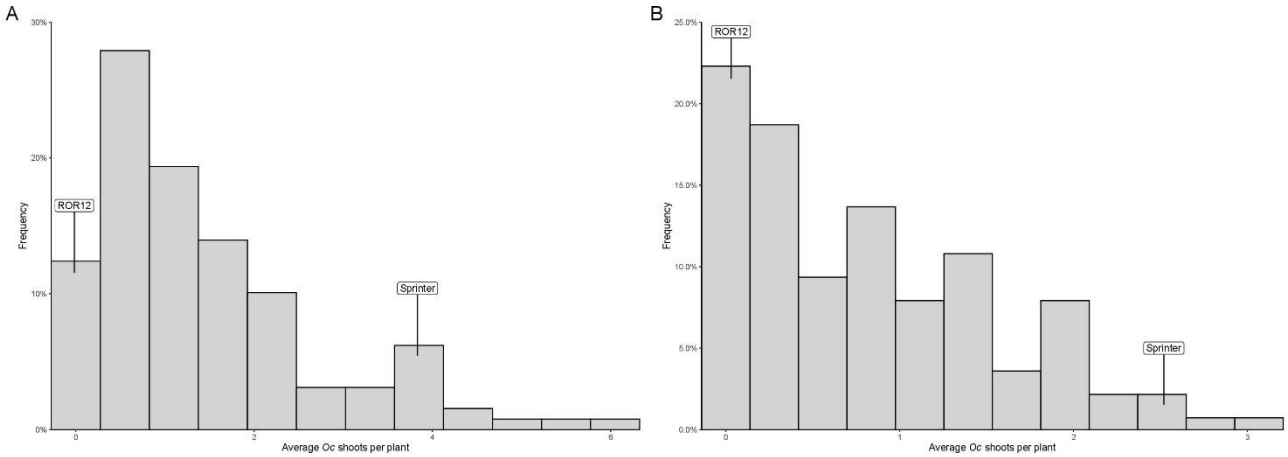

Figure 1. Frequency distribution of the average number of *Orobanche crenata* Forsk. (*Oc*) shoots emerged aboveground per host plant recorded for the parental lines 'Sprinter' and 'ROR12' and their RIL F7 population in 2020 **(A)** and 2021 **(B)**.

Construction of and evaluation of a GBS-based SNP linkage map

Sequencing of an *ApeK*I-GBS library obtained from the DNA of the parental genotypes and the RIL population resulted in about 2.2 million reads/sample. About 33% of the reads were successfully mapped onto the pea reference genome (Kreplak et al., 2019). After the SNP call and quality control procedures, 6,182 polymorphic loci were identified. Further filtering to eliminate potentially spurious SNP calls, associated with loci displaying skewed segregation or associated with double cross-over, resulted in a final panel of 4,489 markers. Of these, 4,127 were located on the seven pea chromosomes, whereas the remaining ones were located on pea superscaffolds and scaffolds. The number of polymorphic loci per chromosome and chromosome length displayed a moderate correlation (R^2=0.55, p=0.03), indicating a quite uniform distribution of variants across the genome.

Linkage analysis resulted in a genetic map containing seven linkage groups (LGs), in accordance with the pea haploid chromosome number (Figure 2A). Genetic length, physical length, and recombination rate associated with each linkage group are presented in Table 2. Good collinearity was found between the position of markers in the genetic map and the one in the pea reference genome (Figure 2B). Most notable exceptions were represented by two regions of the chromosomes 4LG4 and 7LG7 (Figure 2B), and the mapping of 59 markers on a different chromosome than in the reference genome (Supplementary Table S1). In addition, 362 SNP loci positioned on 9 superscaffolds and 125 scaffolds were anchored to the seven linkage groups (Supplementary Table S2).

Table 2. Genetic length, physical length, and recombination rate associated with the linkage groups detected in this study

Linkage Groups	Genetic length (cM)	Physical length (Mb)	Recombination rate (cM/Mb)
1LG6	291.76	371.83	0.78
2LG1	239.19	423.88	0.56
3LG5	306.22	436.66	0.70
4LG4	284.12	418.68	0.64
5LG3	291.33	572.87	0.50
6LG2	316.46	476.61	0.66
7LG7	360.01	490.63	0.73

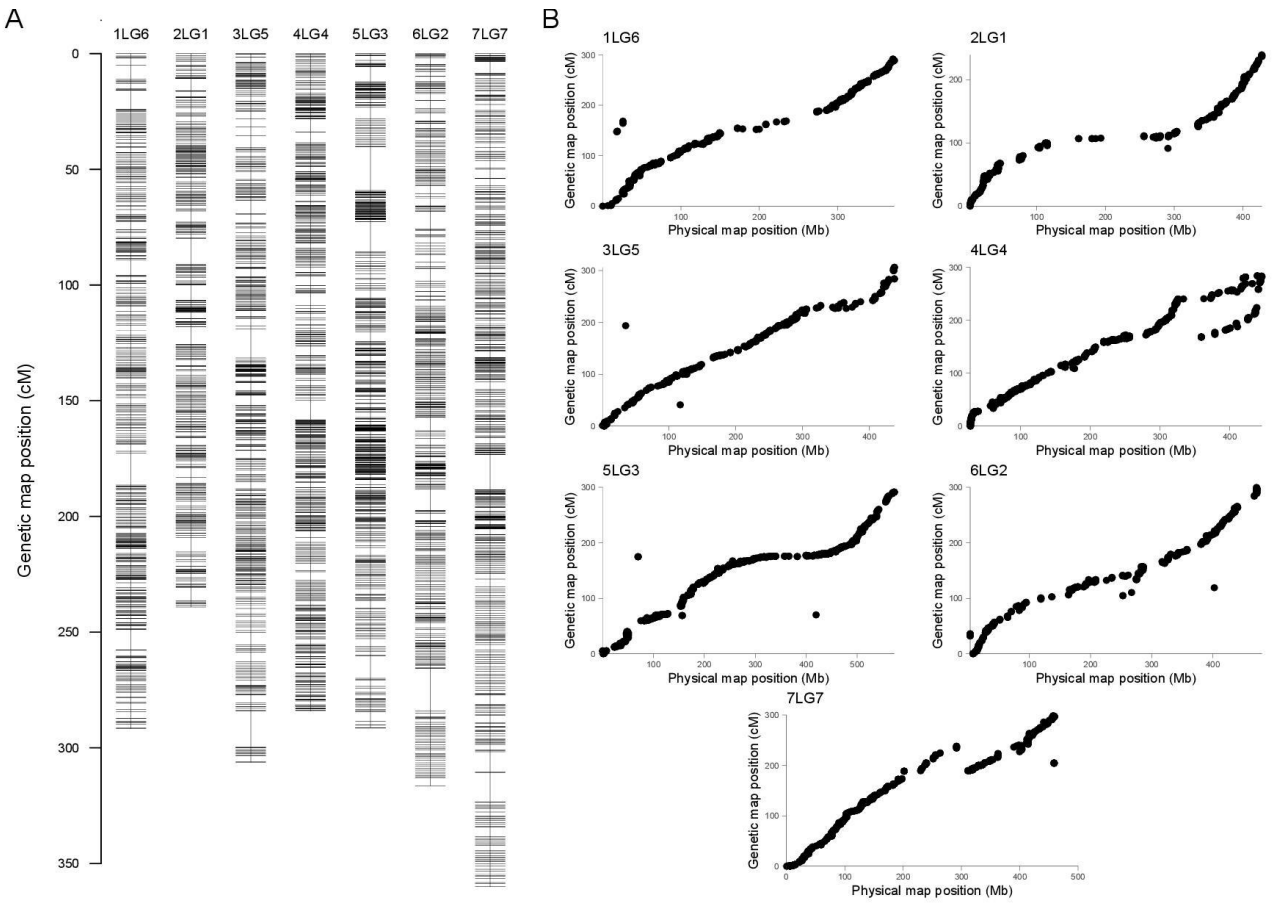

Figure 2. **(A)** Pea genetic map constructed with 4,489 single nucleotide polymorphism (SNP) markers generated by genotyping-by-sequencing (GBS). Each horizontal bar indicates the marker position, expressed in centiMorgan (cM). Each linkage group (LG) has the same name of the corresponding chromosome **(B).** Comparison between the pea genetic and physical maps. For each LG/chromosome, SNPs are represented by dots, whose coordinates on the x and y axes are given by their positions on the genetic map (cM) and the physical map (Mb), respectively.

Identification and annotation of three QTLs associated with response to *Oc* infection

Testing for the effect of variance components indicated a non-significant contribution of the genotype-by-year interaction term (Supplementary Table S3). Therefore, QTL mapping was performed using two-year data, which were combined to obtain BLUPs of RIL genotypic effects on the phenotype (i.e., genotypic values). Three QTLs with LOD score peak above the significance threshold of 4.89 were identified. The QTL on chromosome 4LG4, named *PsOcr-1*, was associated with the highest LOD score peak (36.74), corresponding to 69.3% of the genotypic variance (σ^2_G) (Figure 3). The other two QTLs, located on chromosomes 1LG6 and 5LG3, were named *PsOcr-2* and *PsOcr-3*, respectively. *PsOcr-2* displayed a LOD score peak of 10.73 and explained 29.4% of σ^2_G, whereas *PsOcr-3* displayed a LOD score peak of 4.96 and explained 15% of σ^2_G. The *PsOcr-3* LOD score peak was mapped 14.98 Mb apart from the SSR marker AD174, previously associated with 'ROR12' resistance (Bardaro et al., 2016). The *PsOcr-2* LOD score peak was mapped about 17 Mb apart from the carbonic anhydrase gene *Psat1g058960*. This gene, according to the linkage map reported by Carrillo et al. (2014), is linked to the RAPD marker OPAA19_702, which was in turn linked to the *Oc* resistance QTL N°br04 by Fondevilla et al. (2010).

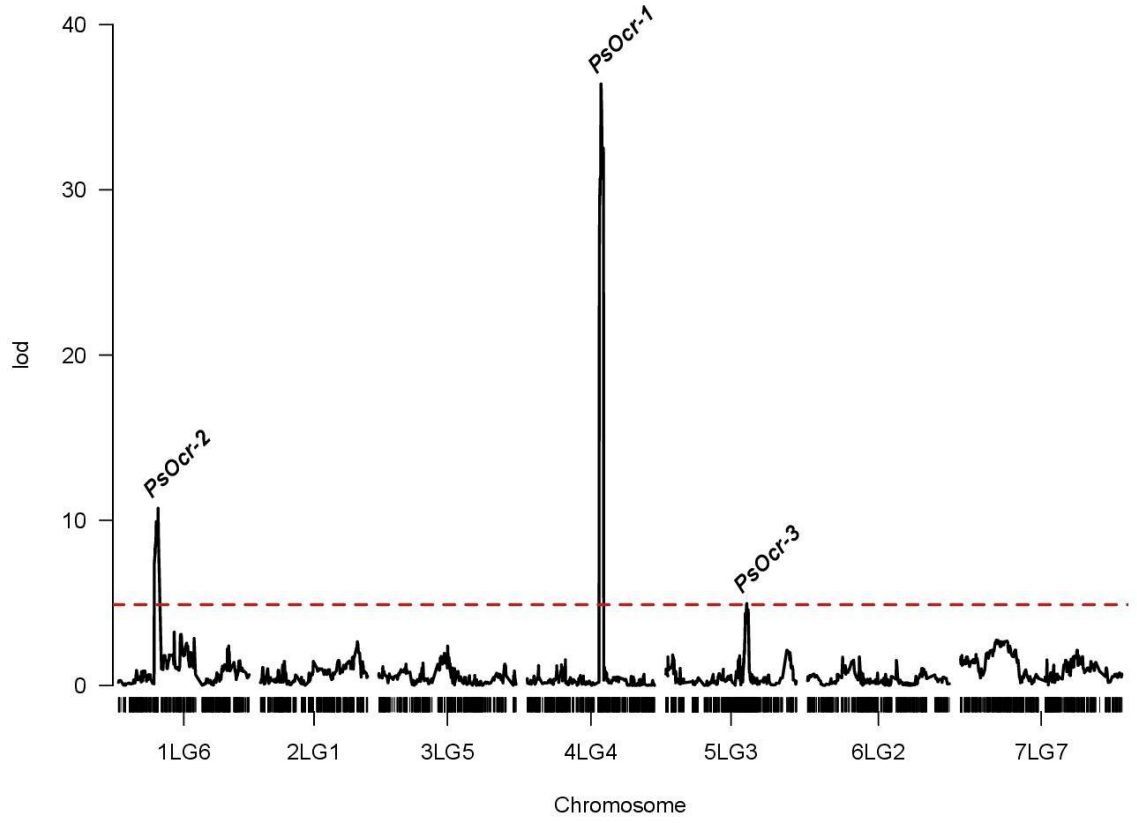

Figure 3. Logarithm of odds (LOD) score curves of quantitative trait loci (QTLs) associated with response to *Orobanche crenata* infection. The dashed red line indicated the significance threshold identified by permutation analysis. The three QTL above the threshold (*PsOcr-1*, *PsOcr-2* and *PsOcr-3*) are indicated in correspondence of their LOD score peaks.

The QTL confidence intervals spanned physical regions of 17.2 Mb for *PsOcr-1*, 7.2 Mb for *PsOcr-2* and 51.2 Mb for *PsOcr-3*, and contained 159, 99 and 617 genes, respectively (Supplementary Table S4). Among these genes, five in *PsOcr-1* and 25 in *PsOcr-3* were annotated with the gene ontology (GO) term GO:0006952, 'defense response biological process' (Supplementary Table S4). Enrichment analysis showed significant enrichment of *PsOcr-3* for this GO term (p-value = 7.08^{-10}). The SNP loci corresponding to the *PsOcr-1*, *PsOcr-2* and *PsOcr-3* LOD score peaks were positioned within genes encoding an F-box domain protein (*Psat4g128720*), a phenylalanine ammonia lyase (*Psat1g046920*) and a proton-dependent oligopeptide transporter (*Psat5g221320*), respectively (Supplementary Table S4).

'ROR12' was previously shown to be a low-strigolactone line, which causes a reduced germination of *Oc* seeds (Pavan et al., 2016). Thus, we searched, within the QTL confidence intervals, for predicted genes showing homology with genes involved in the strigolactone biosynthetic pathway. This resulted in the identification, in *PsOcr-2*, of one *2-oxoglutarate-dependent dioxygenase* (*2OGD*) (*Psat1g046960*) and, in *PsOcr-3*, of one cytochrome P450 oxygenase of the CYP711A subfamily (*Psat5g201640*), two cytochrome P450 oxygenases of the CYP722C subfamily (*Psat5g209960* and *Psat5g209880*), and two *2OGD*s *(Psat5g206640* and *Psat5g206800*) (Supplementary Table S4).

QTLs for *Oc* resistance display both additive and epistatic effects

Information on the genotypic values and QTL genotypes of individual RILs was used to investigate the genetic effect of different QTL combinations. This indicated additivity between *PsOcr-1* and *PsOcr-2*, and between *PsOcr-1* and *PsOcr-3* (Figure 4A-B), with the three QTL alleles contributing to *Oc* resistance all deriving from 'ROR12'. Conversely, the genotype occurring at *PsOcr-3*, homozygous for either the 'ROR12' allele (R) or the 'Sprinter' allele (S), did not affect the genotypic value of RILs homozygous for the R allele at *PsOcr-2* (Figure 4C), thus indicating epistasis of *PsOcr-2* over *PsOcr-3*.

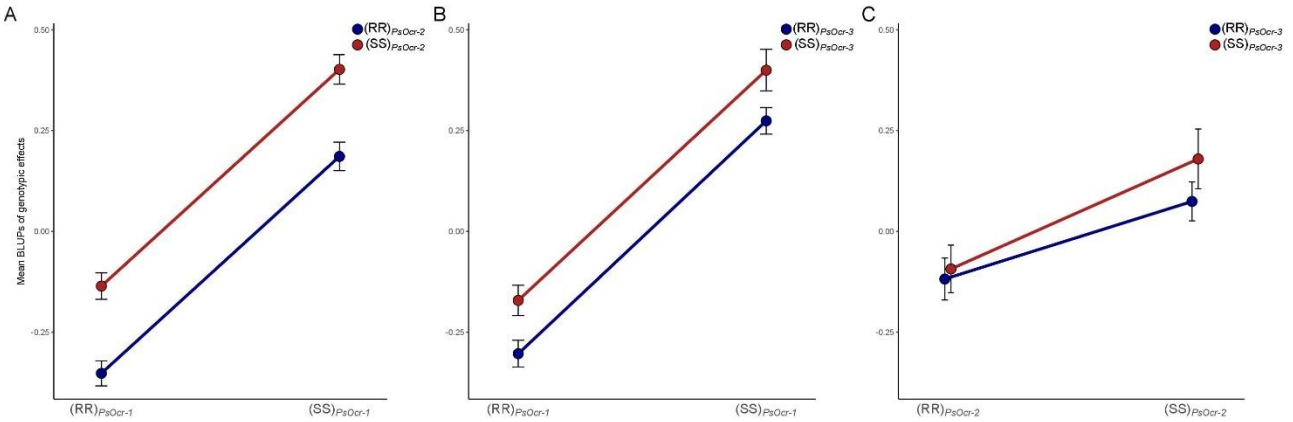

Figure 4. Combined effects on the phenotype of the QTL pairs *PsOcr-1:PsOcr-2* **(A)**, *PsOcr-1:PsOcr-3* **(B)**, and *PsOcr-2:PsOcr-3* **(C)**. Each plot reports: on the x-axis, the genotype for the marker locus corresponding to the first QTL LOD score peak; as a color code, the genotype for the marker locus corresponding to the second QTL LOD score peak; on the y-axis, mean best linear unbiased predictors (BLUPs) of genotypic effects on the phenotype. Black bars indicate ±se of BLUP means. Lines express, for a given genotype of the second QTL, the BLUP mean change when varying the genotype at the first QTL. R and S indicate the 'ROR12' and 'Sprinter' alleles, respectively.

Development of QTL-specific KASP markers

KASP assays were designed on the SNPs corresponding to the LOD score peaks of the QTLs *PsOcr-1*, *PsOcr-2* and *PsOcr-3*. These were validated on the parental lines, as well as three different RIL panels, each one predicted from GBS data to include ten lines homozygous for the 'ROR12' allele, ten lines homozygous for the 'Sprinter' allele, and at least one heterozygous line. Each KASP assays yielded three fluorescence groups (Figure 5). In addition, KASP genotypic calls were fully consistent with GBS calls.

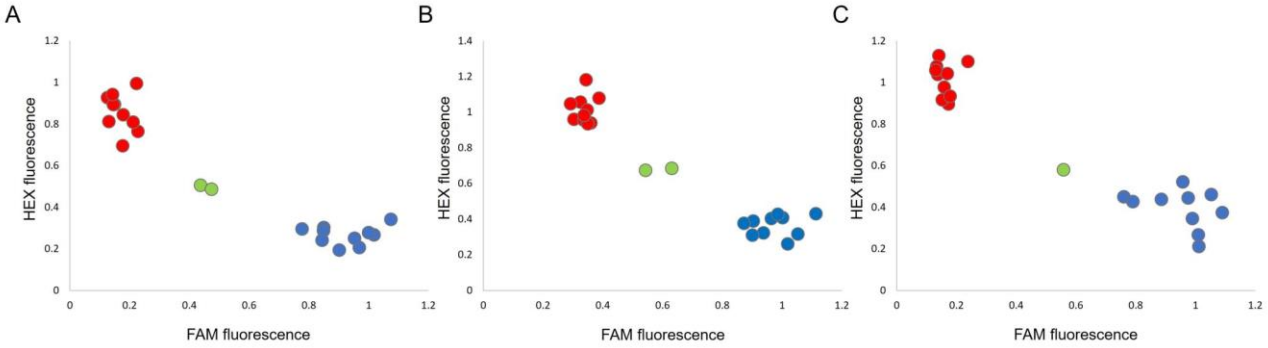

Figure 5. KASP assays for the *PsOcr-1* **(A)**, *PsOcr-2* **(B)** *and PsOcr-3* **(C)** quantitative trait loci (QTLs) for resistance to *Orobanche crenata*. Each recombinant inbred line (RIL) is associated with a dot, whose coordinates are given by the fluorescence levels recorded for the FAM and HEX dyes. The red and blue colors indicate homozygous calls for the 'Sprinter' and 'ROR12' alleles, respectively, whereas the green color indicates heterozygous calls.

DISCUSSION

Here we show that 'ROR12' resistance, highly effective against *Oc*, is controlled by three QTLs, including one (*PsOcr-1*) explaining as much as 69.3% of the genetic variance. In contrast, other *Oc* resistance sources previously identified in wild or cultivated *Pisum* germplasm confer incomplete immunity and are under the control of several minor effect QTLs (Rubiales et al., 2003; Valderrama et al., 2004; Pérez-de-Luque et al., 2005; Rubiales et al., 2005; Fondevilla et al., 2010; Rubiales et al., 2021; Wohor et al., 2022;). High heritability (0.84) and the absence of pleiotropic phenotypes affecting the agronomic performance, such as severe dwarfism and extreme branching occurring in other strigolactone-defective mutants (Rameau et al., 1997; Morris et al., 2001; Pavan et al., 2016), are other features of 'ROR12' resistance of value for breeding purposes. KASP technology provides a robust, high-throughput and cost-effective solution for assisted selection (Ma et al., 2017b; Broccanello et al., 2018), therefore the three KASP assays designed and validated in this study are expected to be of great value for the introgression of 'ROR12' resistance into new pea cultivars. The KASP markers designed on the *PsOcr-2* and *PsOcr-3* LOD score peaks were mapped in proximity of the markers OPAA19_702 and AD174, suggesting that *PsOcr-2* and *PsOcr-3* might coincide with the *Oc* resistance QTLs previously detected by Fondevilla et al. (2010) and Bardaro et al. (2016), respectively.

The study of combined genetic effects indicated additivity between *PsOcr-1* and *PsOcr-2*, and between *PsOcr-1* and *PsOcr-3*, and epistasis of *PsOcr-2* over *PsOcr-3.* In further support of the epistasis of *PsOcr-2* over *PsOcr-3*, we found that two QTLs, *PsOcr-1* and *PsOcr-2*, are alone sufficient to explain about 100% of the RIL population genotypic variance. Overall, our results support the hypothesis that 'ROR12' resistance originates from two independent defense mechanisms, one involving *PsOcr-1* and the other both *PsOcr-2* and *PsOcr-3*.

Several defense response genes were identified in the *PsOcr-1* and *PsOcr-3* QTL confidence intervals. Most of them encode a nucleotide-binding domain shared by apoptotic protease-activating factor-1, resistance proteins and *Caenorhabditis elegans death-4* protein (referred to as NB-ARC domain), which was predicted to play a major role in the activation of defense responses against parasitic plants (Li et al., 2009; Hu et al., 2020). Interestingly, the SNP corresponding to the *PsOcr-2* LOD score peak is associated, in the resistant line, with a missense (Thr699Ile) mutation in the phenylalanine ammonia lyase (PAL) protein encoded by the gene *Psat1g046920*. PAL catalyzes the first committed step in the phenylpropanoid pathway, and its expression is typically induced as a defense mechanism towards biotic agents, including broomrapes (Mabrouk et al., 2016; Briache et al., 2020).

‘ROR12’ resistance was previously associated with reduced production of strigolactones and, consequently, reduced *Oc* seed germination (Pavan et al., 2016). Interestingly, the QTL confidence intervals identified in this study do not contain the two pea strigolactone biosynthetic genes characterized so far, *Rms1* and *Rms5*, encoding the Carotenoid Cleavage Dioxygenase 7 (CCD7) and Carotenoid Cleavage Dioxygenase 8 (CCD7) enzymes. However, the intervals do encompass several homologs of genes that were shown to play a role in strigolactone biosynthesis in other plant species, namely cytochrome P450s of the CYP711A and CYP722C subfamilies and 2OGD enzymes. Members of the CYP711A subfamily play a highly important and varied role in strigolactone biosynthesis. They, for example, convert carlactone into carlactonoic acid in Arabidopsis (Abe at al., 2014), and carlactone into 4-deoxyorobanchol and 4-deoxyorobanchol into orobanchol in rice (Zhang et al., 2014). Enzymes of the CYP722C subfamily were shown to catalyse the formation of 5-deoxystrigol from carlactonoic acid in cotton (Wakabayashi et al., 2020), and of orobanchol from carlactonoic acid in tomato and cowpea (Wakabayashi et al., 2019, Wakabayashi et al., 2022). 2OGDs were associated with the biosynthesis of non-canonical strigolactones in the pea relative *Medicago truncatula* (Xie, 2016; Mashiguchi et al., 2021), however non-canonical strigolactones have not been identified in pea. Interestingly, a recent study showed that pea is lacking a *CYP712G1* orthologue that was postulated to be required for non-canonical strigolactone biosynthesis in *M. truncatula* (Wang et al., 2022). It will be intriguing to see whether the OGDs identified in the present study play a role in the biosynthesis of so far unknown strigolactones in pea.

This study provides another successful example of mapping genes of economic interest in pea by GBS (Holdsworth et al., 2017; Gali et al., 2018; Gali et al., 2019; Pavan et al., 2022). The quality of the linkage map provided in this study is suggested by its overall collinearity with the pea reference genome (Kreplak et al., 2019). Notably, we also highlight a few exceptions to this collinearity, and provide genomic context to unanchored physical scaffolds and superscaffolds, thus delivering elements for the refinement of pea genomic resources.

In conclusion, the results of this study might contribute to foster pea cultivation in the Mediterranean Basin and the Middle East, two areas in which *Oc* infestations discourage farmers from using legumes in crop rotations (Renna et al., 2015; Negewo et al., 2022). Future research might be addressed to the further refinement of the QTL mapping resolution. Pea is considered recalcitrant to stable genetic transformation protocols (Choudhury et al., 2021), therefore transient transformation or TILLING (Dalmais et al., 2008; Li et al., 2023b) may be used for the functional characterization of candidate genes.

Data availability statement

The datasets presented in this study can be found in online repositories. The names of the repository/repositories and accession number(s) can be found below: https://figshare.com/, doi: 10.6084/m9.figshare.22741481.

REFERENCES

Abe, S., Sado, A., Tanaka, K., Kisugi, T., Asami, K., Ota, S., ... & Nomura, T. (2014). Carlactone is converted to carlactonoic acid by MAX1 in *Arabidopsis* and its methyl ester can directly interact with AtD14 in vitro. *Proceedings of the National Academy of Sciences*, *111*(50), 18084-18089.

Allard, A., Bink, M. C., Martinez, S., Kelner, J. J., Legave, J. M., Di Guardo, M., ... & Costes, E. (2016). Detecting QTLs and putative candidate genes involved in budbreak and flowering time in an apple multiparental population. *Journal of Experimental Botany*, *67*(9), 2875-2888.

Bardaro, N., Marcotrigiano, A. R., Bracuto, V., Mazzeo, R., Ricciardi, F., Lotti, C., ... & Ricciardi, L. (2016). Genetic analysis of resistance to *Orobanche crenata* (Forsk.) in a pea (*Pisum sativum* L.) low-strigolactone line. *Journal of Plant Pathology*, 671-675.

Barilli, E., Cobos, M. J., Carrillo, E., Kilian, A., Carling, J., & Rubiales, D. (2018). A high-density integrated DArTseq SNP-based genetic map of *Pisum fulvum* and identification of QTLs controlling rust resistance. *Frontiers in Plant Science*, *9*, 167.

Bates, D., Mächler, M., Bolker, B., & Walker, S. (2015). Fitting linear mixed-effects models using lme4. *Journal of Statistical Software*, *67*, 1-48.

Ben Sadok, I., Celton, J. M., Essalouh, L., El Aabidine, A. Z., Garcia, G., Martinez, S., ... & Khadari, B. (2013). QTL mapping of flowering and fruiting traits in olive. *Plose One*, *8*(5), e62831.

Bouwmeester, H., Li, C., Thiombiano, B., Rahimi, M., & Dong, L. (2021). Adaptation of the parasitic plant lifecycle: germination is controlled by essential host signaling molecules. *Plant Physiology*, *185*(4), 1292-1308.

Bradbury, P. J., Zhang, Z., Kroon, D. E., Casstevens, T. M., Ramdoss, Y., & Buckler, E. S. (2007). TASSEL: software for association mapping of complex traits in diverse samples. *Bioinformatics*, *23*(19), 2633-2635.

Briache, F. Z., Ennami, M., Mbasani-Mansi, J., Lozzi, A., Abousalim, A., El Rodeny, W., ... & Mentag, R. (2020). Effects of salicylic acid and indole acetic acid exogenous applications on induction of faba bean resistance against *Orobanche crenata*. *The Plant Pathology Journal*, *36*(5), 476.

Broccanello, C., Chiodi, C., Funk, A., McGrath, J. M., Panella, L., & Stevanato, P. (2018). Comparison of three PCR-based assays for SNP genotyping in plants. *Plant Methods*, *14*, 1-8.

Broman, K. W., Wu, H., Sen, Ś., & Churchill, G. A. (2003). R/qtl: QTL mapping in experimental crosses. *Bioinformatics*, *19*(7), 889-890.

Broman, K. W. (2015). R/qtlcharts: interactive graphics for quantitative trait locus mapping. *Genetics*, *199*(2), 359-361.

Carrillo, E., Satovic, Z., Aubert, G., Boucherot, K., Rubiales, D., & Fondevilla, S. (2014). Identification of quantitative trait loci and candidate genes for specific cellular resistance responses against *Didymella pinodes* in pea. *Plant Cell Reports*, *33*, 1133-1145.

Catchen, J., Hohenlohe, P. A., Bassham, S., Amores, A., & Cresko, W. A. (2013). Stacks: an analysis tool set for population genomics. *Molecular Ecology*, *22*(11), 3124-3140.

Centrone, M., Gena, P., Ranieri, M., Di Mise, A., D'Agostino, M., Mastrodonato, M., ... & Tamma, G. (2020). In vitro and in vivo nutraceutical characterization of two chickpea accessions: differential effects on hepatic lipid over-accumulation. *Antioxidants*, *9*(3), 268.

Choudhury, A., & Rajam, M.V. (2021). Genetic transformation of legumes: an update. *Plant Cell Reports.* 40, 1813–1830.

Costantini, M., Summo, C., Centrone, M., Rybicka, I., D'agostino, M., Annicchiarico, P., ... & Pasqualone, A. (2021). Macro-and micro-nutrient composition and antioxidant activity of chickpea and pea accessions. *Polish Journal of Food and Nutrition Sciences*, *71*(2), 177-185.

Dalmais, M., Schmidt, J., Le Signor, C., Moussy, F., Burstin, J., Savois, V., ... & Bendahmane, A. (2008). UTILLdb, a *Pisum sativum* in silico forward and reverse genetics tool. *Genome Biology*, *9*, 1-12.

Daryanto, S., Wang, L., & Jacinthe, P. A. (2015). Global synthesis of drought effects on food legume production. *Plose One*, *10*(6), e0127401.

Elshire, R. J., Glaubitz, J. C., Sun, Q., Poland, J. A., Kawamoto, K., Buckler, E. S., & Mitchell, S. E. (2011). A robust, simple genotyping-by-sequencing (GBS) approach for high diversity species. *Plose One*, *6*(5), e19379.

FAOSTAT data (2021) Available at: http://www.fao.org/faostat/ [Accessed January 2023].

Fernández-Aparicio, M., Reboud, X., & Gibot-Leclerc, S. (2016a). Broomrape weeds. Underground mechanisms of parasitism and associated strategies for their control: a review. *Frontiers in Plant Science*, *7*, 135.

Fernández-Aparicio, M., Flores, F., & Rubiales, D. (2016b). The effect of *Orobanche crenata* infection severity in faba bean, field pea, and grass pea productivity. *Frontiers in Plant Science*, *7*, 1409.

Fernández-Aparicio, M., Kisugi, T., Xie, X., Rubiales, D., & Yoneyama, K. (2014). Low strigolactone root exudation: a novel mechanism of broomrape (*Orobanche* and *Phelipanche* spp.) resistance available for faba bean breeding. *Journal of Agricultural and Food Chemistry*, *62*(29), 7063-7071.

Fierst, J. L. (2015). Using linkage maps to correct and scaffold de novo genome assemblies: methods, challenges, and computational tools. *Frontiers in Genetics*, *6*, 220.

Fondevilla, S., Fernández-Aparicio, M., Satovic, Z., Emeran, A. A., Torres, A. M., Moreno, M. T., & Rubiales, D. (2010). Identification of quantitative trait loci for specific mechanisms of resistance to *Orobanche crenata* Forsk. in pea (*Pisum sativum* L.). *Molecular Breeding*, *25*, 259-272.

Gali, K. K., Liu, Y., Sindhu, A., Diapari, M., Shunmugam, A. S., Arganosa, G., ... & Warkentin, T. D. (2018). Construction of high-density linkage maps for mapping quantitative trait loci for multiple traits in field pea (*Pisum sativum* L.). *BMC Plant Biology*, *18*, 1-25.

Gali, K. K., Sackville, A., Tafesse, E. G., Lachagari, V. R., McPhee, K., Hybl, M., ... & Warkentin, T. D. (2019). Genome-wide association mapping for agronomic and seed quality traits of field pea (*Pisum sativum* L.). *Frontiers in Plant Science*, *10*, 1538.

Guindon, M. F., Martin, E., Cravero, V., Gali, K. K., Warkentin, T. D., & Cointry, E. (2019). Linkage map development by GBS, SSR, and SRAP techniques and yield-related QTLs in pea. *Molecular Breeding*, *39*, 1-16.

Holdsworth, W. L., Gazave, E., Cheng, P., Myers, J. R., Gore, M. A., Coyne, C. J., ... & Mazourek, M. (2017). A community resource for exploring and utilizing genetic diversity in the USDA pea single plant plus collection. *Horticulture Research*, *4*.

Hu, L., Wang, J., Yang, C., Islam, F., Bouwmeester, H. J., Muños, S., & Zhou, W. (2020). The effect of virulence and resistance mechanisms on the interactions between parasitic plants and their hosts. *International Journal of Molecular Sciences*, *21*(23), 9013.

Jamil, M., Rodenburg, J., Charnikhova, T., & Bouwmeester, H. J. (2011). Pre-attachment *Striga hermonthica* resistance of New Rice for Africa (NERICA) cultivars based on low strigolactone production. *New Phytologist*, *192*(4), 964-975.

Jamil, M., Kountche, B. A., & Al-Babili, S. (2021). Current progress in *Striga* management. *Plant Physiology*, *185*(4), 1339-1352.

Liis, K., Uku, R., Kuzmin, I., Jaak, V., & Peterson, H. (2020). gprofiler2--an R package for gene list functional enrichment analysis and namespace conversion toolset g: Profiler. *F1000Research*, *9*.

Kreplak, J., Madoui, M. A., Cápal, P., Novák, P., Labadie, K., Aubert, G., ... & Burstin, J. (2019). A reference genome for pea provides insight into legume genome evolution. *Nature Genetics*, *51*(9), 1411-1422.

Kuznetsova, A., Brockhoff, P. B., & Christensen, R. H. (2017). lmerTest package: tests in linear mixed effects models. *Journal of Statistical Software*, *82*, 1-26.

Langmead, B., & Salzberg, S. L. (2012). Fast gapped-read alignment with Bowtie 2. *Nature Methods*, *9*(4), 357-359.

Li, C., Dong, L., Durairaj, J., Guan, J. C., Yoshimura, M., Quinodoz, P., ... & Bouwmeester, H. J. (2023a). Maize resistance to witchweed through changes in strigolactone biosynthesis. *Science*, *379*(6627), 94-99.

Li, G., Liu, R., Xu, R., Varshney, R. K., Ding, H., Li, M., ... & Yang, T. (2023b). Development of an Agrobacterium-mediated CRISPR/Cas9 system in pea (*Pisum sativum* L.). *The Crop Journal*, *11*(1), 132-139.

Li, J., & Timko, M. P. (2009). Gene-for-gene resistance in *Striga*-cowpea associations. *Science*, *325*(5944), 1094-1094.

Loridon, K., McPhee, K., Morin, J., Dubreuil, P., Pilet-Nayel, M. L., Aubert, G., ... & Burstin, J. (2005). Microsatellite marker polymorphism and mapping in pea (*Pisum sativum* L.). *Theoretical and Applied Genetics*, *111*, 1022-1031.

Ma, Y., Coyne, C. J., Grusak, M. A., Mazourek, M., Cheng, P., Main, D., & McGee, R. J. (2017a). Genome-wide SNP identification, linkage map construction and QTL mapping for seed mineral concentrations and contents in pea (*Pisum sativum* L.). *BMC Plant Biology*, *17*, 1-17.

Ma, Y., Coyne, C. J., Main, D., Pavan, S., Sun, S., Zhu, Z., ... & McGee, R. J. (2017b). Development and validation of breeder-friendly KASPar markers for *er1*, a powdery mildew resistance gene in pea (*Pisum sativum* L.). *Molecular Breeding*, *37*, 1-7.

Mabrouk, Y., Mejri, S., Hemissi, I., & Belhadj, O. (2016). Biochemical analysis of induced resistance in chickpea against broomrape (*Orobanche foetida*) by rhizobia inoculation. *Phytopathologia Mediterranea*, 54-61.

Mashiguchi, K., Seto, Y., & Yamaguchi, S. (2021). Strigolactone biosynthesis, transport and perception. *The Plant Journal*, *105*(2), 335-350.

Molenaar, H., Boehm, R., & Piepho, H. P. (2018). Phenotypic selection in ornamental breeding: it's better to have the BLUPs than to have the BLUEs. *Frontiers in Plant Science*, *9*, 1511.

Morris, S. E., Turnbull, C. G., Murfet, I. C., & Beveridge, C. A. (2001). Mutational analysis of branching in pea. Evidence that *Rms1* and *Rms5* regulate the same novel signal. *Plant physiology*, *126*(3), 1205-1213.

Murray, K. D., & Borevitz, J. O. (2018). Axe: rapid, competitive sequence read demultiplexing using a trie. *Bioinformatics*, *34*(22), 3924-3925.

Negewo, T., Ahmed, S., Tessema, T., & Tana, T. (2022). Biological characteristics, impacts, and management of crenate broomrape (*Orobanche crenata*) in faba bean (*Vicia faba*): a review. *Frontiers in Agronomy*, *4*, 708187.

Pavan, S., Schiavulli, A., Marcotrigiano, A. R., Bardaro, N., Bracuto, V., Ricciardi, F., ... & Ricciardi, L. (2016). Characterization of low-strigolactone germplasm in pea (*Pisum sativum* L.) resistant to crenate broomrape (*Orobanche crenata* Forsk.). *Molecular Plant-Microbe Interactions*, *29*(10), 743-749.

Pavan, S., Delvento, C., Ricciardi, L., Lotti, C., Ciani, E., & D'Agostino, N. (2020). Recommendations for choosing the genotyping method and best practices for quality control in crop genome-wide association studies. *Frontiers in Genetics*, *11*, 447.

Pavan, S., Delvento, C., Nazzicari, N., Ferrari, B., D'Agostino, N., Taranto, F., ... & Annicchiarico, P. (2022). Merging genotyping-by-sequencing data from two *ex situ* collections provides insights on the pea evolutionary history. *Horticulture Research*, *9*, uhab062.

Pérez-de-Luque, A., Jorrín, J., Cubero, J. I., & Rubiales, D. (2005). *Orobanche crenata* resistance and avoidance in pea (*Pisum* spp.) operate at different developmental stages of the parasite. *Weed Research*, *45*(5), 379-387.

R Core Team. (2013). R: A language and environment for statistical computing. R Foundation for Statistical Computing, Vienna, Austria. http://www.R-project.org/

Rameau, C., Bodelin, C., Cadier, D., Grandjean, O., Miard, F., & Murfet, I.C. (1997). New *ramosus* mutants at loci *Rms1*, *Rms3* and *Rms4* resulting from the mutation breeding program at Versailles. *Pisum Genetics.* 29, 7-12.

Renna, M., Serio, F., & Santamaria, P. (2015). Crenate broomrape (*Orobanche crenata* Forskal): prospects as a food product for human nutrition. *Genetic Resources and Crop Evolution*, *62*, 795-802.

Rubiales, D., Pérez-de-Luque, A., Cubero, J. I., & Sillero, J. C. (2003). Crenate broomrape (*Orobanche crenata*) infection in field pea cultivars. *Crop Protection*, *22*(6), 865-872.

Rubiales, D., Moreno, M. T., & Sillero, J. C. (2005). Search for resistance to crenate broomrape (*Orobanche crenata* Forsk.) in pea germplasm. *Genetic Resources and Crop Evolution*, *52*, 853-861.

Rubiales, D. (2014). Legume breeding for broomrape resistance. *Czech Journal of Genetics and Plant Breeding, 50*(4), 144–150.

Rubiales, D., Fondevilla, S., & Fernández-Aparicio, M. (2020). Development of pea breeding lines with resistance to *Orobanche crenata* derived from pea landraces and wild *Pisum* spp. *Agronomy*, *11*(1), 36.

Schmidt, P., Hartung, J., Bennewitz, J., & Piepho, H. P. (2019). Heritability in plant breeding on a genotype-difference basis. *Genetics*, *212*(4), 991-1008.

Taylor, J., & Butler, D. (2017). R package ASMap: efficient genetic linkage map construction and diagnosis. *Journal of Statistical Software*, *79*, 1-29.

Valderrama, M. R., Román, B., Satovic, Z., Rubiales, D., Cubero, J. I., & Torres, A. M. (2004). Locating quantitative trait loci associated with *Orobanche crenata* resistance in pea. *Weed Research*, *44*(4), 323-328.

Wakabayashi, T., Hamana, M., Mori, A., Akiyama, R., Ueno, K., Osakabe, K., ... & Sugimoto, Y. (2019). Direct conversion of carlactonoic acid to orobanchol by cytochrome P450 CYP722C in strigolactone biosynthesis. *Science Advances*, *5*(12), eaax9067.

Wakabayashi, T., Shida, K., Kitano, Y., Takikawa, H., Mizutani, M., & Sugimoto, Y. (2020). CYP722C from *Gossypium arboreum* catalyzes the conversion of carlactonoic acid to 5-deoxystrigol. *Planta*, *251*(5), 97.

Wakabayashi, T., Ueno, K., & Sugimoto, Y. (2022). Structure elucidation and biosynthesis of orobanchol. *Frontiers in Plant Science*, *13*, 835160.

Walve, R., Rastas, P., & Salmela, L. (2019). Kermit: linkage map guided long read assembly. *Algorithms for Molecular Biology*, *14*, 1-10.

Wang, Y., Durairaj, J., Suárez Duran, H. G., van Velzen, R., Flokova, K., Liao, C. Y., ... & Bouwmeester, H. J. (2022). The tomato cytochrome P450 CYP712G1 catalyses the double oxidation of orobanchol *en route* to the rhizosphere signalling strigolactone, solanacol. *New Phytologist*, *235*(5), 1884-1899.

Wang, Y., Fang, Y., Ning, S., Xia, L., Zhan, J., Yang, Z., ... & Chen, J. (2023). QTL mapping for ovary-and fruit-related traits in *Cucumis sativus-c*. *hystrix* introgression line IL52. *Genes*, *14*(6), 1133.

Wickham, H. (2016) ggplot2: Elegant Graphics for Data Analysis. (2016). https://ggplot2.tidyverse.org

Wohor, O. Z., Rispail, N., Ojiewo, C. O., & Rubiales, D. (2022). Pea breeding for resistance to rhizospheric pathogens. *Plants*, *11*(19), 2664.

Wu, Y., Bhat, P. R., Close, T. J., & Lonardi, S. (2008). Efficient and accurate construction of genetic linkage maps from the minimum spanning tree of a graph. *PLOS Genetics*, *4*(10), e1000212.

Xie, X., Yoneyama, K., & Yoneyama, K. (2010). The strigolactone story. *Annual Review of Phytopathology*, *48*(1), 93-117.

Xie, X. (2016). Structural diversity of strigolactones and their distribution in the plant kingdom. *Journal of Pesticide Science*, *41*(4), 175-180.

Yang, T., Liu, R., Luo, Y., Hu, S., Wang, D., Wang, C., ... & Zong, X. (2022). Improved pea reference genome and pan-genome highlight genomic features and evolutionary characteristics. *Nature Genetics*, *54*(10), 1553-1563.

Yoneyama, K., Awad, A. A., Xie, X., Yoneyama, K., & Takeuchi, Y. (2010). Strigolactones as germination stimulants for root parasitic plants. *Plant and Cell Physiology*, *51*(7), 1095-1103.

Zhang, Y., Van Dijk, A. D., Scaffidi, A., Flematti, G. R., Hofmann, M., Charnikhova, T., ... & Bouwmeester, H. J. (2014). Rice cytochrome P450 MAX1 homologs catalyze distinct steps in strigolactone biosynthesis. *Nature Chemical Biology*, *10*(12), 1028-1033.

Due to their size, the supplementary tables associated with this chapter are not included in the thesis, but they can be accessed online in its published version: https://www.frontiersin.org/journals/plant-science/articles/10.3389/fpls.2023.1216297/full

Supplementary Table S1. List of SNPs whose chromosomal location, indicated in the SNP name, does not match with the one in the pea linkage map.

Supplementary Table S2. Linkage map coordinates of SNPs that are assigned to superscaffolds or scaffolds in the pea reference genome. The table is sorted by the SNP map position within each of the seven linkage groups (LGs), expressed in centiMorgan (cM).

Supplementary Table S3. Results of ANOVA-like test for the significance of random effect terms of a model in which the number of *O. crenata* shoots emerged aboveground at crop maturity is a function of the year, year by replicate, line, and line by year random effect terms.

Supplementary Table S4. Name and function of genes included in the three QTL confidence intervals identified in this study. Genes highlighted in yellow, green and red indicate, respectively: 1) genes associated with the defense response biological process gene ontology (GO) term; homologs of genes involved in the strigolactone biosynthetic pathway; genes including the SNP corresponding to the QTL LOD peak.

Chapter 3

Field resistance to *Orobanche crenata* in pea (*Pisum sativum* L.): beyond strigolactones

Field resistance to *Orobanche crenata* in pea (*Pisum sativum* L.): beyond strigolactones

Francesco Arcieri[1§], Gaetano Giudice[1§], Marzia Guerriero[1], Chiara Delvento[1], Mario Schilder[2], Angelica Giancaspro[3], Pasquale Luca Curci[4], Catherine Rameau[5], Luigi Ricciardi[1], Concetta Lotti[3], Harro Bouwmeester[2], Imran Haider[1*], Stefano Pavan[1*]

[1]Department of Soil, Plant and Food Sciences, University of Bari Aldo Moro, Via Amendola 165/A, 70126 Bari, Italy

[2]Plant Hormone Biology Group, Swammerdam Institute for Life Sciences, University of Amsterdam, Amsterdam, Netherlands

[3]Department of Agricultural, Food and Environmental Sciences, University of Foggia, Foggia, Italy

[4]Institute of Biosciences and Bioresources, National Research Council (CNR), Bari, Italy

[5]Institut Jean-Pierre Bourgin, INRAE, AgroParisTech, Universite Paris-Saclay, Versailles, France

§ These authors equally contributed to this work

*Corresponding authors: Stefano Pavan, email: stefano.pavan@uniba.it; Imran Haider, email: imran.haider@uniba.it

Submitted to BMC Plant Biology (currently under revision).

Submission ID: 7b38bf85-ce08-48f1-9bab-76d998793ffa

ABSTRACT

Orobanchaceae are parasitic weeds causing substantial yield losses in many crops, including pea (*Pisum sativum* L.). Within host species, genotypes that display enhanced resistance to Orobanchaceae often exude low levels of strigolactones (SLs) from their roots, in line with evidence that SLs stimulate the germination of Orobanchaceae. However, to which extent genetically determined low SL exudation contributes to field resistance to Orobanchaceae was poorly investigated. Here, we studied the relation between SL exudation and field response to *Orobanche crenata* Forsk. (*Oc*) in pea.

The screening of a germplasm panel identified three novel sources of field resistance to *Oc* and revealed an association between field resistance and low SL exudation. Although the SL-deficient mutants *rms1* and *rms5* were more resistant than their wild-type backgrounds, they still suffered substantial *Oc* parasitization. Genetic analysis and RNA-seq of recombinant inbred lines uncovered both SL-dependent and SL-independent mechanisms contributing to the near-complete resistance to *Oc* previously reported in the breeding line ROR12, and identified candidate genes possibly underlying resistance loci.

Besides identifying novel sources of resistance to *Oc*, our study indicates that reduced or absent SL exudation alone is not sufficient to confer complete field resistance to *Oc* in pea. This suggests the necessity of exploring SL-independent resistance mechanisms for breeding purposes. Further investigations are needed to clarify whether a similar scenario applies to other crops affected by Orobanchaceae, and to characterize genes causally related to *Oc* resistance.

Keywords: Orobanchaceae, pea, *Orobanche crenata*, resistance, strigolactones

INTRODUCTION

Orobanchaceae include root parasitic weeds, witchweeds (*Striga* spp.) and broomrapes (*Orobanche* and *Phelipanche* spp.), causing agricultural losses of about 10 billion US dollars annually (Xu et al., 2022). Crenate broomrape (*Orobanche crenata* Forsk.) (*Oc*) is a major threat to the cultivation of cool-season legumes in the Mediterranean area, and may cause up to complete yield loss in pea (*Pisum sativum* L.), one of the most important legume species globally with a production of about 35 million metric tons (Parker, 2009; Fernández-Aparicio et al., 2016; FAO, 2022; Pavan et al., 2022).

Orobanchaceae are extremely difficult to control using agronomic and chemical methods, as their life cycle mostly occurs underground and they produce large amounts of small, long-lived seeds (Rispail et al., 2007). No commercially available pea cultivar displays significant resistance to *Oc*, therefore confining pea cultivation to non-infested areas (Rubiales, 2014; Renna et al., 2015; Wohor et al., 2022).

Strigolactones (SLs) are carotenoid-derived compounds exuded by the roots of land plants that induce the germination of Orobanchaceae at concentrations as low as 10 pM (Xie et al., 2010; Pavan et al., 2016; Bouwmeester et al., 2021; Li et al., 2023a). Besides this, SLs act as recognition signals for symbiotic arbuscular mycorrhizal fungi and as plant hormones involved in a range of endogenous physiological processes, such as root architecture, leaf senescence, secondary growth, and response to environmental stresses (Matusova et al., 2005; Umehara et al., 2008; Zhang et al., 2013; Wu et al., 2022; Wang et al., 2024). The initial steps in SL biosynthesis are conserved across the plant kingdom and involve enzymes that convert β-carotene to carlactone (CL) (Alder et al., 2012). *DWARF27* (*D27*) encodes a β-carotene isomerase that converts all-*trans*- to 9-*cis*-β-carotene. This is then converted into CL by CAROTENOID CLEAVAGE DEOXYGENASE 7 (CCD7) and CCD8 (Johnson et al., 2006; Gomez-Roldan et al., 2008; Al-Babili et al., 2015; Jia et al., 2018). CL undergoes additional modifications to a range of different SLs (Yoneyama et al. 2018; Bouwmeester et al. 2021; Guercio et al., 2023). The SLs orobanchol, orobanchyl acetate and fabacyl acetate have been previously reported in legume root exudates (Pavan et al., 2016; Trabelsi et al., 2017).

In accordance with the role of SLs as Orobanchaceae germination stimulants, host genotypes displaying enhanced field resistance to Orobanchaceae, such as the rice cultivars NERICA, the faba bean breeding lines Navio and Quijote, and the pea breeding line ROR12, often secrete low SL levels in their root exudates (Jamil et al., 2011; Fernández-Aparicio et al., 2014; Bardaro et al., 2016; Pavan et al., 2016). However, whether resistance of this germplasm is solely due to this low SL exudation has not been investigated. Indeed, it was suggested that the attachment of Orobanchaceae to their hosts can be prevented by SL-independent resistance mechanisms, involving other germination

stimulants, germination inhibitors and host-derived haustorium initiation factors (Brun et al., 2018; Uraguchi et al., 2018; Fishman et al., 2021; Jhu et al., 2022; Jhu et al., 2023; Jamil et al., 2024). Additionally, post-attachment defense mechanisms to Orobanchaceae were documented (Martín-Sanz et al., 2020; Albert et al., 2021; Fishman et al., 2021). The low-SL pea breeding line ROR12, displaying nearly complete resistance to *Oc* without an obvious yield penalty (Pavan et al., 2016), is also likely to exhibit SL-independent resistance mechanisms, as it carries resistance alleles at three distinct quantitative trait loci (QTLs), previously named *PsOcr-1*, *PsOcr-2*, and *PsOcr-3* (Delvento et al., 2023).

Loss-of function mutants of key SL biosynthetic genes have been reported in several species, including the pea mutant lines *rms1* and *rms5* (Beveridge, 2000; Morris et al., 2001). Although these mutants are expected to display enhanced resistance to Orobanchaceae, they exhibit severe pleiotropic phenotypes as a result of the complete loss of SLs, such as extreme branching and dwarfism, which makes them unsuitable for breeding purposes (Sorefan et al., 2003; Johnson et al., 2006; Gomez-Roldan et al., 2008). Notably, the response of SL biosynthetic mutants to Orobanchaceae was mostly assessed *in vitro,* by means of seed germination assays, rather than under field conditions (Matusova et al., 2005; Gomez-Roldan et al., 2008; Butt et al., 2018; Hao et al., 2023).

Here, we integrated liquid chromatography multiple reaction monitoring mass spectrometry (LC-MS/MS), RNA-seq and field trials to evaluate different pea germplasm, i.e. a global collection, the mutant lines *rms1* and *rms5*, and a set of recombinant inbred lines (RILs) originating from ROR12 as resistant parent. This allowed us to identify new sources of resistance to *Oc*, evaluate the relation between SL exudation and field resistance to *Oc*, and characterize QTLs underlying ROR12 resistance to *Oc.*

MATERIALS AND METHODS

Field trials

Three pea lines, selected from the DISSPA-UNIBA germplasm collection, along with 133 lines from the U.S. Department of Agriculture (USDA) Pea Single Plant Plus (PSPP) collection (Supplementary Table S1), were evaluated over two growing seasons (2022-2023 and 2023-2024) (Supplementary Figure S1 and Supplementary Figure S2). The trials were conducted at the University of Bari (41°01′22.1″N 16°54′21.0″E), in a silty–clayey experimental field continuously cultivated with legumes and heavily infested by the *Oc* seed bank. Plants were sown according to randomized block designs with three blocks (2022-2023) or four blocks (2023-2024), which were placed orthogonally to a gradient of infestation observed in previous years. Each experimental unit consisted of two plants spaced 0.3 m apart along the row. Experimental units were spaced 1 m apart within the row and 1 m

between adjacent rows. No fertilization and irrigation were applied during the crop cycle. Pest and pathogen management was carried out using single applications of deltamethrin, acetamiprid and difenoconazole, while weed control was performed with pendimethalin in pre-emergence and manual weeding in post-emergence. Response to *Oc* was evaluated by counting the number of parasitic shoots emerged aboveground per plant at crop maturity. To assess the homogeneity of *Oc* infestation, ten plants of the susceptible cultivar 'Sprinter' were randomly allocated in each block, and the standard deviation of the mean was calculated. Data on *Oc* emergence were normalized by square root transformation and further analysed by analysis of variance (ANOVA). As no significant genotype by year interaction was detected, data averaged over two years were used to obtain a frequency histogram of genotypic responses to *Oc*, using the ggplot2 and ggrepel R packages (Wickham, 2016; Slowikowski et al., 2021).

Another field trial was conducted using the pea SL mutants *rms1* and *rms5* (Beveridge, 2000; Morris et al., 2001), provided by the French National Institute for Agriculture, Food, and Environment (INRAE) along with their wild-type genetic background (cv. Térèse), and the breeding line ROR12 (Pavan et al., 2016). Plants were sown in 2022 according to a randomized block design with seven blocks. Experimental units, consisting of five plants 0.2 m apart along the row, were spaced 1 m within and between rows. Crop management and *Oc* response evaluation were carried out as previously described. After data normalization by square root transformation and ANOVA, means were compared using the Tukey's Honest Significant Difference (HSD) post-hoc test implemented by the R package Agricolae, with significant level α set to 0.05 (De Mendiburu et al., 2020). Finally, a box plot was obtained with the ggplot2 R package (Wickham, 2016).

Strigolactone quantification

Pea seeds were surface sterilized with 70% ethanol for 30s and 2% sodium hypochlorite (v/v) for 30 min. They were then rinsed five times in sterile double-distilled water and kept in a petri dish on wet filer paper in the dark at 25°C for two days to induce germination. Germinated seeds were transferred to pots filled with vermiculite and kept for one week. Afterwards, seedlings were moved to an aeroponic system arranged in a randomized block design with three replicates, in which each experimental unit consisted of a tank with eight plants. Plants were initially grown in 3 liters of Hoagland's nutrient solution with $K_2HPO_4 \cdot 3H_2O$ (+Pi) for 2 weeks, followed by $K_2HPO_4 \cdot 3H_2O$ (–Pi) for another 10 days (Wang et al., 2019). The aeroponic growing conditions were 23°C during the day, 22°C during the night, 16-hour light/8-hour dark photoperiod, and 60% relative humidity.

SL quantification was performed as previously described, with minor modifications (Pavan et al., 2016). Briefly, root exudates (1 liter) were concentrated by loading onto a pre-equilibrated SPE C18-

Fast column (500mg/ 3 mL, Grace Pure) and eluted with 3 mL 100% ethyl acetate. The solvent was evaporated in the nitrogen flow, and the dried extract was dissolved in 100 µl of acetonitrile:water (25:75, v:v) and filtered through a 0.22 µm filter for LC-MS/MS with MRM mode analysis. Chromatographic separation was performed using the Waters Acquity UPLC^{TM} I-class system with Acquity UPLC^{TM} bridged ethylene hybrid (BEH) C18 column (2.1 mm x 100 mm, 1.7 µm, Waters). This ultra-high pressure liquid chromatography (UHPLC) system is coupled to a Xevo® TQ-S quadrupole mass spectrometer with electrospray (ESI) ionization interface (Waters). The injection volume was set to 5 µl and analytes were eluted at a flow rate of 0.45 mL/min. Water + 15mM formic acid (A) and acetonitrile + 15mM formic acid (B) were used to generate a solvent gradient with the following profile: isocratic elution 0.4 min (15% B), 0.65 min (27% B), 5 min (40% B), 8 min (65% B), 9.5 min (95% B). The column was washed for one minute (95% B) and then equilibrated to initial conditions for 1.5 min (15% B). The ESI source was operated in positive mode and multiple reaction monitoring (MRM) was used to detect SLs using the following transitions: orobanchol_347>97, orobanchyl acetate_389>97, fabacyl acetate_405>97. Mass spectrometry data were processed using the MassLynx^{TM} software (V4.2, Waters). Mass spectrometry data with a signal to noise ratio less than 10 were considered zero.

Statistical analyses for individual SLs were carried out using the Agricolae R package (De Mendiburu et al., 2020). The Student's t-test ($\alpha = 0.05$) was used to compare the means of lines displaying contrasting response to *Oc*, or alternative alleles at the *PsOcr-1*, *PsOcr-2* and *PsOcr-3* QTLs. The ANOVA and the Tukey's HSD post-hoc test ($\alpha = 0.05$) were performed to compare the lines *rms1*, *rms5* and Térèse. Data were graphically represented with barplots, which were obtained using the ggplot2 R package (Wickham, 2016).

RNA-seq analysis

ROR12, the *Oc* susceptible cultivar Sprinter and six F_6 RILs originating from their cross were selected, based on available genotyping by sequencing (GBS) data and the KASP marker assays described by (Delvento et al., 2023), to encompass all the 2^3 possible homozygous configurations of resistance (R) and susceptibility (S) alleles at *PsOcr-1*, *PsOcr-2* and *PsOcr-3* (Table 1). Total RNA was extracted from root tissues using the TRI-Reagent with a Direct-zol RNA MiniPrep Kit, according to the manufacturer's instruction (Zymo Research). RNA concentration, quality and integrity were checked using a NanoDrop 2000 UV-Vis spectrophotometer (Thermo Scientific) and standard gel electrophoresis. After total RNA isolation, complementary DNA (cDNA) libraries were prepared using the Hieff NGS Ultima Dual-mode mRNA Library Prep Kit for Illumina (Yeasen). In detail, mRNA was enriched using oligo(dT) beads, sheared using a fragmentation buffer and reverse

transcribed into cDNA with random primers. After synthesizing the second strand, cDNA fragments underwent end-repair, poly(A) addition, and ligation to Illumina sequencing adapters. Size selection of the ligation products was performed using Hieff NGS DNA Selection Beads (Superior Ampure XP alternative|12601ES56, Yeasen). Ligated fragments were finally PCR amplified. Library sequencing was performed on an Illumina Novaseq 6000 platform (Illumina). Raw sequencing data were assessed for quality using FASTQC (https://www.bioinformatics.babraham.ac.uk/projects/fastqc) before and after trimming. The Trimmomatic software (Bolger et al., 2014) was employed to remove sequencing adapters, low-quality bases (Phred < 25), short reads (< 35 nt), and the first 10 base pairs from each read. The kraken2/bracken pipeline (Lu et al., 2020) and a database comprising all bacteria and fungi species listed in RefSeq were used to assess potential contamination with pathogens. The STAR software (Dobin et al., 2013) was used to index the *P. sativum* ZW6 reference genome (Yang et al., 2022) and to map the trimmed reads. Qualimap (Okonechnikov et al., 2016) was used to evaluate the mapping quality and infer strand specificity. Gene-level read summarization was conducted with FeatureCounts (Liao et al., 2014), focusing on reads with a mapping quality greater than 30 and counting fragments due to the paired-end nature of the data. The DESeq2 package (Love et al., 2014) was used to normalize counts, filter out poorly expressed genes by setting a minimum of 10 counts in at least 3 samples, and to assess relations among samples by principal component analysis (PCA).

The DESeq2 package was also used to detect differentially expressed genes between lines carrying resistance (R) or susceptibility (S) alleles at each of the three previously identified QTLs *PsOcr-1*, *PsOcr-2* and *PsOcr-3* (Delvento et al., 2023). To reduce the number of statistically significant genes with a weak effect, the analysis was conducted using a testing log2 fold-change threshold of 0.5. After performing shrinkage of log2 foldchange (LFC) estimates with the *lfcShrink* function, genes with adjusted p-value < 0.01 and |log2FC| >1 were considered differentially expressed genes (DEGs). DEGs within the *PsOcr-1*, *PsOcr-2* and *PsOcr-3* confidence intervals were identified by aligning the interval ends, previously determined on the Cameor genome (Kreplak et al., 2019; Delvento et al., 2023), on the newly published high-quality ZW6 genome (Yang et al., 2022). Finally, a Volcano plot for each of the three comparisons was obtained using the EnhancedVolcano R package (Blighe et al., 2024).

Enrichment analysis of DEGs for Gene Ontology–Biological Process (GO–BP) terms was performed using the hypergeometric test and the false discovery rate (FDR) multiple comparison correction implemented by the gProfiler2 R package (version 0.2.3) (Kolberg et al., 2020).

RESULTS

Identification of new sources of resistance to *Oc* in pea

Preliminary screenings carried out on the pea *ex situ* germplasm collection held at the Department of Soil, Plant and Food Sciences, University of Bari (DISSPA-UNIBA), resulted in the detection of three lines, PS-00168, PS-00169 and PS-00300, showing low levels of *Oc* infection. These were further evaluated for two consecutive years in experimental fields severely infested by *Oc*, together with 133 lines from the Pea Single Plant Plus (PSPP) collection of the U.S. Department of Agriculture (USDA) (Supplementary Table S1). Within each experimental block, ten randomly allocated plants of the susceptible cultivar Sprinter displayed relatively low variation with respect to the average number of *Oc* shoots emerged per plant, indicating a fairly uniform level of *Oc* pressure within the blocks (Supplementary Table S2).

The ANOVA indicated significant genetic variation for response to *Oc*, and non-significant genotype by year interaction (Supplementary Table S3). The lines PS-00168, PS-00169 and PS-00300 showed the highest level of resistance, with the average number of *Oc* shoots emerged per plant ranging from 1.5 (PS-00300) to 1.83 (PS-00168 and PS-00169) across the two years (Figure 1A and Supplementary Table S4).

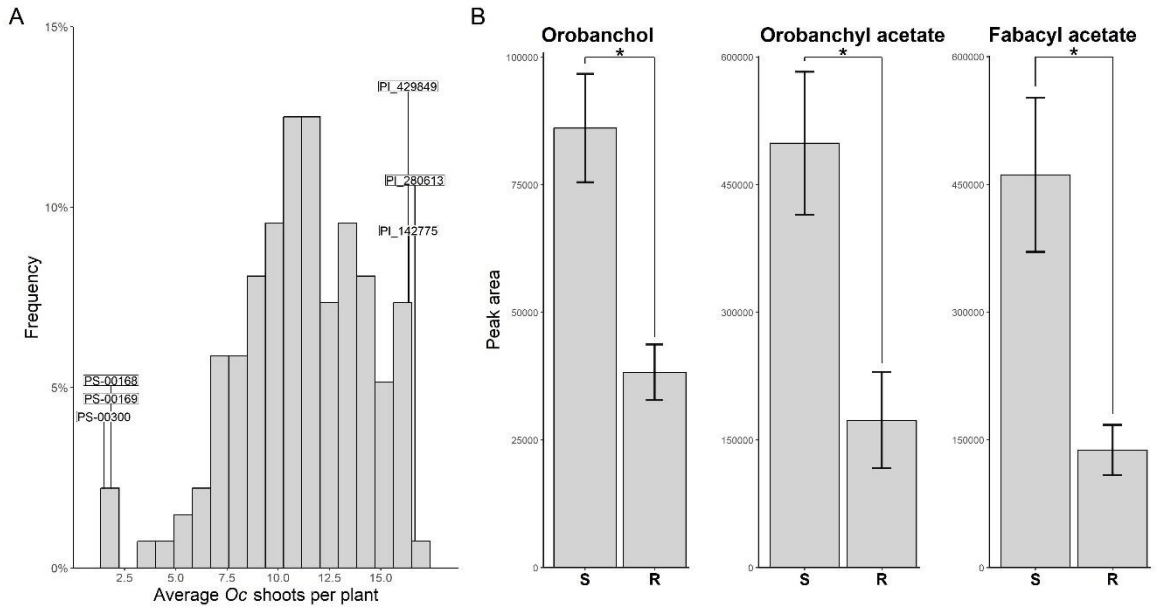

Figure 1. (A) Distribution of the number of *Orobanche crenata* Forsk. (*Oc*) shoots emerged aboveground per host plant on a pea germplasm panel. Data are presented as the means of two growing seasons. Labels indicate six lines displaying extreme phenotypes, which were further analyzed for strigolactone quantification. **(B)** Orobanchol, orobanchyl acetate and fabacyl acetate peak areas associated with the root exudates of lines displaying resistant (R) and susceptible (S) phenotypes to *Oc*. Data are presented as means ± SE (n = 3). Asterisks indicate significant differences ($p < 0.05$, Student's t-test).

Pea field resistance to *Oc* is associated with lower SL exudation

Aiming to study the relation between SL exudation and field resistance to *Oc*, we quantified SLs in root exudates collected from the resistant lines mentioned above and the lines PI_142775, PI_280613, and PI_429849. These showed the highest level of susceptibility, with the average number of *Oc* shoots emerged per plant ranging from 16.33 (PI_429849) to 16.67 (PI_280613) (Figure 1A). Significantly lower levels of SLs were detected in the resistant group (Figure 1B). Specifically, orobanchol, orobanchyl acetate and fabacyl acetate were reduced by 55.56%, 65.26% and 70.07%, respectively (Figure 1B).

Pea SL-deficient *rms* mutants only display partial resistance to *Oc*

To further explore the role of SLs in field resistance to *Oc*, we evaluated the previously reported *rms1* and *rms5* SL biosynthetic mutants (Beveridge, 2000; Morris et al., 2001). No SL was detected in the root exudates of these mutants, in contrast to their wild-type genetic background, i.e the cv. Térèse (Figure 2A). Surprisingly, both *rms1* and *rms5* displayed substantial parasitization, with an average of 9.43 and 8.57 *Oc* shoots emerged per plant, respectively, although they were significantly more resistant than Térèse, with an average of 22 *Oc* shoots emerged per plant (Figure 2B). The level of *Oc* parasitization was not significantly different between *rms1* and *rms5* (Figure 2B). Nearly complete field resistance was displayed by ROR12, associated with 0.5 *Oc* shoots emerged per plant on average (Figure 2B).

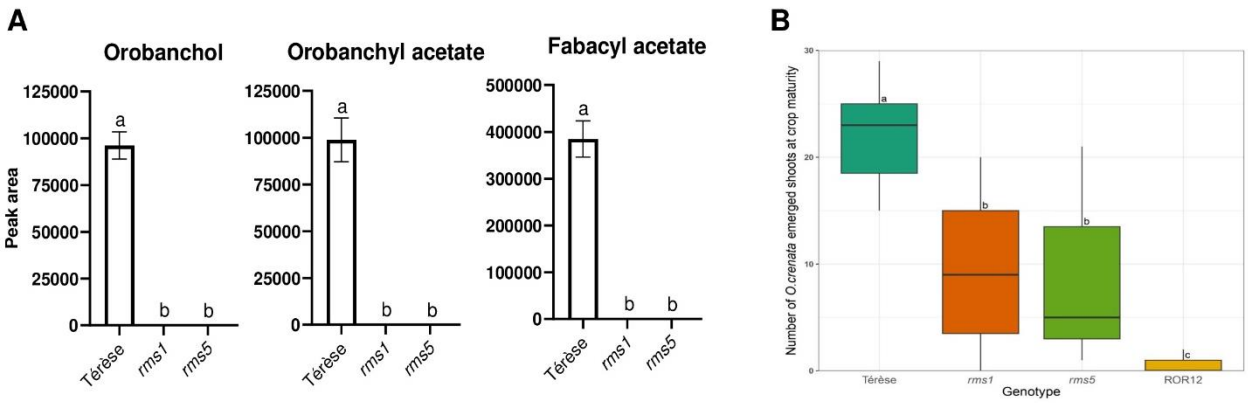

Figure 2. (A) Orobanchol, orobanchyl acetate and fabacyl acetate peak areas associated with the root exudates of the mutants *rms5* and *rms1*, and their -genetic background (cv. Térèse). Data are shown as mean ± SE (n = 3). Different letters indicate significant differences ($p < 0.05$, Tukey's HSD test). **(B)** Box plots showing the distribution of the number of *Orobanche crenata* Forsk. (Oc) shoots emerged aboveground on Térèse, *rms1*, *rms5* and the breeding line ROR12. Data are presented as mean ± SE (n = 7). Different letters indicate significant differences ($p < 0.05$, Tukey's HSD test).

Both SL-dependent and SL-independent mechanisms play a role in the resistance to *Oc* displayed by the breeding line ROR12

The pea breeding line ROR12 carries *Oc* resistance alleles at three different QTLs, previously named *PsOcr-1* to *PsOcr-3* (Delvento et al., 2023). Based on available genotyping-by-sequencing data (Delvento et al., 2023), we selected a panel of eight homozygous lines, i.e. ROR12, the *Oc* susceptible cultivar Sprinter and six F_6 recombinant inbred lines derived from their cross, together encompassing the 2^3 possible homozygous configurations of resistance (R) and susceptibility (S) alleles at the three QTLs (Table 1). These configurations were validated using Kompetitive Allele Specific PCR (KASP) marker assays previously developed on the QTL significance peaks (Delvento et al., 2023) (Supplementary Figure S3).

The root exudates of lines carrying the *PsOcr-1* R allele displayed, compared to lines carrying the *PsOcr-1* S allele, significantly lower levels of orobanchol, orobanchyl acetate and fabacyl acetate, indicating that the resistance mechanism associated with *PsOcr-1* relates to lower SL exudation (Figure 3). Notably, no significant difference in SL exudation was found by the analysis of lines carrying alternative alleles at either *PsOcr-2* or *PsOcr-3* (Supplementary Figure S4), indicating that ROR12 resistance also involves SL-independent resistance mechanisms.

Table 1. Homozygous genotypes at the QTLs PsOcr-1, PsOcr-2 and PsOcr-3 displayed by the breeding line ROR12, the cultivar Sprinter and six recombinant inbred lines (RILs) originating from their cross. S and R indicate the susceptibility and resistance allele, respectively.

ID	*PsOcr-1*	*PsOcr-2*	*PsOcr-3*
ROR12	RR	RR	RR
Sprinter	SS	SS	SS
144 RIL	RR	SS	SS
113 RIL	SS	RR	SS
164 RIL	SS	SS	RR
155 RIL	RR	RR	SS
27 RIL	RR	SS	RR
23 RIL	SS	RR	RR

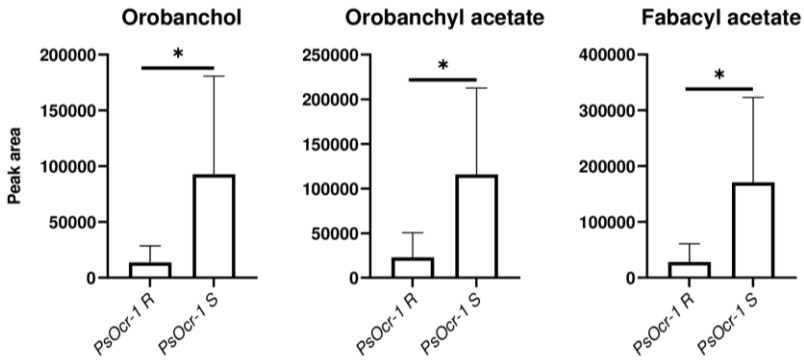

Figure 3. Orobanchol, orobanchyl acetate and fabacyl acetate peak areas associated with root exudates of RILs homozygous for the resistance (R) or the susceptibility (S) allele at *PsOcr-1*. Data are shown as means ± SE (n = 4). Asterisks indicate significant differences ($p < 0.05$, Student's t-test).

Characterization of transcriptional profiles associated with different resistance mechanisms to *Oc*

To gain further insights into the molecular basis of ROR12 resistance to *Oc*, we performed RNA-seq to analyze gene expression in the roots of the eight pea lines above mentioned carrying different *PsOcr* allele combinations. Sequencing generated from 32.52 to 49.07 million raw reads per sample (Supplementary Table S5). Reads mapped onto the *P. sativum* 'ZW6' reference genome (Yang et al., 2022) ranged from 23.66 to 46.72 million, while uniquely mapped reads ranged from 67.41% to 92.26% (Supplementary Table S5). Principal component analysis showed a high level of consistency among the expression profile of biological replicates (Supplementary Figure S5). Data from the cv. Sprinter were excluded from further analysis due to significant contamination with reads from *Fusarium* spp.

Comparing lines homozygous for alternative alleles at *PsOcr-1* led to the identification of 15 differentially expressed genes (DEGs) (Supplementary Figure S6A and Supplementary Table S6). Two of them, encoding a 2-methylene-furan-3-one reductase and a carbonic anhydrase 2-like protein, resided in the *PsOcr-1* confidence interval and were downregulated in lines carrying the R allele (Figure 4A). As for lines carrying alternative alleles at *PsOcr-2,* 108 DEGs were found (Supplementary Figure S6B and Supplementary Table S6). Among them, three genes resided in the *PsOcr-2* confidence interval, including two (encoding a phenylalanine ammonia-lyase 1-like protein and an uncharacterized proteins) down-regulated and one (encoding a lachrymatory-factor synthase-like protein) up-regulated in lines carrying the R allele (Figure 4A). Finally, 54 DEGs were found between lines carrying alternative alleles at *PsOcr-3* (Supplementary Figure S6C and Supplementary Table S6). One of them, encoding a G-type lectin S-receptor-like serine/threonine-protein kinase, resided in the *PsOcr-3* confidence interval and was up-regulated in lines carrying the R allele (Figure 4A).

DEGs between lines differing for the allelic configuration at *PsOcr-1* were not significantly enriched for any gene ontology (GO) biological process (BP) term. In contrast, the GO BP terms GO:0006749 and GO:0006355, indicating glutathione metabolic process and regulation of DNA-templated transcription, respectively, were significantly enriched in DEGs between lines carrying alternative allelic configurations at *PsOcr-2* (Figure 4B). Finally, the GO BP term GO:0098542, indicating defense response to other organisms, was enriched in DEGs between lines carrying alternative allelic configurations at *PsOcr-3* (Figure 4B).

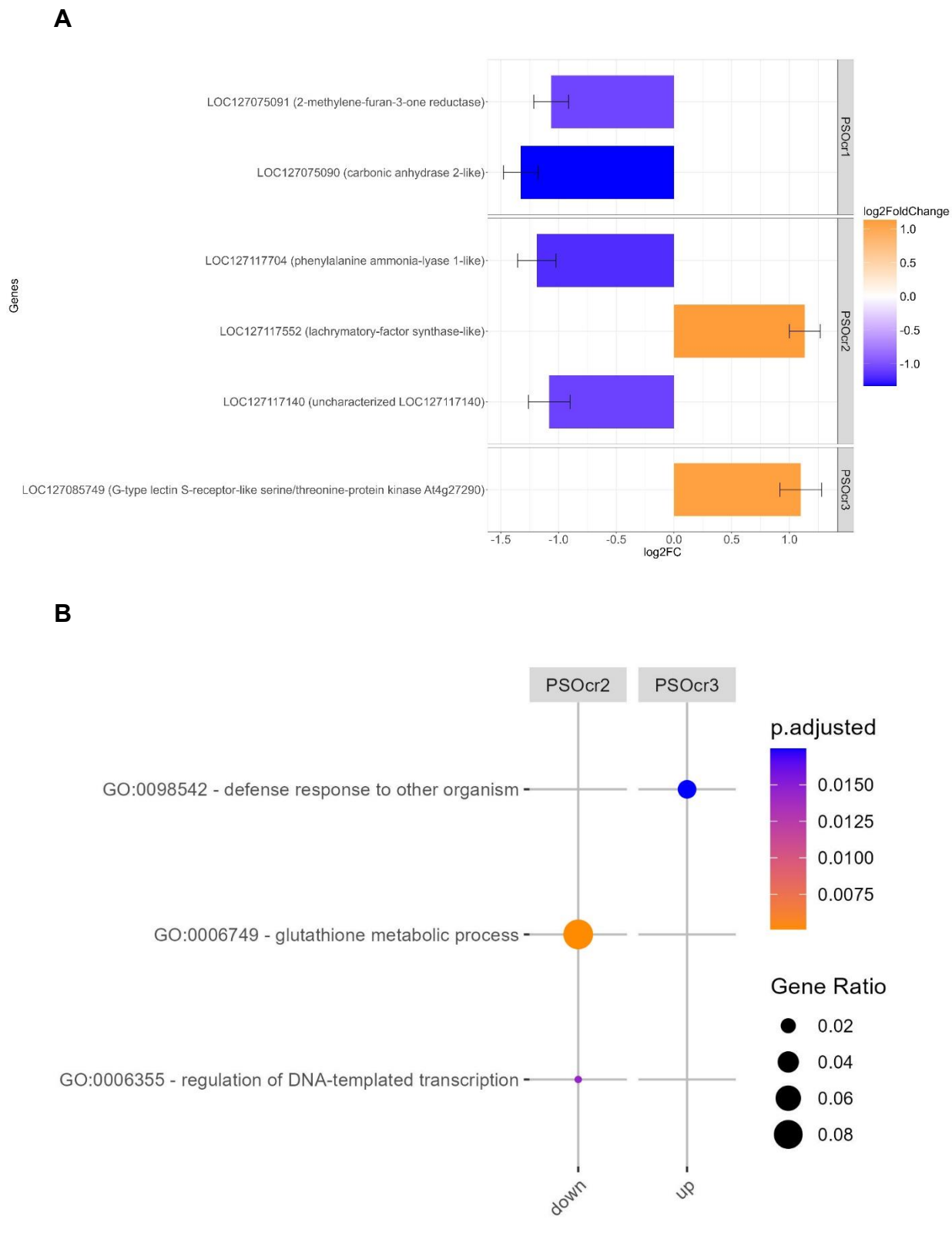

Figure 4. (A) Differentially expressed genes (DEGs) between lines homozygous for alternative alleles at the QTLs *PsOcr-1*, *PsOcr-2* and *PsOcr-3*. Bars indicate DEGs within QTL confidence intervals. The bar colors represent log2 fold changes (LFC) value, according to a blue (down-regulated)/orange (up-regulated) scale. **(B)** Gene ontology enrichment analysis for DEGs between lines homozygous for alternative alleles at *PsOcr-2* and *PsOcr-3*. Dot sizes indicate the proportion of DEGs in each set, while dot colors indicate the significance level, according to a blue (less significant)/orange (more significant) scale.

DISCUSSION

We report the identification of three pea lines, PS-00168, PS-00169, and PS-00300, representing novel sources of resistance to *Oc* (Figure 1A), a root parasitic weed severely affecting pea cultivation in the Mediterranean region. Notably, all the lines mentioned above, as well as the previously described *Oc*-resistant line ROR12 (Pavan et al., 2016), originate from southern Italy (Supplementary Table S1). This geographic clustering raises important questions regarding the origin, spread, and potentially shared genetic basis of resistance within this regional germplasm.

The characterization of pea genotypes with contrasting response to *Oc* showed that pea field resistance is commonly associated with low SL exudation (Figure 1B), in line with previous studies relating low SL exudation with resistance to Orobanchaceae in rice and faba bean (Jamil et al., 2011; Fernández-Aparicio et al., 2014). Another SL-dependent mechanism of resistance to Orobanchaceae, reported in sorghum and maize, involves qualitative differences in SL composition, as individual SLs may differ in their activity as germination stimulants (Gobena et al., 2017; Mohemed et al., 2018; Li et al., 2023a). However, this mechanism does not appear to apply to PS-00168, PS-00169, PS-00300, which show similar ratios among the three pea SLs orobanchol, orobanchyl acetate and fabacyl acetate compared to susceptible germplasm (Figure 1B).

Although low SL exudation is known to reduce germination of Orobanchaceae (Bouwmeester et al., 2021), its translation into effective field resistance has been poorly explored. Indeed, SL-biosynthetic mutants have been primarily tested by *in vitro* germination assays or by pot assays (Kohlen et al., 2012; Butt et al., 2018; Galili et al., 2021; Hao et al., 2023). The only exceptions are represented by the tomato mutants *sb1* and *sb2*, which carry loss-of-function mutations in the *CCD7* and *CCD8* genes, respectively, and were recently reported to exhibit complete field resistance to the broomrape species *Phelipanche aegyptiaca* (Dor et al., 2010; Karniel et al., 2024). In contrast, as a key novelty of this study, we show that compared with their wild-type genetic background, the SL biosynthetic mutants *rms1* and *rms5*, which do not produce detectable SL levels, only show a moderate reduction in *Oc* parasitization under field conditions (Figure 2B). This highlights the limitations of relying solely on SL exudation as a breeding strategy to introduce *Oc* resistance in pea. Our findings are in line with earlier *in vitro* observations, showing significant germination of *Oc* on *rms1* root exudates (Gomez-Roldan et al., 2008). Incomplete resistance of *rms* mutants could be attributed to the presence of non-SL germination stimulants, which have been previously reported in pea root exudates (Brun et al., 2018; Jamil et al., 2024).

Consistent with the partial contribution of SL deficiency to resistance, we showed that only one of the three QTLs associated with the nearly complete field resistance of ROR12, *PsOcr-1,* is correlated

with lower SL exudation (Figure 3 and Supplementary Figure S4). Nevertheless, no known SL biosynthetic or catabolic gene is located within the *PsOcr-1* confidence interval, nor is differentially expressed between lines with alternative alleles at *PsOcr-1*. However, one of the two DEGs in *PsOcr-1* encodes a 2-methylene-furan-3-one reductase. Although there are no reports on a possible role of 2-methylene-furan-3-one reductases in the modification of SLs, the strigolactone D-ring is a furanone. In addition, non-SL furanones, termed debranones, mimic SLs in inhibiting shoot branching and stimulating the germination of *Striga* and *Orobanche* (Fukui et al., 2011; Takahashi et al., 2016; Kawada et al., 2024). Functional analysis of this gene could clarify its potential impact on SL activity or mimicry.

Within *PsOcr-2*, a differentially expressed gene encodes a phenylalanine ammonia-lyase (PAL), a well-known enzyme associated with response to various biotic and abiotic stresses (Cass et al., 2015; Chen et al., 2017). *PAL* expression is induced upon infection by the root parasitic plant species *Striga hermonthica*, *Orobanche foetida* and *Oc* in rice, chickpea and faba bean (Swarbrick et al., 2008; Mabrouk et al., 2016; Briache et al., 2020), respectively, making it a strong candidate gene underlying *Oc* resistance in pea.

Finally, the sole DEG within the *PsOcr-3* confidence interval encodes a G-type lectin S-receptor-like serine/threonine-protein kinase. Increasing evidence supports the role of lectin receptor-like kinases (LecRLKs) in the activation of defense pathways against pathogens (Sun et al., 2020). In addition, the RLK HAOR7 in sunflowers provides resistance against *O. cumana* (Duriez et al., 2019). Furthermore, lines carrying contrasting alleles at *PsOcr-3* show significant enrichment of the GO-BP term *defense response to other organism*, suggesting that this QTL may contribute to enhanced defense signaling.

Taken together, our results provide evidence that achieving substantial field resistance to *Oc* in pea requires the integration of low SL exudation with SL-independent resistance mechanisms. It will be particularly interesting to investigate whether this finding also applies to other legumes affected by *Oc* or to crops targeted by other Orobanchaceae species. The identification of candidate genes within resistance QTLs offers promising avenues for downstream functional studies. To this end, we are currently employing TILLING to functionally characterize the role of selected candidates. Additional approaches, such as conventional mutagenesis and recently established genome editing technologies in pea (Ludvíková et al., 2022; Li et al., 2023b), are also feasible and may complement our efforts.

In conclusion, we identified three new potential sources of field resistance to *Oc* in pea. This finding is highly relevant, as no commercially available cultivars currently provide resistance to this parasitic species, which remains a major constraint on pea cultivation in Mediterranean agro-ecosystems.

By integrating SL quantification with field phenotyping of diverse genetic resources, we demonstrated that low or absent SL exudation can confer only partial resistance to *Oc*. This highlights the need to expand breeding strategies beyond SL-based mechanisms, thus targeting additional SL-independent pathways.

Our results not only provide valuable information for pea improvement, but also offer new insights into the genetic complexity of resistance to parasitic Orobanchaceae. The identification of DEGs within QTLs associated with resistance points to molecular mechanisms potentially involved in both SL-dependent and independent responses. These findings lay the groundwork for functional validation of these genes by reverse genetics approaches.

Finally, the conceptual framework and methodologies applied in this study may be extended to other legume species and crops affected by Orobanchaceae, thereby broadening the impact of our research in the context of sustainable agriculture and parasitic weed management.

REFERENCES

Al-Babili, S., & Bouwmeester, H. J. (2015). Strigolactones, a novel carotenoid-derived plant hormone. *Annual Review of Plant Biology*, *66*(1), 161-186.

Albert, M., Axtell, M. J., & Timko, M. P. (2021). Mechanisms of resistance and virulence in parasitic plant–host interactions. *Plant Physiology*, *185*(4), 1282-1291.

Alder, A., Jamil, M., Marzorati, M., Bruno, M., Vermathen, M., Bigler, P., ... & Al-Babili, S. (2012). The path from β-carotene to carlactone, a strigolactone-like plant hormone. *Science*, *335*(6074), 1348-1351.

Bardaro, N., Marcotrigiano, A. R., Bracuto, V., Mazzeo, R., Ricciardi, F., Lotti, C., ... & Ricciardi, L. (2016). Genetic analysis of resistance to *Orobanche crenata* (Forsk.) in a pea (*Pisum sativum* L.) low-strigolactone line. *Journal of Plant Pathology*, 671-675.

Beveridge, C. A. (2000). Long-distance signalling and a mutational analysis of branching in pea. *Plant Growth Regulation*, *32*, 193-203.

Blighe, K., Rana, S., & Lewis, M. (2024). EnhancedVolcano: Publication-ready volcano plots with enhanced colouring and labeling. R package version 1.24.0. Available at: https://github.com/kevinblighe/EnhancedVolcano (Accessed December 16, 2024).

Bolger, A. M., Lohse, M., & Usadel, B. (2014). Trimmomatic: a flexible trimmer for Illumina sequence data. *Bioinformatics*, *30*(15), 2114-2120.

Bouwmeester, H., Li, C., Thiombiano, B., Rahimi, M., & Dong, L. (2021). Adaptation of the parasitic plant lifecycle: germination is controlled by essential host signaling molecules. *Plant Physiology*, *185*(4), 1292-1308.

Briache, F. Z., Ennami, M., Mbasani-Mansi, J., Lozzi, A., Abousalim, A., El Rodeny, W., ... & Mentag, R. (2020). Effects of salicylic acid and indole acetic acid exogenous applications on induction of faba bean resistance against *Orobanche crenata*. *The Plant Pathology Journal*, *36*(5), 476.

Brun, G., Braem, L., Thoiron, S., Gevaert, K., Goormachtig, S., & Delavault, P. (2018). Seed germination in parasitic plants: what insights can we expect from strigolactone research?. *Journal of Experimental Botany*, *69*(9), 2265-2280.

Butt, H., Jamil, M., Wang, J. Y., Al-Babili, S., & Mahfouz, M. (2018). Engineering plant architecture via CRISPR/Cas9-mediated alteration of strigolactone biosynthesis. *BMC Plant Biology*, *18*, 1-9.

Cass, C. L., Peraldi, A., Dowd, P. F., Mottiar, Y., Santoro, N., Karlen, S. D., ... & Sedbrook, J. C. (2015). Effects of *PHENYLALANINE AMMONIA LYASE* (*PAL*) knockdown on cell wall composition, biomass digestibility, and biotic and abiotic stress responses in *Brachypodium*. *Journal of Experimental Botany*, *66*(14), 4317-4335.

Chen, Y., Li, F., Tian, L., Huang, M., Deng, R., Li, X., ... & Wu, G. (2017). The phenylalanine ammonia lyase gene *LjPAL1* is involved in plant defense responses to pathogens and plays diverse roles in *Lotus japonicus*-rhizobium symbioses. *Molecular Plant-Microbe Interactions*, *30*(9), 739-753.

De Mendiburu, F., & Yaseen, M. (2020). AGRICOLAE: statistical procedures for agricultural research, version 1.2-4.

Delvento, C., Arcieri, F., Marcotrigiano, A. R., Guerriero, M., Fanelli, V., Dellino, M., ... & Pavan, S. (2023). High-density linkage mapping and genetic dissection of resistance to broomrape (*Orobanche crenata* Forsk.) in pea (*Pisum sativum* L.). *Frontiers in Plant Science*, *14*, 1216297.

Dobin, A., Davis, C. A., Schlesinger, F., Drenkow, J., Zaleski, C., Jha, S., ... & Gingeras, T. R. (2013). STAR: ultrafast universal RNA-seq aligner. *Bioinformatics*, *29*(1), 15-21.

Dor, E., Alperin, B., Wininger, S., Ben-Dor, B., Somvanshi, V. S., Koltai, H., ... & Hershenhorn, J. (2010). Characterization of a novel tomato mutant resistant to the weedy parasites *Orobanche* and *Phelipanche* spp. *Euphytica*, *171*, 371-380.

Duriez, P., Vautrin, S., Auriac, M. C., Bazerque, J., Boniface, M. C., Callot, C., ... & Muños, S. (2019). A receptor-like kinase enhances sunflower resistance to *Orobanche cumana*. *Nature Plants*, *5*(12), 1211-1215.

FAO (2022). FAOSTAT data. Available at: http://www.fao.org/faostat/

Fernández-Aparicio, M., Kisugi, T., Xie, X., Rubiales, D., & Yoneyama, K. (2014). Low strigolactone root exudation: a novel mechanism of broomrape (*Orobanche* and *Phelipanche* spp.) resistance available for faba bean breeding. *Journal of Agricultural and Food Chemistry*, *62*(29), 7063-7071.

Fernández-Aparicio, M., Reboud, X., & Gibot-Leclerc, S. (2016). Broomrape weeds. Underground mechanisms of parasitism and associated strategies for their control: a review. *Frontiers in Plant Science*, *7*, 135.

Fishman, M. R., & Shirasu, K. (2021). How to resist parasitic plants: pre-and post-attachment strategies. *Current Opinion in Plant Biology*, *62*, 102004.

Fukui, K., Ito, S., Ueno, K., Yamaguchi, S., Kyozuka, J., & Asami, T. (2011). New branching inhibitors and their potential as strigolactone mimics in rice. *Bioorganic & Medicinal Chemistry Letters*, *21*(16), 4905-4908.

Galili, S., Hershenhorn, J., Smirnov, E., Yoneyama, K., Xie, X., Amir-Segev, O., ... & Dor, E. (2021). Characterization of a chickpea mutant resistant to *Phelipanche aegyptiaca* Pers. and *Orobanche crenata* Forsk. *Plants*, *10*(12), 2552.

Gobena, D., Shimels, M., Rich, P. J., Ruyter-Spira, C., Bouwmeester, H., Kanuganti, S., ... & Ejeta, G. (2017). Mutation in sorghum *LOW GERMINATION STIMULANT 1* alters strigolactones and causes *Striga* resistance. *Proceedings of the National Academy of Sciences*, *114*(17), 4471-4476.

Gomez-Roldan, V., Fermas, S., Brewer, P. B., Puech-Pagès, V., Dun, E. A., Pillot, J. P., ... & Rochange, S. F. (2008). Strigolactone inhibition of shoot branching. *Nature*, *455*(7210), 189-194.

Guercio, A. M., Palayam, M., & Shabek, N. (2023). Strigolactones: diversity, perception, and hydrolysis. *Phytochemistry Reviews*, *22*(2), 339-359.

Hao, J., Yang, Y., Futrell, S., Kelly, E. A., Lorts, C. M., Nebie, B., ... & Schachtman, D. P. (2023). CRISPR/Cas9-mediated mutagenesis of *carotenoid cleavage dioxygenase* (*CCD*) genes in sorghum alters strigolactone biosynthesis and plant biotic interactions. *Phytobiomes Journal*, *7*(3), 339-351.

Jamil, M., Rodenburg, J., Charnikhova, T., & Bouwmeester, H. J. (2011). Pre-attachment *Striga hermonthica* resistance of New Rice for Africa (NERICA) cultivars based on low strigolactone production. *New Phytologist*, *192*(4), 964-975.

Jamil, M., Margueritte, O., Yonli, D., Wang, J. Y., Navangi, L., Mudavadi, P., ... & Al-Babili, S. (2024). Evaluation of granular formulated strigolactone analogs for *Striga* suicidal germination. *Pest Management Science*, *80*(9), 4314-4321.

Jhu, M. Y., & Sinha, N. R. (2022). Parasitic plants: an overview of mechanisms by which plants perceive and respond to parasites. *Annual Review of Plant Biology*, *73*(1), 433-455.

Jhu, M. Y., Kawa, D., & Brady, S. M. (2023). The genetic basis of plants' battle against witchweeds: linking immune responses to distinct resistance mechanisms. *Journal of Experimental Botany*, *74*(17), 4903-4909.

Jia, K. P., Baz, L., & Al-Babili, S. (2018). From carotenoids to strigolactones. *Journal of Experimental Botany*, *69*(9), 2189-2204.

Johnson, X., Brcich, T., Dun, E. A., Goussot, M., Haurogné, K., Beveridge, C. A., & Rameau, C. (2006). Branching genes are conserved across species. Genes controlling a novel signal in pea are coregulated by other long-distance signals. *Plant Physiology*, *142*(3), 1014-1026.

Karniel, U., Koch, A., Bar Nun, N., Zamir, D., & Hirschberg, J. (2024). Tomato Mutants Reveal Root and Shoot Strigolactone Involvement in Branching and Broomrape Resistance. *Plants*, *13*(11), 1554.

Kawada, K., Takahashi, I., Takei, S., Nomura, A., Seto, Y., Fukui, K., & Asami, T. (2024). The Evaluation of Debranone Series Strigolactone Agonists for Germination Stimulants in *Orobanche* Species. *Journal of Agricultural and Food Chemistry*, *72*(35), 19517-19525.

Kohlen, W., Charnikhova, T., Lammers, M., Pollina, T., Tóth, P., Haider, I., ... & López-Ráez, J. A. (2012). The tomato *CAROTENOID CLEAVAGE DIOXYGENASE 8* (*SlCCD8*) regulates rhizosphere signaling, plant

architecture and affects reproductive development through strigolactone biosynthesis. *New Phytologist*, *196*(2), 535-547.

Kolberg, L., Raudvere, U., Kuzmin, I., Vilo, J., & Peterson, H. (2020). gprofiler2--an R package for gene list functional enrichment analysis and namespace conversion toolset g: Profiler. *F1000Research*, *9*, ELIXIR-709.

Kreplak, J., Madoui, M. A., Cápal, P., Novák, P., Labadie, K., Aubert, G., ... & Burstin, J. (2019). A reference genome for pea provides insight into legume genome evolution. *Nature Genetics*, *51*(9), 1411-1422.

Li, C., Dong, L., Durairaj, J., Guan, J. C., Yoshimura, M., Quinodoz, P., ... & Bouwmeester, H. J. (2023a). Maize resistance to witchweed through changes in strigolactone biosynthesis. *Science*, *379*(6627), 94-99.

Li, G., Liu, R., Xu, R., Varshney, R. K., Ding, H., Li, M., ... & Yang, T. (2023b). Development of an Agrobacterium-mediated CRISPR/Cas9 system in pea (*Pisum sativum* L.). *The Crop Journal*, *11*(1), 132-139.

Liao, Y., Smyth, G. K., & Shi, W. (2014). featureCounts: an efficient general purpose program for assigning sequence reads to genomic features. *Bioinformatics*, *30*(7), 923-930.

Love, M. I., Huber, W., & Anders, S. (2014). Moderated estimation of fold change and dispersion for RNA-seq data with DESeq2. *Genome Biology*, *15*, 1-21.

Lu, J., & Salzberg, S. L. (2020). Ultrafast and accurate 16S rRNA microbial community analysis using Kraken 2. *Microbiome*, *8*(1), 124.

Ludvíková, M., & Griga, M. (2022). Pea transformation: History, current status and challenges. *Czech Journal of Genetics and Plant Breeding*, *58*(3), 127-161.

Mabrouk, Y., Mejri, S., Hemissi, I., & Belhadj, O. (2016). Biochemical analysis of induced resistance in chickpea against broomrape (*Orobanche foetida*) by rhizobia inoculation. *Phytopathologia Mediterranea*, 54-61.

Martín-Sanz, A., Pérez-Vich, B., Rueda, S., Fernández-Martínez, J. M., & Velasco, L. (2020). Characterization of post-haustorial resistance to sunflower broomrape. *Crop Science*, *60*(3), 1188-1198.

Matusova, R., Rani, K., Verstappen, F. W., Franssen, M. C., Beale, M. H., & Bouwmeester, H. J. (2005). The strigolactone germination stimulants of the plant-parasitic *Striga* and *Orobanche* spp. are derived from the carotenoid pathway. *Plant Physiology*, *139*(2), 920-934.

Mohemed, N., Charnikhova, T., Fradin, E. F., Rienstra, J., Babiker, A. G., & Bouwmeester, H. J. (2018). Genetic variation in *Sorghum* bicolor strigolactones and their role in resistance against *Striga hermonthica*. *Journal of Experimental Botany*, *69*(9), 2415-2430.

Morris, S. E., Turnbull, C. G., Murfet, I. C., & Beveridge, C. A. (2001). Mutational analysis of branching in pea. Evidence that *Rms1* and *Rms5* regulate the same novel signal. *Plant Physiology*, *126*(3), 1205-1213.

Okonechnikov, K., Conesa, A., & García-Alcalde, F. (2016). Qualimap 2: advanced multi-sample quality control for high-throughput sequencing data. *Bioinformatics*, *32*(2), 292-294.

Parker, C. (2009). Observations on the current status of *Orobanche* and *Striga* problems worldwide. *Pest Management Science: formerly Pesticide Science*, *65*(5), 453-459.

Pavan, S., Schiavulli, A., Marcotrigiano, A. R., Bardaro, N., Bracuto, V., Ricciardi, F., ... & Ricciardi, L. (2016). Characterization of low-strigolactone germplasm in pea (*Pisum sativum* L.) resistant to crenate broomrape (*Orobanche crenata* Forsk.). *Molecular Plant-Microbe Interactions*, *29*(10), 743-749.

Pavan, S., Delvento, C., Nazzicari, N., Ferrari, B., D'Agostino, N., Taranto, F., ... & Annicchiarico, P. (2022). Merging genotyping-by-sequencing data from two *ex situ* collections provides insights on the pea evolutionary history. *Horticulture Research*, *9*, uhab062.

Renna, M., Serio, F., & Santamaria, P. (2015). Crenate broomrape (*Orobanche crenata* Forskal): prospects as a food product for human nutrition. *Genetic Resources and Crop Evolution*, *62*, 795-802.

Rispail, N., Dita, M. A., González-Verdejo, C., Pérez-de-Luque, A., Castillejo, M. A., Prats, E., ... & Rubiales, D. (2007). Plant resistance to parasitic plants: molecular approaches to an old foe. *New Phytologist*, *173*(4), 703-712.

Rubiales, D. (2014). Legume breeding for broomrape resistance. *Czech Journal of Genetics and Plant Breeding*, 50, 144–150.

Slowikowski, K., Schep, A., & Hughes, S. (2021). ggrepel: Automatically position non-overlapping text labels with 'ggplot2.' R package version 0.9 1.

Sorefan, K., Booker, J., Haurogné, K., Goussot, M., Bainbridge, K., Foo, E., ... & Leyser, O. (2003). *MAX4* and *RMS1* are orthologous dioxygenase-like genes that regulate shoot branching in *Arabidopsis* and pea. *Genes & Development*, *17*(12), 1469-1474.

Sun, Y., Qiao, Z., Muchero, W., & Chen, J. G. (2020). Lectin receptor-like kinases: the sensor and mediator at the plant cell surface. *Frontiers in Plant Science*, *11*, 596301.

Swarbrick, P. J., Huang, K., Liu, G., Slate, J., Press, M. C., & Scholes, J. D. (2008). Global patterns of gene expression in rice cultivars undergoing a susceptible or resistant interaction with the parasitic plant *Striga hermonthica*. *New Phytologist*, *179*(2), 515-529.

Takahashi, I., Fukui, K., & Asami, T. (2016). Chemical modification of a phenoxyfuranone-type strigolactone mimic for selective effects on rice tillering or *Striga hermonthica* seed germination. *Pest Management Science*, *72*(11), 2048-2053.

Trabelsi, I., Yoneyama, K., Abbes, Z., Amri, M., Xie, X., Kisugi, T., ... & Kharrat, M. (2017). Characterization of strigolactones produced by *Orobanche foetida* and *Orobanche crenata* resistant faba bean (*Vicia faba* L.) genotypes and effects of phosphorous, nitrogen, and potassium deficiencies on strigolactone production. *South African Journal of Botany*, *108*, 15-22.

Umehara, M., Hanada, A., Yoshida, S., Akiyama, K., Arite, T., Takeda-Kamiya, N., ... & Yamaguchi, S. (2008). Inhibition of shoot branching by new terpenoid plant hormones. *Nature*, *455*(7210), 195-200.

Uraguchi, D., Kuwata, K., Hijikata, Y., Yamaguchi, R., Imaizumi, H., Am, S., ... & Tsuchiya, Y. (2018). A femtomolar-range suicide germination stimulant for the parasitic plant *Striga hermonthica*. *Science*, *362*(6420), 1301-1305.

Wang, J. Y., Haider, I., Jamil, M., Fiorilli, V., Saito, Y., Mi, J., ... & Al-Babili, S. (2019). The apocarotenoid metabolite zaxinone regulates growth and strigolactone biosynthesis in rice. *Nature Communications*, *10*(1), 810.

Wang, J. Y., Chen, G. T. E., Braguy, J., & Al-Babili, S. (2024). Distinguishing the functions of canonical strigolactones as rhizospheric signals. *Trends in Plant Science*, *29*, 925-936.

Wickham, H., & Sievert, C. (2009). ggplot2: elegant graphics for data analysis (Vol. 10, pp. 978-0). New York: Springer.

Wohor, O. Z., Rispail, N., Ojiewo, C. O., & Rubiales, D. (2022). Pea breeding for resistance to rhizospheric pathogens. *Plants*, *11*(19), 2664.

Wu, F., Gao, Y., Yang, W., Sui, N., & Zhu, J. (2022). Biological functions of strigolactones and their crosstalk with other phytohormones. *Frontiers in Plant Science*, *13*, 821563.

Xie, X., Yoneyama, K., & Yoneyama, K. (2010). The strigolactone story. *Annual Review of Phytopathology*, *48*(1), 93-117.

Xu, Y., Zhang, J., Ma, C., Lei, Y., Shen, G., Jin, J., ... & Wu, J. (2022). Comparative genomics of *orobanchaceous* species with different parasitic lifestyles reveals the origin and stepwise evolution of plant parasitism. *Molecular Plant*, *15*(8), 1384-1399.

Yang, T., Liu, R., Luo, Y., Hu, S., Wang, D., Wang, C., ... & Zong, X. (2022). Improved pea reference genome and pan-genome highlight genomic features and evolutionary characteristics. *Nature Genetics*, *54*(10), 1553-1563.

Yoneyama, K., Xie, X., Yoneyama, K., Kisugi, T., Nomura, T., Nakatani, Y., ... & McErlean, C. S. (2018). Which are the major players, canonical or non-canonical strigolactones?. *Journal of Experimental Botany*, *69*(9), 2231-2239.

Zhang, Y., Haider, I., Ruyter-Spira, C., & Bouwmeester, H. J. (2013). Strigolactone biosynthesis and biology. *Molecular Microbial Ecology of the Rhizosphere*, *1*, 355-371.

Supplementary materials

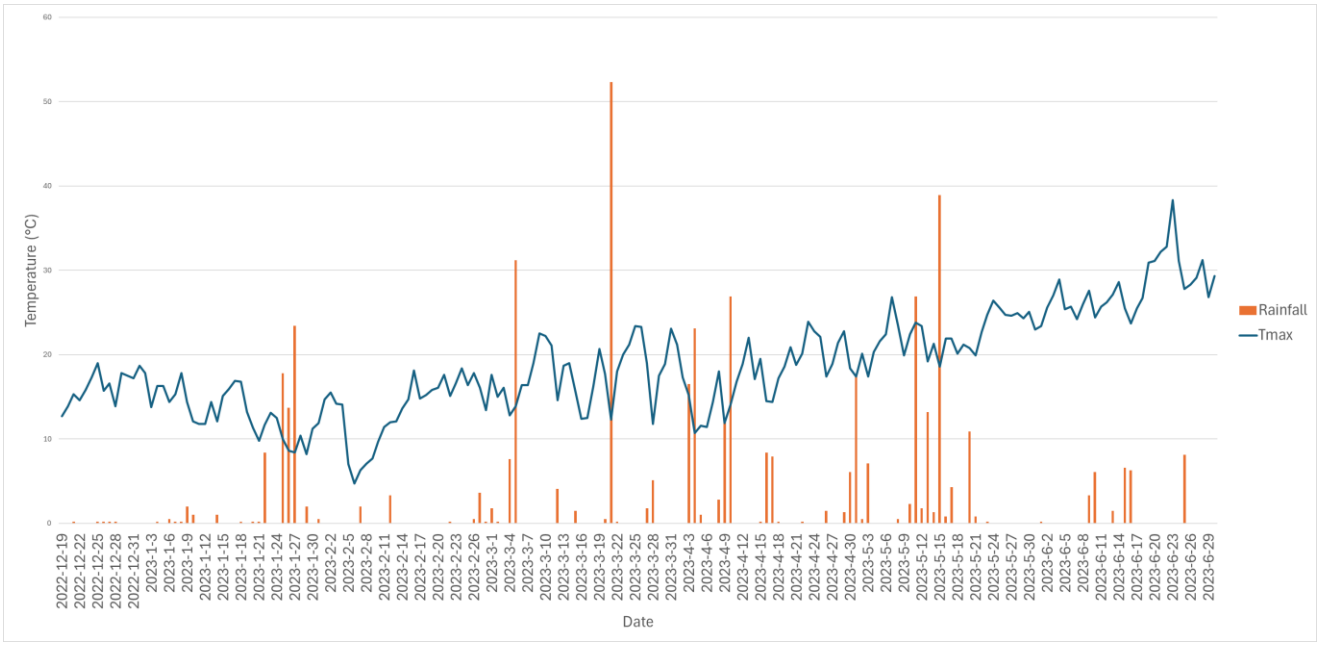

Supplementary Figure S1. Climatic data for the field trial conducted in 2022–2023.

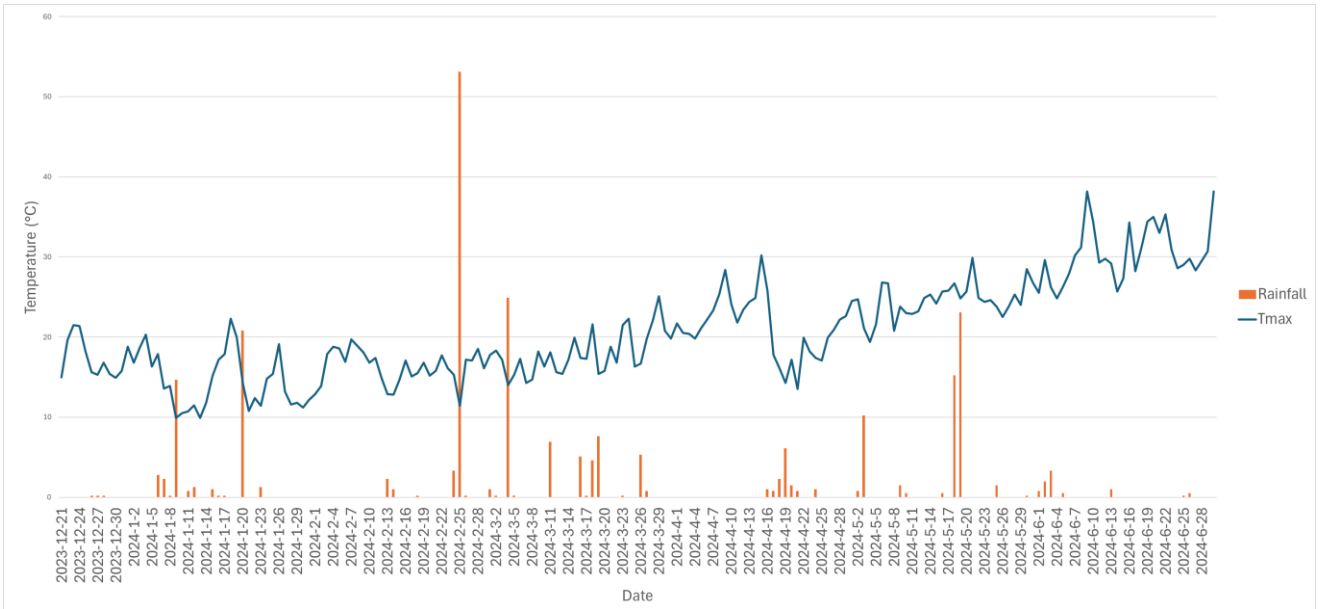

Supplementary Figure S2. Climatic data for the field trial conducted in 2023–2024.

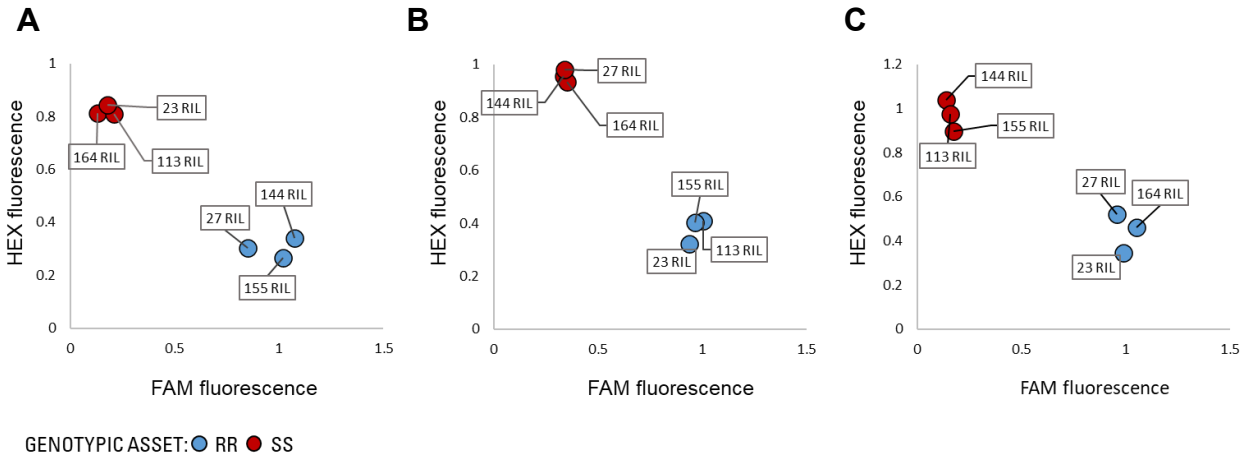

Supplementary Figure S3. KASP assays for the *PsOcr-1* **(A)**, *PsOcr-2* **(B)**, and *PsOcr-3* **(C)** quantitative trait loci (QTLs) associated with pea resistance to *O. crenata*.

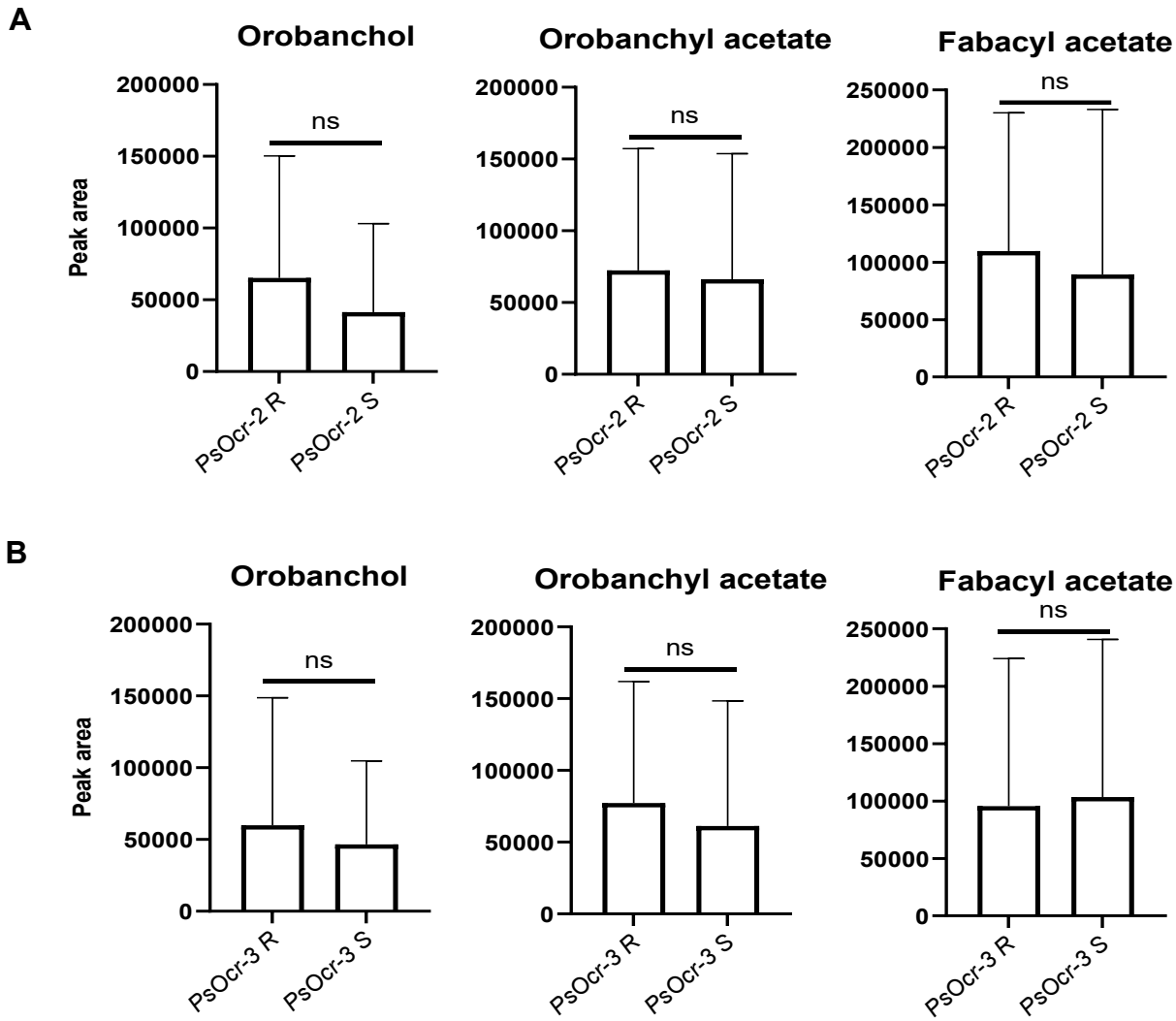

Supplementary Figure S4. Orobanchol, orobanchyl acetate and fabacyl acetate peak areas associated with the root exudates of RILs homozygous for the resistance (R) or susceptibility (S) allele at **(A)** *PsOcr-2* and **(B)** *PsOcr-3*. Data are shown as means ± SE (n = 4). ns indicate no significant difference ($p > 0.05$, Student's t-test)

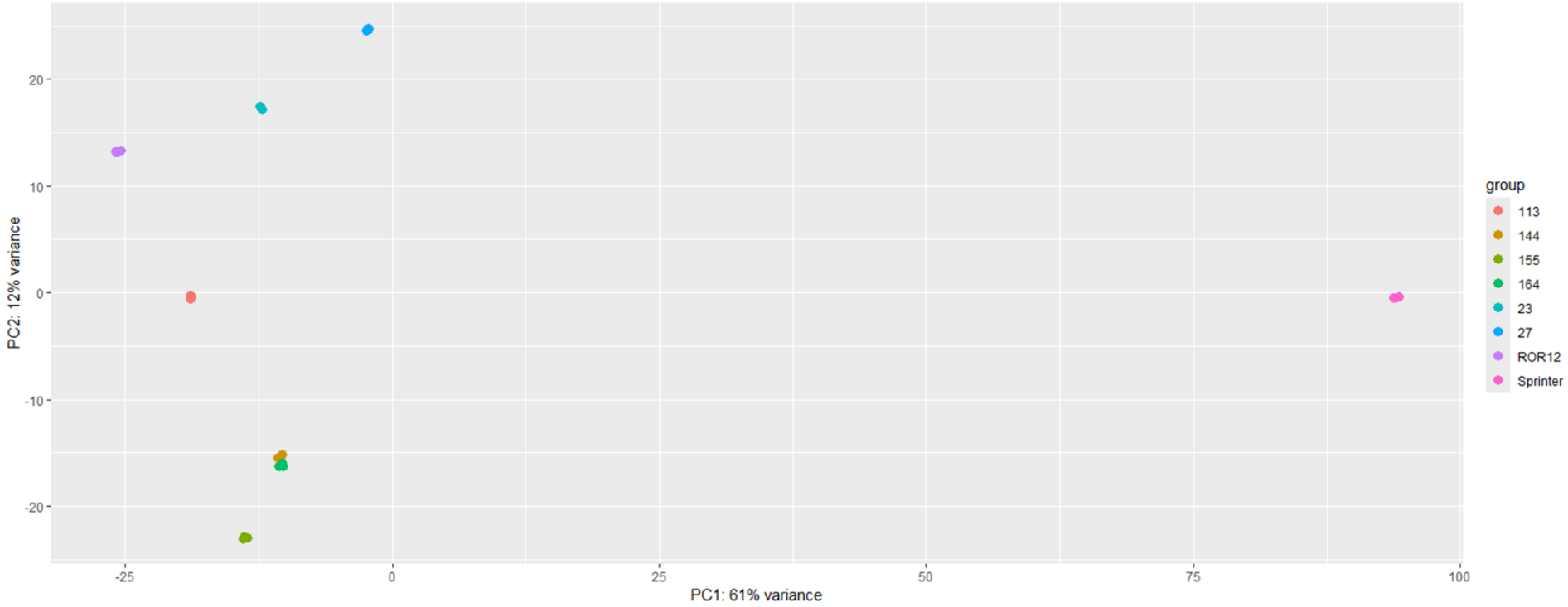

Supplementary Figure S5. Principal component analysis for the transcriptional profiles of ROR12, Sprinter and six recombinant inbred lines originating from their cross. Dots of the same color indicate biological replicates of the same genotype (n = 3)

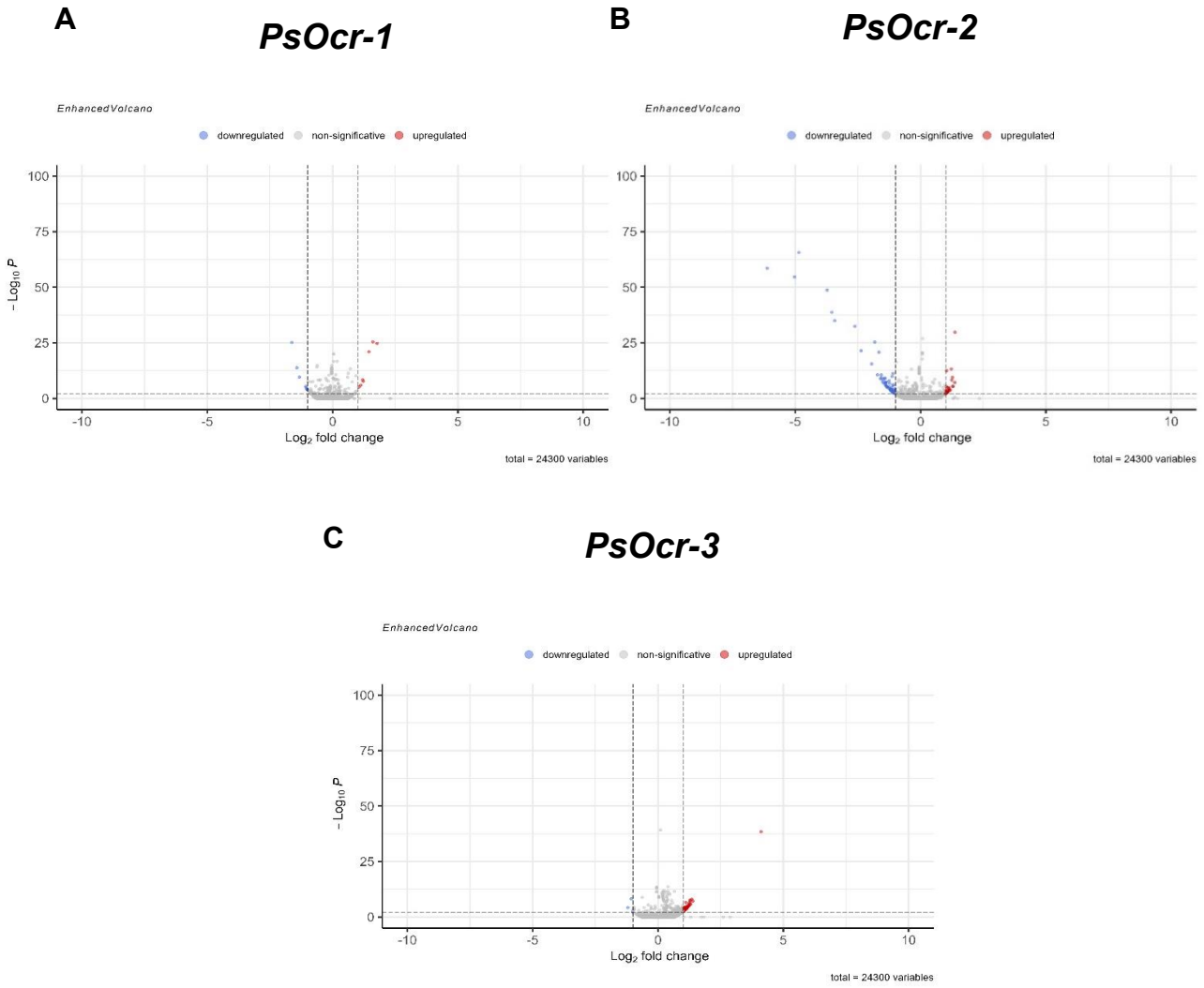

Supplementary Figure S6. Volcano plots showing differentially expressed genes between lines homozygous for the resistance (R) and susceptibility (S) allele at **(A)** *PsOcr-1*, **(B)** *PsOcr-2*, and **(C)** *PsOcr-3*.

Supplementary Table S1. Information on the germplasm panel evaluated in this study for response to *O. crenata*

Accession number	Origin	Genebank
PI_102888	CHN	USDA_PSPP
PI_103058	CHN	USDA_PSPP
PI_116056	IND	USDA_PSPP
PI_117264	TUR	USDA_PSPP
PI_117998	BRA	USDA_PSPP
PI_118501	BRA	USDA_PSPP
PI_121352	IND	USDA_PSPP
PI_134271	AFG	USDA_PSPP
PI_142775	MEX	USDA_PSPP
PI_143485	AZE	USDA_PSPP
PI_156647	ETH	USDA_PSPP
PI_162909	PRY	USDA_PSPP
PI_163126	IND	USDA_PSPP
PI_163129	IND	USDA_PSPP
PI_164612	IND	USDA_PSPP
PI_164971	TUR	USDA_PSPP
PI_166159	NPL	USDA_PSPP
PI_169608	TUR	USDA_PSPP
PI_179449	TUR	USDA_PSPP
PI_179450	SYR	USDA_PSPP
PI_179451	SYR	USDA_PSPP
PI_179459	TUR	USDA_PSPP
PI_179722	IND	USDA_PSPP
PI_180329	IND	USDA_PSPP
PI_180702	GER	USDA_PSPP
PI_181799	LBN	USDA_PSPP
PI_181801	LBN	USDA_PSPP
PI_181958	SYR	USDA_PSPP
PI_184784	GIN	USDA_PSPP
PI_193578	ETH	USDA_PSPP
PI_193584	ETH	USDA_PSPP
PI_195020	ETH	USDA_PSPP
PI_195631	ETH	USDA_PSPP
PI_197990	NLD	USDA_PSPP
PI_198074	SWE	USDA_PSPP
PI_203068	FIN	USDA_PSPP
PI_204306	AUS	USDA_PSPP
PI_206838	USA	USDA_PSPP
PI_210561	RUS	USDA_PSPP
PI_210569	FIN	USDA_PSPP
PI_210571	FIN	USDA_PSPP
PI_212917	IND	USDA_PSPP
PI_221697	IDN	USDA_PSPP
PI_236492	USA	USDA_PSPP
PI_241593	TWN	USDA_PSPP
PI_242028	DNK	USDA_PSPP
PI_248181	RWA	USDA_PSPP
PI_250440	CSK	USDA_PSPP
PI_250441	CSK	USDA_PSPP
PI_250446	CSK	USDA_PSPP
PI_261622	SPA	USDA_PSPP
PI_263014	NLD	USDA_PSPP
PI_263030	FRA	USDA_PSPP
PI_263032	FRA	USDA_PSPP
PI_263871	GRC	USDA_PSPP
PI_269762	UK	USDA_PSPP
PI_269777	UK	USDA_PSPP
PI_269778	UK	USDA_PSPP
PI_269782	UK	USDA_PSPP
PI_269802	UK	USDA_PSPP
PI_269825	UK	USDA_PSPP
PI_271038	NPL	USDA_PSPP
PI_272148	FIN	USDA_PSPP
PI_272171	GER	USDA_PSPP
PI_272184	GRC	USDA_PSPP
PI_272194	GER	USDA_PSPP
PI_272215	GER	USDA_PSPP
PI_272216	BGR	USDA_PSPP
PI_273605	ECU	USDA_PSPP

Accession number	Origin	Genebank
PI_274584	NOR	USDA_PSPP
PI_275822	SWE	USDA_PSPP
PI_280609	RUS	USDA_PSPP
PI_280613	RUS	USDA_PSPP
PI_280614	RUS	USDA_PSPP
PI_280619	EST	USDA_PSPP
PI_280626	RUS	USDA_PSPP
PI_285718	POL	USDA_PSPP
PI_285747	POL	USDA_PSPP
PI_286607	THA	USDA_PSPP
PI_288025	FRA	USDA_PSPP
PI_293426	BGR	USDA_PSPP
PI_306591	HUN	USDA_PSPP
PI_314794	AUS	USDA_PSPP
PI_324695	HUN	USDA_PSPP
PI_324697	HUN	USDA_PSPP
PI_324700	HUN	USDA_PSPP
PI_324702	HUN	USDA_PSPP
PI_324703	HUN	USDA_PSPP
PI_331414	ETH	USDA_PSPP
PI_343338	USA	USDA_PSPP
PI_343987	TUR	USDA_PSPP
PI_347295	IND	USDA_PSPP
PI_347490	IND	USDA_PSPP
PI_347496	IND	USDA_PSPP
PI_355906	JPN	USDA_PSPP
PI_356974	IND	USDA_PSPP
PI_356980	IND	USDA_PSPP
PI_356986	IND	USDA_PSPP
PI_356992	IND	USDA_PSPP
PI_393490	CSK	USDA_PSPP
PI_409031	GER	USDA_PSPP
PI_413678	HUN	USDA_PSPP
PI_413698	HUN	USDA_PSPP
PI_413703	HUN	USDA_PSPP
PI_429849	UZB	USDA_PSPP
PI_476409	LVA	USDA_PSPP
PI_476413	RUS	USDA_PSPP
PI_486131	ECU	USDA_PSPP
PI_494077	CHL	USDA_PSPP
PI_499982	CHN	USDA_PSPP
PI_505062	GRC	USDA_PSPP
PI_505080	CYP	USDA_PSPP
PI_505108	GRC	USDA_PSPP
PI_505122	ALB	USDA_PSPP
PI_505127	ALB	USDA_PSPP
PI_601516	NLD	USDA_PSPP
PI_619079	USA	USDA_PSPP
PI_639974	GEO	USDA_PSPP
PI_639980	BGR	USDA_PSPP
PI_639981	BGR	USDA_PSPP
PS-00168	ITA	DISSPA
PS-00169	ITA	DISSPA
PS-00300	ITA	DISSPA
W6_15008	ISR	USDA_PSPP
W6_26160	GEO	USDA_PSPP
W6_31707	RUS	USDA_PSPP
W6_44716	CHN	USDA_PSPP
W6_44718	CHN	USDA_PSPP
W6_44720	CHN	USDA_PSPP
W6_44724	CHN	USDA_PSPP
W6_44725	CHN	USDA_PSPP
W6_44726	CHN	USDA_PSPP
W6_44766	CHN	USDA_PSPP
W6_44768	CHN	USDA_PSPP
W6_44769	CHN	USDA_PSPP
W6_44770	CHN	USDA_PSPP

Supplementary Table S2. Number of *O. crenata* shoots emerged on the cultivar Sprinter within each experimental block of the field trials carried out in 2022-2023 and 2023-2024. Data are presented as means ± SD.

Genotype	Block	Growing season	Average *Oc* shoots	SD
Sprinter	1	2022-2023	10	1.732
Sprinter	2	2022-2023	11.4	1.342
Sprinter	3	2022-2023	13.8	1.789
Sprinter	1	2023-2024	9.6	1.140
Sprinter	2	2023-2024	6.8	0.837
Sprinter	3	2023-2024	4.6	0.548
Sprinter	4	2023-2024	5	0.816

Supplementary Table S3. ANOVA for response to *O. crenata* of the pea germplasm panel evaluated in this study.

	Df	Sum Sq	Mean Sq	F value	Pr(>F)
Genotype	135	117.23207	0.86838571	1.4974133	0.00134825
Replication	1	0.7648095	0.76480954	1.3188102	0.25146088
Year	1	287.66838	287.668375	496.04506	4.51E-73
Genotype:Year	135	42.346641	0.31367882	0.5408965	0.99998131
Residuals	419	242.9881	0.57992387		

Supplementary Table S4. Mean infestation data of *O. crenata* recorded on the pea germplasm panel over two growing seasons (2022–2023 and 2023–2024). Means were calculated using three replicates in 2022–2023 and four replicates in 2023–2024.

Accession number	Growing season	Mean number of emerged *Oc* shoot	Origin	Genebank
PI_102888	2022-2023	11	CHN	USDA_PSPP
PI_102888	2023-2024	4	CHN	USDA_PSPP
PI_103058	2022-2023	10.5	CHN	USDA_PSPP
PI_103058	2023-2024	2.5	CHN	USDA_PSPP
PI_116056	2022-2023	14.67	IND	USDA_PSPP
PI_116056	2023-2024	7	IND	USDA_PSPP
PI_117264	2022-2023	18.67	TUR	USDA_PSPP
PI_117264	2023-2024	5	TUR	USDA_PSPP
PI_117998	2022-2023	22.67	BRA	USDA_PSPP
PI_117998	2023-2024	8.33	BRA	USDA_PSPP
PI_118501	2022-2023	17.67	BRA	USDA_PSPP
PI_118501	2023-2024	3.5	BRA	USDA_PSPP
PI_121352	2022-2023	17	IND	USDA_PSPP
PI_121352	2023-2024	3.67	IND	USDA_PSPP
PI_134271	2022-2023	11	AFG	USDA_PSPP
PI_134271	2023-2024	4	AFG	USDA_PSPP
PI_142775	2022-2023	25.5	MEX	USDA_PSPP
PI_142775	2023-2024	7.25	MEX	USDA_PSPP
PI_143485	2022-2023	14.67	AZE	USDA_PSPP
PI_143485	2023-2024	5.67	AZE	USDA_PSPP
PI_156647	2022-2023	25	ETH	USDA_PSPP
PI_156647	2023-2024	6.33	ETH	USDA_PSPP
PI_162909	2022-2023	16.67	PRY	USDA_PSPP
PI_162909	2023-2024	3	PRY	USDA_PSPP
PI_163126	2022-2023	11.67	IND	USDA_PSPP
PI_163126	2023-2024	5	IND	USDA_PSPP
PI_163129	2022-2023	13.33	IND	USDA_PSPP
PI_163129	2023-2024	8.5	IND	USDA_PSPP
PI_164612	2022-2023	11.5	IND	USDA_PSPP
PI_164612	2023-2024	7	IND	USDA_PSPP

Accession number	Growing season	Mean number of emerged *Oc* shoot	Origin	Genebank
PI_263030	2022-2023	13	FRA	USDA_PSPP
PI_263030	2023-2024	4.5	FRA	USDA_PSPP
PI_263032	2022-2023	10.67	FRA	USDA_PSPP
PI_263032	2023-2024	7	FRA	USDA_PSPP
PI_263871	2022-2023	11.33	GRC	USDA_PSPP
PI_263871	2023-2024	7	GRC	USDA_PSPP
PI_269762	2022-2023	10.33	UK	USDA_PSPP
PI_269762	2023-2024	4.33	UK	USDA_PSPP
PI_269777	2022-2023	20.33	UK	USDA_PSPP
PI_269777	2023-2024	4	UK	USDA_PSPP
PI_269778	2022-2023	16.33	UK	USDA_PSPP
PI_269778	2023-2024	4	UK	USDA_PSPP
PI_269782	2022-2023	11.33	UK	USDA_PSPP
PI_269782	2023-2024	4	UK	USDA_PSPP
PI_269802	2022-2023	16	UK	USDA_PSPP
PI_269802	2023-2024	6.75	UK	USDA_PSPP
PI_269825	2022-2023	18.67	UK	USDA_PSPP
PI_269825	2023-2024	7	UK	USDA_PSPP
PI_271038	2022-2023	20	NPL	USDA_PSPP
PI_271038	2023-2024	8	NPL	USDA_PSPP
PI_272148	2022-2023	10.67	FIN	USDA_PSPP
PI_272148	2023-2024	4	FIN	USDA_PSPP
PI_272171	2022-2023	20	GER	USDA_PSPP
PI_272171	2023-2024	7.33	GER	USDA_PSPP
PI_272184	2022-2023	18.33	GRC	USDA_PSPP
PI_272184	2023-2024	5	GRC	USDA_PSPP
PI_272194	2022-2023	20.33	GER	USDA_PSPP
PI_272194	2023-2024	5.67	GER	USDA_PSPP
PI_272215	2022-2023	21	GER	USDA_PSPP
PI_272215	2023-2024	4	GER	USDA_PSPP

Accession number	Growing season	Mean number of emerged *Oc* shoot	Origin	Genebank
PI_164971	2022-2023	15.33	TUR	USDA_PSPP
PI_164971	2023-2024	8.5	TUR	USDA_PSPP
PI_166159	2022-2023	14.67	NPL	USDA_PSPP
PI_166159	2023-2024	8	NPL	USDA_PSPP
PI_169608	2022-2023	11	TUR	USDA_PSPP
PI_169608	2023-2024	5	TUR	USDA_PSPP
PI_179449	2022-2023	18.67	TUR	USDA_PSPP
PI_179449	2023-2024	3.67	TUR	USDA_PSPP
PI_179450	2022-2023	17	SYR	USDA_PSPP
PI_179450	2023-2024	5	SYR	USDA_PSPP
PI_179451	2022-2023	25.33	SYR	USDA_PSPP
PI_179451	2023-2024	7	SYR	USDA_PSPP
PI_179459	2022-2023	16.67	TUR	USDA_PSPP
PI_179459	2023-2024	2.5	TUR	USDA_PSPP
PI_179722	2022-2023	6.67	IND	USDA_PSPP
PI_179722	2023-2024	2	IND	USDA_PSPP
PI_180329	2022-2023	7.67	IND	USDA_PSPP
PI_180329	2023-2024	2.5	IND	USDA_PSPP
PI_180702	2022-2023	17	GER	USDA_PSPP
PI_180702	2023-2024	2.33	GER	USDA_PSPP
PI_181799	2022-2023	16.5	LBN	USDA_PSPP
PI_181799	2023-2024	3	LBN	USDA_PSPP
PI_181801	2022-2023	21.67	LBN	USDA_PSPP
PI_181801	2023-2024	6.5	LBN	USDA_PSPP
PI_181958	2022-2023	18.33	SYR	USDA_PSPP
PI_181958	2023-2024	7	SYR	USDA_PSPP
PI_184784	2022-2023	21.33	GIN	USDA_PSPP
PI_184784	2023-2024	4	GIN	USDA_PSPP
PI_193578	2022-2023	7	ETH	USDA_PSPP
PI_193578	2023-2024	5	ETH	USDA_PSPP
PI_193584	2022-2023	12.67	ETH	USDA_PSPP
PI_193584	2023-2024	5	ETH	USDA_PSPP
PI_195020	2022-2023	21	ETH	USDA_PSPP
PI_195020	2023-2024	5.33	ETH	USDA_PSPP
PI_195631	2022-2023	17.33	ETH	USDA_PSPP
PI_195631	2023-2024	5.5	ETH	USDA_PSPP
PI_197990	2022-2023	19.33	NLD	USDA_PSPP
PI_197990	2023-2024	5.5	NLD	USDA_PSPP
PI_198074	2022-2023	23	SWE	USDA_PSPP
PI_198074	2023-2024	6	SWE	USDA_PSPP
PI_203068	2022-2023	9	FIN	USDA_PSPP
PI_203068	2023-2024	5	FIN	USDA_PSPP
PI_204306	2022-2023	24.67	AUS	USDA_PSPP
PI_204306	2023-2024	7.5	AUS	USDA_PSPP
PI_206838	2022-2023	16.33	USA	USDA_PSPP
PI_206838	2023-2024	4	USA	USDA_PSPP
PI_210561	2022-2023	11	RUS	USDA_PSPP
PI_210561	2023-2024	4	RUS	USDA_PSPP
PI_210569	2022-2023	18.67	FIN	USDA_PSPP
PI_210569	2023-2024	3	FIN	USDA_PSPP
PI_210571	2022-2023	26.33	FIN	USDA_PSPP
PI_210571	2023-2024	5.5	FIN	USDA_PSPP
PI_212917	2022-2023	19.33	IND	USDA_PSPP
PI_212917	2023-2024	4	IND	USDA_PSPP
PI_221697	2022-2023	10	IDN	USDA_PSPP
PI_221697	2023-2024	6.5	IDN	USDA_PSPP
PI_236492	2022-2023	25	USA	USDA_PSPP
PI_236492	2023-2024	7	USA	USDA_PSPP
PI_241593	2022-2023	18	TWN	USDA_PSPP
PI_241593	2023-2024	3.5	TWN	USDA_PSPP
PI_242028	2022-2023	22.33	DNK	USDA_PSPP
PI_242028	2023-2024	4	DNK	USDA_PSPP
PI_248181	2022-2023	18.67	RWA	USDA_PSPP
PI_248181	2023-2024	5	RWA	USDA_PSPP
PI_250440	2022-2023	15.67	CSK	USDA_PSPP
PI_250440	2023-2024	3	CSK	USDA_PSPP
PI_272216	2022-2023	24.33	BGR	USDA_PSPP
PI_272216	2023-2024	4	BGR	USDA_PSPP
PI_273605	2022-2023	24	ECU	USDA_PSPP
PI_273605	2023-2024	5.33	ECU	USDA_PSPP
PI_274584	2022-2023	23.33	NOR	USDA_PSPP
PI_274584	2023-2024	8.33	NOR	USDA_PSPP
PI_275822	2022-2023	10.67	SWE	USDA_PSPP
PI_275822	2023-2024	4.5	SWE	USDA_PSPP
PI_280609	2022-2023	15	RUS	USDA_PSPP
PI_280609	2023-2024	3	RUS	USDA_PSPP
PI_280613	2022-2023	26.33	RUS	USDA_PSPP
PI_280613	2023-2024	7	RUS	USDA_PSPP
PI_280614	2022-2023	13	RUS	USDA_PSPP
PI_280614	2023-2024	6	RUS	USDA_PSPP
PI_280619	2022-2023	20	EST	USDA_PSPP
PI_280619	2023-2024	4	EST	USDA_PSPP
PI_280626	2022-2023	17.67	RUS	USDA_PSPP
PI_280626	2023-2024	4	RUS	USDA_PSPP
PI_285718	2022-2023	18	POL	USDA_PSPP
PI_285718	2023-2024	5	POL	USDA_PSPP
PI_285747	2022-2023	5	POL	USDA_PSPP
PI_285747	2023-2024	2	POL	USDA_PSPP
PI_286607	2022-2023	21	THA	USDA_PSPP
PI_286607	2023-2024	5	THA	USDA_PSPP
PI_288025	2022-2023	18	FRA	USDA_PSPP
PI_288025	2023-2024	7	FRA	USDA_PSPP
PI_293426	2022-2023	19.67	BGR	USDA_PSPP
PI_293426	2023-2024	8	BGR	USDA_PSPP
PI_306591	2022-2023	13.5	HUN	USDA_PSPP
PI_306591	2023-2024	7	HUN	USDA_PSPP
PI_314794	2022-2023	20.67	AUS	USDA_PSPP
PI_314794	2023-2024	7.75	AUS	USDA_PSPP
PI_324695	2022-2023	14.33	HUN	USDA_PSPP
PI_324695	2023-2024	6.5	HUN	USDA_PSPP
PI_324697	2022-2023	22.33	HUN	USDA_PSPP
PI_324697	2023-2024	5.5	HUN	USDA_PSPP
PI_324700	2022-2023	10.33	HUN	USDA_PSPP
PI_324700	2023-2024	4	HUN	USDA_PSPP
PI_324702	2022-2023	21	HUN	USDA_PSPP
PI_324702	2023-2024	6.5	HUN	USDA_PSPP
PI_324703	2022-2023	26.33	HUN	USDA_PSPP
PI_324703	2023-2024	5.33	HUN	USDA_PSPP
PI_331414	2022-2023	12.67	ETH	USDA_PSPP
PI_331414	2023-2024	7.33	ETH	USDA_PSPP
PI_343338	2022-2023	23	USA	USDA_PSPP
PI_343338	2023-2024	6.67	USA	USDA_PSPP
PI_343987	2022-2023	21.33	TUR	USDA_PSPP
PI_343987	2023-2024	7.33	TUR	USDA_PSPP
PI_347295	2022-2023	16.33	IND	USDA_PSPP
PI_347295	2023-2024	5.75	IND	USDA_PSPP
PI_347490	2022-2023	18.67	IND	USDA_PSPP
PI_347490	2023-2024	7	IND	USDA_PSPP
PI_347496	2022-2023	15	IND	USDA_PSPP
PI_347496	2023-2024	6	IND	USDA_PSPP
PI_355906	2022-2023	20.67	JPN	USDA_PSPP
PI_355906	2023-2024	6.33	JPN	USDA_PSPP
PI_356974	2022-2023	12	IND	USDA_PSPP
PI_356974	2023-2024	4.67	IND	USDA_PSPP
PI_356980	2022-2023	17	IND	USDA_PSPP
PI_356980	2023-2024	6.67	IND	USDA_PSPP
PI_356986	2022-2023	20	IND	USDA_PSPP
PI_356986	2023-2024	6.5	IND	USDA_PSPP
PI_356992	2022-2023	12.33	IND	USDA_PSPP
PI_356992	2023-2024	5	IND	USDA_PSPP
PI_393490	2022-2023	18.67	CSK	USDA_PSPP
PI_393490	2023-2024	5	CSK	USDA_PSPP

Accession number	Growing season	Mean number of emerged *Oc* shoot	Origin	Genebank
PI_250441	2022-2023	24.67	CSK	USDA_PSPP
PI_250441	2023-2024	5	CSK	USDA_PSPP
PI_250446	2022-2023	16.67	CSK	USDA_PSPP
PI_250446	2023-2024	3	CSK	USDA_PSPP
PI_261622	2022-2023	6	SPA	USDA_PSPP
PI_261622	2023-2024	5	SPA	USDA_PSPP
PI_263014	2022-2023	22	NLD	USDA_PSPP
PI_263014	2023-2024	4.5	NLD	USDA_PSPP
PI_429849	2022-2023	24.67	UZB	USDA_PSPP
PI_429849	2023-2024	8	UZB	USDA_PSPP
PI_476409	2022-2023	26.33	LVA	USDA_PSPP
PI_486131	2022-2023	23.33	ECU	USDA_PSPP
PI_486131	2023-2024	6.33	ECU	USDA_PSPP
PI_494077	2022-2023	13.33	CHL	USDA_PSPP
PI_494077	2023-2024	3.67	CHL	USDA_PSPP
PI_499982	2022-2023	18.67	CHN	USDA_PSPP
PI_499982	2023-2024	3.5	CHN	USDA_PSPP
PI_505062	2022-2023	24	GRC	USDA_PSPP
PI_505062	2023-2024	6	GRC	USDA_PSPP
PI_505080	2022-2023	25.33	CYP	USDA_PSPP
PI_505080	2023-2024	5	CYP	USDA_PSPP
PI_505108	2022-2023	13.33	GRC	USDA_PSPP
PI_505108	2023-2024	7	GRC	USDA_PSPP
PI_505122	2022-2023	10.33	ALB	USDA_PSPP
PI_505122	2023-2024	3	ALB	USDA_PSPP
PI_505127	2022-2023	20.67	ALB	USDA_PSPP
PI_505127	2023-2024	6.5	ALB	USDA_PSPP
PI_601516	2022-2023	11.33	NLD	USDA_PSPP
PI_601516	2023-2024	5.5	NLD	USDA_PSPP
PI_619079	2022-2023	17.67	USA	USDA_PSPP
PI_619079	2023-2024	4.67	USA	USDA_PSPP
PI_639974	2022-2023	16.33	GEO	USDA_PSPP
PI_639974	2023-2024	4.33	GEO	USDA_PSPP
PI_639980	2022-2023	18.33	BGR	USDA_PSPP
PI_639980	2023-2024	5	BGR	USDA_PSPP
PI_639981	2022-2023	19	BGR	USDA_PSPP
PI_639981	2023-2024	5	BGR	USDA_PSPP
PS-00168	2022-2023	2.33	ITA	DISSPA
PS-00168	2023-2024	1.33	ITA	DISSPA
W6_26160	2022-2023	16.67	GEO	USDA_PSPP
W6_26160	2023-2024	8	GEO	USDA_PSPP
PS-00169	2022-2023	2	ITA	DISSPA

Accession number	Growing season	Mean number of emerged *Oc* shoot	Origin	Genebank
PI_409031	2022-2023	16.67	GER	USDA_PSPP
PI_409031	2023-2024	3	GER	USDA_PSPP
PI_413678	2022-2023	17.67	HUN	USDA_PSPP
PI_413678	2023-2024	3.33	HUN	USDA_PSPP
PI_413698	2022-2023	15	HUN	USDA_PSPP
PI_413698	2023-2024	2	HUN	USDA_PSPP
PI_413703	2022-2023	16	HUN	USDA_PSPP
PI_413703	2023-2024	5.5	HUN	USDA_PSPP
PI_476409	2023-2024	2	LVA	USDA_PSPP
PI_476413	2022-2023	14	RUS	USDA_PSPP
PI_476413	2023-2024	7.5	RUS	USDA_PSPP
PS-00300	2022-2023	2	ITA	DISSPA
PS-00300	2023-2024	1	ITA	DISSPA
W6_15008	2022-2023	11.67	ISR	USDA_PSPP
W6_15008	2023-2024	4.33	ISR	USDA_PSPP
W6_26160	2022-2023	16.67	GEO	USDA_PSPP
W6_26160	2023-2024	8	GEO	USDA_PSPP
W6_31707	2022-2023	21.67	RUS	USDA_PSPP
W6_31707	2023-2024	5.5	RUS	USDA_PSPP
W6_44716	2022-2023	20	CHN	USDA_PSPP
W6_44716	2023-2024	6.33	CHN	USDA_PSPP
W6_44718	2022-2023	20.5	CHN	USDA_PSPP
W6_44718	2023-2024	6.67	CHN	USDA_PSPP
W6_44720	2022-2023	26	CHN	USDA_PSPP
W6_44720	2023-2024	6.67	CHN	USDA_PSPP
W6_44724	2022-2023	24	CHN	USDA_PSPP
W6_44724	2023-2024	6	CHN	USDA_PSPP
W6_44725	2022-2023	12.67	CHN	USDA_PSPP
W6_44725	2023-2024	8	CHN	USDA_PSPP
W6_44726	2022-2023	18.5	CHN	USDA_PSPP
W6_44726	2023-2024	6	CHN	USDA_PSPP
W6_44766	2022-2023	10	CHN	USDA_PSPP
W6_44766	2023-2024	6	CHN	USDA_PSPP
W6_44768	2022-2023	20	CHN	USDA_PSPP
W6_44768	2023-2024	7.67	CHN	USDA_PSPP
W6_44769	2022-2023	18.33	CHN	USDA_PSPP
W6_44769	2023-2024	5.75	CHN	USDA_PSPP
W6_44770	2022-2023	12.33	CHN	USDA_PSPP
W6_44770	2023-2024	5	CHN	USDA_PSPP
W6_15008	2022-2023	11.67	ISR	USDA_PSPP
W6_15008	2023-2024	4.33	ISR	USDA_PSPP
PS-00169	2023-2024	1,67	ITA	DISSPA

Supplementary Table S5. Summary for the results of the RNA-seq experiment.

Attribute	23A	23B	23C	27A	27B	27C	113A	113B	113C	144A	144B	144C	155A	155B	155C	164A	164B	164C	ROR12A	ROR12B	ROR12C	SprinterA	SprinterB	SprinterC
Number of input reads	34506398	33807167	33786805	33357426	35582888	36706618	34828852	35223543	36516076	33880864	35220402	35949340	35602310	35324129	32526808	35952287	34136167	35524096	37697656	36167632	49087508	35491731	33571229	34085506
Average input read length	278	279	279	279	279	278	278	279	278	278	278	278	278	279	279	278	278	278	278	278	278	279	279	278
UNIQUE READS:																								
Uniquely mapped reads number	31326844	30730894	30942439	30597745	32753866	33519633	31957184	32374497	33468951	31057499	32046220	32922457	32524092	32590590	29998929	32948111	31427293	32678994	34368054	32930195	44931006	24067652	22630672	23090757
Uniquely mapped reads %	90.79%	90.90%	91.58%	91.73%	92.05%	91.32%	91.75%	91.91%	91.66%	91.67%	90.99%	91.58%	91.35%	92.26%	92.23%	91.64%	92.06%	91.99%	91.17%	91.05%	91.53%	67.81%	67.41%	67.74%
Average mapped length	277.46	277.74	277.63	277.72	277.9	277.62	277.5	277.59	277.36	277.42	277.51	277.55	277.39	277.69	277.71	277.49	277.37	277.55	277.07	276.73	277	277.87	277.79	277.58
Number of splices: Total	28469438	27899552	28064811	28170782	30221213	30810248	29579956	30060865	31039045	28212682	29285191	30063497	29406974	29810233	27445873	29922351	28499352	29795722	31535548	30008759	41086136	22210720	20872807	21150632
Number of splices: Annotated (sjdb)	26820511	26229017	26389340	26484474	28480417	28979129	27874256	28321219	29264758	26514095	27587112	28300434	27569885	28008546	25792410	28127098	26790799	28032914	29742397	28265620	38642272	20857434	19597785	19809858
Number of splices: GT/AG	28091873	27531920	27695867	27826805	29850041	30432185	29204738	29679692	30647578	27851747	28909539	29678132	29023433	29417599	27086013	29536077	28131508	29409214	31124435	29619879	40552058	21961309	20638575	20915931
Number of splices: GC/AG	297843	288642	289796	269589	292366	297039	292626	296642	305029	284627	297349	304049	294645	303420	278898	303791	289623	304748	319354	300478	410709	197546	184969	183546
Number of splices: AT/AC	28278	28339	28727	24231	26021	26663	28785	29312	30275	27671	27579	29080	30422	31314	28144	26795	25697	26852	30156	29204	40200	12912	12248	12370
Number of splices: Non-canonical	51444	50651	50421	50157	52785	54361	53807	55219	56163	48637	50724	52236	58474	57900	52818	55688	52524	54908	61603	59198	83169	38953	37015	38785
Mismatch rate per base, %	0.56%	0.52%	0.52%	0.47%	0.49%	0.50%	0.55%	0.52%	0.56%	0.49%	0.53%	0.51%	0.50%	0.50%	0.49%	0.50%	0.49%	0.51%	0.60%	0.60%	0.58%	0.46%	0.47%	0.42%
Deletion rate per base	0.02%	0.02%	0.02%	0.02%	0.02%	0.02%	0.02%	0.02%	0.02%	0.02%	0.02%	0.02%	0.02%	0.02%	0.02%	0.02%	0.02%	0.02%	0.02%	0.02%	0.02%	0.02%	0.02%	0.02%
Deletion average length	2.34	2.36	2.33	2.33	2.32	2.32	2.27	2.27	2.26	2.29	2.27	2.27	2.29	2.28	2.29	2.23	2.22	2.23	2.41	2.41	2.42	2.28	2.31	2.28
Insertion rate per base	0.02%	0.02%	0.02%	0.02%	0.02%	0.02%	0.02%	0.02%	0.02%	0.02%	0.02%	0.02%	0.02%	0.02%	0.02%	0.02%	0.02%	0.02%	0.02%	0.02%	0.02%	0.02%	0.02%	0.02%
Insertion average length	1.75	1.75	1.75	1.73	1.74	1.74	1.71	1.71	1.71	1.68	1.71	1.71	1.79	1.78	1.77	1.67	1.69	1.7	1.87	1.88	1.89	1.59	1.57	1.6
MULTI-MAPPING READS:																								
Number of reads mapped to multiple loci	1283585	1253427	1258080	1138435	1210105	1243550	1142563	1158055	1196619	1123525	1159686	1177915	1185793	1173516	1073862	1176943	1126085	1157300	1305122	1264334	1736579	1049267	978544	1018051
% of reads mapped to multiple loci	3.72%	3.71%	3.72%	3.41%	3.40%	3.39%	3.28%	3.29%	3.28%	3.32%	3.29%	3.28%	3.33%	3.32%	3.30%	3.27%	3.30%	3.26%	3.46%	3.50%	3.54%	2.96%	2.91%	2.99%
Number of reads mapped to too many loci	34832	30904	30815	40465	42244	44696	35891	36408	36861	34627	35425	36316	48183	46998	43241	49144	46230	45469	39994	38886	53114	59742	52966	60168
% of reads mapped to too many loci	0.10%	0.09%	0.09%	0.12%	0.12%	0.12%	0.10%	0.10%	0.10%	0.10%	0.10%	0.10%	0.14%	0.13%	0.13%	0.14%	0.14%	0.13%	0.11%	0.11%	0.11%	0.17%	0.16%	0.18%
UNMAPPED READS:																								
Number of reads unmapped: too many mismatches	0	0	0	0	0	0	0	0	0	0	0	0	0	0	0	0	0	0	0	0	0	0	0	0
% of reads unmapped: too many mismatches	0.00%	0.00%	0.00%	0.00%	0.00%	0.00%	0.00%	0.00%	0.00%	0.00%	0.00%	0.00%	0.00%	0.00%	0.00%	0.00%	0.00%	0.00%	0.00%	0.00%	0.00%	0.00%	0.00%	0.00%
Number of reads unmapped: too short	1754535	1725342	1490889	1516067	1509533	1834193	1618030	1581171	1742852	1598433	1917306	1742116	1759157	1436828	1334517	1695316	1462864	1572757	1921847	1866620	2245363	10264607	9869946	9862257
% of reads unmapped: too short	5.08%	5.10%	4.41%	4.54%	4.24%	5.00%	4.65%	4.49%	4.77%	4.72%	5.44%	4.85%	4.94%	4.07%	4.10%	4.72%	4.29%	4.43%	5.10%	5.16%	4.57%	28.92%	29.40%	28.93%
Number of reads unmapped: other	106602	66600	64582	64714	67140	64546	75184	73412	70793	66780	61765	70536	85085	76197	76259	82773	73695	69576	62639	67597	121446	50463	39101	54273
% of reads unmapped: other	0.31%	0.20%	0.19%	0.19%	0.19%	0.18%	0.22%	0.21%	0.19%	0.20%	0.18%	0.20%	0.24%	0.22%	0.23%	0.23%	0.22%	0.20%	0.17%	0.19%	0.25%	0.14%	0.12%	0.16%
CHIMERIC READS:																								
Number of chimeric reads	0	0	0	0	0	0	0	0	0	0	0	0	0	0	0	0	0	0	0	0	0	0	0	0
% of chimeric reads	0.00%	0.00%	0.00%	0.00%	0.00%	0.00%	0.00%	0.00%	0.00%	0.00%	0.00%	0.00%	0.00%	0.00%	0.00%	0.00%	0.00%	0.00%	0.00%	0.00%	0.00%	0.00%	0.00%	0.00%

Supplementary Table S6. List of differentially expressed genes between lines carrying the resistance (R) and susceptible (S) allele at *PsOcr-1*, *PsOcr-2*, and *PsOcr-3*.

Gene	Description	baseMean	log2FoldChange	lfcSE	stat	pvalue	padj	comparison
LOC127083728	cytochrome P450 89A2-like	305.0615329	-1.026113494	0.149612614	-6.81456128	3.57475E-07	8.0429E-05	*PsOcr-1*
LOC127129437	probable L-gulonolactone oxidase 6	205.2120266	1.050225948	0.118526156	8.85657085	2.37616E-08	7.8025E-06	*PsOcr-1*
LOC127074893	uncharacterized LOC127074893	104.6161319	1.449848182	0.148632961	11.6640869	1.68232E-25	1.022E-21	*PsOcr-1*
LOC127075090	carbonic anhydrase 2-like	310.4818074	-1.325879881	0.15056881	-8.8150569	4.1995E-13	2.6854E-10	*PsOcr-1*
LOC127075091	2-methylene-furan-3-one reductase	107.6845367	-1.063412353	0.149938789	-7.088634	1.19482E-08	4.2077E-06	*PsOcr-1*
LOC127075586	uncharacterized LOC127075586	599.2275523	-1.011727914	0.150306246	-6.69092109	4.10628E-07	9.154E-05	*PsOcr-1*
LOC127076717	patatin-like protein 4	2222.695453	-1.008491745	0.121558092	-8.27921197	2.73439E-07	6.5785E-05	*PsOcr-1*
LOC127107152	pentatricopeptide repeat-containing protein At3g04130, mitochondrial-like	143.9111969	1.199366029	0.117413004	10.1805879	7.65179E-12	3.8736E-09	*PsOcr-1*
LOC127107167	beta-amyrin synthase-like	134.8291588	1.606381161	0.147232485	12.077277	1.49216E-30	3.6258E-26	*PsOcr-1*
LOC127107223	uncharacterized LOC127107223	27.3280791	-1.626466644	0.143135521	-12.0197773	5.80243E-30	7.0497E-26	*PsOcr-1*
LOC127101186	putative cyclic nucleotide-gated ion channel 8	193.0920309	-1.055068377	0.124599477	-8.44678497	5.29307E-08	1.5311E-05	*PsOcr-1*
LOC127105390	uncharacterized LOC127105390	18.72265308	-1.423833387	0.14173039	-9.22287415	8.7489E-18	1.6353E-14	*PsOcr-1*
LOC127107595	uncharacterized LOC127107595	1056.800256	1.225116182	0.135305963	9.13281098	4.65705E-11	2.0575E-08	*PsOcr-1*
LOC127107613	probable inactive nicotinamidase At3g16190	128.6479353	1.777119739	0.122438434	14.3517718	2.186E-29	1.7706E-25	*PsOcr-1*
LOC127107619	boron transporter 4-like	620.3953094	1.130611606	0.131326361	8.65618168	2.83916E-09	1.0951E-06	*PsOcr-1*
LOC127115339	uncharacterized LOC127115339	70.16504323	1.366656486	0.193741035	7.51742363	2.15215E-10	7.6889E-08	*PsOcr-2*
LOC127119670	9-cis-epoxycarotenoid dioxygenase NCED1, chloroplastic-like	402.1872954	-1.048388507	0.191969866	-5.42726962	3.92293E-05	0.00387414	*PsOcr-2*
LOC127105415	putative pentatricopeptide repeat-containing protein At1g12700, mitochondrial	281.1253444	-1.32574594	0.193342135	-6.84034193	2.31868E-08	5.5772E-06	*PsOcr-2*
LOC127116366	uncharacterized LOC127116366	244.8254627	-1.029621642	0.188522854	-5.42945961	7.28842E-05	0.00668169	*PsOcr-2*
LOC127117140	uncharacterized LOC127117140	425.288682	-1.079753044	0.180471659	-5.95464965	2.3927E-05	0.00254948	*PsOcr-2*
LOC127117552	lachrymatory-factor synthase-like	2532.636779	1.132872475	0.132803061	8.54093562	6.17276E-08	1.3607E-05	*PsOcr-2*
LOC127117704	phenylalanine ammonia-lyase 1-like	1025.826129	-1.188205692	0.166651736	-7.10697633	6.42975E-07	0.00011238	*PsOcr-2*
LOC127121838	uncharacterized LOC127121838	933.5101713	-1.135090309	0.1805304	-6.25763955	6.20548E-06	0.00081933	*PsOcr-2*
LOC127122595	AAA-ATPase ASD, mitochondrial-like	406.9399089	-1.104821851	0.184872006	-5.94417979	1.40855E-05	0.00162177	*PsOcr-2*
LOC127122600	AAA-ATPase ASD, mitochondrial-like	286.6398773	-1.14544145	0.19013983	-5.98887178	4.88166E-06	0.00066254	*PsOcr-2*
LOC127124183	(-)-isopiperitenol/(-)-carveol dehydrogenase, mitochondrial-like	558.2872976	1.014084223	0.169049869	6.0297535	6.40662E-05	0.00596331	*PsOcr-2*
LOC127127885	2-methylene-furan-3-one reductase-like	1884.65497	-1.060395899	0.189789975	-5.66651924	1.96709E-06	0.00029318	*PsOcr-2*
LOC127128640	sucrose transport protein SUC8-like	599.8615474	1.065349298	0.167958158	6.37614203	1.68145E-05	0.00186526	*PsOcr-2*
LOC127130165	uncharacterized LOC127130165	477.7602549	-1.182304407	0.175773775	-6.69761862	1.45088E-06	0.00022451	*PsOcr-2*
LOC127130518	albumin-2-like	3393.754511	1.253526304	0.121442825	10.3303642	1.29351E-11	5.5131E-09	*PsOcr-2*
LOC127130584	carboxylesterase 1-like	327.0735259	1.054980043	0.176442457	6.02509393	2.83801E-05	0.00287277	*PsOcr-2*
LOC127131240	kunitz-type trypsin inhibitor-like 2 protein	852.1670675	1.141395165	0.162307335	7.06310888	1.41281E-06	0.000222	*PsOcr-2*
LOC127104962	ubiquitin carboxyl-terminal hydrolase 9-like	16.73787757	-1.595305253	0.193754214	-8.05565795	3.21056E-12	1.4716E-09	*PsOcr-2*
LOC127135361	IQ domain-containing protein IQM4-like	1131.778664	-1.02496849	0.164353317	-6.2194959	4.95172E-05	0.00471753	*PsOcr-2*
LOC127136497	putative transcription factor bHLH041	454.5814938	-1.078936711	0.186378832	-5.75644281	2.57175E-05	0.00267834	*PsOcr-2*
LOC127080314	heat shock 70 kDa protein-like	793.3039258	-1.469945972	0.184067564	-7.94491761	3.55878E-10	1.1683E-07	*PsOcr-2*
LOC127118421	metal tolerance protein 4-like	98.35087917	-1.007521309	0.1807813	-5.91273384	2.40233E-07	4.6439E-05	*PsOcr-2*
LOC127118479	exocyst complex component EXO70B1-like	541.4489061	-1.112834947	0.181727844	-6.09368984	1.11096E-05	0.00135627	*PsOcr-2*
LOC127120714	transcription factor MYB3R-3-like	231.021827	-1.476612383	0.159961104	-9.19768348	7.08578E-12	3.1299E-09	*PsOcr-2*
LOC127126126	sulfate transporter 3.1-like	3515.887615	1.100971056	0.158597963	6.96868398	3.60859E-06	0.00050383	*PsOcr-2*
LOC127129065	non-structural maintenance of chromosomes element 4 homolog A-like	161.3310511	-1.191534708	0.176266434	-6.72853329	1.15791E-06	0.00018879	*PsOcr-2*
LOC127126711	probable xyloglucan endotransglucosylase/hydrolase protein B	2582.577343	1.378547113	0.074208647	18.5740937	5.62208E-34	1.7073E-30	*PsOcr-2*
LOC127130706	ubiquitin carboxyl-terminal hydrolase 9-like	8.074580101	-1.378542287	0.185424053	-6.92706211	2.28903E-10	8.0594E-08	*PsOcr-2*
LOC127127168	BON1-associated protein 1-like	37.7497206	-1.366428972	0.182743248	-7.40902406	1.04316E-08	2.7546E-06	*PsOcr-2*
LOC127127538	probable glutathione S-transferase	302.9481305	-1.005412908	0.138690738	-7.24056688	1.45789E-05	0.00166282	*PsOcr-2*
LOC127127805	metallothionein-like protein 4B	121.0607831	-1.23571621	0.186293339	-7.0289902	6.60866E-10	2.1125E-07	*PsOcr-2*
LOC127138655	protein ANTAGONIST OF LIKE HETEROCHROMATIN PROTEIN 1-like	427.4666146	-1.321430656	0.188916189	-6.95681607	4.62856E-08	1.0608E-05	*PsOcr-2*
LOC127073649	uncharacterized LOC127073649	151.9205899	-1.160205432	0.192011136	-6.09732588	3.28557E-07	6.2359E-05	*PsOcr-2*
LOC127073672	eukaryotic translation initiation factor 5A-3-like	25038.43476	1.297890501	0.190748085	7.05069676	1.79501E-08	4.4957E-06	*PsOcr-2*
LOC127073732	flavonoid 3-monooxygenase-like	246.6565798	1.138704759	0.193685472	6.29064168	2.30762E-07	4.5211E-05	*PsOcr-2*
LOC127073906	U-box domain-containing protein 19-like	154.4026074	-1.094330295	0.188115006	-5.78396227	1.74729E-05	0.0019121	*PsOcr-2*
LOC127074153	lipid transfer protein EARLI 1-like	29996.46304	1.073067329	0.120167627	8.93652545	8.74789E-08	1.848E-05	*PsOcr-2*
LOC127074278	uncharacterized LOC127074278	94.71057972	-1.112096817	0.182051645	-6.57364702	6.73039E-09	1.9236E-06	*PsOcr-2*
LOC127077615	small nucleolar RNA Z101	62.32189286	-1.439479025	0.189582654	-7.98490479	1.64974E-12	7.8586E-10	*PsOcr-2*
LOC127077612	small nucleolar RNA Z101	31.87025081	-1.087554664	0.178647617	-6.66642656	2.57461E-09	7.8185E-07	*PsOcr-2*
LOC127136726	uncharacterized LOC127136726	61.16654306	-1.065888121	0.188140309	-5.78281369	8.74092E-07	0.0001485	*PsOcr-2*
LOC127074602	ABC transporter F family member 4-like	154.4675212	-1.367700158	0.190864273	-7.40707424	1.22443E-10	4.5764E-08	*PsOcr-2*
LOC127074695	uncharacterized LOC127074695	83.83156926	-1.301403099	0.191853093	-6.74578078	6.91745E-08	1.4872E-05	*PsOcr-2*
LOC127074725	uncharacterized LOC127074725	250.7300335	-1.393429912	0.193122079	-7.20037548	3.24013E-09	9.718E-07	*PsOcr-2*

Gene	Description	baseMean	log2FoldChange	lfcSE	stat	pvalue	padj	comparison
LOC127074759	uncharacterized LOC127074759	45.76395012	-1.138820126	0.193721403	-5.84953565	2.7751E-06	0.0004013	*PsOcr-2*
LOC127075149	IAA-amino acid hydrolase ILR1-like 4	264.8630425	1.019789992	0.188238417	5.51286973	5.36406E-05	0.00505095	*PsOcr-2*
LOC127075773	transcription factor bHLH130-like	128.4242952	-1.057370209	0.19366742	-5.43188701	2.03392E-05	0.00219609	*PsOcr-2*
LOC127076164	NAC domain-containing protein 69-like	58.38312479	-1.197253042	0.182760301	-6.51419328	1.30409E-06	0.00020843	*PsOcr-2*
LOC127076513	xyloglucan endotransglucosylase/hydrolase protein 2-like	66.24761274	-1.074316812	0.187097188	-5.70676078	2.8142E-05	0.00287261	*PsOcr-2*
LOC127076798	uncharacterized LOC127076798	47.51131419	-1.078188208	0.19343268	-5.54177961	1.44558E-05	0.00165655	*PsOcr-2*
LOC127084351	uncharacterized LOC127084351	572.2334025	1.272007531	0.190263889	8.16189362	6.13325E-13	3.1702E-10	*PsOcr-2*
LOC127087897	probable WRKY transcription factor 50	292.2086489	-1.177165423	0.177978854	-6.58416114	1.86857E-06	0.00028022	*PsOcr-2*
LOC127081195	protein DOWNY MILDEW RESISTANCE 6	302.7965092	-1.065828258	0.169341396	-6.27331514	2.24774E-05	0.00240558	*PsOcr-2*
LOC127083583	uncharacterized LOC127083583	301.6838516	-1.517231991	0.192863282	-7.86179197	5.81105E-11	2.3372E-08	*PsOcr-2*
LOC127083979	zinc finger CCCH domain-containing protein 29-like	1074.95395	-1.21335417	0.158128317	-7.65406248	1.23635E-07	2.5672E-05	*PsOcr-2*
LOC127083981	zinc finger CCCH domain-containing protein 29-like	1015.332768	-1.244654552	0.157506347	-7.88246689	3.91045E-08	9.1347E-06	*PsOcr-2*
LOC127084384	probable glutathione S-transferase parA	1250.438619	-1.560363061	0.155261798	-10.0223288	4.68339E-14	2.5284E-11	*PsOcr-2*
LOC127084385	probable glutathione S-transferase parA	246.3994167	-1.950986841	0.179088466	-10.8358027	2.45177E-19	2.9782E-16	*PsOcr-2*
LOC127084687	uncharacterized LOC127084687	46.50623246	1.020826509	0.193672533	5.5237899	8.74535E-06	0.00110083	*PsOcr-2*
LOC127086624	uncharacterized LOC127086624	416.3550845	1.018475673	0.192829788	5.7103932	2.76539E-06	0.0004013	*PsOcr-2*
LOC127087010	proteasome subunit beta type-4-like	1835.32432	1.043444374	0.069708511	14.9665169	4.66462E-16	3.434E-13	*PsOcr-2*
LOC127087108	ruBisCO-associated protein-like	579.3735693	1.028176831	0.102884993	9.99048462	1.85029E-08	4.5868E-06	*PsOcr-2*
LOC127087401	putative leucine-rich repeat receptor-like protein kinase At2g19210	580.0219435	-1.213033143	0.171481837	-7.04710739	4.52653E-07	8.2065E-05	*PsOcr-2*
LOC127087457	uncharacterized LOC127087457	21.26443998	-1.380208065	0.193722152	-7.05509924	3.71758E-09	1.1014E-06	*PsOcr-2*
LOC127097427	probable disease resistance protein At4g33300	216.264717	-1.09929679	0.171645751	-8.40515752	1.1113E-14	6.4281E-12	*PsOcr-2*
LOC127098170	WAT1-related protein At4g15540-like	650.0252311	1.083102293	0.163091598	6.66845207	8.17151E-06	0.00103936	*PsOcr-2*
LOC127091933	uncharacterized LOC127091933	97.18086082	1.078799448	0.192945349	5.77890855	6.04406E-06	0.00080237	*PsOcr-2*
LOC127097737	uncharacterized LOC127097737	18.0560531	-1.250571131	0.181859511	-7.34487158	3.09426E-11	1.2741E-08	*PsOcr-2*
LOC127091891	rust resistance kinase Lr10-like	537.5577572	-1.387940019	0.157336116	-8.79717562	1.67151E-10	6.1527E-08	*PsOcr-2*
LOC127092388	LEAF RUST 10 DISEASE-RESISTANCE LOCUS RECEPTOR-LIKE PROTEIN KINASE-like 2.2	172.2000165	-1.718909148	0.188313347	-9.08829859	4.46442E-14	2.465E-11	*PsOcr-2*
LOC127097566	uncharacterized LOC127097566	44.7152854	-1.828080192	0.186325482	-11.8541515	1.9099E-29	4.6399E-26	*PsOcr-2*
LOC127097940	uncharacterized LOC127097940	28.57575483	-1.658511874	0.1839253	-10.8549655	8.39903E-25	1.7004E-21	*PsOcr-2*
LOC127092444	protein HUA2-LIKE 2-like	237.2427426	-1.573016592	0.170872202	-9.16320286	1.15692E-12	5.6212E-10	*PsOcr-2*
LOC127093369	uncharacterized LOC127093369	918.6223722	1.286622398	0.16403731	7.88730756	1.3963E-08	3.5335E-06	*PsOcr-2*
LOC127091328	uncharacterized LOC127091328	236.7006389	-2.614993227	0.192869754	-13.9831028	1.04609E-36	3.6305E-33	*PsOcr-2*
LOC127098022	uncharacterized LOC127098022	11350.38948	-1.422744289	0.169257949	-8.37421205	3.24009E-10	1.0933E-07	*PsOcr-2*
LOC127091037	probable L-type lectin-domain containing receptor kinase S.5	69.86424405	1.189178707	0.17984029	6.64370763	9.8709E-07	0.00016425	*PsOcr-2*
LOC127096771	uncharacterized LOC127096771	283.2485942	-6.11979166	0.163573963	-17.5919797	2.30073E-63	2.7947E-59	*PsOcr-2*
LOC127097788	uncharacterized LOC127097788	14.45468915	-2.370861724	0.193619634	-11.120949	1.51553E-25	3.3471E-22	*PsOcr-2*
LOC127091679	uncharacterized LOC127091679	138.0934296	-3.72468705	0.192342311	-16.0626815	2.94907E-53	1.7911E-49	*PsOcr-2*
LOC127091676	uncharacterized LOC127091676	56.15664469	-3.535003098	0.191358494	-14.4861423	3.78162E-43	1.8374E-39	*PsOcr-2*
LOC127092792	uncharacterized LOC127092792	7.168262988	-1.135246384	0.171753523	-7.81958946	2.63488E-13	1.3916E-10	*PsOcr-2*
LOC127092112	ethylene-responsive transcription factor ERF098-like	362.8020895	-1.052642283	0.185258708	-5.65147189	4.66497E-05	0.00446184	*PsOcr-2*
LOC127092118	uncharacterized LOC127092118	523.998908	-4.85510358	0.187486101	-18.6002421	1.00598E-70	2.4439E-66	*PsOcr-2*
LOC127097222	uncharacterized LOC127097222	49.24974933	-3.425834566	0.191517448	-13.8297224	2.6176E-39	1.0599E-35	*PsOcr-2*
LOC127091757	histone H1-like	918.9328534	1.228219269	0.091714673	13.3875726	7.06746E-17	6.3591E-14	*PsOcr-2*
LOC127095671	uncharacterized LOC127095671	180.3295712	-5.026802749	0.180361946	-16.9975439	2.47367E-59	2.0032E-55	*PsOcr-2*
LOC127092262	uncharacterized LOC127092262	50.82440949	-1.349680185	0.190416932	-7.03519053	1.97995E-08	4.8587E-06	*PsOcr-2*
LOC127097171	glucomannan 4-beta-mannosyltransferase 9-like	105.6153299	1.135956688	0.159281528	7.13068603	1.42996E-06	0.00022269	*PsOcr-2*
LOC127093161	transcription factor bHLH92	155.6674154	-1.133927896	0.19043972	-5.91693183	6.36984E-06	0.00083648	*PsOcr-2*
LOC127092651	MYB-like transcription factor EOBII	184.4817463	-1.020383442	0.19015664	-5.3328647	8.25506E-05	0.00745534	*PsOcr-2*
LOC127091782	dehydration-responsive element-binding protein 1A-like	74.91282364	-1.163866558	0.193651777	-5.98522542	1.60304E-06	0.00024493	*PsOcr-2*
LOC127098408	early light-induced protein, chloroplastic	244.5137791	-1.015551931	0.191754299	-5.31081852	1.36009E-05	0.00158096	*PsOcr-2*
LOC127097117	cysteine-rich receptor-like protein kinase 25	70.36264203	-1.21180194	0.176361383	-6.83487299	6.60572E-07	0.00011463	*PsOcr-2*
LOC127091317	cysteine-rich receptor-like protein kinase 10	531.4796086	-1.145530566	0.160817111	-7.10424705	1.41237E-06	0.000222	*PsOcr-2*
LOC127108462	nudix hydrolase 17, mitochondrial-like	51.76989097	-1.030704048	0.164623079	-6.24021307	4.31191E-05	0.00419014	*PsOcr-2*
LOC127108465	nudix hydrolase 18, mitochondrial-like	57.8628026	-1.173838927	0.19172872	-6.07719969	2.19003E-06	0.00032442	*PsOcr-2*
LOC127108236	probable WRKY transcription factor 41	785.0083543	-1.097991081	0.183446473	-5.95456714	1.63754E-05	0.00182488	*PsOcr-2*
LOC127107829	calmodulin-binding transcription activator 3	1319.857855	-1.123116859	0.153338177	-7.30943765	1.4164E-06	0.000222	*PsOcr-2*
LOC127101314	cytochrome P450 CYP82D47-like	566.6715833	-1.069802345	0.179995602	-5.91624239	2.98954E-05	0.00301361	*PsOcr-2*
LOC127106187	ethylene-responsive transcription factor ERF109-like	13.1312921	-1.407640098	0.18349655	-7.65064884	1.73745E-12	8.1172E-10	*PsOcr-2*
LOC127107106	uncharacterized LOC127107106	1933.417984	1.089483949	0.189530772	5.88446775	8.85855E-06	0.00110933	*PsOcr-2*
LOC127100691	disease resistance protein RPP13-like	921.9702738	-1.045729988	0.143797812	-7.26208507	6.54684E-06	0.0008551	*PsOcr-2*
LOC127106484	uncharacterized LOC127106484	77.98812264	-1.126334706	0.183804215	-6.09131584	8.33904E-06	0.00105515	*PsOcr-2*

Gene	Description	baseMean	log2FoldChange	lfcSE	stat	pvalue	padj	comparison
LOC127106000	uncharacterized LOC127106000	452017.3924	1.003288568	0.167315507	6.02800303	7.83279E-05	0.00710037	*PsOcr-2*
LOC127106478	ethylene-responsive transcription factor ERF039-like	66.4654401	-1.108741855	0.155851218	-7.09143791	2.81489E-06	0.00040464	*PsOcr-2*
LOC127102733	transcription factor MYB114-like	1821.586826	-1.163996397	0.157462854	-7.37464863	5.81112E-07	0.0001023	*PsOcr-2*
LOC127106747	transcription factor MYB13-like	86.1719583	-1.149499404	0.189386764	-6.20451158	1.16454E-07	2.4389E-05	*PsOcr-2*
LOC127117817	receptor-like protein kinase HSL1	259.9789682	1.015920197	0.170403083	6.02174554	2.51298E-05	0.00316284	*PsOcr-3*
LOC127128432	uncharacterized LOC127128432	363.2984268	-1.01641059	0.172730755	-5.85340055	3.70584E-05	0.00445636	*PsOcr-3*
LOC127117994	protein LYK5-like	823.4643237	1.030522358	0.174966448	5.9872095	1.45563E-05	0.00196437	*PsOcr-3*
LOC127118410	NDR1/HIN1-like protein 6	450.2484483	1.082210282	0.169805171	6.44475394	4.17775E-06	0.00065052	*PsOcr-3*
LOC127118799	probable trehalose-phosphate phosphatase C	939.7912415	1.005216904	0.131829368	7.63476547	4.56911E-06	0.00070246	*PsOcr-3*
LOC127123124	putative disease resistance protein RGA4	689.5834608	1.227659883	0.173156356	7.2167468	4.5658E-08	1.4219E-05	*PsOcr-3*
LOC127119403	putative disease resistance protein RGA4	255.4845555	1.084805872	0.177111543	6.25071053	2.86003E-06	0.00046315	*PsOcr-3*
LOC127119405	UDP-glycosyltransferase 74B1-like	191.6328833	1.043055312	0.180054984	6.33622075	1.44767E-07	3.8643E-05	*PsOcr-3*
LOC127119409	uncharacterized LOC127119409	1473.725655	1.232433453	0.180589851	7.14167749	9.47871E-09	3.5084E-06	*PsOcr-3*
LOC127119425	metalloendoproteinase 2-MMP-like	237.2729745	1.0617572	0.176938763	6.11672722	5.53871E-06	0.0008305	*PsOcr-3*
LOC127120635	chalcone synthase 5	1920.27112	1.059200949	0.129968107	8.1612365	4.89044E-07	9.9827E-05	*PsOcr-3*
LOC127132549	chitinase 10-like	233.9114958	1.157521186	0.17402339	6.75763394	4.32468E-07	9.2965E-05	*PsOcr-3*
LOC127125580	NDR1/HIN1-like protein 10	421.6727074	1.151247	0.174908427	6.70393993	4.86537E-07	9.9827E-05	*PsOcr-3*
LOC127126628	spermidine hydroxycinnamoyl transferase-like	402.4789993	1.145360903	0.178422024	6.59369803	3.90557E-07	8.6246E-05	*PsOcr-3*
LOC127127449	omega-3 fatty acid desaturase, chloroplastic-like	206.208035	1.109889394	0.175185703	6.44089902	1.6751E-06	0.00029064	*PsOcr-3*
LOC127128273	enoyl-CoA delta isomerase 1, peroxisomal-like	1461.312633	1.295928873	0.139677533	9.30361642	9.29208E-11	4.4258E-08	*PsOcr-3*
LOC127074296	protein NRT1/ PTR FAMILY 7.3-like	1182.864763	1.136198411	0.159477919	7.17205467	5.94266E-07	0.00011928	*PsOcr-3*
LOC127075656	protein ENHANCED PSEUDOMONAS SUSCEPTIBILITY 1-like	740.7425252	1.091913011	0.176686872	6.31071412	2.38783E-06	0.00039458	*PsOcr-3*
LOC127076049	protein SUPPRESSOR OF PHYA-105 1-like	319.6722006	1.1890777	0.178619905	6.85000095	9.54416E-08	2.6345E-05	*PsOcr-3*
LOC127137937	aconitate hydratase, cytoplasmic-like	96.06903461	-1.063301116	0.163746008	-7.55222979	1.0405E-11	6.4807E-09	*PsOcr-3*
LOC127076696	dol-P-Man:Man(7)GlcNAc(2)-PP-Dol alpha-1,6-mannosyltransferase-like	522.3879343	-1.204135207	0.17351602	-6.90128961	2.33855E-07	5.8563E-05	*PsOcr-3*
LOC127085997	uncharacterized LOC127085997	124.2164933	1.162087594	0.178101169	6.67336498	2.6798E-07	6.5095E-05	*PsOcr-3*
LOC127080312	uncharacterized LOC127080312	311.1472217	1.111507162	0.162339292	6.89111912	1.52439E-06	0.00026833	*PsOcr-3*
LOC127082960	ATP-dependent RNA helicase DEAH12, chloroplastic-like	228.0638741	1.130522138	0.179643302	6.48646056	4.70111E-07	9.8728E-05	*PsOcr-3*
LOC127082993	putative multidrug resistance protein	39.29710729	1.120073349	0.181336256	6.49496838	9.09237E-08	2.5387E-05	*PsOcr-3*
LOC127084140	uncharacterized LOC127084140	332.5577926	1.109630442	0.176009517	6.42555599	1.55663E-06	0.00027203	*PsOcr-3*
LOC127084294	uncharacterized LOC127084294	131.3762471	1.164552229	0.177449373	6.70027186	2.74492E-07	6.6017E-05	*PsOcr-3*
LOC127084427	uncharacterized LOC127084427	184.1565321	1.094980496	0.155485349	7.06210302	1.7992E-06	0.00030778	*PsOcr-3*
LOC127084482	putative receptor protein kinase ZmPK1	85.32080961	1.06235187	0.18010907	6.0506548	3.27727E-06	0.00052031	*PsOcr-3*
LOC127084526	uncharacterized LOC127084526	168.1200059	1.350980131	0.181481638	8.01646636	1.49966E-11	8.7138E-09	*PsOcr-3*
LOC127084542	uncharacterized LOC127084542	379.6590808	1.141509453	0.181425526	6.63979133	8.4426E-08	2.3846E-05	*PsOcr-3*
LOC127084543	uncharacterized LOC127084543	334.5690175	1.285338406	0.181258602	7.79321054	4.25854E-11	2.1551E-08	*PsOcr-3*
LOC127084558	gibberellin 2-beta-dioxygenase 8	152.9154311	1.258718057	0.181137654	7.30288886	2.43666E-09	9.7031E-07	*PsOcr-3*
LOC127084680	uncharacterized LOC127084680	126.6775522	1.031742678	0.176249365	5.94384175	1.35341E-05	0.00184695	*PsOcr-3*
LOC127085229	uncharacterized LOC127085229	361.3522192	4.112308113	0.173565216	14.4249975	3.15289E-43	3.8293E-39	*PsOcr-3*
LOC127085336	uncharacterized LOC127085336	266.7422957	1.03296904	0.153635879	6.7441488	1.04118E-05	0.00147903	*PsOcr-3*
LOC127085749	G-type lectin S-receptor-like serine/threonine-protein kinase At4g27290	234.5027604	1.098341512	0.181459046	6.37146694	3.23589E-07	7.4154E-05	*PsOcr-3*
LOC127083052	uncharacterized LOC127083052	299.5019843	1.135658681	0.177551241	6.54639111	6.11637E-07	0.00011982	*PsOcr-3*
LOC127086793	probable terpene synthase 11	48.42803345	1.111735143	0.177584469	7.12778344	6.76506E-10	2.8333E-07	*PsOcr-3*
LOC127087224	ADP,ATP carrier protein, mitochondrial-like	233.6562301	1.038330499	0.18098876	6.15689731	5.19703E-07	0.0001052	*PsOcr-3*
LOC127087278	B-box zinc finger protein 25-like	82.67173484	1.03926172	0.174234381	6.02405041	1.31726E-05	0.00180777	*PsOcr-3*
LOC127096647	patatin-like protein 2	173.1839492	1.203650517	0.180695103	6.93686769	2.73897E-08	9.162E-06	*PsOcr-3*
LOC127096622	WAT1-related protein At4g08290-like	9088.403937	1.164460987	0.175877702	6.76759748	2.93123E-07	6.9039E-05	*PsOcr-3*
LOC127093569	aluminum-activated malate transporter 10-like	427.6299232	1.259198505	0.181480563	7.43831496	7.00008E-10	2.882E-07	*PsOcr-3*
LOC127093516	probable aspartic proteinase GIP2	437.7161881	1.124199608	0.147819476	7.62631427	3.56682E-07	8.0224E-05	*PsOcr-3*
LOC127097674	geraniol 8-hydroxylase-like	213.4114946	1.255994843	0.173980625	7.34457038	1.81766E-08	6.3736E-06	*PsOcr-3*
LOC127097564	ethylene-response factor C3-like	181.7971608	1.02315739	0.171368713	6.03141087	2.07478E-05	0.0026951	*PsOcr-3*
LOC127096982	putative F-box/LRR-repeat protein At4g15060	111.7634593	1.016464939	0.181412304	5.83224343	4.79737E-06	0.00073291	*PsOcr-3*
LOC127097504	heavy metal-associated isoprenylated plant protein 39-like	448.5645132	1.145657873	0.177066627	6.6196259	4.75535E-07	9.8728E-05	*PsOcr-3*
LOC127097506	heavy metal-associated isoprenylated plant protein 12-like	583.3037447	1.18833925	0.180218469	6.8534632	5.61465E-08	1.7048E-05	*PsOcr-3*
LOC127098405	early light-induced protein, chloroplastic-like	83.48501663	1.302638193	0.171345222	7.66347157	4.48086E-09	1.7277E-06	*PsOcr-3*
LOC127098410	early light-induced protein, chloroplastic-like	66.74867118	1.390828179	0.176038803	8.01054064	1.65246E-10	7.4333E-08	*PsOcr-3*
LOC127108027	(+)-6a-hydroxymaackiain 3-O-methyltransferase 2	1039.124299	1.159222917	0.179606249	6.67513831	1.83857E-07	4.7511E-05	*PsOcr-3*
LOC127113357	cytochrome P450 CYP736A12-like	357.855106	1.085929019	0.180919847	6.24168433	9.93246E-07	0.00018418	*PsOcr-3*

Chapter 4

Transcriptome analysis of pea *ramosus* mutants reveals strigolactone- dependent and independent processes associated with stress adaptation and plant development

Transcriptome analysis of pea *ramosus* mutants reveals strigolactone- dependent and independent processes associated with stress adaptation and plant development

Francesco Arcieri[1§], Gaetano Giudice[1§], Marzia Guerriero[1], Chiara Delvento[1], Kit Xi Liew[2], Lamis Berqdar[2], Pasquale Luca Curci[3], Concetta Lotti[4], Luigi Ricciardi[1], Salim Al-Babili[2], Imran Haider[1*], Stefano Pavan[1*]

[1]Department of Soil, Plant and Food Sciences, University of Bari "Aldo Moro", Via Amendola 165/A, 70126 Bari, Italy.

[2]The BioActives Lab, Biological and Environmental Sciences and Engineering (BESE), King Abdullah University of Science and Technology (KAUST), 23955-6900, Thuwal, Kingdom of Saudi Arabia.

[3]Institute of Biosciences and Bioresources, National Research Council (CNR), Bari, Italy.

[4]Department of Agricultural, Food and Environmental Sciences, University of Foggia, Foggia, Italy.

§These authors equally contributed to this work

*Corresponding authors: Stefano Pavan, email: stefano.pavan@uniba.it; Imran Haider, email: imran.haider@uniba.it

Submitted to Frontiers in Plant Science, section Plant Physiology.

Submission ID: 1657499

ABSTRACT

Strigolactones (SLs) are carotenoid-derived molecules with dual functions as rhizosphere signals and plant hormones. However, knowledge on the physiological processes regulated by SLs, including plant growth and adaptation to abiotic stresses, is still limited. In this study, a comprehensive picture of SL biological roles was obtained by comparing the root transcriptomic profiles of the pea mutants *ramosus5* (*rms5*) and *rms1*, impaired for the SL biosynthetic genes *CAROTENOID CLEAVAGE DIOXYGENASE 7* (*CCD7*) and *CCD8*, respectively, with those of their corresponding wild-type (WT) genotype. Gene Ontology (GO) enrichment analysis revealed significant downregulation of genes involved in abiotic and oxidative stress responses, hormonal and cell cycle regulation, DNA maintenance and cell division, as well as structural and metabolic processes in *rms* mutants. In contrast, genes related to response to phosphate starvation were notably upregulated. Hormonal quantification using LC-MS/MS indicated that the absence of SLs in *rms* mutants is associated with significantly higher levels of jasmonic acid, and significantly lower levels of abscisic acid.

To explore whether CCD7, previously associated *in vitro* with broad carotenoid substrate specificity, also functions is involved in processes beyond SL biosynthesis, we searched for genes and biological processes that are specifically up- or downregulated in the *rms5* mutant relative compared to both *rms1* and WT, but and that are not significantly enriched in the *rms1* when comparing to WT. SL-independent downregulated processes resulting from CCD7 impairment included plant cell wall organization, cell wall modification, and nucleosome assembly, while the upregulated processes were primarily associated with light-dependent energy production. Overall, our study provides insights on the broad biological role of SLs and suggests that CCD7 activity may influence photosynthetic, chromatin and cell wall-related processes beyond its canonical function in SL biosynthesis. As a non-mutually exclusive hypothesis, carotenoids cleaved by CCD7, or apocarotenoids originating from their non-enzymatic cleavage, might act as signalling molecules regulating these processes.

Keywords: Transcriptomics; *ramosus* mutants; carotenoid cleavage dioxygenase; pea (*Pisum sativum* L.); hormonal quantification; strigolactone biosynthesis

INTRODUCTION

Plant hormones are small molecules produced through various metabolic pathways that govern plant growth and developmental processes (Chaiwanon et al., 2016). Their significance is emphasized by their ability to help plants respond to multiple environmental challenges, including biotic and abiotic stresses (Benitez-Alfonso et al., 2023). These represent major factors contributing to crop failure, and pose significant challenges to sustainable agricultural practices (Araújo et al., 2015; Parihar et al., 2022).

Strigolactones (SLs) are a group of over 35 carotenoid-derived molecules that are exudated by the roots of around 80% of terrestrial plant species (Al-Babili et al., 2015; Stra et al., 2023). Initially discovered as exogenous signals that trigger the germination of root parasitic plants such as *Striga* and *Orobanche* from the Orobanchaceae family (Cook et al., 1966; Bouwmeester et al., 2021), SLs were later recognized for their role in promoting symbiotic relationships between plant roots and arbuscular mycorrhizal fungi (AMF), particularly under nutrient-deficient conditions (Akiyama et al., 2005; Lanfranco et al., 2018; Fiorilli et al., 2019). In addition to their external signaling role, SLs also act as endogenous hormones that regulate plant architecture above ground, with roles in lateral bud outgrowth, internode elongation, leaf senescence, and secondary stem growth, as well as below ground, with effects on adventitious root formation and root hair density (Waters et al., 2017; Wu et al., 2022; Wang et al., 2024). Our understanding of biological roles of SLs continues to expand, with emerging research suggesting their potential to enhance plant tolerance and resilience to various abiotic stresses, including drought, salinity, temperature extremes, and oxidative stress (Haider et al., 2018; Guan et al., 2025).

Two carotenoid cleavage dioxygenase enzymes, CCD7 and CCD8, play a major role in SL biosynthesis, occuring in plant roots. The functions and characteristics of CCD7 and CCD8 have been subjects of extensive discussion (Walter et al., 2010). CCD7 is responsible for cleaving 9-*cis*-β-carotene (C40), resulting in the production of β-ionone and 9-*cis*-β-apo-10'-carotenal (C27) (Al-Babili et al., 2015; Jia et al. 2018). Next, CCD8 cleaves 9-*cis*-apo-10'-carotenal to form the SL precursor carlactone (C19) (Alder et al., 2012; Bouwmeester et al., 2021).

CCD7 exhibits a wide range of substrate specificity, whereas CCD8 appears to be more specialized for the SL biosynthesis (Bruno et al., 2014; Hou et al., 2016). Indeed, CCD7 has been also associated with the cleavage of unknown carotenoid substrates in C27 apocarotenoids, which are further oxidized to C13 and C14 cyclohexenone and mycorradicin derivatives (Floss et al., 2008).

Here, the transcritomic and the hormonal profiles of the pea mutants *ramosus5* (*rms5*) and *rms1*, impaired for the *CCD7* and *CCD8* genes, respectively, and their respective wild-type cultivar, were

produced. Data analysis provided a picture of the biological functions and hormonal cross talks involving SLs. Remarkably, biological processes independent from SL biosynthesis and associated with CCD7 activity were identified.

MATERIALS AND METHODS

Plant materials and growth conditions

Seeds of the pea SL mutants *rms1* and *rms5*, along with their wild-type genetic background (cv. Térèse), were obtained from the French National Institute for Agriculture, Food, and Environment (INRAE). After placing seeds for two days at 25°C in a dark environment on moist filter paper, seedlings were transferred to an aeroponic tanks arranged in a randomized block design with three replicates, in which each experimental unit consisted of a tank with eight plants. Plants were grown in 3-liters Hoagland's nutrient solution with $K_2HPO_4.3H_2O$ (+Pi) for 2 weeks, followed by $K_2HPO_4.3H_2O$ (–Pi) for another 10 days. The experiment was carried out under controlled conditions, maintaining a temperature of 23°C during the day and 22°C at night, a photoperiod of 16 hours of light and 8 hours of darkness, and a relative humidity of 60%.

Total RNA isolation, library preparation and sequencing

Total RNA was extracted from root tissues, using the Direct-zol RNA MiniPrep Kit with TRI-Reagent ®, according to the manufacturer's instruction (Zymo Research). RNA concentration, quality and integrity were checked using a NanoDrop 2000 UV-Vis spectrophotometer (Thermo Scientific) and standard gel electrophoresis.

After total RNA isolation, complementary DNA (cDNA) libraries were prepared using the Hieff NGS Ultima Dual-mode mRNA Library Prep Kit for Illumina (Yeasen). In detail, mRNA was enriched using oligo(dT) beads, sheared using a fragmentation buffer and reverse transcribed into cDNA with random primers. After synthesizing the second strand, cDNA fragments underwent end-repair, poly(A) addition, and ligation to Illumina sequencing adapters. Size selection of the ligation products was performed using Hieff NGS DNA Selection Beads (Superior Ampure XP alternative|12601ES56, Yeasen). Ligated fragments were finally PCR amplified. Library sequencing was performed on an Illumina Novaseq 6000 platform (Illumina).

Transcriptomic analysis

Raw sequencing data were assessed for quality using FASTQC both before and after trimming. Trimmomatic was used to remove sequencing adapters, low-quality bases (Phred score < 25), short reads (<35 nucleotides), and to trim the first 10 base pairs from all reads. The STAR aligner was then used to index the *Pisum sativum* reference genome (GCF_024323335.1) and to map the trimmed

reads to the genome, and the software Qualimap was then used to obtain a report of the mapping quality and to infer strand specificity. Read summarization at gene level was performed using FeatureCounts, using reads with mapping quality higher than 30 and counting fragments since the data was paired-end. Raw counts were imported into R to perform statistical analysis.

The DESeq2 package (Love et al., 2014) was used to normalize counts, filter out poorly expressed genes by setting a minimum of 10 counts in at least 3 samples, and to assess relations among samples by principal component analysis (PCA). Comparisons were conducted between the *rms1* mutant and the wild-type (*rms*1 vs WT), the *rms5* mutant and the wild type (*rms5* vs WT), and the two mutants (*rms1* vs *rms5*), using the second term of each comparison as reference. Following shrinkage of log2 foldchange (LFC) estimates with the lfcShrink function, genes with an adjusted p-value < 0.01 and |log2FC| > 1 were considered differentially expressed genes (DEGs). Finally, a Volcano plot was obtained using the EnhancedVolcano R package (Blighe et al., 2024).

Functional enrichment analysis

Gene Ontology (GO) enrichment analysis was carried out using the *gost()* function of the gProfiler2 R package (version 0.2.3) (Kolberg et al., 2020). Multiple testing correction was applied using the Benjamini–Hochberg method to control the false discovery rate (FDR). Biological processes (BPs) associated with SL production were inferred based on a matching trend between the *rms1* vs WT and *rms5* vs WT comparisons; BPs specifically associated with CCD7 activity were inferred based on a matching trend between the *rms5* vs WT and *rms5* vs *rms1* comparisons.

Hormonal profiling

To quantify plant hormones in root tissues, approximately 20 mg of dry powder was combined with an internal standard, D6-ABA (2.0 ng), in 1.8 mL of methanol through vortex mixing. Following a 15-minute sonication (Branson 3510 ultrasonic bath), the samples were centrifuged for 8 minutes at 4000 rpm and 4°C, and the supernatant was transferred to a 4 mL glass vial. The extraction was repeated with an additional 1.8 mL of methanol (without IS) and the combined solutions were concentrated using a speed vacuum. After drying, the residue was re-dissolved in 120 µL of 90% acetonitrile and filtered using a Minisart syringe prior to injection for LC-MS analysis.

For MS parameters setting, the Vanquish™ Duo UHPLC Systems were integrated with a TSQ Altis™ triple quadrupole mass spectrometer (Thermo Scientific), featuring a heated-electrospray ionization source. Chromatographic separation utilized an ACQUITY UPLC HSS T3 column (2.1 × 100 mm, 1.8 µm, Waters) along with a VanGuard pre-column (2.1 × 5 mm, 1.8 µm, Waters), both maintained at a temperature of 40°C. The mobile phases comprised 5% aqueous acetonitrile (A) and acetonitrile (B), each containing 0.01% formic acid, facilitating the elution of hormones through a gradient

program: from 5% B to 80% B over 0–12 minutes, transitioning to 100% B from 12 to 13 minutes, maintaining 100% B for 13–16 minutes at a flow rate of 0.4 mL/min, and reverting to 5% B at 16.5 minutes for a hold of 3.5 minutes. The mass spectrometry parameters included a positive and negative ion mode at 3500 V, sheath gas at 45 Arb, auxiliary gas at 10 Arb, sweep gas at 1 Arb, ion transfer tube temperature at 325°C, vaporizer temperature at 300°C, a cycle time of 1 second, Q1 and Q3 resolutions (FWHM) at 0.7, CID gas at 1.5 mTorr, and a chromatographic peak width of 6 seconds.

Analysis of variance (ANOVA), followed by the least significant difference (LSD) post-hoc test ($\alpha = 0.05$), implemented using the R package *agricolae* (De Mendiburu et al., 2020), was performed to assess significant differences among the hormonal profiles of *rms1*, *rms5*, and the cv. Térèse.

RESULTS

RNA-seq data production and quality control

RNA-seq was performed to obtain root transcriptomic profiles from two null SL mutants, *rms1* and *rms5*, along with their corresponding wild-type genetic background, the cultivar Térèse. Prior to sampling, plants were subjected to phosphate starvation, a condition known to induce SL biosynthesis, thereby enhancing physiological differences between wild-type and mutant plants. On average, each sample yielded 38,965,129 reads with a length of 278 bp. Uniquely mapped reads to the *Pisum sativum* reference genome (GCF_024323335.1) accounted for 81% of the total, with no chimeric reads detected, indicating that the preprocessing parameters were suitable for downstream analyses (Supplementary Table S1). Principal component analysis (PCA) revealed minimal variation among biological replicates (Figure 1), while clearly distinct transcriptomic profiles were observed among the three genotypes, which clustered separately in the PCA biplot (Figure 1).

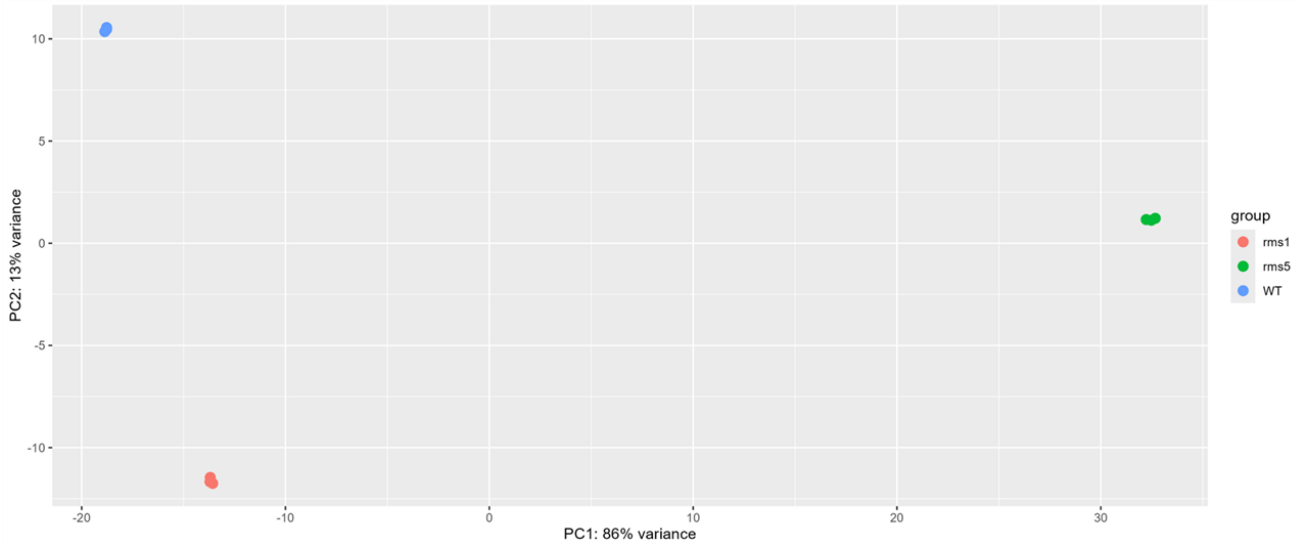

Figure 1. Principal component analysis (PCA) of pea *ramosus* (*rms*) mutants and their wild-type genetic background (cv. Térèse) transcript profiles.

Identification of differentially expressed genes, biological processes and biochemical pathways associated with SL biosynthesis

To gain insights on the effect of the biological roles of SLs, we compared the trascriptomic profiles of the *rms* mutants to the one of Térèse (WT), in search for differentially expressed genes (DEGs). The comparison between *rms1* and WT yielded 1,185 DEGs, including 953 downregulated and 232 upregulated genes (Figure 2A). An about four-fold higher number of DEGs (4,444) was observed for the comparison between *rms5* and WT, including 3,179 downregulated and 1,265 upregulated genes (Figure 2B).

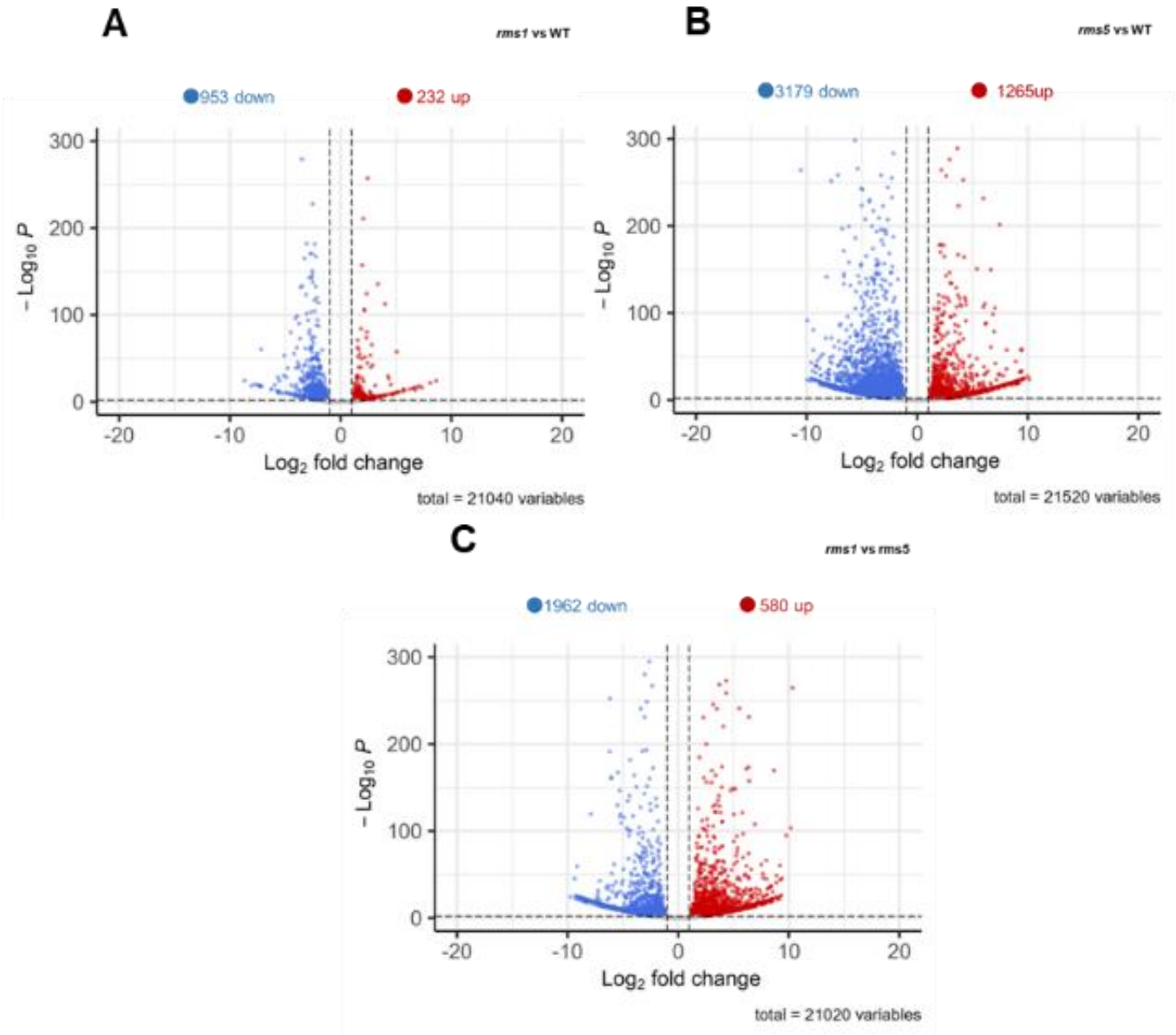

Figure 2. Differentially expressed genes (DEGs) in the comparison between SL-deficient *rms* mutants and wild-type cv. Térèse plants, specifically: *rms1* vs WT, *rms5* vs WT, and *rms1* vs *rms5*. **(A)**Volcano plot of DEGs for comparison *rms1* vs WT **(B)** Volcano plot of DEGs for comparison *rms5* vs WT **(C)** Volcano plot of DEGs for comparison *rms1* vs *rms5*.

Gene Ontology (GO) enrichment analysis was conducted on DEGs showing matching trend between the *rms1* vs WT and *rms5* vs WT comparisons, in order to detect biological processes (BPs) associated with SLs. This resulted in the identification of 15 downregulated and one upregulated BPs (Figure 3, Supplementary Table S2). Downregulated BPs included five related to response to stresses (oxidative stress, response to hydrogen peroxide, hydrogen peroxide catabolic process, response to sal stress, response to heat), five related to cell cycle and division (cyclin-dependent protein serine/threonine kinase activity, mitotic cell phase transition, microtubule-based movement, DNA replication initiation and double strand break repair), two related to catabolic pathways (L-phenylalanine and lignin), two related to protein metabolism (proteolysis and protein complex oligomerization), and carbohydrate metabolism. The only BP upregulated in *rms* mutants was response to phosphate starvation (Figure 3, Supplementary Table S2).

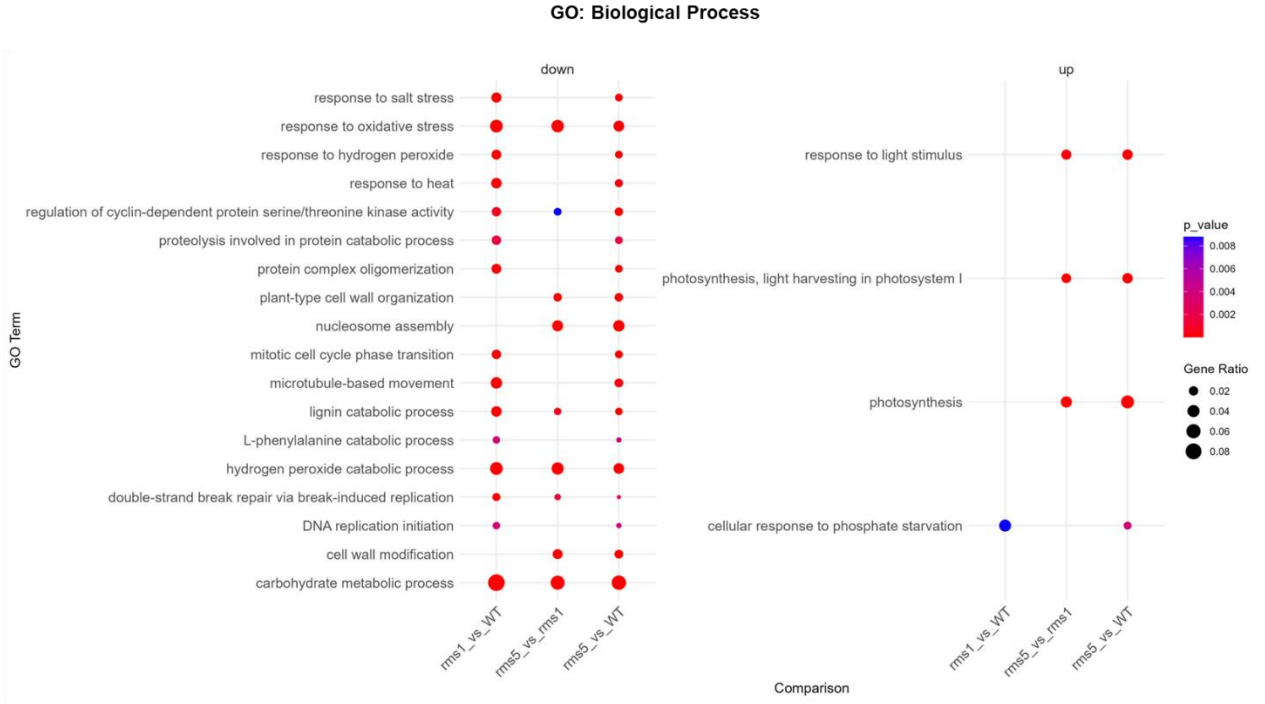

Figure 3. GO:BP enrichment analyses of DEGs identified in the comparisons between SL-deficient *rms* mutants and wild-type (cv. Térèse) plants, specifically: *rms1* vs WT, *rms5* vs WT, and *rms1* vs *rms5*. GO: gene ontology; BP: biological processes.

SL deficiency is associated with lower abscissic acid and higher jasmonic acid levels

In order to investigate the interplay between SLs and other plant hormones, we quantified abscisic acid (ABA), auxin, cytokinin, gibberellin, jasmonic acid (JA) and salicylic acid levels in *rms* mutants and Térèse roots under phosphate starvation. JA levels were significantly higher in mutants (16.55 pg/mg DW in *rms1*, 24.99 pg/mg DW in *rms5*) compared to Térèse (5.86 pg/mg DW). An opposite trend was observed for ABA, whose levels were markably lower in mutants (7.36 pg/mg DW in *rms1*, 14.32 pg/mg DW in *rms5*) compared to Térèse (37.96 pg/mg DW) (Figure 4A). No significant difference was observed with respect to all the other hormonal quantifications (Supplementary Figure S1).

To further investigate the relations between SLs and JA, and SLs and ABA, we examined the JA and ABA metabolic processes within our transcriptomic dataset. Notably, a gene annotated as *METHYL JASMONATE ESTERASE 1-LIKE* (*MJE 1-L*) was significantly upregulated by 3.3-fold in the *rms* mutants compared to the wild-type roots, suggesting that higher JA levels in mutants may derive from higher hydrolysis of methyl jasmonate (MeJA) into JA. On the other hand, two *ALLENE OXIDE CYCLASE-LIKE* (*AOC*) genes, possibly involved in JA biosynthesis, were downregulated by 2.8-fold in the *rms* mutants. Finally, the stress response gene *DDR48*, associated with ABA metabolism, showed an increase (4.4-fold) in expression in the *rms* mutants (Figure 4B). This suggests that SL may play a role in modulating the interaction between ABA and JA, thereby affecting the plant's defense mechanisms against stress.

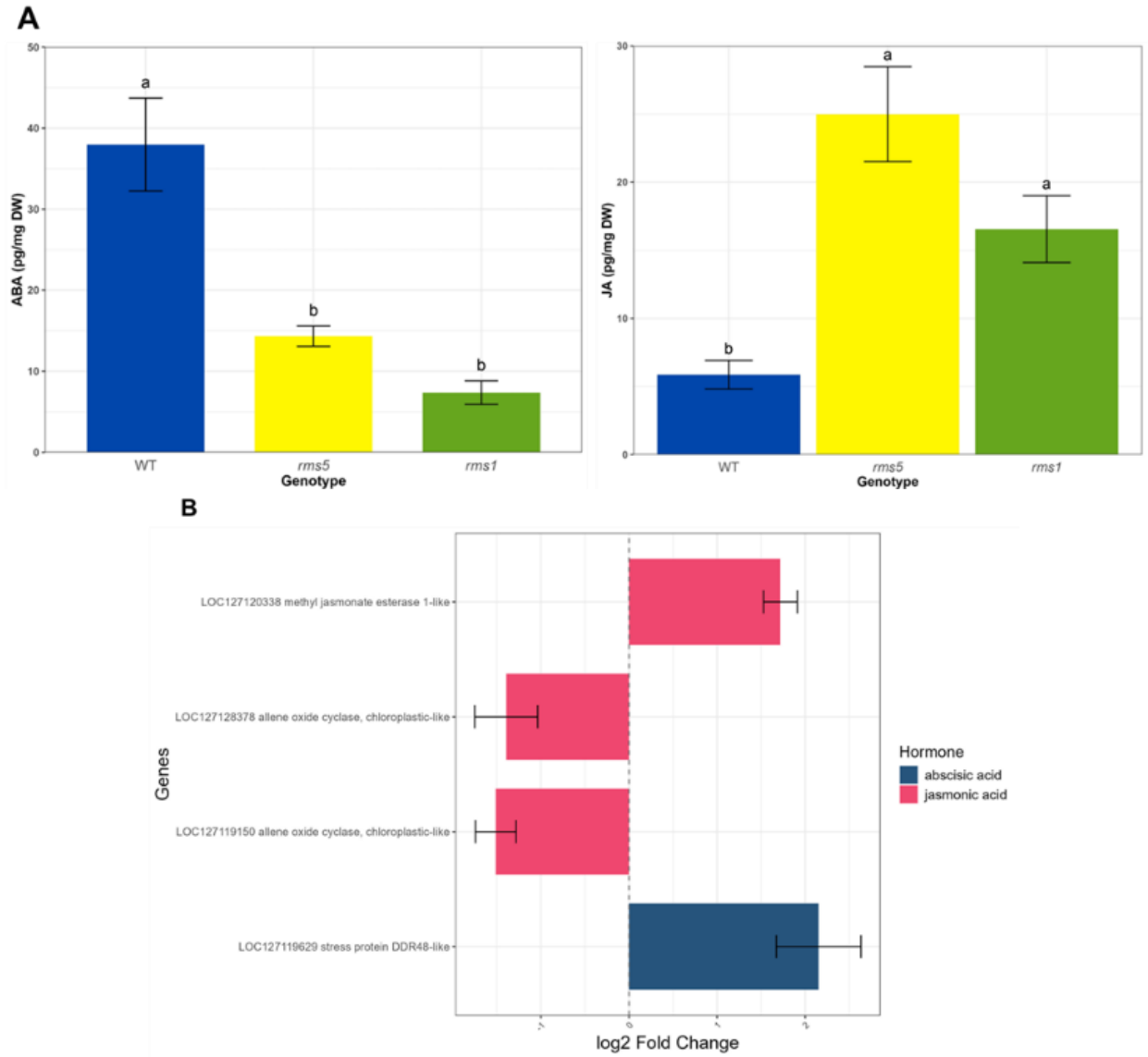

Figure 4. Quantification of abscisic acid (ABA) and jasmonic acid (JA) levels, along with the analysis of related DEGs, in plant roots of *rms* mutants and wild-type (cv. Térèse) under phosphate-starved conditions. **(A)** Bar plot showing ABA and JA levels in *rms* mutants compared to wild-type roots. Data are shown as mean ± SE ($n = 3$). Different letters indicate significant differences ($p < 0.05$, LSD test). **(B)** Bar plot showing DEGs related to ABA and JA metabolic processes in the *rms* mutants compared to wild-type roots.

Analysis of DEGs between *rms1* and *rms5* mutants

To explore the potential involvement of CCD7 and/or CCD8 enzymes in biological processes beyond SL biosynthesis, we next examined the GO-BP enrichment analysis results to search for terms specifically upregulated or downregulated in one mutant compared with the other two genotypes. To this aim, we used data from the *rms1* vs WT, *rms5* vs WT, and the *rms1* vs *rms5* comparisons, the latter resulting in the identification of 2,642 DEGs (1,962 downregulated and 580 upregulated) (Figure 2C). This resulted in the identification of six biological processes differentially expressed in *rms5*, including three downregulated (cell wall modification, plant cell-type organization and

nucleosome assembly), and three upregulated (response to light stimulus, light harvesting in photosystem I and photosynthesis) (Figure 3; Supplementary Table S2).

DISCUSSION

By comparing the transcriptomes of SL-deficient pea mutants and their wild-type genotype, this study highlights a wide range of SL-regulated biological processes, reinforcing the idea that SLs are key integrators of developmental and stress-related signaling pathways. Specifically, we found a significant downregulation of genes involved in the response to oxidative, salt, and heat stresses, and L-phenylalanine and lignin catabolic pathways (Figure 3). This is in line with our finding that SL mutants display significantly lower levels of ABA (Figure 4A), that is known to enhance the plant's antioxidant defense system, stress adaptation, and the phenylpropanoid pathway (Li et al., 2022; Singh et al., 2023; Dong et al., 2021; Omoarelojie et al., 2021). Prior to this study, cross-talk between SLs and ABA was repeatedly reported (Haider et al., 2018; Korek et al., 2023). In addition, reduced ABA levels in SL-deficient mutants were described in tomato, rice, and *Lotus japonicus* (Liu et al., 2015; Liu et al., 2020; Visentin et al., 2020), and SL deficiency was associated with ABA-mediated response to heat stress (Chi et al., 2021). Notably, we did not observe significant differential expression of genes directly involved in ABA biosynthesis (Figure 4B). This suggests that ABA accumulation is regulated post-transcriptionally, possibly via enhanced catabolism, altered transport, or reduced enzymatic activity.

SLs support root growth by promoting meristem activity and lateral root formation (Kapulnik et al., 2011; Ruyter-Spira et al., 2011; Koren et al., 2013). This explains why SL mutants also exhibited a significant downregulation of biological processes related to cell cycle and division, namely cyclin-dependent protein serine/threonine kinase activity, mitotic cell phase transition, microtubule-based movement, DNA replication initiation and double strand break repair (Figure 3, Supplementary Table S2). With this respect, it is worth noticing that significant changes in cortical microtubule organization were reported in Arabidopsis hypocotyl cells following treatment with the synthetic SL analog GR24 (Krasylenko et al., 2021). Reduced root growth, and thus lower demand for energy in root tissues, may explain the downregulation of genes involved in carbohydrate metabolism, as part of a broader adjustment in resource allocation (Figure 3, Supplementary Table S2).

Although it is well-established that SLs are as key mediators of plant adaptation to phosphate deficiency, this study is, to our knowledge, the first reporting the upregulation, in SL biosynthetic mutants, of genes involved in cellular response with phosphate starvation, likely as a compensatory response to impaired SL signaling (Figure 3, Supplementary Table S2).

Remarkably, our study identifies biological processes that are specifically upregulated (photosynthesis, light harvesting in photosystem I) or downregulated (plant cell wall organization, cell wall modification, and nucleosome assembly) in *rms5* mutant (Figure 3, Supplementary Table

S2). Unlike *rms1* mutants, *rms5* mutants, impaired in *CCD7*, accumulate 9-*cis*-β-carotene and related carotenoides, which may undergo non-enzymatic oxidative cleavage to yield various apocarotenoids. Compelling evidance suggests that carotenoids and/or apocarotenoids can trigger retrograde signaling pathways that modulate nuclear gene expression and influence key developmental processes, including plastid biogenesis (Moreno et al., 2020; Wang et al., 2021; Sierra et al., 2022). Alternatively, the specific transcriptomic shifts observed in *rms5* could be attributed to the broader substrate specificity of CCD7, as previously reported (Bruno et al., 2014; Hou et al., 2016), which may result in the formation of additional bioactive apocarotenoids. Notably, CCD7 has been implicated in the initial enzymatic step leading to the production of cyclohexenone (C13) and mycorradicin (C14) derivatives from an as-yet unidentified carotenoid precursor (Walter et al., 2007). Supporting the hypothesis of CCD7-specific roles beyond SL biosynthesis, we found that *rms5* and *rms1* mutants, despite both lacking detectable SL levels, exhibit clearly distinct transcriptomic profiles (Figure 1).

In addition to relations between SL and ABA, our study also highlighted significantly higher levels of JA in *rms* mutants (Figure 4A). This finding is consistent with previous works reporting that rice SL biosynthetic and signalling mutants accumulate higher JA in both roots and leaves compared with wild-type (Lahari et al., 2019; Liu et al., 2022; Lahari et al., 2023). Notably, our data suggest a molecular link between SL and JA pathways, as we found that SL depletion was associated with the higher expression of a gene encoding a methyl jasmonate esterase possibly responsible for the production of JA from MeJA (Liu et al., 2021) (Figure 4B).

Overall, our study sheds light on the biological role of SLs and unveils SL-independent roles for carotenoid cleavage operated by CCD7 , thus paving the way to future functional studies.

REFERENCES

Akiyama, K., Matsuzaki, K. I., & Hayashi, H. (2005). Plant sesquiterpenes induce hyphal branching in arbuscular mycorrhizal fungi. *Nature*, *435*(7043), 824-827.

Al-Babili, S., & Bouwmeester, H. J. (2015). Strigolactones, a novel carotenoid-derived plant hormone. *Annual Review of Plant Biology*, *66*(1), 161-186.

Alder, A., Jamil, M., Marzorati, M., Bruno, M., Vermathen, M., Bigler, P., ... & Al-Babili, S. (2012). The path from β-carotene to carlactone, a strigolactone-like plant hormone. *Science*, *335*(6074), 1348-1351.

Aliche, E. B., Screpanti, C., De Mesmaeker, A., Munnik, T., & Bouwmeester, H. J. (2020). Science and application of strigolactones. *New Phytologist*, *227*(4), 1001-1011.

Araújo, S. S., Beebe, S., Crespi, M., Delbreil, B., González, E. M., Gruber, V., ... & Patto, M. C. V. (2015). Abiotic stress responses in legumes: strategies used to cope with environmental challenges. *Critical Reviews in Plant Sciences*, *34*(1-3), 237-280.

Benitez-Alfonso, Y., Soanes, B. K., Zimba, S., Sinanaj, B., German, L., Sharma, V., ... & Foyer, C. H. (2023). Enhancing climate change resilience in agricultural crops. *Current Biology*, *33*(23), R1246-R1261.

Blighe, K., Rana, S., & Lewis, M. (2024). EnhancedVolcano: Publication-ready volcano plots with enhanced colouring and labeling. R package version 1.24.0.

Bouwmeester, H., Li, C., Thiombiano, B., Rahimi, M., & Dong, L. (2021). Adaptation of the parasitic plant lifecycle: germination is controlled by essential host signaling molecules. *Plant Physiology*, *185*(4), 1292-1308.

Bruno, M., Hofmann, M., Vermathen, M., Alder, A., Beyer, P., & Al-Babili, S. (2014). On the substrate-and stereospecificity of the plant carotenoid cleavage dioxygenase 7. *FEBS Letters*, *588*(9), 1802-1807.

Chaiwanon, J., Wang, W., Zhu, J. Y., Oh, E., & Wang, Z. Y. (2016). Information integration and communication in plant growth regulation. *Cell*, *164*(6), 1257-1268.

Chi, C., Xu, X., Wang, M., Zhang, H., Fang, P., Zhou, J., ... & Yu, J. (2021). Strigolactones positively regulate abscisic acid-dependent heat and cold tolerance in tomato. *Horticulture Research*, *8*.

Cook, C. E., Whichard, L. P., Turner, B., Wall, M. E., & Egley, G. H. (1966). Germination of witchweed (*Striga lutea* Lour.): isolation and properties of a potent stimulant. *Science*, *154*(3753), 1189-1190.

De Mendiburu, F., & Yaseen, M. (2020). AGRICOLAE: statistical procedures for agricultural research, version 1.2-4.

Dong, N. Q., & Lin, H. X. (2021). Contribution of phenylpropanoid metabolism to plant development and plant–environment interactions. *Journal of Integrative Plant Biology*, *63*(1), 180-209.

Floss, D. S., Schliemann, W., Schmidt, J., Strack, D., & Walter, M. H. (2008). RNA interference-mediated repression of *MtCCD1* in mycorrhizal roots of *Medicago truncatula* causes accumulation of C27 apocarotenoids, shedding light on the functional role of CCD1. *Plant Physiology*, *148*(3), 1267-1282.

Gomez-Roldan, V., Fermas, S., Brewer, P. B., Puech-Pagès, V., Dun, E. A., Pillot, J. P., ... & Rochange, S. F. (2008). Strigolactone inhibition of shoot branching. *Nature*, *455*(7210), 189-194.

Guan, Y., Li, L., Wang, D., Zhou, J., Qi, W., Cheng, Y., ... & Quan, M. (2025). Multifaceted functions of strigolactones in annual and perennial plants: developmental regulation, phytohormone crosstalk and abiotic stresses. *Plant Stress*, *16*, 100895.

Haider, I., Andreo-Jimenez, B., Bruno, M., Bimbo, A., Floková, K., Abuauf, H., ... & Ruyter-Spira, C. (2018). The interaction of strigolactones with abscisic acid during the drought response in rice. *Journal of Experimental Botany*, *69*(9), 2403-2414.

Hill, E. M., Robinson, L. A., Abdul-Sada, A., Vanbergen, A. J., Hodge, A., & Hartley, S. E. (2018). Arbuscular mycorrhizal fungi and plant chemical defence: effects of colonisation on aboveground and belowground metabolomes. *Journal of Chemical Ecology*, *44*, 198-208.

Hou, X., Rivers, J., León, P., McQuinn, R. P., & Pogson, B. J. (2016). Synthesis and function of apocarotenoid signals in plants. *Trends in Plant Science*, *21*(9), 792-803.

Johnson, X., Brcich, T., Dun, E. A., Goussot, M., Haurogné, K., Beveridge, C. A., & Rameau, C. (2006). Branching genes are conserved across species. Genes controlling a novel signal in pea are coregulated by other long-distance signals. *Plant Physiology*, *142*(3), 1014-1026.

Kapulnik, Y., Delaux, P. M., Resnick, N., Mayzlish-Gati, E., Wininger, S., Bhattacharya, C., ... & Koltai, H. (2011). Strigolactones affect lateral root formation and root-hair elongation in *Arabidopsis*. *Planta*, *233*, 209-216.

Kolberg, L., Raudvere, U., Kuzmin, I., Vilo, J., & Peterson, H. (2020). gprofiler2--an R package for gene list functional enrichment analysis and namespace conversion toolset g: Profiler. *F1000Research*, *9*, ELIXIR-709.

Koren, D., Resnick, N., Gati, E. M., Belausov, E., Weininger, S., Kapulnik, Y., & Koltai, H. (2013). Strigolactone signaling in the endodermis is sufficient to restore root responses and involves SHORT HYPOCOTYL 2 (SHY2) activity. *New Phytologist*, *198*(3), 866-874.

Korek, M., & Marzec, M. (2023). Strigolactones and abscisic acid interactions affect plant development and response to abiotic stresses. *BMC Plant Biology*, *23*(1), 314.

Krasylenko, Y., Komis, G., Hlynska, S., Vavrdová, T., Ovečka, M., Pospíšil, T., & Šamaj, J. (2021). GR24, a synthetic strigolactone analog, and light affect the organization of cortical microtubules in Arabidopsis hypocotyl cells. *Frontiers in Plant Science*, *12*, 675981.

Lahari, Z., Ullah, C., Kyndt, T., Gershenzon, J., & Gheysen, G. (2019). Strigolactones enhance root-knot nematode (*Meloidogyne graminicola*) infection in rice by antagonizing the jasmonate pathway. *New Phytologist*, *224*(1), 454-465.

Lahari, Z., van Boerdonk, S., Omoboye, O. O., Reichelt, M., Höfte, M., Gershenzon, J., ... & Ullah, C. (2024). Strigolactone deficiency induces jasmonate, sugar and flavonoid phytoalexin accumulation enhancing rice defense against the blast fungus *Pyricularia oryzae*. *New Phytologist*, *241*(2), 827-844.

Lanfranco, L., Fiorilli, V., & Gutjahr, C. (2018). Partner communication and role of nutrients in the arbuscular mycorrhizal symbiosis. *New Phytologist*, *220*(4), 1031-1046.

Liu, H., & Timko, M. P. (2021). Jasmonic acid signaling and molecular crosstalk with other phytohormones. *International Journal of Molecular Sciences*, *22*(6), 2914.

Liu, J., He, H., Vitali, M., Visentin, I., Charnikhova, T., Haider, I., ... & Cardinale, F. (2015). Osmotic stress represses strigolactone biosynthesis in *Lotus japonicus* roots: exploring the interaction between strigolactones and ABA under abiotic stress. *Planta*, *241*, 1435-1451.

Liu, L., Li, K., Zhou, X., & Fang, C. (2022). Integrative analysis of metabolome and transcriptome reveals the role of strigolactones in wounding-induced rice metabolic re-programming. *Metabolites*, *12*(9), 789.

Liu, X., Hu, Q., Yan, J., Sun, K., Liang, Y., Jia, M., ... & Wang, B. (2020). ζ-Carotene isomerase suppresses tillering in rice through the coordinated biosynthesis of strigolactone and abscisic acid. *Molecular Plant*, *13*(12), 1784-1801.

Love, M. I., Huber, W., & Anders, S. (2014). Moderated estimation of fold change and dispersion for RNA-seq data with DESeq2. *Genome Biology*, *15*, 1-21.

Moreno, J. C., Mi, J., Alagoz, Y., & Al-Babili, S. (2021). Plant apocarotenoids: from retrograde signaling to interspecific communication. *The Plant Journal*, *105*(2), 351-375.

Omoarelojie, L. O., Kulkarni, M. G., Finnie, J. F., & Van Staden, J. (2021). Strigolactone analog (rac-GR24) enhances chilling tolerance in mung bean seedlings. *South African Journal of Botany*, *140*, 173-181.

Parihar, A. K., Kumar, J., Gupta, D. S., Lamichaney, A., Naik Sj, S., Singh, A. K., ... & Toklu, F. (2022). Genomics enabled breeding strategies for major biotic stresses in pea (*Pisum sativum* L.). *Frontiers in Plant Science*, *13*, 861191.

Richmond, B. L., Coelho, C. L., Wilkinson, H., McKenna, J., Ratchinski, P., Schwarze, M., ... & Gifford, M. L. (2022). Elucidating connections between the strigolactone biosynthesis pathway, flavonoid production and root system architecture in *Arabidopsis thaliana*. *Physiologia Plantarum*, *174*(2), e13681.

Ruyter-Spira, C., Kohlen, W., Charnikhova, T., van Zeijl, A., van Bezouwen, L., De Ruijter, N., ... & Bouwmeester, H. (2011). Physiological effects of the synthetic strigolactone analog GR24 on root system architecture in Arabidopsis: another belowground role for strigolactones?. *Plant physiology*, *155*(2), 721-734.

Stra, A., Almarwaey, L. O., Alagoz, Y., Moreno, J. C., & Al-Babili, S. (2023). Carotenoid metabolism: New insights and synthetic approaches. *Frontiers in Plant Science*, *13*, 1072061.

Visentin, I., Pagliarani, C., Deva, E., Caracci, A., Turečková, V., Novák, O., ... & Cardinale, F. (2020). A novel strigolactone-miR156 module controls stomatal behaviour during drought recovery. *Plant, Cell & Environment*, *43*(7), 1613-1624.

Walter, M. H., Floss, D. S., & Strack, D. (2010). Apocarotenoids: hormones, mycorrhizal metabolites and aroma volatiles. *Planta*, *232*, 1-17.

Wang, J. Y., Haider, I., Jamil, M., Fiorilli, V., Saito, Y., Mi, J., ... & Al-Babili, S. (2019). The apocarotenoid metabolite zaxinone regulates growth and strigolactone biosynthesis in rice. *Nature Communications*, *10*(1), 810.

Wang, J. Y., Lin, P. Y., & Al-Babili, S. (2021). On the biosynthesis and evolution of apocarotenoid plant growth regulators. In *Seminars in cell & developmental biology* (Vol. 109, pp. 3-11). Academic Press.

Wang, J. Y., Chen, G. T. E., Braguy, J., & Al-Babili, S. (2024). Distinguishing the functions of canonical strigolactones as rhizospheric signals. *Trends in Plant Science*, *29*, 925-936.

Waters, M. T., Gutjahr, C., Bennett, T., & Nelson, D. C. (2017). Strigolactone signaling and evolution. *Annual Review of Plant Biology*, *68*(1), 291-322.

Wu, F., Gao, Y., Yang, W., Sui, N., & Zhu, J. (2022). Biological functions of strigolactones and their crosstalk with other phytohormones. *Frontiers in Plant Science*, *13*, 821563.

Supplementary materials

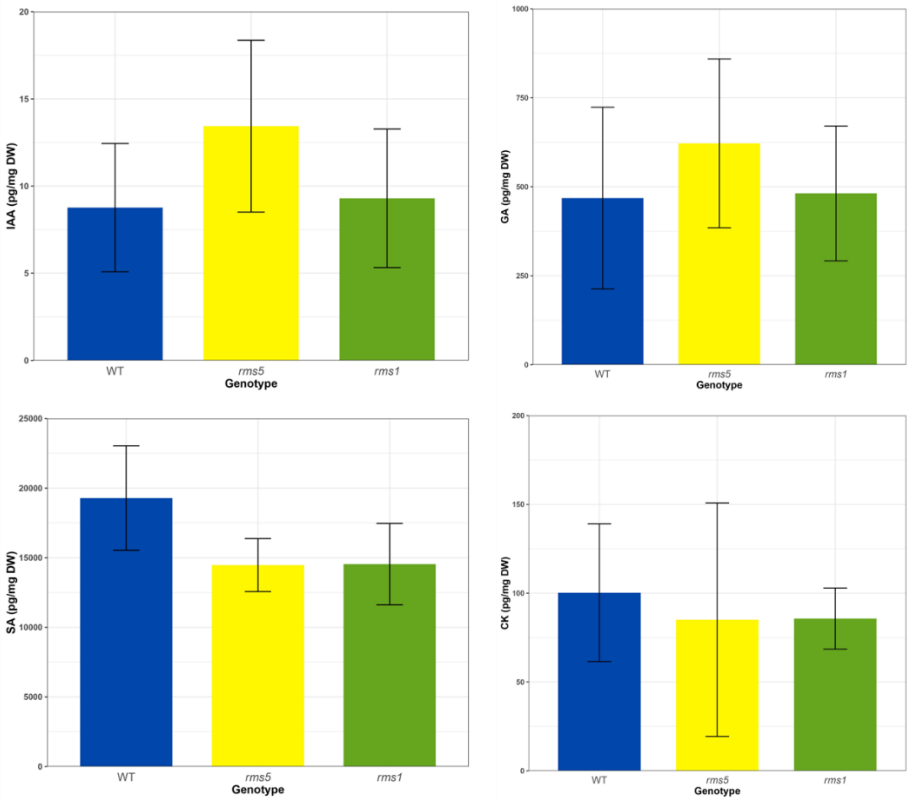

Supplementary Figure S1. Bar plot showing auxin (IAA), gibberellin (GA), salicylic acid (SA), and cytokinin (iPR-CK) levels in *rms* mutants and wild-type (cv. Térèse) roots under phosphate-starved conditions. Data are shown as mean ± SE (n = 3).

Supplementary Table S1. Read mapping summary of the RNA-seq experiment.

Attribute	rms1_A	rms1_B	rms1_C	rms5_A	rms5_B	rms5_C	WT_A	WT_B	WT_C	Average
Number of input reads |	39882166	35728567	35082612	42666017	42802112	42395767	42481351	36763640	32883929	38965129
Average input read length |	279	278	278	279	278	278	278	278	278	278.222222
UNIQUE READS:										
Uniquely mapped reads number |	35329608	31582264	30982749	35856659	34690228	35335071	30581690	26889976	24226513	31719417.6
Uniquely mapped reads % |	88.58%	88.39%	88.31%	84.04%	81.05%	83.35%	71.99%	73.14%	73.67%	81.39%
Average mapped length |	277.98	277.67	277.77	277.78	277.34	277.31	277.56	277.72	277.56	277.632222
Number of splices: Total |	34067062	30138645	29861908	34422668	33216683	33934718	28806905	25261072	22486256	30243990.8
Number of splices: Annotated (sjdb) |	33374494	29520133	29250093	33643742	32456513	33136841	28195693	24720178	22002225	29588879.1
Number of splices: GT/AG |	33627589	29747878	29479991	33939494	32747657	33461426	28436664	24935746	22194926	29841263.4
Number of splices: GC/AG |	337767	298879	292621	374797	362211	363381	275353	241310	217245	307062.667
Number of splices: AT/AC |	18591	16726	17082	19174	18732	19434	15287	13212	11556	16643.7778
Number of splices: Non-canonical |	83115	75162	72214	89203	88083	90477	79601	70804	62529	79020.8889
Mismatch rate per base, % |	0.41%	0.42%	0.40%	0.49%	0.51%	0.49%	0.45%	0.44%	0.46%	0.00452222
Deletion rate per base |	0.02%	0.02%	0.02%	0.02%	0.02%	0.02%	0.02%	0.02%	0.02%	0.0002
Deletion average length |	2.99	3	2.94	3.19	3.2	3.19	3.03	3.04	3.06	3.07111111
Insertion rate per base |	0.02%	0.02%	0.02%	0.02%	0.02%	0.02%	0.02%	0.02%	0.02%	0.02%
Insertion average length |	2.42	2.44	2.36	2.69	2.69	2.7	2.5	2.52	2.52	2.53777778
MULTI-MAPPING READS:										
Number of reads mapped to multiple loci |	1025944	917016	904119	1331693	1338101	1326189	1237013	1081014	969716	1125645
% of reads mapped to multiple loci |	2.57%	2.57%	2.58%	3.12%	3.13%	3.13%	2.91%	2.94%	2.95%	2.88%
Number of reads mapped to too many loci |	61413	56403	57932	162867	206143	159000	204144	159140	141874	134324
% of reads mapped to too many loci |	0.15%	0.16%	0.17%	0.38%	0.48%	0.38%	0.48%	0.43%	0.43%	0.34%
UNMAPPED READS:										
Number of reads unmapped: too many mismatches |	0	0	0	0	0	0	0	0	0	0
% of reads unmapped: too many mismatches |	0.00%	0.00%	0.00%	0.00%	0.00%	0.00%	0.00%	0.00%	0.00%	0.00%
Number of reads unmapped: too short |	2980131	2751110	2672061	4191358	4714305	4321866	8030480	6781616	6074938	4724207.22
% of reads unmapped: too short |	7.47%	7.70%	7.62%	9.82%	11.01%	10.19%	18.90%	18.45%	18.47%	12.18%
Number of reads unmapped: other |	485070	421774	465751	1123440	1853335	1253641	2428024	1851894	1470888	1261535.22
CHIMERIC READS:										
% of reads unmapped: other |	1.22%	1.18%	1.33%	2.63%	4.33%	2.96%	5.72%	5.04%	4.47%	3.21%
Number of chimeric reads |	0	0	0	0	0	0	0	0	0	0
% of chimeric reads |	0.00%	0.00%	0.00%	0.00%	0.00%	0.00%	0.00%	0.00%	0.00%	0.00%

Supplementary Table S2. GO enrichment analyses of DEGs identified in the comparisons between SL-deficient *rms* mutants and wild-type (cv. Térèse) plants, specifically: *rms1* vs WT, *rms5* vs WT, and *rms1* vs *rms5*.

Term ID	Term name	Term size	Effective domain size	Query size	Intersection size	p value	Precision	Recall	Intersection	comparison	trend
GO:0006334	nucleosome assembly	83	8860	1282	43	3.14E-13	3.35E-02	5.18E-01	LOC127080296,LOC127080288,LOC127118786,LOC127125921,LOC127125928,LOC127158567,LOC127158568,LOC127084627,LOC127084626,LOC127084628,LOC127084631,LOC127086881,LOC127086882,LOC127095518,LOC127096599,LOC127096600,LOC127092249,LOC127092253,LOC127106054,LOC127106059,LOC127118787,LOC127125922,LOC127125924,LOC127126078,LOC127127928,LOC127138565,LOC127075708,LOC127075709,LOC127075710,LOC127080832,LOC127082474,LOC127084632,LOC127084654,LOC127086883,LOC127098573,LOC127096601,LOC127100730,LOC127106140,LOC127106053,LOC127106057,LOC127106061,LOC127100838,LOC127101330	rms5_vs_WT	down
GO:0005975	carbohydrate metabolic process	245	8860	1282	80	3.86E-11	6.24E-02	3.27E-01	LOC127108310,LOC127135496,LOC127107895,LOC127137695,LOC127137722,LOC127073819,LOC127118002,LOC127113385,LOC127118913,LOC127120469,LOC127132161,LOC127127959,LOC127158386,LOC127074635,LOC127075987,LOC127138058,LOC127138059,LOC127138060,LOC127085218,LOC127082888,LOC127084449,LOC127083797,LOC127085522,LOC127086101,LOC127085629,LOC127087108,LOC127083668,LOC127097834,LOC127098626,LOC127097449,LOC127098294,LOC127091213,LOC127092922,LOC127098105,LOC127100450,LOC127108428,LOC127104235,LOC127101623,LOC127100904,LOC127107418,LOC127075205,LOC127104405,LOC127079138,LOC127132062,LOC127107868,LOC127107877,LOC127119306,LOC127132061,LOC127107874,LOC127107941,LOC127074795,LOC127138057,LOC127076592,LOC127085058,LOC127084521,LOC127084179,LOC127087961,LOC127079103,LOC127079102,LOC127082801,LOC127087529,LOC127087556,LOC127091283,LOC127062412,LOC127093037,LOC127091936,LOC127098624,LOC127097511,LOC127091587,LOC127098104,LOC127102819,LOC127105784,LOC127107412,LOC127101211,LOC127105764,LOC127100903,LOC127100907,LOC127107314,LOC127105107	rms5_vs_WT	down
GO:0009664	plant-type cell wall organization	26	8860	1282	20	1.53E-10	1.56E-02	7.69E-01	LOC127127150,LOC127127624,LOC127080761,LOC127084599,LOC127087176,LOC127087221,LOC127095435,LOC127093250,LOC127097601,LOC127105211,LOC127101389,LOC127119494,LOC127120693,LOC127128567,LOC127135289,LOC127082286,LOC127095255,LOC127095828,LOC127091291,LOC127106782	rms5_vs_WT	down
GO:0006979	response to oxidative stress	83	8860	1282	38	4.43E-10	2.96E-02	4.58E-01	LOC127119991,LOC127115786,LOC127075601,LOC127085516,LOC127118460,LOC127120101,LOC127120205,LOC127120460,LOC127125461,LOC127126220,LOC127127386,LOC127135082,LOC127138368,LOC127135043,LOC127074375,LOC127074623,LOC127074731,LOC127081188,LOC127086766,LOC127087290,LOC127093438,LOC127092343,LOC127093400,LOC127091787,LOC127098134,LOC127106951,LOC127102428,LOC127096705,LOC127075525,LOC127075576,LOC127075616,LOC127118458,LOC127118462,LOC127080557,LOC127080576,LOC127092597	rms5_vs_WT	down
GO:0042744	hydrogen peroxide catabolic process	76	8860	1282	36	4.43E-10	2.81E-02	4.74E-01	LOC127108310,LOC127135496,LOC127107895,LOC127137695,LOC127137722,LOC127073819,LOC127118002,LOC127113385,LOC127118913,LOC127120469,LOC127132161,LOC127127959,LOC127138368,LOC127135043,LOC127074375,LOC127074623,LOC127074731,LOC127081188,LOC127086766,LOC127087290,LOC127093438,LOC127092343,LOC127093400,LOC127091787,LOC127098134,LOC127106951,LOC127102428,LOC127096705,LOC127075525,LOC127075576,LOC127075616,LOC127118458,LOC127118462,LOC127080557,LOC127080576,LOC127092597	rms5_vs_WT	down
GO:0046274	lignin catabolic process	18	8860	1282	15	7.05E-09	1.17E-02	8.33E-01	LOC127102230,LOC127127615,LOC127127617,LOC127127646,LOC127127702,LOC127127705,LOC127084619,LOC127104669,LOC127118091,LOC127118481,LOC127118581,LOC127120232,LOC127127704,LOC127076095,LOC127084023	rms5_vs_WT	down
GO:0044772	mitotic cell cycle phase transition	27	8860	1282	17	3.77E-07	1.33E-02	6.30E-01	LOC127117867,LOC127120030,LOC127126470,LOC127074768,LOC127086204,LOC127082788,LOC127087524,LOC127120474,LOC127075138,LOC127088064,LOC127088066,LOC127088069,LOC127088075,LOC127088423,LOC127086812,LOC127095907,LOC127097925	rms5_vs_WT	down
GO:0042545	cell wall modification	42	8860	1282	22	3.77E-07	1.72E-02	5.24E-01	LOC127132649,LOC127132650,LOC127127855,LOC127127864,LOC127135583,LOC127135585,LOC127076198,LOC127079494,LOC127082034,LOC127078397,LOC127085963,LOC127086041,LOC127104142,LOC127127112,LOC127128120,LOC127136348,LOC127120619,LOC127132415,LOC127132652,LOC127126257,LOC127085964,LOC127101825	rms5_vs_WT	down
GO:0000079	regulation of cyclin-dependent protein serine/threonine kinase activity	36	8860	1282	20	3.77E-07	1.56E-02	5.56E-01	LOC127117867,LOC127120030,LOC127126470,LOC127126901,LOC127074768,LOC127076698,LOC127086204,LOC127082788,LOC127087524,LOC127120474,LOC127127914,LOC127075138,LOC127088064,LOC127088066,LOC127088069,LOC127088075,LOC127086423,LOC127086812,LOC127095907,LOC127097925	rms5_vs_WT	down
GO:0042542	response to hydrogen peroxide	27	8860	1282	16	3.05E-06	1.25E-02	5.93E-01	LOC127097931,LOC127097930,LOC127097909,LOC127108315,LOC127108329,LOC127101306,LOC127101062,LOC127123594,LOC127118223,LOC127076221,LOC127087891,LOC127087893,LOC127087892,LOC127097228,LOC127103818,LOC127101307	rms5_vs_WT	down
GO:0009651	response to salt stress	29	8860	1282	16	9.92E-06	1.25E-02	5.52E-01	LOC127097931,LOC127097930,LOC127097909,LOC127108315,LOC127108329,LOC127101306,LOC127101062,LOC127123594,LOC127118223,LOC127076221,LOC127087891,LOC127087893,LOC127087892,LOC127097228,LOC127103818,LOC127101307	rms5_vs_WT	down
GO:0051259	protein complex oligomerization	29	8860	1282	16	9.92E-06	1.25E-02	5.52E-01	LOC127097931,LOC127097930,LOC127097909,LOC127108315,LOC127108329,LOC127101306,LOC127101062,LOC127123594,LOC127118223,LOC127076221,LOC127087891,LOC127087893,LOC127087892,LOC127097228,LOC127103818,LOC127101307	rms5_vs_WT	down
GO:0019438	aromatic compound biosynthetic process	27	8860	1282	15	1.90E-05	1.17E-02	5.56E-01	LOC127117487,LOC127117488,LOC127121036,LOC127128508,LOC127128603,LOC127074970,LOC127076154,LOC127128642,LOC127128644,LOC127128645,LOC127108081,LOC127132055,LOC127126089,LOC127095599,LOC127106487	rms5_vs_WT	down
GO:0032259	methylation	41	8860	1282	18	1.21E-04	1.40E-02	4.39E-01	LOC127117487,LOC127117488,LOC127121036,LOC127128508,LOC127128603,LOC127074609,LOC127074970,LOC127076154,LOC127084846,LOC127128642,LOC127128644,LOC127128645,LOC127108081,LOC127132055,LOC127126089,LOC127074608,LOC127098595,LOC127106487	rms5_vs_WT	down
GO:0048364	root development	15	8860	1282	10	1.31E-04	7.80E-03	6.67E-01	LOC127085076,LOC127084729,LOC127107057,LOC127107558,LOC127120053,LOC127120061,LOC127078439,LOC127085876,LOC127078515,LOC127105234	rms5_vs_WT	down
GO:0009408	response to heat	43	8860	1282	18	2.32E-04	1.40E-02	4.19E-01	LOC127097931,LOC127097930,LOC127097909,LOC127108315,LOC127108329,LOC127101306,LOC127101062,LOC127123594,LOC127118223,LOC127076221,LOC127087891,LOC127087893,LOC127087892,LOC127081434,LOC127088066,LOC127103818,LOC127101307	rms5_vs_WT	down
GO:0007018	microtubule-based movement	59	8860	1282	22	2.32E-04	1.72E-02	3.73E-01	LOC127085316,LOC127117548,LOC127126549,LOC127127682,LOC127084516,LOC127088267,LOC127093105,LOC127055521,LOC127121645,LOC127114423,LOC127117645,LOC127132640,LOC127125628,LOC127084806,LOC127085710,LOC127093565,LOC127105579,LOC127105001,LOC127100656,LOC127100761	rms5_vs_WT	down
GO:0048367	shoot system development	14	8860	1282	9	5.08E-04	7.02E-03	6.43E-01	LOC127084729,LOC127107057,LOC127107558,LOC127120053,LOC127120061,LOC127078439,LOC127085876,LOC127078515,LOC127105234	rms5_vs_WT	down
GO:0051603	proteolysis involved in protein catabolic process	41	8860	1282	16	1.71E-03	1.25E-02	3.90E-01	LOC127115670,LOC127080882,LOC127115171,LOC127080918,LOC127080929,LOC127080940,LOC127080949,LOC127074010,LOC127101580,LOC127080901,LOC127080908,LOC127115173,LOC127080958,LOC127082715,LOC127101749,LOC127106876	rms5_vs_WT	down
GO:0000727	double-strand break repair via break-induced replication	10	8860	1282	7	1.76E-03	5.46E-03	7.00E-01	LOC127152618,LOC127127778,LOC127073431,LOC127104488,LOC127102825,LOC127108178,LOC127073171	rms5_vs_WT	down
GO:0006559	L-phenylalanine catabolic process	14	8860	1282	8	3.82E-03	6.24E-03	5.71E-01	LOC127117704,LOC127125697,LOC127117466,LOC127125805,LOC127125806,LOC127126312,LOC127098546,LOC127092228	rms5_vs_WT	down
GO:0006270	DNA replication initiation	14	8860	1282	8	3.82E-03	6.24E-03	5.71E-01	LOC127152618,LOC127127778,LOC127073431,LOC127105083,LOC127104488,LOC127119528,LOC127085026,LOC127084592	rms5_vs_WT	down
GO:0006629	lipid metabolic process	92	8860	1282	26	6.32E-03	2.03E-02	2.83E-01	LOC127127471,LOC127120370,LOC127120372,LOC127120820,LOC127132036,LOC127125886,LOC127126151,LOC127074690,LOC127075248,LOC127076717,LOC127097864,LOC127107471,LOC127124040,LOC127117639,LOC127120581,LOC127076174,LOC127084563,LOC127084836,LOC127086566,LOC127088446,LOC127088647,LOC127094753,LOC127002265,LOC127106069,LOC127101115,LOC127105648	rms5_vs_WT	down
GO:0015979	photosynthesis	36	8860	376	18	1.10E-13	4.79E-02	5.00E-01	LOC127075655,LOC127126512,LOC127073792,LOC127076748,LOC127076816,LOC127087878,LOC127083038,LOC127085270,LOC127086091,LOC127087483,LOC127091001,LOC127091850,LOC127093202,LOC127126980,LOC127079879,LOC127104989,LOC127122918,LOC127138567	rms5_vs_WT	up
GO:0009768	photosynthesis, light harvesting in photosystem I	13	8860	376	10	3.92E-10	2.66E-02	7.69E-01	LOC127126478,LOC127131099,LOC127084779,LOC127117465,LOC127117511,LOC127076171,LOC127085378,LOC127107008,LOC127105163,LOC127086414	rms5_vs_WT	up
GO:0009416	response to light stimulus	13	8860	376	10	3.93E-05	2.66E-02	3.03E-01	LOC127126478,LOC127131099,LOC127084779,LOC127117465,LOC127117511,LOC127076171,LOC127085378,LOC127107008,LOC127105163,LOC127086414	rms5_vs_WT	up
GO:0016036	cellular response to phosphate starvation	12	8860	376	5	3.77E-03	1.33E-02	4.17E-01	LOC127107345,LOC127092838,LOC127073554,LOC127087337,LOC127093215	rms5_vs_WT	up
GO:0046274	lignin catabolic process	18	8750	438	12	5.31E-10	2.74E-02	6.67E-01	LOC127127615,LOC127127617,LOC127127702,LOC127127705,LOC127084619,LOC127104669,LOC127118209,LOC127118481,LOC127120232,LOC127084023,LOC127118112,LOC127106115	rms1_vs_WT	down
GO:0005975	carbohydrate metabolic process	243	8750	438	39	5.64E-09	8.90E-02	1.60E-01	LOC127137695,LOC127073819,LOC127118002,LOC127118585,LOC127118913,LOC127120469,LOC127074635,LOC127082888,LOC127084449,LOC127083797,LOC127083668,LOC127097834,LOC127097449,LOC127098294,LOC127091213,LOC127108428,LOC127100904,LOC127107877,LOC127119306,LOC127087179,LOC127087028,LOC127091283,LOC127092412,LOC127093037,LOC127091587,LOC127100903,LOC127100907,LOC127105107,LOC127126364,LOC127127443,LOC127074985,LOC127087296,LOC127087352,LOC127107402,LOC127106530,LOC127093131,LOC127093133,LOC127086285	rms1_vs_WT	down
GO:0042744	hydrogen peroxide catabolic process	77	8750	438	20	3.88E-08	4.57E-02	2.60E-01	LOC127120101,LOC127135043,LOC127074623,LOC127074731,LOC127087290,LOC127093400,LOC127096705,LOC127075576,LOC127118458,LOC127118462,LOC127080557,LOC127080573,LOC127092597,LOC127075557,LOC127122953,LOC127120542,LOC127084434,LOC127091129,LOC127118084,LOC127086538	rms1_vs_WT	down
GO:0006979	response to oxidative stress	85	8750	438	20	1.91E-07	4.57E-02	2.35E-01	LOC127120101,LOC127135043,LOC127074623,LOC127074731,LOC127087290,LOC127093400,LOC127096705,LOC127075576,LOC127118458,LOC127118462,LOC127080557,LOC127080573,LOC127092597,LOC127075557,LOC127122953,LOC127120542,LOC127084434,LOC127091129,0 C127118084,LOC127086538	rms1_vs_WT	down
GO:0009651	response to salt stress	29	8750	438	11	2.34E-06	2.51E-02	3.79E-01	LOC127097009,LOC127108315,LOC127101306,LOC127118223,LOC127087891,LOC127087892,LOC127103831,LOC127101307,LOC127092040,LOC127092226,LOC127108328	rms1_vs_WT	down
GO:0007018	microtubule-based movement	59	8750	438	15	3.75E-06	3.42E-02	2.54E-01	LOC127085316,LOC127117548,LOC127126549,LOC127127682,LOC127093105,LOC127093521,LOC127121645,LOC127114423,LOC127117645,LOC127132640,LOC127125628,LOC127084806,LOC127105001,LOC127100761,LOC127107898	rms1_vs_WT	down
GO:0042542	response to hydrogen peroxide	27	8750	438	10	8.77E-06	2.28E-02	3.70E-01	LOC127097009,LOC127108315,LOC127101306,LOC127118223,LOC127087891,LOC127087892,LOC127103831,LOC127101307,LOC127092226,LOC127108328	rms1_vs_WT	down
GO:0009408	response to heat	42	8750	438	12	1.31E-05	2.74E-02	2.86E-01	LOC127097009,LOC127108315,LOC127101306,LOC127118223,LOC127087891,LOC127087892,LOC127084885,LOC127103818,LOC127101307,LOC127092226,LOC127108328,LOC127100551	rms1_vs_WT	down
GO:0051259	protein complex oligomerization	29	8750	438	10	1.48E-05	2.28E-02	3.45E-01	LOC127097009,LOC127108315,LOC127101306,LOC127118223,LOC127087891,LOC127087892,LOC127103831,LOC127101307,LOC127092226,LOC127108328	rms1_vs_WT	down
GO:0000727	double-strand break repair via break-induced replication	10	8750	438	6	4.73E-05	1.37E-02	6.00E-01	LOC127152618,LOC127073431,LOC127104488,LOC127102825,LOC127108178,LOC127073171	rms1_vs_WT	down
GO:0044772	mitotic cell cycle phase transition	27	8750	438	9	6.08E-05	2.05E-02	3.33E-01	LOC127117867,LOC127120030,LOC127126470,LOC127074768,LOC127086204,LOC127082788,LOC127087524,LOC127088066,LOC127097925	rms1_vs_WT	down
GO:0000079	regulation of cyclin-dependent protein serine/threonine kinase activity	35	8750	438	9	5.87E-04	2.05E-02	2.57E-01	LOC127117867,LOC127120030,LOC127126470,LOC127074768,LOC127086204,LOC127082788,LOC127087524,LOC127088066,LOC127097925	rms1_vs_WT	down
GO:0009833	plant-type primary cell wall biogenesis	23	8750	438	7	1.24E-03	1.60E-02	3.04E-01	LOC127138081,LOC127080647,LOC127132638,LOC127138457,LOC127075131,LOC127096570,LOC127086715	rms1_vs_WT	down
GO:0051603	proteolysis involved in protein catabolic process	40	8750	438	9	1.56E-03	2.05E-02	2.25E-01	LOC127115171,LOC127080918,LOC127080929,LOC127080901,LOC127080908,LOC127080958,LOC127082715,LOC127101749,LOC127106876	rms1_vs_WT	down
GO:0030244	cellulose biosynthetic process	25	8750	438	7	1.93E-03	1.60E-02	2.80E-01	LOC127138081,LOC127080647,LOC127132638,LOC127138457,LOC127075131,LOC127096570,LOC127086715	rms1_vs_WT	down
GO:0030639	polyketide biosynthetic process	13	8750	438	5	3.11E-03	1.14E-02	3.85E-01	LOC127120635,LOC127120889,LOC127120888,LOC127120633,LOC127120637	rms1_vs_WT	down
GO:0006559	L-phenylalanine catabolic process	14	8750	438	5	3.71E-03	1.14E-02	3.57E-01	LOC127117466,LOC127125808,LOC127126312,LOC127098546,LOC127092228	rms1_vs_WT	down
GO:0010497	plasmodesmata-mediated intercellular transport	8	8750	438	4	3.71E-03	9.13E-03	5.00E-01	LOC127091470,LOC127091469,LOC127098021,LOC127096961	rms1_vs_WT	down
GO:0006270	DNA replication initiation	14	8750	438	5	3.71E-03	1.14E-02	3.57E-01	LOC127152618,LOC127073431,LOC127105083,LOC127104488,LOC127119528	rms1_vs_WT	down
GO:0006268	DNA unwinding involved in DNA replication	14	8750	438	5	3.71E-03	1.14E-02	3.57E-01	LOC127152618,LOC127073720,LOC127104488,LOC127108178,LOC127073171	rms1_vs_WT	down
GO:0006260	DNA replication	38	8750	438	8	4.02E-03	1.83E-02	2.11E-01	LOC127132618,LOC127073431,LOC127073720,LOC127102825,LOC127108178,LOC127119528,LOC127120402,LOC127073171	rms1_vs_WT	down
GO:0006271	DNA strand elongation involved in DNA replication	5	8750	438	3	9.24E-03	6.85E-03	6.00E-01	LOC127132618,LOC127102825,LOC127108178	rms1_vs_WT	down
GO:0016036	cellular response to phosphate starvation	12	8750	78	3	8.77E-03	3.85E-02	2.50E-01	LOC127107345,LOC127073554,LOC127087337	rms1_vs_WT	up
GO:0015979	photosynthesis	34	8678	408	13	1.65E-07	3.19E-02	3.82E-01	LOC127075655,LOC127126512,LOC127073792,LOC127076748,LOC127076816,LOC127087878,LOC127083038,LOC127085270,LOC127086091,LOC127087483,LOC127091001,LOC127091850,LOC127093202	rms1_vs_rms5	down
GO:0009768	photosynthesis, light harvesting in photosystem I	14	8678	408	9	1.65E-07	2.21E-02	6.43E-01	LOC127126478,LOC127131099,LOC127084779,LOC127117465,LOC127117511,LOC127076171,LOC127085378,LOC127107008,LOC127105163	rms1_vs_rms5	down
GO:0009416	response to light stimulus	34	8678	408	10	1.44E-04	2.45E-02	2.94E-01	LOC127126478,LOC127131099,LOC127080885,LOC127084779,LOC127117485,LOC127117511,LOC127076171,LOC127085378,LOC127107008,LOC127105163	rms1_vs_rms5	down
GO:0006979	response to oxidative stress	81	8678	715	31	1.51E-11	4.34E-02	3.83E-01	LOC127119991,LOC127115786,LOC127075601,LOC127085516,LOC127118460,LOC127120101,LOC127120205,LOC127120460,LOC127125461,LOC127126220,LOC127126260,LOC127125482,LOC127135082,LOC127138368,LOC127135043,LOC127074375,LOC127074623,LOC127074731,LOC127081188,LOC127086766,LOC127087290,LOC127093438,LOC127092343,LOC127093400,LOC127091787,LOC127098134,LOC127106951,LOC127102428,LOC127105470	rms1_vs_rms5	up
GO:0042744	hydrogen peroxide catabolic process	74	8678	715	29	2.42E-11	4.06E-02	3.92E-01	LOC127119991,LOC127115786,LOC127075601,LOC127085516,LOC127118460,LOC127120101,LOC127120205,LOC127120556,LOC127120460,LOC127125461,LOC127126220,LOC127135082,LOC127138368,LOC127135043,LOC127138651,LOC127074375,LOC127074623,LOC127074731,LOC127081188,LOC127086766,LOC127087290,LOC127093438,LOC127092343,LOC127093400,LOC127091787,LOC127098134,LOC127106951,LOC127102428,LOC127105470	rms1_vs_rms5	up
GO:0042545	cell wall modification	40	8678	715	17	3.92E-07	2.38E-02	4.25E-01	LOC127132649,LOC127132650,LOC127127855,LOC127127864,LOC127135583,LOC127135585,LOC127076198,LOC127079494,LOC127082034,LOC127078397,LOC127085963,LOC127086041,LOC127105503,LOC127105505,LOC127104142,LOC127107112	rms1_vs_rms5	up
GO:0009664	plant-type cell wall organization	21	8678	715	11	2.19E-05	1.54E-02	5.00E-01	LOC127127150,LOC127127624,LOC127080761,LOC127084599,LOC127087176,LOC127087221,LOC127095435,LOC127093250,LOC127097601,LOC127105211,LOC127101389	rms1_vs_rms5	up
GO:0006334	nucleosome assembly	83	8678	715	22	2.97E-05	3.08E-02	2.65E-01	LOC127127926,LOC127080296,LOC127080288,LOC127118786,LOC127125921,LOC127125923,LOC127138567,LOC127138568,LOC127084627,LOC127084626,LOC127084628,LOC127084631,LOC127086881,LOC127086882,LOC127091752,LOC127095518,LOC127096599,LOC127096600,LOC127092249,LOC127092253,LOC127106054,LOC127106059	rms1_vs_rms5	up
GO:0005975	carbohydrate metabolic process	233	8678	715	42	3.86E-05	5.87E-02	1.80E-01	LOC127108310,LOC127135496,LOC127107895,LOC127137695,LOC127137722,LOC127073819,LOC127118002,LOC127113385,LOC127118913,LOC127120469,LOC127132161,LOC127127959,LOC127135082,LOC127073689,LOC127074635,LOC127075987,LOC127138058,LOC127138059,LOC127138060,LOC127085218,LOC127082888,LOC127083449,LOC127083797,LOC127085522,LOC127085101,LOC127086629,LOC127087108,LOC127083668,LOC127097834,LOC127098626,LOC127097449,LOC127098294,LOC127091213,LOC127092922,LOC127092922,LOC127098105,LOC127100450,LOC127108428,LOC127104235,LOC127101623,LOC127100904,LOC127107418,LOC127102230,LOC127127615,LOC127127617,LOC127127646,LOC127127702,LOC127127705,LOC127084619,LOC127104669	rms1_vs_rms5	up
GO:0046274	lignin catabolic process	16	8678	715	8	5.42E-04	1.12E-02	5.00E-01		rms1_vs_rms5	up
GO:0000727	double-strand break repair via break-induced replication	10	8678	715	6	1.40E-03	8.39E-03	6.00E-01	LOC127152618,LOC127127778,LOC127073431,LOC127104488,LOC127102825,LOC127108178	rms1_vs_rms5	up
GO:0042546	cell wall biogenesis	28	8678	715	10	1.40E-03	1.40E-02	3.57E-01	LOC127106797,LOC127115455,LOC127126705,LOC127126711,LOC127138539,LOC127138618,LOC127086798,LOC127097127,LOC127106489,LOC127107069	rms1_vs_rms5	up
GO:0010411	xyloglucan metabolic process	28	8678	715	9	7.19E-03	1.26E-02	3.21E-01	LOC127115455,LOC127126705,LOC127126711,LOC127138539,LOC127138618,LOC127086798,LOC127097127,LOC127106489,LOC127107069	rms1_vs_rms5	up
GO:0000079	regulation of cyclin-dependent protein serine/threonine kinase activity	29	8678	715	9	8.79E-03	1.26E-02	3.10E-01	LOC127117867,LOC127120030,LOC127126470,LOC127126901,LOC127074768,LOC127086204,LOC127082788,LOC127087524	rms1_vs_rms5	up
GO:0034440	lipid oxidation	24	8678	715	8	9.96E-03	1.12E-02	3.33E-01	LOC127076359,LOC127076541,LOC127076551,LOC127076550,LOC127076533,LOC127076534,LOC127076535,LOC127076536	rms1_vs_rms5	up

Chapter 5

Characterization of relations among seed color, phenolic profile and antioxidant activity in lentil

INTRODUCTION

Lentil (*Lens culinaris* Medik.) is a staple food legume cultivated in over 70 countries covering 5.50 million hectares (Parihar et al., 2025). Global lentil production in 2024 was about 6.6 million tonnes, indicating an increase of 15% compared to the 5.7 million tonnes produced in 2023 (Crop Production Statistics, 2024). A wide range of landraces and local varieties are spread in different regions thus representing a valuable source of genetic diversity for breeding programs to both improve plant adaptation to climate constraints, and to meet consumer's preferences (Piergiovanni, 2000). Canada, Australia, and India are the major producers of red lentils, while Canada and the US lead green lentil production and exports. Worldwide, lentil types comprise 70% small-seeded lentils with red cotyledons, 25% green large-seeded and only 5% brown lentils. In Europe, lentils used to be an important crop until the Second World War, but their cultivation drastically decreased in the subsequent decades, becoming unprofitable for farmers and largely replaced by meat as source of proteins in the human diet (Yanni et al., 2023). However, the interest in lentils has been renewed worldwide and in Europe also due to their significance for human health and for sustainable agriculture (Alrosan et al., 2022).

Growing lentils contributes to a significant reduction of nitrogen fertilizer because of the ability of legumes to fix nitrogen in symbiosis with rhizobia and to improve both soil fertility and soil-building capacity (Warne et al., 2019). Several lentil genotypes are drought-tolerant and drought-adapted being resilient in water-limited and rain-fed environments (Warne et al., 2019). In fact, lentils are a primary component of farming systems in Middle East and North Africa (MENA) that are the most water-scarce region in the world, playing a significant role in human and animal nutrition (Noor et al., 2024).

Lentils are rich source of high quality proteins complementing the essential amino acid of staple cereals (Ganesan et al., 2017). In addition to proteins, ranging from approximately 20% to 30% of dry seed weight, lentils contain complex carbohydrates (60–64%) and dietary fibre (11–31%) with known beneficial effects against metabolic disorders and non-communicable diseases (Bennet et al., 2018; Guo et al., 2022; Venter de Villiers et al., 2024). The consumption of lentils is associated with low blood cholesterol and lipid levels, and reduced risks of obesity, type 2 diabetes, colon and breast cancer (Adebamowo et al., 2005; Aslani et al., 2015; Hafiz et al., 2022). These positive effects depend on the abundance of health-promoting components such as unsaturated fatty acids, B vitamins, minerals, and polyphenols (Kushi et al., 1999; Ganesan et al., 2017; Lastras et al., 2021). Among the ppolyphenols, flavonoids are particularly abundant in lentils exhibiting important health-promoting properties aciting against non-communicable diseases (Ganesan et al., 2017; Dhull et al., 2022; Jung et al, 2022; Peng et al, 2022). Moreover, lentil polyphenols reduce the risks of several types of cancers

like thyroid, liver, breast, and prostate cancers (Adebamowo et al., 2005; Caccialupi et al., 2010; Ganesan et al., 2017; Kushi et al., 2017;).

A major concentration of polyphenols was found in the lentil seed coat than in the cotyledons (Manco et al., 2023). Besides their nutraceutical role, lentil polyphenols contributes also on organoleptic properties and seed color (Mirali et al., 2016, 2017).The seed coat color shows a large variation in lentil germplasm depending on the genotype varying from green, tan, grey, brown, black or mottled. Also, cotyledons color vary from yellow, green, or orange-red (Ganesan, 2017; Mirali et al., 2017). In marketing contexts, lentils with uniform and green color are the most appreciated in the United States and Europe, whereas brown seeds are more appreciated across the Mediterranean Basin, and shelled seeds with intense bright red color are the most preferred in Eastern countries (Erdoğan, 2015; Fiocchetti et al., 2009). Besides the background color, lentil seedcoats show a large variability for patterns that can be dotted, spotted, or marbled contributing to the overall color of whole seeds (AGPG, 1985; Irakli et al., 2021).

Red lentil varieties are the most common in global trade and the most consumed worldwide. The red color is putatively contributed by polyphenolic compounds such as tannins and anthocyanins (Giusti et al., 2017). The red color has been attracting the attention of geneticists and producers not only for the health-promoting properties that are associated to these components, but also for their ability to mimic meat color and to be used as plant based substitutes in vegan meat without the need for added colorings which may have stability or safety issues (Muehlbauer et al., 2009; Erdoğan, 2015). Red lentil flour is currently used also to make healthier legume-based pasta and snacks, and traditional Italian gluten-free pasta. Evaluating natural variation in the red lentil genotypes for polyphenols can help the development of lentil-based foods with improved functional value (Purves et al., 2025). However, the treasure of genetic variability for red colour in lentil germplasm has not fully characterized in large red lentil collections (Mirali et al, 2017; Guerra-García et al., 2021; Manco et al., 2023).

In this paper, for the first time we analyzed a broad lentil collection composed by 59 lentil varieties differing for cotyledons color and seed coat background color, showing multiform seed coat pattern (Del Coco et al., 2022) with the aim to assess the correlation between polyphenol content and composition and antioxidant capacity with seed color.

The content of individual flavonoids including anthocyanidins, flavonols, flavans and flavones, and phenolic acids were analyzed by HPLC-DAD whereas total polyphenol content was measured by spectrophotometric assay. The antioxidant capacity of phenolic extracts was evaluated by ABTS assay and by a direct ABTS assay (ABTS*dir*) that was conducted directly on the wholemeal flour.

The results of our study provide fundamental information about red lentil genotypes that could be selected and used for developing novel legume-based foods with health benefits.

MATERIALS AND METHODS

Chemicals

Authentic reference standards of phenolic compounds (caffeic acid, *p*-coumaric acid, gallic acid, *p*-hydroxybenzoic acid, protocatechuic acid, syringic acid, vanillic acid, sinapic acid and ferulic acid, (+)-catechin, (-)-epicatechin, kaempferol, luteolin, myricetin, delphinidin and cyanidin), ABTS (2,2'-Azino-bis(3-ethylbenzothiazoline-6-sulfonic acid), Trolox (6-hydroxy-2,5,7,8-tetramethylchroman-2-carboxylic acid), potassium persulfate, AAPH [2,2′-azobis (2-methyl-propionamide)] were obtained from Sigma-Aldrich (Milan, Italy), and Folin-Ciocalteu reagent, sodium hydroxide, formic acid and HPLC (high performance liquid chromatography) grade solvents were obtained from Carlo Erba Reagent (Milan, Italy).

Plant materials

Fifty-nine red lentil varieties, with different pedigree, year of release, country of origin, and seed morphology were received by ICARDA, Lebanon (Supplementary Table S1). The plants were grown at ICARDA experimental station, Terbol, Lebanon (33.81° N, 35.98° E), in the 2018/19 growing season.

Morphological analyses

Lentils seed coat color was assessed using a Minolta CR-400 model spectrophotometer (Minolta Camera Co, Osaka, Japan) according to the International Commission on Illumination (CIELab, 1978). Whole seeds were transferred into the Minolta collector, and lightness (L*) and color (a*, red index; b*: yellow, index) were assessed. Seed coat patterns and cotyledons colors were classified based on the descriptors reported by AGPG (1985).

Extraction of total polyphenols and flavonoids analyses by HPLC

Total polyphenols were extracted following Manco et al. (2023) with slight modifications. Briefly, 0.1 g of whole-meal flour was extracted by adding 1 mL of methanol/water/formic acid (80/15/5) at room temperature and incubating overnight. Samples were centrifuged at 4,000 x g for 10 min, and the slurry was re-extracted with an additional 10 mL of solvent on a rotary shaker for 1 h, at room temperature. Sample extractions were performed in triplicate.

Flavonoids were extracted from whole-meal samples using two different procedures according to Lee et al. (2017). Flavonoid-enriched extracts were obtained adding 1.2 mL of 50 % methanol containing 1.2 M HCl to 0.1 g of seed fraction powder (hull and cotyledon). The samples were heated in a water

bath at 80 °C for 2 hours and then centrifuged at 10,000 x g at 4 °C for 5 min. Anthocyanin-enriched extracts were achieved from 0.1 g of lentil hull or cotyledon seed powder by adding 0.95 mL of acidified methanol (85 methanol / 15 HCl 1 N v/v) followed by sonication for 1 min. The samples were incubated at 38 °C for 5 min with a mixing frequency of 300 rpm, and subsequently hydrolyzed with 0.2 mL 6 N HCl at 90 °C for 2 h. The extracts were separated through centrifugation at 10,000 x g at 4 °C for 5 min. All analyses were carried out in triplicate.

For flavonoids analysis the conditions were those described by Manco et al. (2023). The identification and quantification of individual phenolic acids was carried out following the conditions described in Alzuwaid et al. (2020).

Folin-Ciocalteu Assay

Total phenol contents were determined following the method by Magalhães et al. (2010) and using a microplate reader (Tecan, Infinite M200). Folin-Ciocalteu reagent diluted in water from Milli-Q system (1:5 v/v) (50 µL) was placed in each well of a microplate, and then 100 µL of sodium hydroxide solution (0.35 M) was added. The absorbance value at 760 nm was recorded after 5 min of incubation. Gallic acid was used to obtain a calibration curve in the range from 2.5 to 40.0 mg/L. The total phenol content of each sample was expressed as gallic acid equivalents (GAE). The analyses were carried out in triplicate.

Total antioxidant capacity assays

ABTS assay was performed on total polyphenols extracts and flavonoid-enriched extracts according to Manco et al. (2023). The absorbance of samples was measured at 734 nm after 6 min using a plate reader (Infinite 200 Pro, Tecan, Männedorf, Switzerland). Antioxidant capacity values were expressed as Trolox equivalents (mmol Trolox Equivalent (TE)/g). Magellan v7.2 software (Tecan, Männedorf, Switzerland) was used to check the plate reader. The analyses were carried out in triplicate.

Total antioxidant capacity of whole-meal flours from the five lentil varieties were assessed following a direct procedure described in Romano et al. (2022) using the ABTS assay. The antioxidant capacity was expressed as mmol Trolox equivalent antioxidant capacity (ABTS*dir*) per gram of whole-meal flour sample. The analyses were carried out in triplicate.

In this manuscript, the total antioxidant capacity obtained with the three different assays (ABTS on extracts, direct ABTS and ORAC) will be referred to as ABTS, ORAC and ABTS*dir*.

Statistical analysis

Normal distribution of the data was verified using the Shapiro-Wilk normality test implemented in the stats R package. Non-normal data were transformed with the bestNormalize package for further analysis. Genotype effects on individual polyphenols, total polyphenol content, antioxidant activity and CIELab indices were tested by one-way ANOVA. Three-way ANOVAs, followed by the Tukey's HSD test, were conducted to assess the effects of cotyledon color (CC), tegument color (TC), and tegument pigmentation pattern (TPP) on individual polyphenols, total polyphenol content (TPC), and antioxidant capacity. The same approach was applied to evaluate the effects of CIELAB color indices. Statistical significance was determined at $P \leq 0.05$ using post hoc LSD test in the Agricolae R package (de Mendiburu, 2023).

Principal Components Analysis (PCA) was performed with the *prcomp* function implemented in the basic stats R package and the results visualized using ggplot2 (Wickham, 2016).

Hierarchical clustering of genotypes and physicochemical variables based on collected data was performed using the complete method implemented in the hclust function of the basic stats R package and rendered with pheatmap (Kolde, 2019).

RESULTS

Biochemical and morphological characterization

ANOVA indicated significant genotypic effects ($p<0.01$) with respect to all the parameters tested, including individual polyphenols (delphinidin, cyanidin, gallic acid, catechin, epicatechin, luteolin, kaempferol and myricetin), total polyphenol content (TPC), antioxidant capacity (expressed as both ABTS*dir* and ABTS) and the three CIELab color space indexes L*, a* and b* (Supplementary Table S2).

Three-way ANOVAs were also performed to determine whether different cotyledon color (CC), tegument color (TC) and tegument pigmentation pattern (TPP) classes were significantly associated with variation of individual polyphenols, TPC and antioxidant capacity. Except for kaempferol, the results were highly significant ($p < 0.01$, Table 1), suggesting that internal and external seed pigmentation is associated with variation of the other variables under test.

Running linear regression models revealed significant associations between at least one of the three CIELab color space indexes and several polyphenols (gallic acid, catechin, epicatechin, luteolin and myricetin), TPC and ABTS ($p < 0.05$, Supplementary Table S3). non-significant results were obtained for cyanidin and kaempferol, delphinidin and TEAC-DIR-TE results were slightly above significance.

Table 1. Three-way ANOVA results effects of cotyledon color (CC), tegument color (TC), and tegument pigmentation pattern (TPP) effects on the concentration of individual polyphenols, total polyphenol content (TPC), and antioxidant capacity in lentil genotypes. Different letters indicate significant differences ($p < 0.01$, LSD test).

		Delphinidin	Cyanidin	Gallic_acid	Catechin	Epicatechin	Luteolin	Kaempferol	Myricetin	TPC	ABTS	ABTSdir
CC	Orange	99.53 ± 30.73 a	56.93 ± 20.44 a	98.5 ± 21.4 b	348.3 ± 96.61 a	466.06 ± 381.85 b	3.34 ± 2.69 a	158.89 ± 37.54 a	3.45 ± 1.75 a	4.08 ± 0.72 b	0.06 ± 0.01 a	0.1 ± 0.02 a
CC	Orange/Red	83.83 ± 32.84 a	50.45 ± 24.12 a	97.64 ± 9.14 ab	424.79 ± 124.18 a	343.96 ± 34.98 b	1.58 ± 0.7 a	149.28 ± 12.2 a	2.87 ± 0.62 a	4.35 ± 0.58 ab	0.06 ± 0.01 a	0.1 ± 0.01 a
CC	Orange/Yellow	96.49 ± 9.5 a	56.62 ± 13.42 a	137.1 ± 36.16 a	378.01 ± 64.69 a	435.56 ± 81.05 ab	2.65 ± 1.14 a	165.76 ± 11.62 a	3.22 ± 0.82 a	4.49 ± 0.39 ab	0.07 ± 0.01 a	0.11 ± 0.01 a
CC	Yellow	108.03 ± 33.12 a	55.91 ± 23.23 a	91.83 ± 25.32 b	353.14 ± 95.63 a	825.12 ± 836.37 a	3.15 ± 2.56 a	165.99 ± 42.31 a	3.52 ± 0.87 a	4.65 ± 0.63 a	0.07 ± 0.01 a	0.1 ± 0.03 a
TPP	Absent	97.39 ± 33.7 b	52.33 ± 21.6 b	96.14 ± 25.94 a	381.56 ± 92.36 a	646.23 ± 643.69 a	2.19 ± 0.95 b	156.61 ± 37.87 a	3.11 ± 0.89 b	4.46 ± 0.69 a	0.07 ± 0.01 a	0.1 ± 0.02 a
TPP	Complex	126.85 ± 19.11 a	76.52 ± 9.25 a	108.93 ± 18.24 a	229 ± 71.72 c	348.95 ± 108.82 b	8.03 ± 2.35 a	169.53 ± 38.44 a	5.72 ± 3.23 a	3.83 ± 0.57 b	0.05 ± 0.01 b	0.09 ± 0.01 a
TPP	Dotted	102.88 ± 25.76 ab	62.58 ± 19.95 ab	94.97 ± 5.59 a	300.62 ± 73.13 bc	390.5 ± 122.14 ab	5.36 ± 3.61 a	179.11 ± 41.9 a	3.82 ± 1.06 a	3.43 ± 0.48 b	0.05 ± 0.01 b	0.09 ± 0.02 a
TPP	Spotted	95.55 ± 17.15 b	54.7 ± 12.98 b	103.85 ± 26.11 a	364.49 ± 37.13 ab	349.25 ± 62.56 ab	2.13 ± 0.89 b	152.45 ± 21.95 a	2.8 ± 0.4 b	4.34 ± 0.45 a	0.06 ± 0.01 a	0.1 ± 0.03 a
TC	Brown/Orange	104.17 ± 32.31 a	60.79 ± 19.85 a	101.22 ± 22.83 a	350.26 ± 102.13 a	465.44 ± 338.95 a	4.02 ± 3.07 a	163.22 ± 33.68 a	3.68 ± 1.94 a	4.03 ± 0.65 b	0.06 ± 0.01 b	0.09 ± 0.02 b
TC	Pink/Red	98.8 ± 33.31 a	54.66 ± 22.83 ab	89.54 ± 18.84 b	359.95 ± 101.77 a	684.78 ± 751.95 a	2.47 ± 1.91 b	153.87 ± 42.62 a	3.02 ± 0.6 a	4.38 ± 0.81 a	0.06 ± 0.01 b	0.1 ± 0.02 a
TC	Yellow/Green	94.33 ± 11.13 a	44.43 ± 11.4 b	114.1 ± 31.08 a	341.9 ± 40.89 a	424.47 ± 116.44 a	2.3 ± 0.61 ab	170.88 ± 33.54 a	3.79 ± 1.46 a	4.63 ± 0.45 a	0.07 ± 0.01 a	0.1 ± 0.02 ab
	F-statistic	2.73	3.07	4.71	6.54	4.03	9.95	1.48	6.58	10.79	8.91	2.72
	p-value (F-test)	8.83E-03	3.74E-03	5.56E-05	6.05E-07	3.17E-04	2.54E-10	1.73E-01	5.47E-07	3.31E-12	3.95E-10	7.69E-03

Principal component analysis and hierarchical clustering

Relationships among genotypes were further investigated by Principal Component Analysis (PCA). The first two components explained 28.55% (PC1) and 18.62% (PC2) of the dataset variation (Figure 1). Notably, the PCA biplot successfully separated accessions with complex or dotted TPP from those with spotted or no TPP.

Hierarchical clustering provided information on variables with similar variation trends and genotypes with similar physicochemical features (Figure 2). Three main variable clusters were found. The first (V1) included luteolin, myricetin, kaempferol and gallic acid, with the first two variables exhibiting the most similar variation patterns (Figure 2). The second cluster (V2) revealed very similar variation patterns for delphinidin and cyanidin, and relation of these two compounds with epicatechin and ABTS*dir*. The third cluster (V3) grouped the remaining variables, with L and b*, TPC and ABTS, and a* and catechin forming three sub-clusters with most similar variation patterns.

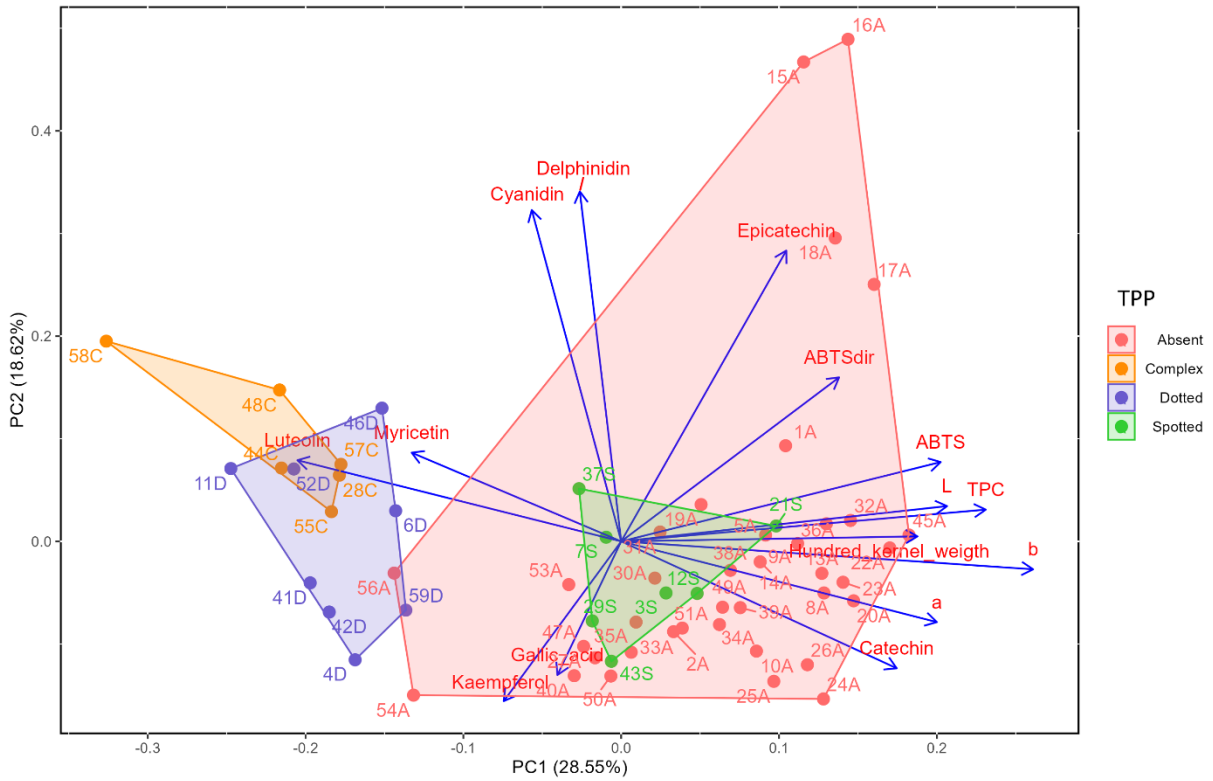

Figure 1. Principal Component Analysis (PCA) for physicochemical features of 59 lentil genotypes. The results are reported for the first (PC1) and the second (PC2) PCs. Genotypes are indicated by dots with different colors according to the seed coat pattern. Arrows refer to loadings for each variable. L*, a*, b*: CIELAB color space indexes; TPC: Total phenolic content; ABTS: Antioxidant capacity by the 2,2'-azino-bis(3-ethylbenzothiazoline-6-sulfonic acid) (ABTS) assay on extracts; ABTS*dir*: Antioxidant capacity by direct ABTS assay.

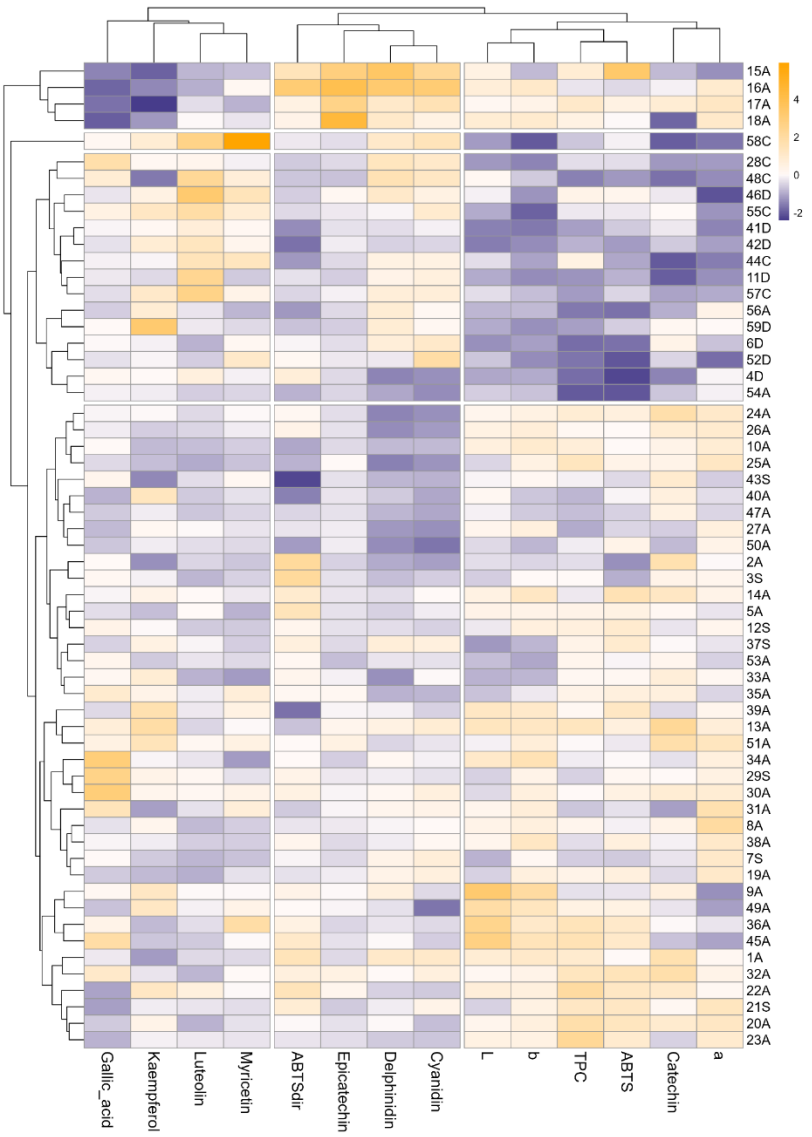

Figure 2. Heatmap and hierarchical clustering based on the physicochemical features of 59 lentil genotypes. The color scale refers to scaled average values for each variable. L*, a*, b*: CIELAB color space indexes; TPC: Total phenolic content; ABTS: Antioxidant capacity by the 2,2'-azino-bis(3-ethylbenzothiazoline-6-sulfonic acid) (ABTS) assay on extracts; ABTS*dir*: Antioxidant capacity by direct ABTS assay.

Concerning the genotypes, PCA results were confirmed, as two main clusters were identified, one mostly containing complex and dotted TPP genotypes, and the other absent or spotted TPP genotypes. The first was characterized by below-average levels of variables included in V3; the second lacked a clear pattern of variation. In addition, a divergent cluster was found, including the accessions 15A, 16A, 17A and 18A, all characterized by no TPP. This was characterized by below-average levels of variables included in the V1 group, and above-average levels of variables included in the V2 group. The genotype 58C, displaying a complex TPP, showed a clearly distinct profile, with above-average levels of variables included in the V1 cluster (including the highest level of myricetin), and below-average levels of variables included in the V3 group (including the lowest value of the b* color index).

DISCUSSION

From a breeding perspective, the whole-seed phenolic and antioxidant profile is an important selection criterion, as it may improve the nutritional quality of lentils without compromising yield or agronomic performance. Moreover, phenolic-rich seeds can support the development of functional food products that meet growing consumer demand for plant-based foods with added health benefits. Given the increasing interest in clean-label and naturally fortified ingredients, lentil-derived products enriched in specific polyphenols could find applications in the formulation of bakery goods, meat alternatives, ready-to-eat meals, and nutraceuticals. Phenolic compounds are key contributors to the antioxidant properties found in plant-derived foods (Sun et al.,2023) and therefore are assumed to be highly correlated with each other. In addition, they are often associated with specific pigmentation patterns, therefore seed color and patterns can serve as a practical indicator for identifying polyphenol-rich genotypes. However, the extent of these relationships still needed to be clarified in lentil.

In this study, relations among phenolic content and composition, antioxidant capacity, and seed color and pattern were assessed on a lentil germplasm collection. Most of the genotypes selected by this study were indicated by the ICARDA genebank as drought tolerant, therefore of main interest for breeding or direct use in Mediterranean agricultural settings. Significant genotypic effects were found for all the parameters under test, indicating the possibility to obtain genetic gains by breeding. As expected, cotyledon color (CC), tegument color (TC) and tegument pigmentation pattern (TPP) classes were significantly associated with variation of individual polyphenols, TPC and antioxidant capacity, as showed by ANOVA and regression analysis for CIELab indexes (Table 1, Supplementary Table S3).

Variation in biochemical features and color could be associated with TTPs (Figure 1 and Table 1). Specifically, complex and dotted TPPs were associated with overall lower TPC levels and antioxidant capacity, and higher levels of anthocyanins, luteolin and myricetin. In contrast, genotypes with spotted TPP or lacking tegument patterns showed high TPC and antioxidant capacity. Genotypes lacking TPP also exhibit the highest levels of catechin and epicatechin, whereas those with complex TPP show the lowest.

CC was significatively associated with gallic acid, epicatechin and total polyphenols content (Table 1). Specifically, the highest TPC levels were observed for yellow cotyledons, which were significantly different from the orange ones. Antioxidant capacity was not affected by variation in this trait, in line with the notion that most antioxidant compounds accumulate in the seed coat. Consistently, Differences in TPC, antioxidant activity, luteolin gallic acid and cyanidin were

associated with variation in TC (Table 1). In detail, yellow/green teguments had the highest antioxidant capacity and increased TPC with respect to brown/orange. In addition, yellow/green teguments presented the highest level of gallic acid, significantly higher of pink/red and a significant lower cyanidin content compared to brown/orange TC.

A strong correlation was also observed between CIELab color indexes and Gallic acid, Catechin, Epicatechin, Luteolin, Kaempferol, Myricetin, TPC and ABTS antioxidant capacity. Notably, this suggests the possibility to select these traits with the aid of spectophotemetric analysis (Figure 2).

Overall, this work provides an overview of lentil genetic variation for traits of importance for the development of functional food products. Importantly, our study indicates that seed phenotypic traits can be taken as proxies for the selection of genotypes with superior profile of bioactive compounds.

REFERENCES

Adebamowo, C. A., Cho, E., Sampson, L., Katan, M. B., Spiegelman, D., Willett, W. C., & Holmes, M. D. (2005). Dietary flavonols and flavonol-rich foods intake and the risk of breast cancer. *International Journal of Cancer*, *114*(4), 628-633.

AGPG, 1985. AGPG. Lentil Descriptor; International Board for Plant Genetic Resources: Rome, Italy, 1985.

Alrosan, M., Tan, T. C., Easa, A. M., Gammoh, S., & Alu'datt, M. H. (2022). Recent updates on lentil and quinoa protein-based dairy protein alternatives: Nutrition, technologies, and challenges. *Food Chemistry*, *383*, 132386.

Alzuwaid, N. T., Fellows, C. M., Laddomada, B., & Sissons, M. (2020). Impact of wheat bran particle size on the technological and phytochemical properties of durum wheat pasta. *Journal of Cereal Science*, *95*, 103033.

Aslani, Z., Alipour, B., Mirmiran, P., & Bahadoran, Z. (2015). Lentil's (*Lens culinaris* L.) functional properties in prevention and treatment of non-communicable chronic diseases: A review. *International Journal of Nutrition and Food Sciences*, *4*(2-1), 15-20.

Bennett, J. E., Stevens, G. A., Mathers, C. D., Bonita, R., Rehm, J., Kruk, M. E., ... & Ezzati, M. (2018). NCD Countdown 2030: worldwide trends in non-communicable disease mortality and progress towards Sustainable Development Goal target 3.4. *The Lancet*, *392*(10152), 1072-1088.

Caccialupi, P., Ceci, L. R., Siciliano, R. A., Pignone, D., Clemente, A., & Sonnante, G. (2010). Bowman-Birk inhibitors in lentil: Heterologous expression, functional characterisation and anti-proliferative properties in human colon cancer cells. *Food Chemistry*, *120*(4), 1058-1066.

Calabriso, N., Massaro, M., Scoditti, E., Pasqualone, A., Laddomada, B., & Carluccio, M. A. (2020). Phenolic extracts from whole wheat biofortified bread dampen overwhelming inflammatory response in human endothelial cells and monocytes: Major role of VCAM-1 and CXCL-10. *European Journal of Nutrition*, *59*, 2603-2615.

CIELab, 1978. International Commission on Illumination / Comission internationale de l'Eclairage / Internationale Beleuchtungskommission [WWW Document]. URL https://cie.co.at/ (accessed 5.16.23).

Crop Production Statistics, 2024. https://data.tuik.gov.tr/Bulten/Index?p=Crop-Production-Statistics-2024-53447&dil=2, accessed on March 5th, 2025.

Day, L. (2013). Proteins from land plants–potential resources for human nutrition and food security. *Trends in Food Science & Technology*, *32*(1), 25-42.

De Mendiburu, F., & Yaseen, M. (2020). AGRICOLAE: statistical procedures for agricultural research, version 1.2-4.

Del Coco, M., Laddomada, B., Romano, G., Carcagnì, P., Kumar, S., & Leo, M. (2022). Characterization of a collection of colored lentil genetic resources using a novel computer vision approach. *Foods*, *11*(24), 3964.

Dhull, S. B., Kinabo, J., & Uebersax, M. A. (2023). Nutrient profile and effect of processing methods on the composition and functional properties of lentils (*Lens culinaris* Medik): A review. *Legume Science*, *5*(1), e156.

Erdoğan, C. (2015). Genetic characterization and cotyledon color in lentil. *Chilean Journal of Agricultural Research*, *75*(4), 383-389.

FAOSTAT Database. Food and Agriculture Organization of the United Nations. Available online: http://faostat3.fao.org

Faris, M. E. A. I. E., Takruri, H. R., & Issa, A. Y. (2012). Role of lentils (*Lens culinaris* L.) in human health and nutrition: A review. *Mediterranean Journal of Nutrition and Metabolism*, *6*(1), 3-16.

Fiocchetti, F., Laddomada, B., Roselli, M., Crinò, P., & Lucretti, S. (2009). Fingerprinting of three typical macrosperma Italian lentil (*Lens culinaris* Medik.) landraces using fluorescence-based AFLP markers. *Scientia Horticulturae*, *121*(3), 383-387.

Ganesan, K., & Xu, B. (2017). Polyphenol-rich lentils and their health promoting effects. *International Journal of Molecular Sciences*, *18*(11), 2390.

Giusti, F., Caprioli, G., Ricciutelli, M., Vittori, S., & Sagratini, G. (2017). Determination of fourteen polyphenols in pulses by high performance liquid chromatography-diode array detection (HPLC-DAD) and correlation study with antioxidant activity and colour. *Food Chemistry*, *221*, 689-697.

Guerra-García, A., Gioia, T., von Wettberg, E., Logozzo, G., Papa, R., Bitocchi, E., & Bett, K. E. (2021). Intelligent characterization of lentil genetic resources: evolutionary history, genetic diversity of germplasm, and the need for well-represented collections. *Current Protocols*, *1*(5), e134.

Guo, F., Danielski, R., Santhiravel, S., & Shahidi, F. (2024). Unlocking the nutraceutical potential of legumes and their by-products: Paving the way for the circular economy in the agri-food industry. *Antioxidants*, *13*(6), 636.

Hafiz, M. S., Campbell, M. D., O'Mahoney, L. L., Holmes, M., Orfila, C., & Boesch, C. (2022). Pulse consumption improves indices of glycemic control in adults with and without type 2 diabetes: a systematic review and meta-analysis of acute and long-term randomized controlled trials. *European Journal of Nutrition*, *61*(2), 809-824.

Han, H., & Baik, B. K. (2008). Antioxidant activity and phenolic content of lentils (*Lens culinaris*), chickpeas (*Cicer arietinum* L.), peas (*Pisum sativum* L.) and soybeans (*Glycine max*), and their quantitative changes during processing. *International Journal of Food Science and Technology*, *43*(11), 1971-1978.

Irakli, M., Kargiotidou, A., Tigka, E., Beslemes, D., Fournomiti, M., Pankou, C., ... & Vlachostergios, D. N. (2021). Genotypic and environmental effect on the concentration of phytochemical contents of lentil (*Lens culinaris* L.). *Agronomy*, *11*(6), 1154.

Jung, Y. S., Lee, S. H., Chun, S. Y., Kim, D. H., Jang, B. I., Han, M. H., & Lee, S. O. (2021). In vitro and in vivo protective effects of lentil (*Lens culinaris*) extract against oxidative stress-induced hepatotoxicity. *Molecules*, *27*(1), 59.

Kushi, L. H., Meyer, K. A., & Jacobs Jr, D. R. (1999). Cereals, legumes, and chronic disease risk reduction: evidence from epidemiologic studies. *The American Journal of Clinical Nutrition*, *70*(3), 451S-458S.

Lastras, C., Revilla, I., González-Martín, M. I., & Vivar-Quintana, A. M. (2021). Prediction of fatty acid and mineral composition of lentils using near infrared spectroscopy. *Journal of Food Composition and Analysis*, *102*, 104023.

Lee, S. Y., Yeo, Y. S., Park, S. Y., Lee, S. G., Lee, S. M., Cho, H. S., ... & Oh, S. W. (2017). Compositional analysis of lentil (*Lens culinaris*) cultivars related to colors and their antioxidative activity. *Plant Breeding and Biotechnology*, *5*(3), 192-203.

Magalhães, L. M., Santos, F., Segundo, M. A., Reis, S., & Lima, J. L. (2010). Rapid microplate high-throughput methodology for assessment of Folin-Ciocalteu reducing capacity. *Talanta*, *83*(2), 441-447.

Manco, A., Gerardi, C., Romano, G., D'Amico, L., Blanco, A., Milano, F., ... & Laddomada, B. (2023). Phenolic profile of whole seeds and seed fractions of lentils and its impact on antioxidant activity. *Food Bioscience*, *54*, 102887.

Mirali, M., Purves, R. W., Stonehouse, R., Song, R., Bett, K., & Vandenberg, A. (2016). Genetics and biochemistry of zero-tannin lentils. *Plose One*, *11*(10), e0164624.

Mirali, M., Purves, R. W., & Vandenberg, A. (2017). Profiling the phenolic compounds of the four major seed coat types and their relation to color genes in lentil. *Journal of Natural Products*, *80*(5), 1310-1317.

Muehlbauer, F. J., Mihov, M., Vandenberg, A., Tullu, A., & Materne, M. (2009). Improvement in developed countries. In *The lentil: Botany, production and uses* (pp. 137-154). Wallingford UK: CABI.

Noor, M. M. A., Tahjib-Ul-Arif, M., Alim, S. A., Islam, M. M., Hasan, M. T., Babar, M. A., ... & Mostofa, M. G. (2024). Lentil adaptation to drought stress: response, tolerance, and breeding approaches. *Frontiers in Plant Science*, *15*, 1403922.

Parihar, A. K., Hazra, K. K., Lamichaney, A., Gupta, D. S., Kumar, J., Singh, A. K., ... & Dixit, G. P. (2025). Adaptive responses of large-seeded lentils across diverse Indian climates. *Heliyon*, *11*(3).

Peng, L., Guo, F., Pei, M., Tsao, R., Wang, X., Jiang, L., ... & Xiong, H. (2022). Anti-inflammatory effect of lentil hull (*Lens culinaris*) extract via MAPK/NF-κB signaling pathways and effects of digestive products on

intestinal barrier and inflammation in Caco-2 and Raw264. 7 co-culture. *Journal of Functional Foods*, *92*, 105044.

Purves, R. W., Khazaei, H., Elessawy, F. M., Munro, R., Shurmer, B. O., & Vandenberg, A. (2025). Investigation of polyphenol diversity among lentil species (*Lens* spp.) using mass spectrometry-based metabolomics guided by photodiode array detection. *Food Research International*, *209*, 116154.

Sun, W., & Shahrajabian, M. H. (2023). Therapeutic potential of phenolic compounds in medicinal plants—Natural health products for human health. *Molecules*, *28*(4), 1845.

Venter de Villiers, M., Cheng, J., & Truter, L. (2024). The Shift Towards Plant-Based Lifestyles: Factors Driving Young Consumers' Decisions to Choose Plant-Based Food Products. *Sustainability*, *16*(20), 9022.

Yanni, A. E., Iakovidi, S., Vasilikopoulou, E., & Karathanos, V. T. (2023). Legumes: A vehicle for transition to sustainability. *Nutrients*, *16*(1), 98.

Xu, B., & Chang, S. K. (2009). Phytochemical profiles and health-promoting effects of cool-season food legumes as influenced by thermal processing. *Journal of Agricultural and Food Chemistry*, *57*(22), 10718-10731.

Warne, T., Ahmed, S., Byker Shanks, C., & Miller, P. (2019). Sustainability dimensions of a North American lentil system in a changing world. *Frontiers in Sustainable Food Systems*, *3*, 88.

Wickham, H., & Sievert, C. (2009). ggplot2: elegant graphics for data analysis (Vol. 10, pp. 978-0). New York: Springer.

Kolde, R. (2019). Pheatmap: pretty heatmaps. *R package version*, *1*(2), 726.

Zulueta, A., Esteve, M. J., & Frígola, A. (2009). ORAC and TEAC assays comparison to measure the antioxidant capacity of food products. *Food Chemistry*, *114*(1), 310-316.

Supplementary materials

Supplementary Table S1. List of lentil genotypes used in this study, including their origin, cotyledon coat color, tegument coat color and seed coat pattern infromation.

Genotype	Variety	Cotyledon_Coat_Color	Tegument_Coat_Color	Seed_Coat_Pattern	Year_of_Release	Country	ID	Pedigree
1A	IG358	Orange	Brown/Orange	Absent	1984	Ethiopia	PI 299127	NEL358
2A	IG590	Orange	Pink/Red	Absent	1998	Australia	PI 339319	Selection from PI339319
3S	IG481	Orange	Pink/Red	Spotted	1989	Canada	PI 300561	Lebanese landrace NEL481
4D	IG784	Orange	Pink/Red	Dotted	1991	USA	GIZA 9	Egyptian local, Giza 9
5A	IG854	Yellow	Brown/Orange	Absent	1991	Turkey	60	Egyptian germplasm, 60
6D	IG1005	Orange	Pink/Red	Dotted	1973	Chile	33-032-10403	-
7S	IG4399	Orange/Red	Pink/Red	Spotted	1987	Turkey	Lebanese Local	Selection from L1278
8A	IG4400	Yellow	Yellow/Green	Absent	1988	Algeria	SYRIAN	Selection from landrace
9A	IG4605	Yellow	Pink/Red	Absent	1989	ICARDA	PRECOZ	Selection from landrace
10A	IG73661	Orange	Pink/Red	Absent	2001	Syria	FLIP 89-39L	ILL 223 X 79SH4901
11D	IG76027	Orange	Pink/Red	Dotted	1990	Nepal	LN0077	-
12S	IG5562	Orange/Yellow	Pink/Red	Spotted	1999	Morocco	76TA 66005	ILL 1 selection
13A	IG5582	Yellow	Brown/Orange	Absent	1987	Syria	78S 26002	ILL 8 selection
14A	IG5588	Orange	Brown/Orange	Absent	1995	Australia	78S 26013	ILL 16 selection
15A	IG5722	Orange	Brown/Orange	Absent	2001	Turkey	FLIP 84-51L	ILL 883 X ILL 470
16A	IG5748	Yellow	Pink/Red	Absent	1995	Ethiopia	FLIP 84-78L	ILL 883 X ILL 470
17A	IG69492	Orange	Pink/Red	Absent	2000	Syria	81S15	UJL 197 X ILL 4400
18A	IG70043	Yellow	Pink/Red	Absent	1995	Lebanon	FLIP 86-2L	ILL 466 X ILL 212
19A	IG73979	Orange	Pink/Red	Absent	1989	USA	WH-80	-
20A	IG70076	Orange	Pink/Red	Absent	2003	Morocco	FLIP 86-35L	ILL 4354 X ILL 922
21S	IG156736	Orange	Pink/Red	Spotted	2014	Afghanistan	95S 35195-17	ILL 7949 X ILL 7686
22A	IG70092	Yellow	Pink/Red	Absent	2012	Iran	FLIP 86-51L	ILL 4349 X ILL 4605
23A	IG71144	Yellow	Pink/Red	Absent	1999	Iran	FLIP 87-22L	ILL 4349 X ILL 4605
24A	IG117646	Orange/Red	Pink/Red	Absent	1999	Syria	FLIP 96-14 L	ILL 6209 X ILL 5671
25A	IG71178	Orange	Pink/Red	Absent	2000	Lebanon	FLIP 87-56L	ILL 2129 X ILL 13
26A	IG117679	Yellow	Brown/Orange	Absent	1996	ICARDA	FLIP 96-47 L	-
27A	IG73685	Orange	Brown/Orange	Absent	1998	Ethiopia	FLIP 89-63L	ILL 4225 X ILL 4605
28C	IG122918	Orange	Brown/Orange	Complex	1998	Pakistan	91516	-
29S	IG73858	Orange	Brown/Orange	Spotted	2002	Syria	FLIP 90-25L	ILL 5588 X ILL 99
30A	IG73874	Orange/Yellow	Brown/Orange	Absent	2006	Turkey	FLIP 90-41L	Sel. 80S42188 X ILL 223
31A	IG75896	Yellow	Pink/Red	Absent	2009	Iran	FLIP 92-12L	ILL 5582 X ILL 707
32A	IG122934	Orange	Brown/Orange	Absent	1998	ICARDA	FLIP 98-15 L	ILL 6243 X ILL 1939
33A	IG75920	Orange	Brown/Orange	Absent	2002	Syria	FLIP 92-36L	ILL 5879 X ILL 5714
34A	IG75932	Orange	Yellow/Green	Absent	2000	Lesotho	FLIP 92-48L	ILL 5583 X ILL 5726
35A	IG76232	Orange	Yellow/Green	Absent	2007	Syria	FLIP 93-12L	ILL 5538 X ILL 5782
36A	IG114687	Orange	Yellow/Green	Absent	2015	Syria	FLIP 95-29L	-
37S	IG114688	Orange	Brown/Orange	Spotted	2006	Turkey	FLIP 95-30L	ILL5604 X ILL6015
38A	IG114713	Orange	Brown/Orange	Absent	1999	Portugal	FLIP 95-55L	-
39A	IG117647	Yellow	Yellow/Green	Absent	2007	Azerbaijan	FLIP 96-15 L	ILL 6209 X ILL 5671
40A	IG117680	Orange	Brown/Orange	Absent	2004	Ethiopia	FLIP 96-48 L	-
41D	IG117682	Orange	Brown/Orange	Dotted	2009	Nepal	FLIP 96-50 L	Laird X VW000412
42D	ILL8006	Orange	Brown/Orange	Dotted	1996	Bangladesh	-	ILL7888 X ILL5782
43S	IG129142	Orange	Brown/Orange	Spotted	2000	ICARDA	FLIP 00-19 L	ILL 5883 X ILL 6994
44C	ILL8009	Orange	Brown/Orange	Complex	1990	Nepal	-	Local land race, LG7
45A	IG122878	Yellow	Yellow/Green	Absent	2007	Uzbekistan	FLIP 97-4L	ILL 6002 X ILL 6435
46D	IG122880	Yellow	Brown/Orange	Dotted	1997	ICARDA	FLIP 97-6L	ILL 5582 X ILL 5845
47A	IG142268	Orange	Brown/Orange	Absent	2006	ICARDA	FLIP 07-57L	ILL 5883 X ILL 590
48C	IG156670	Orange	Brown/Orange	Complex	2006	Bangladesh	BARIMASUR 5	ILL 2501 X ILL 7616
49A	IG156514	Yellow	Yellow/Green	Absent	2018	Syria	97-39L, 98S029	-
50A	IG156631	Orange	Pink/Red	Absent	1995	ICARDA	95S 36115-01	ILL 7620 X 88522
51A	IG156693	Orange	Pink/Red	Absent	-	Ethiopia	ALEMAYA	-
52D	IG156695	Orange	Brown/Orange	Dotted	1998	India	SUBRATA	WBL
53A	10867/10174/6SPS	Orange	Brown/Orange	Absent	2018	ICARDA	-	ILL 10867 X ILL 10174
54A	F1X2011S-132/F1X2011S-110/23-10	Orange	Brown/Orange	Absent	2018	ICARDA	-	F1X2011S-132 X F1X2011S-110
55C	8114/7663/2SPS	Orange	Brown/Orange	Complex	2018	ICARDA	-	ILL 8114 X ILL7663
56A	F1X2011S-132/F1X2011S-110/6-2	Orange	Brown/Orange	Absent	2018	ICARDA	-	F1X2011S-132 X F1X2011S-110
57C	7978/DPL 62/10-8	Orange	Brown/Orange	Complex	2018	ICARDA	-	ILL 7978 X DPL 62
58C	4605/3596/2SPS	Orange	Brown/Orange	Complex	2018	ICARDA	-	ILL 4605 X ILL 3596
59D	10072/1712/10-3	Orange	Pink/Red	Dotted	2018	ICARDA	-	ILL 10072 X ILL1712

Supplementary Table S2. One-way ANOVA results from testing the genotype effect on individual polyphenols, total polyphenol content, antioxidant activity and CIELab indices.

Response	Delphinidin	Cyanidin	Gallic_acid	Catechin	Epicatechin	Luteolin	Kaempferol	Myricetin	TPC	ABTS	ABTS *dir*	L*	a*	b*
R^2	0.947	0.962	0.923	0.951	0.969	0.988	0.958	0.961	0.927	0.913	0.830	0.994	0.996	0.994
Adjusted R^2	0.895	0.925	0.848	0.904	0.939	0.975	0.916	0.922	0.891	0.871	0.746	0.989	0.992	0.988
F-statistic	18.206	25.758	12.270	19.914	32.247	80.889	23.110	24.989	25.784	21.286	9.920	182.049	243.618	167.736
p-value (F-test)	1.06815E-22	9.26928E-27	2.91452E-18	9.80333E-24	1.89202E-29	8.91885E-41	1.77888E-25	2.12034E-26	5.9414E-46	2.3299E-41	1.24785E-25	5.34134E-51	1.071E-54	5.8219E-50

Supplementary Table S3. Three-way ANOVA results examining the effect of CIELab color indices on individual polyphenols, total polyphenol content, and antioxidant activity.

Response	Delphinidin	Cyanidin	Gallic_acid	Catechin	Epicatechin	Luteolin	Kaempferol	Myricetin	TPC	ABTS	ABTS *dir*
R^2	0.063	0.052	0.096	0.152	0.083	0.258	0.031	0.175	0.316	0.247	0.063
Adjusted R^2	0.039	0.027	0.072	0.129	0.059	0.239	0.006	0.153	0.298	0.228	0.039
F-statistic	2.565	2.076	4.047	6.795	3.430	13.219	1.217	8.060	17.542	12.494	2.575
p-value for the model (F-test)	0.0581	0.1073	0.0089	0.0003	0.0195	0.0000	0.3069	0.0001	0.0000	0.0000	0.0574
p-value (coefficient L)	0.2591	0.5209	0.0029	0.9404	0.0326	0.5606	0.2386	0.1408	0.0000	0.0007	0.4618
p-value (coefficient a)	0.0787	0.7161	0.0054	0.0364	0.1589	0.0001	0.1627	0.0015	0.0006	0.0314	0.5123
p-value (coefficient b)	0.5804	0.1743	0.0025	0.3092	0.2975	0.3402	0.4261	0.2961	0.0162	0.2566	0.7004

Chapter 6
Discussion and Conclusions

The low profitability of legumes in Mediterranean countries has led to minimal breeding activities and inadequate exposure of farmers to new cultivars (Rubiales et al., 2021). In Italy, farmers still largely favour cereals over legumes, due to higher yield, well-developed markets, and effective incentives (Ghelfi et al., 2017). Remarkably, imports are meeting most of the Italian grain legume internal demand.

In this scenario, the characterization of legume biodiversity is an essential step for the development of economically valuable legume cultivars, merging high yield potential with adaptation to abiotic and biotic stresses and suitable to market requirements and innovative uses by the food industry. Notably, the promotion of legume cultivation by improved cultivars will lead to increased sustainability of farming systems, given the capacity of legumes to fix atmospheric nitrogen and their positive impact on soil properties and conservation (Sultani et al., 2007). Besides this, information on the genetic features of germplasm collections may pave the way to the characterization of genes underlying economically important genes, and thus scientific advancements in the field of agricultural genetics.

The general aim of this PhD thesis is to characterize legume biodiversity for stress adaptation and innovative industrial uses. Considering the major impact of the parasitic species *Oc* in Mediterranean agro-ecosystems, focus was given to the study of genetic mechanisms of resistance to this parasite.

Some of the experiments conducted in this thesis, described in Chapter 2 and part of Chapter 3, address the genetic dissection and use in breeding of the nearly complete field resistance to *Oc* displayed by the breeding line ROR12, previously characterized at the Department of Soil, Plant and Food Sciences of the University of Bari Aldo Moro. Three QTLs associated with ROR12 resistance were found by a QTL mapping approach, including one (*PsOcr-1*) explaining as much as 69.3% of the genetic variance. This is a relevant finding, as (incomplete) *Oc* resistance sources previously identified in wild or cultivated *Pisum* germplasm were associated with several minor effect QTLs (Rubiales et al., 2003; Valderrama et al., 2004; Rubiales et al., 2005; Pérez-de-Luque et al., 2005; Fondevilla et al., 2010; Rubiales et al., 2020; Wohor et al., 2022).

Interestingly, genetic analysis provided in Chapter 2 indicated additivity between *PsOcr-1* and *PsOcr-2*, and between *PsOcr-1* and *PsOcr-3*, and epistasis of *PsOcr-2* over *PsOcr-3,* indicating that 'ROR12' resistance originates from two independent defense mechanisms, one involving *PsOcr-1* and the other both *PsOcr-2* and *PsOcr-3*. This finding was further confirmed by the analysis of pea lines harbouring contrasting alleles at the three QTLs, indicating that, while resistance provided by *PsOcr-1* relies on low strigolactone (SL) exudation, SL-independent mechanisms are associated with *PsOcr-2* and *PsOcr-3*.

RNA-seq conducted on the same set of lines above mentioned, carrying different allelic combinations at the *PsOcr* QTLs, indicated a 2-methylene-furan-3-one reductase as a candidate gene for *PsOcr-1,* which might act on furanone rings of SLs and/or debranones, mimicking SLs in inhibiting shoot branching and stimulating the germination of *Striga* and *Orobanche* (Fukui et al., 2011; Takahashi et al., 2016; Kawada et al., 2024). Notably, the integration of QTL mapping and RNA-seq data also indicated a *phenylalanine ammonia lyase* (*PAL*) as an obvious candidate gene for *PsOcr-2*. PAL, a key enzyme in the phenylpropanoid pathway, is indeed typically upregulated in response to biotic stresses, including broomrape infection (Mabrouk et al., 2016; Briache et al., 2020). A G-type lectin S-receptor-like serine/threonine-protein kinase, known to be involved in the activation of defense pathways against pathogens (Sun et al., 2020), was identified a possible candidate for *PsOcr-3*. Future research might be addressed to the further refinement of the QTL mapping resolution and the functional characterization of candidate genes. With this respect, transient transformation, TILLING and ECOTILLING appear as the most feasible approaches at the moment, in the absence of efficient transformation protocols (Dalmais et al., 2008; Choudhury et al., 2021; Li et al., 2023).

The use of ROR12 resistance, previously shown to be devoid of obvious pleiotropic effects affecting agronomic performance, in breeding might be facilitated by its high heritability, which was estimated to be equal to 0.84 in our experimental conditions. In addition, assisted selection programs might be prompted by the KASP assays described in this thesis.

Other experimental activities of this thesis, described in Chapter 3, were addressed to identify new sources of *Oc* resistance in pea biodiversity, and to study the role of low SL exudation in determining field resistance to *Oc*. Importantly, three pea lines resistant to *Oc* were identified. Intriguingly, all of them, along with ROR12, originate from southern Italy. This geographic concentration suggests a common origin or dissemination pattern and points to a possibly shared genetic basis for resistance within this regional germplasm.

While reduced strigolactone (SL) exudation is known to limit germination of Orobanchaceae species (Bouwmeester et al., 2021), its effectiveness in conferring field resistance remains largely unexplored. Indeed, SL-biosynthetic mutants have mainly been evaluated through in vitro germination or pot assays (Kohlen et al., 2012; Butt et al., 2018; Galili et al., 2021; Hao et al., 2023). This thesis reports the results of analytical quantification of SLs in germplasm showing contrasting response to *Oc*, revealing an association between low SL exudation and resistance, and suggesting that low SL exudation is common in pea germplasm displaying enhancing resistance to *Oc*. On the other hand, field evaluation of the pea SL biosynthetic mutants *rms1* and *rms5*, impaired for the key SL biosynthetic enzymes CCD8 and CCD7, resulted in substantial parasitization by *Oc* in field

conditions, albeit to a minor extent than their corresponding wild-type genotype (the cv. Térèse). All of this leads to a key conclusion of this thesis, i.e. that low or null SL exudation alone is not sufficient to confer field resistance to *Oc* in pea. Therefore, to cope with this parasitic weed, pea breeding should combine SL-dependent and SL-independent resistance mechanisms, such as those shown to occur in ROR12 resistance. Incomplete resistance of *rms* mutants could be attributed to the presence of non-SL germination stimulants, which have been previously reported in pea root exudates (Brun et al., 2018; Jamil et al., 2024).

Experimental activities described in Chapter 4 aim to investigate, based on RNA-seq and hormone quantifications, emphasize the central role of SLs as integrators of developmental and stress-response signaling the biological roles of SLs. Notably, genes involved in oxidative, salt, and heat stress responses, as well as phenylalanine and lignin catabolism, were significantly downregulated in SL mutants. This aligns with the observed reduction in abscisic acid (ABA) levels (Figure 4A), a plant hormone known to enhance antioxidant defenses, stress adaptation, and the phenylpropanoid pathway (Li et al., 2022; Singh et al., 2023; Dong et al., 2021). Although previous studies have reported crosstalk between SL and ABA pathways (Haider et al., 2018; Korek et al., 2023), we did not observe major changes in the expression of ABA biosynthesis genes (Figure 4B, Supplementary Figure S2), suggesting post-transcriptional regulation via altered catabolism, transport, or enzymatic activity. The interaction between SLs and ABA described indicates, among other things, that breeding strategies for *Oc* resistance based on SL depletion might have pleiotropic deleterious effects on abiotic stress tolerance.

SLs also promote root growth by regulating meristem activity and lateral root formation (Kapulnik et al., 2011; Ruyter-Spira et al., 2011). Accordingly, genes involved in cell cycle progression, DNA replication, and microtubule dynamics showed downregulation upon SL depletion. This lower root activity may in turn lead to decreased energy demand and downregulation of carbohydrate metabolism genes, also observed by the analysis of transcriptomic data.

Interestingly, transcriptomic changes unique to the *rms5* mutant (defective in CCD7), but not to *rms1* (CCD8), were identified, indicating biological processes that are influenced by CCD7 beyond its role as SL biosynthetic enzyme. These include photosynthesis- and light-harvesting-related genes (upregulated by CCD7 depletion), and genes related to cell wall organization and nucleosome assembly. These findings support the idea that CCD7 may act on additional carotenoid substrates, producing apocarotenoids with signaling functions (Bruno et al., 2014; Hou et al., 2016). In this context, we highlight that CCD7 has been linked to the generation of cyclohexenone (C13) and mycorradicin (C14) derivatives (Walter et al., 2007). Another possible explanation for *rms5*-specific

transcriptomic shifts is that carotenoids like 9-*cis*-β-carotene or their cleavage products may contribute to retrograde signaling affecting nuclear gene expression and plastid development (Moreno et al., 2021; Wang et al., 2021; Sierra et al., 2022).

Finally, experimental activities reported in Chapter 5 investigate the relations among phenolic content and composition, antioxidant capacity, and seed color and pattern, aiming to provide useful information for the development of functional food products meeting the growing demand of consumers for plant-based foods with added health benefits. Variation in biochemical features and color could be clearly associated with the tegument pigmentation pattern. Specifically, complex and dotted TPPs were associated with overall lower total phenolic content and antioxidant capacity, and higher levels of anthocyanins, luteolin and myricetin. In contrast, genotypes with spotted TPP or lacking tegument patterns showed high TPC and antioxidant capacity. Genotypes lacking TPP also exhibited the highest levels of catechin and epicatechin, whereas those with complex TPP show the lowest.

A strong correlation was observed between CIELab color indexes and Gallic acid, Catechin, Epicatechin, Luteolin, Kaempferol, Myricetin, TPC and ABTS antioxidant capacity. Notably, this suggests the possibility to select these traits with the aid of spectophotemetric analysis

Overall, the work described in this PhD thesis provides valuable insights for legume genetic improvement, supporting the revitalization of their cultivation in the Mediterranean region. It also lays the foundation for the molecular understanding of complex phenomena such as responses to parasitic plants and abiotic stresses. Currently, reverse genetics strategies are underway to functionally validate the candidate genes reported in the thesis. In addition, targeted analyses are being conducted for a detailed biochemical characterization of pea and lentil germplasm collections, focusing on traits considered important for the agro-industrial sector, such as protein content, macro- and microelement profiles, and the content of trigonelline, an alkaloid of growing interest in the functional food and nutraceutical sectors for its potential health-promoting properties.

REFERENCES

Bouwmeester, H., Li, C., Thiombiano, B., Rahimi, M., & Dong, L. (2021). Adaptation of the parasitic plant lifecycle: germination is controlled by essential host signaling molecules. *Plant Physiology*, *185*(4), 1292-1308.

Briache, F. Z., Ennami, M., Mbasani-Mansi, J., Lozzi, A., Abousalim, A., El Rodeny, W., ... & Mentag, R. (2020). Effects of salicylic acid and indole acetic acid exogenous applications on induction of faba bean resistance against *Orobanche crenata*. *The Plant Pathology Journal*, *36*(5), 476.

Brun, G., Braem, L., Thoiron, S., Gevaert, K., Goormachtig, S., & Delavault, P. (2018). Seed germination in parasitic plants: what insights can we expect from strigolactone research?. *Journal of Experimental Botany*, *69*(9), 2265-2280.

Bruno, M., Hofmann, M., Vermathen, M., Alder, A., Beyer, P., & Al-Babili, S. (2014). On the substrate-and stereospecificity of the plant carotenoid cleavage dioxygenase 7. *FEBS Letters*, *588*(9), 1802-1807.

Butt, H., Jamil, M., Wang, J. Y., Al-Babili, S., & Mahfouz, M. (2018). Engineering plant architecture via CRISPR/Cas9-mediated alteration of strigolactone biosynthesis. *BMC Plant Biology*, *18*, 1-9.

Choudhury, A., & Rajam, M.V. (2021). Genetic transformation of legumes: an update. *Plant Cell Reports.* 40, 1813–1830.

Dalmais, M., Schmidt, J., Le Signor, C., Moussy, F., Burstin, J., Savois, V., ... & Bendahmane, A. (2008). UTILLdb, a *Pisum sativum* in silico forward and reverse genetics tool. *Genome Biology*, *9*, 1-12.

Dong, N. Q., & Lin, H. X. (2021). Contribution of phenylpropanoid metabolism to plant development and plant–environment interactions. *Journal of Integrative Plant Biology*, *63*(1), 180-209.

Fondevilla, S., Fernández-Aparicio, M., Satovic, Z., Emeran, A. A., Torres, A. M., Moreno, M. T., & Rubiales, D. (2010). Identification of quantitative trait loci for specific mechanisms of resistance to *Orobanche crenata* Forsk. in pea (*Pisum sativum* L.). *Molecular Breeding*, *25*, 259-272.

Fukui, K., Ito, S., Ueno, K., Yamaguchi, S., Kyozuka, J., & Asami, T. (2011). New branching inhibitors and their potential as strigolactone mimics in rice. *Bioorganic & Medicinal Chemistry Letters*, *21*(16), 4905-4908.

Galili, S., Hershenhorn, J., Smirnov, E., Yoneyama, K., Xie, X., Amir-Segev, O., ... & Dor, E. (2021). Characterization of a chickpea mutant resistant to *Phelipanche aegyptiaca* Pers. and *Orobanche crenata* Forsk. *Plants*, *10*(12), 2552.

Ghelfi, R., & Palmieri, A. (2017). Pulses production in Italy: Trade, marketing and policy issues. *Italian Journal of Agronomy*, *12*(3), 891.

Haider, I., Andreo-Jimenez, B., Bruno, M., Bimbo, A., Floková, K., Abuauf, H., ... & Ruyter-Spira, C. (2018). The interaction of strigolactones with abscisic acid during the drought response in rice. *Journal of Experimental Botany*, *69*(9), 2403-2414.

Hao, J., Yang, Y., Futrell, S., Kelly, E. A., Lorts, C. M., Nebie, B., ... & Schachtman, D. P. (2023). CRISPR/Cas9-mediated mutagenesis of *carotenoid cleavage dioxygenase* (*CCD*) genes in sorghum alters strigolactone biosynthesis and plant biotic interactions. *Phytobiomes Journal*, *7*(3), 339-351.

Hou, X., Rivers, J., León, P., McQuinn, R. P., & Pogson, B. J. (2016). Synthesis and function of apocarotenoid signals in plants. *Trends in Plant Science*, *21*(9), 792-803.

Jamil, M., Margueritte, O., Yonli, D., Wang, J. Y., Navangi, L., Mudavadi, P., ... & Al-Babili, S. (2024). Evaluation of granular formulated strigolactone analogs for *Striga* suicidal germination. *Pest Management Science*, *80*(9), 4314-4321.

Kapulnik, Y., Delaux, P. M., Resnick, N., Mayzlish-Gati, E., Wininger, S., Bhattacharya, C., ... & Koltai, H. (2011). Strigolactones affect lateral root formation and root-hair elongation in *Arabidopsis*. *Planta*, *233*, 209-216.

Kawada, K., Takahashi, I., Takei, S., Nomura, A., Seto, Y., Fukui, K., & Asami, T. (2024). The Evaluation of Debranone Series Strigolactone Agonists for Germination Stimulants in *Orobanche* Species. *Journal of Agricultural and Food Chemistry*, *72*(35), 19517-19525.

Kohlen, W., Charnikhova, T., Lammers, M., Pollina, T., Tóth, P., Haider, I., ... & López-Ráez, J. A. (2012). The tomato *CAROTENOID CLEAVAGE DIOXYGENASE 8* (*SlCCD8*) regulates rhizosphere signaling, plant architecture and affects reproductive development through strigolactone biosynthesis. *New Phytologist*, *196*(2), 535-547.

Korek, M., & Marzec, M. (2023). Strigolactones and abscisic acid interactions affect plant development and response to abiotic stresses. *BMC Plant Biology*, *23*(1), 314.

Li, G., Liu, R., Xu, R., Varshney, R. K., Ding, H., Li, M., ... & Yang, T. (2023). Development of an Agrobacterium-mediated CRISPR/Cas9 system in pea (*Pisum sativum* L.). *The Crop Journal*, *11*(1), 132-139.

Li, S., Liu, S., Zhang, Q., Cui, M., Zhao, M., Li, N., ... & Wang, L. (2022). The interaction of ABA and ROS in plant growth and stress resistances. *Frontiers in Plant Science*, *13*, 1050132.

Mabrouk, Y., Mejri, S., Hemissi, I., & Belhadj, O. (2016). Biochemical analysis of induced resistance in chickpea against broomrape (*Orobanche foetida*) by rhizobia inoculation. *Phytopathologia Mediterranea*, 54-61.

Moreno, J. C., Mi, J., Alagoz, Y., & Al-Babili, S. (2021). Plant apocarotenoids: from retrograde signaling to interspecific communication. *The Plant Journal*, *105*(2), 351-375.

Pérez-de-Luque, A., Jorrín, J., Cubero, J. I., & Rubiales, D. (2005). *Orobanche crenata* resistance and avoidance in pea (*Pisum* spp.) operate at different developmental stages of the parasite. *Weed Research*, *45*(5), 379-387.

Rubiales, D., Annicchiarico, P., Vaz Patto, M. C., & Julier, B. (2021). Legume breeding for the agroecological transition of global agri-food systems: A European perspective. *Frontiers in Plant Science*, *12*, 782574.

Rubiales, D., Fondevilla, S., & Fernández-Aparicio, M. (2020). Development of pea breeding lines with resistance to *Orobanche crenata* derived from pea landraces and wild *Pisum* spp. *Agronomy*, *11*(1), 36.

Rubiales, D., Moreno, M. T., & Sillero, J. C. (2005). Search for resistance to crenate broomrape (*Orobanche crenata* Forsk.) in pea germplasm. *Genetic Resources and Crop Evolution*, *52*, 853-861.

Rubiales, D., Pérez-de-Luque, A., Cubero, J. I., & Sillero, J. C. (2003). Crenate broomrape (*Orobanche crenata*) infection in field pea cultivars. *Crop Protection*, *22*(6), 865-872.

Ruyter-Spira, C., Kohlen, W., Charnikhova, T., van Zeijl, A., van Bezouwen, L., De Ruijter, N., ... & Bouwmeester, H. (2011). Physiological effects of the synthetic strigolactone analog GR24 on root system architecture in Arabidopsis: another belowground role for strigolactones?. *Plant Physiology*, *155*(2), 721-734.

Sierra, J., McQuinn, R. P., & Leon, P. (2022). The role of carotenoids as a source of retrograde signals: impact on plant development and stress responses. *Journal of Experimental Botany*, *73*(21), 7139-7154.

Singh, A., & Roychoudhury, A. (2023). Abscisic acid in plants under abiotic stress: Crosstalk with major phytohormones. *Plant Cell Reports*, *42*(6), 961-974.

Sultani, M. I., Gill, M. A., Anwar, M. M., & Athar, M. (2007). Evaluation of soil physical properties as influenced by various green manuring legumes and phosphorus fertilization under rain fed conditions. *International Journal of Environmental Science & Technology*, *4*, 109-118.

Sun, Y., Qiao, Z., Muchero, W., & Chen, J. G. (2020). Lectin receptor-like kinases: the sensor and mediator at the plant cell surface. *Frontiers in Plant Science*, *11*, 596301.

Takahashi, I., Fukui, K., & Asami, T. (2016). Chemical modification of a phenoxyfuranone-type strigolactone mimic for selective effects on rice tillering or *Striga hermonthica* seed germination. *Pest Management Science*, *72*(11), 2048-2053.

Valderrama, M. R., Román, B., Satovic, Z., Rubiales, D., Cubero, J. I., & Torres, A. M. (2004). Locating quantitative trait loci associated with *Orobanche crenata* resistance in pea. *Weed Research*, *44*(4), 323-328.

Walter, M. H., Floß, D. S., Hans, J., Fester, T., & Strack, D. (2007). Apocarotenoid biosynthesis in arbuscular mycorrhizal roots: contributions from methylerythritol phosphate pathway isogenes and tools for its manipulation. *Phytochemistry*, *68*(1), 130-138.

Wang, J. Y., Lin, P. Y., & Al-Babili, S. (2021, January). On the biosynthesis and evolution of apocarotenoid plant growth regulators. In *Seminars in cell & developmental biology* (Vol. 109, pp. 3-11). Academic Press.

Wohor, O. Z., Rispail, N., Ojiewo, C. O., & Rubiales, D. (2022). Pea breeding for resistance to rhizospheric pathogens. *Plants*, *11*(19), 2664.